

IJCER

[Volume 4, Issue 2, February, 2014]



Frequency: 12 issues per year
[ISSN: 2250-3005 (online version)]
IJCER

Editorial Board

Editor-In-Chief

Prof. Chetan Sharma

Specialization: Electronics Engineering, India
Qualification: Ph.d, Nanotechnology, IIT Delhi, India

Editorial Committees

DR.Qais Faryadi

Qualification: PhD Computer Science
Affiliation: USIM(Islamic Science University of Malaysia)

Dr. Lingyan Cao

Qualification: Ph.D. Applied Mathematics in Finance
Affiliation: University of Maryland College Park,MD, US

Dr. A.V.L.N.S.H. HARIHARAN

Qualification: Phd Chemistry
Affiliation: GITAM UNIVERSITY, VISAKHAPATNAM, India

DR. MD. MUSTAFIZUR RAHMAN

Qualification: Phd Mechanical and Materials Engineering
Affiliation: University Kebangsaan Malaysia (UKM)

Dr. S. Morteza Bayareh

Qualificatio: Phd Mechanical Engineering, IUT
Affiliation: Islamic Azad University, Lamerd Branch
Daneshjoo Square, Lamerd, Fars, Iran

Dr. Zahéra Mekkioui

Qualification: Phd Electronics
Affiliation: University of Tlemcen, Algeria

Dr. Yilun Shang

Qualification: Postdoctoral Fellow Computer Science
Affiliation: University of Texas at San Antonio, TX 78249

Lugen M.Zake Sheet

Qualification: Phd, Department of Mathematics
Affiliation: University of Mosul, Iraq

Mohamed Abdellatif

Qualification: PhD Intelligence Technology
Affiliation: Graduate School of Natural Science and Technology

Meisam Mahdavi

Qualification: Phd Electrical and Computer Engineering

Affiliation: University of Tehran, North Kargar st. (across the ninth lane), Tehran, Iran

Dr. Ahmed Nabih Zaki Rashed

Qualification: Ph. D Electronic Engineering

Affiliation: Menoufia University, Egypt

Dr. José M. Merigó Lindahl

Qualification: Phd Business Administration

Affiliation: Department of Business Administration, University of Barcelona, Spain

Dr. Mohamed Shokry Nayle

Qualification: Phd, Engineering

Affiliation: faculty of engineering Tanta University Egypt

CONTENTS:

S.No.	Title Name	Page No.
Version I		
1.	Crahid: A New Technique for Web Crawling In Multimedia Web Sites Dr. Ammar Falih Mahdi , Rana Khudhair Abbas Ahmed	01-06
2.	Analysis Of Wavelet And Curvelet Image Denoising For Different Kinds Of Additive Noises Miss Monika Shukla , Dr.Soni Changlani , Mr.Tejinder Singh Marwah	07-12
3.	A More Effective Realization Of BCD Adder By Using A New Reversible Logic BBCDC Shefali Mamataj,Biswajit Das,Anurima Rahaman	13-19
4.	Effect of Chemical Reaction on Mass Transfer over a Stretching Surface Embedded In a Porous Medium E. M. A. Elbashbeshy , A. M. Sedki	20-28
5.	Development and Performance Evaluation of a Recirculatory System Fish Incubator Diabana P.D, Fakunmoju F.A ,Adesina B.S	29-34
6.	Fractional Derivative Associated With the Generalized M-Series and Multivariable Polynomials Ashok Singh Shekhawat , Jyoti Shaktawat	35-39
7.	DMZ: A trusted honeypot for secure transmission M.Buveneswari , M.P. Loganathan	40-42
8.	Efficient Cluster Head Selection Method For Wireless Sensor Network Manjusha M S, K E Kannammal	43-49
9.	Optimal Synthesis of a Single-Dwell 6-Bar Planar Linkage Galal A. Hassaan	50-56
10.	Vehicles Weight Ratio V. Initial Velocity of Vehicle in Chain Accidents on Highways Robert M Brooks, Mehmet Cetin	57-63

11.	To Study and Analyze To Foresee Market Using Data Mining Technique Amit Khedkar, Prof. Rajendra Argiddi	64-67
12.	Multiple Single Input Change Vectors for Built-In Self Test (MSIC-BIST) Praveenkumar.J,Danesh.K	68-72
Version II		
1.	Design and Implementation of Testable Reversible Sequential Circuits Optimized Power Manikandan.B, Vijayaprabhu.A	01-06
2.	Mathematical Methods in Medical Image Processing and Magnetic Resonance Imaging Joyjit patra, Himadri Nath Moulick, Arun Kanti Manna, Rajarshi Roy	07-18
3.	Erbil Guide Application Roojwan Scddeek.Esmael, Shahab WahabKareem, Rami S. Youael	19-24
4.	Algorithm on conditional probability on random graph using Markov Chain Habiba El-Zohny , Hend El- Morsy	25-33
5.	Analysis of Activity Patterns and Design Features Relationships in Urban Public Spaces: A Case Study of the Old City Of As-Salt Dr. Rana Almatarneh	34-51
6.	Modified Approach for Solving Maximum Clique Problem Jaspreet Singh	52-58
Version III		
1.	Optimizing Design Cost of System by using Dynamic Programming KIndira Priyadarsini, Amanulla Mohammad	01-05
2.	Criteria for Choosing An Effective Cloud Storage Provider Audu Jonathan Adoga, Garba M. Rabi,Anyesha Amos Audu	06-13
3.	Design and Implementation of Area and Power Efficient Embedded Transition Inversion Coding For Serial Links C.Jacob Ebbipeni , N.Bamakumari	14-21

4.	An Improved Software Reliability Growth Model B.Anniprincy, Dr. S. Sridhar	22-28
5.	Electronic Waste Status in Jharkhand Cities Umesh Kumar, Dr D N Singh	29-37
6.	Introducing Parallelism in Privacy Preserving Data Mining Algorithms Mrs.P.Cynthia Selvi , Dr.A.R.Mohamed Shanavas	38-41
7.	Comparative Aspects of Single & Multiple PV Arrays Connected With UPQC Payal Deshpande, Amit Shrivastava	42-49
8.	Analytical Solution Of Unsteady Flow Past An Accelerated Vertical Plate With Constant Temperature and Variable Mass Transfer I. J. Uwanta ,I. D. Yale	50-55
9.	Identification of Fault Location in Multiple Transmission Lines by Wavelet Transform Subba Reddy.B, D.Sreenivasulu Reddy,Dr.G.V.Marutheswar	56-65
10.	Data Storage in Secured Multi-Cloud Storage in Cloud Computing Archana Waghmare, Rahul Patil, Pramod Mane, Shruti Bhosale	66-69

Crahid: A New Technique for Web Crawling In Multimedia Web Sites

¹Dr. Ammar Falih Mahdi , ²Rana Khudhair Abbas Ahmed

¹Rafidain University college./Software Engineering Department

². Rafidain University College/ Computer Technical Engineering Department

ABSTRACT

With the quick growth and the huge amount of data that propagate in the web, we spend a lot of our time in finding the exact required information from the huge information retrieved from the web crawlers of search engines. Therefore, a special software is required to collect and find the exact required information and save our time and effort in finding what is good from the huge amount of retrieved data from the web. In our research, we proposed a software called "CRAHID" which uses a new technique to crawl (image, sound, text and video) depending on an information hiding technique for describing media. We supposed a new media format which describes media using hidden information to maintain time and effort for finding the exact information retrieved from the crawler.

KEYWORDS: Computer, Crawling, Information hiding, Multimedia, Search , Technique, Web.

I. INTRODUCTION

A crawler is a computer program which traverses a network and tries to capture the content of the documents within. In general the "crawled" network is the World Wide Web, and the documents are web pages. Due to the fact that the structure of the WWW is unknown, therefore crawlers implement different strategies to traverse it. These strategies calculate which links the crawler should follow and which not. This way the crawler only crawl a relative small subset of the whole network. Policies discussed later make sure that the relevant pages are contained within this crawled subset. Crawls the whole WWW is not possible due to its size and growth [1].

II. REQUIREMENTS FOR A CRAWLER [1]

- [1] **Flexibility:** The design of the crawler should make it possible to use the same parts in different scenarios. For example change the crawler application to implement a different strategy with keeping the crawler system the same.
- [2] **Robustness:** Due to that fact that the crawler downloads documents from a large variety of servers, it has to be able to deal with strange server behavior, badly formed HTML and other glitches that can occur on a network that is open to so many contributors. Also because a one iteration of the crawling can takes weeks, or is a continuous process the crawler should be able to handle crashes and network failures.
- [3] **Etiquette and Speed Control:** Following standard conventions like the robots.txt and robot specific meta-data is very important for any serious crawler.
- [4] **Manageability / Reconfigurability:** The administrator of a crawler should be able to change settings and add elements to a blacklist and monitor the crawler state and memory usage during the crawling process. It should also be possible make changes or adaption to the software after a crash or restart to fix bugs or make improvements based on knowledge gathered during the crawl.

III. WEB CRAWLER STRATEGIES

There are different strategies used in Web crawling, we explain some of these strategies in the section below:

3.1 Breadth First Search Algorithm:

This algorithm aims in the uniform search across the neighbor nodes. It starts at the root node and searches the all the neighbor nodes at the same level. If the objective is reached, then it is reported as success and the search is terminated. If it is not, it proceeds down to the next level weeping the search across the neighbor nodes at that level and so on until the objective is reached. When all the nodes are searched, but the objective is not met then it is reported as failure. Breadth first is well suited for situations where the objective is found on the shallower parts in a deeper tree. It will not perform so well when the branches are so many in a

game tree, especially like chess game and also when all the path leads to the same objective with the same length of the path.

3.2 Depth First Search Algorithm

This is the powerful technique that systematic traverse through the search by starting at the root node and traverse deeper through the child node. If there are more than one child, then priority is given to the left most child and traverse deep until no more child is available. It is backtracked to the next unvisited node and then continues in a similar manner. This algorithm makes sure that all the edges are visited once breadth. It is well suited for search problems, but when the branches are large then this algorithm takes might end up in an infinite loop.

IV. WEB CRAWLER ARCHITECTURE

Web crawlers are a central part of search engines, and details on their algorithms and architecture are kept as business secrets. When crawler designs are published, there is often an important lack of detail that prevents other from reproducing the work. There are also emerging concerns about “search engine spamming”, which prevent major search engines from publishing their ranking algorithms [3]. The typical high-level architecture of Web crawlers is shown in Figure (1).

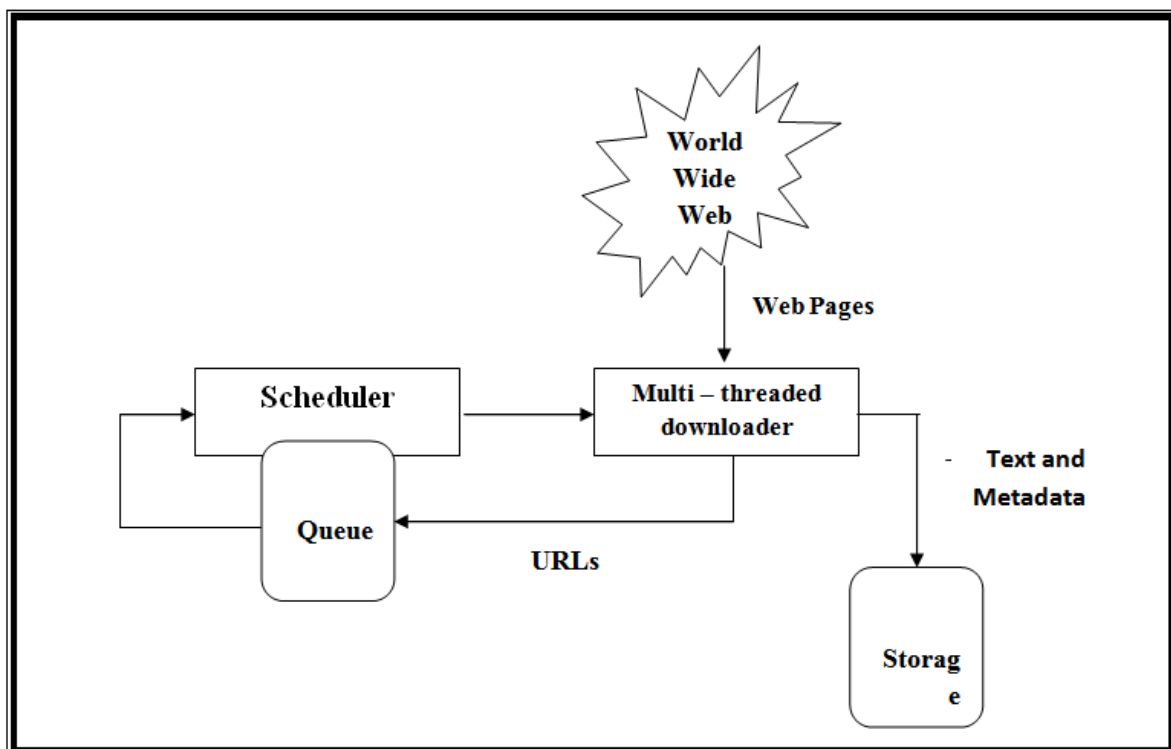


Figure (1): Typical high-level architecture of a Web crawler [4].

While it is fairly easy to build a slow crawler that downloads a few pages per second for a short period of time, building a high-performance system that can download hundreds of millions of pages over several weeks presents a number of challenges in system designed, I/O and network efficiency, and robustness and manageability [4]. Modern crawlers require a flexible robust and effective architecture to accomplish their task of crawling millions of web pages and download hundreds of gigabyte of data in a reasonable amount of time. Depending on the crawlers strategies the requirements may differ. A breadth-first crawler will need to store which URLs have already been crawled, whereas a link analysis crawler may need to store the graph of the crawled network. These requirements must reflect in the architecture of the individual crawler. But on the other hand there are some tasks every crawler will have to perform, allowing for a more general formulation of crawlers architecture [1]. The design of a crawler can be separated into two mayor components, the crawling application and the crawling system. The crawling application decides on what URLs to crawl and analyses the downloaded data supplied by the crawling system. The crawling system is responsible for the actual task of downloading data, taking care of crawler policies e.g. crawler.txt and other crawler relevant meta-data. The crawling application is responsible of implementing the crawling strategy.

With this basic concept the same crawling system can be used to implement a wide variety of crawling strategies by only changing the crawler application [1]. The crawler system seems very primitive, but when taking in account that thousands of pages have to be downloaded every second, this task becomes in fact very complex. In a real-world environment the crawler system will probably be distributed over many servers, and even geographical over different parts of the world to increase download speed. In many cases even the whole crawling application will be distributed over a many servers spread over different locations [1].

V. COMPONENTS OF A WEB CRAWLER

- a. **Multi-threaded Downloader**:-It downloads documents in parallel by various parallel running threads.
- b. **Scheduler**:-Selects the next URL to be downloaded.
- c. **URL Queue**:-A queue having all URL of page.
- d. **Site-ordering Module**:-It score the site based on various factors and order them based on the score.
- e. **New ordered queue**: - URL s sorted based on their score.
- f. **World Wide Web**: - Collection of interlinked documents.
- g. **Storage**:-to save the downloaded documents.

VI. INFORMATION HIDING IN MULTIMEDIA FILES

In General, there are techniques for hiding information in multimedia files, and usually this information is very important to be secret. With this technique we can retrieve the information from the files without changing the size of file before and after hiding the information in it. There are many algorithms for hiding information in multimedia files. One of these algorithms is LSB "Least significant Bit" algorithm which hides the information bits in LSB bits of bytes in a media file. Because of wasting time and effort in finding the exact information that satisfies the user's needs from the retrieved information of the search engine. It is necessary for the search engines to accommodate text description for all hypermedia files (text, sound, ..., etc.). In our proposed web crawler software called CRAHID, we supposed using a new format for saving media file which uses information hiding to describe the media file. This means, when we talk about sound file called "aa.mp3", to know what is the content, of this file, we need to extract the hidden information from it by using LSB algorithm. The extracted information is processed by the populated keywords in the search engine database.

VII. PROPOSED "CRAHID" SOFTWARE

In our research, we proposed a new web crawling software called CRAHID which uses a new technique to crawl not only HTML, Document, PDF and text file but also sound, image and video depending on an information hiding technique. The indexing operation in web site search engine needs text to extract keywords with their properties from the web page in order to help the searching operation, but what about image, sound and videos. Usually, crawling operation reads multimedia file name and some small information related to this file in order to help the indexing operation. But this information does not describe the multimedia file in details, therefore in our CRAHID crawling technique, the crawler reads hidden information in the multimedia file which describes the media in details. Then saves this information as a text for indexing to maintain time and effort to find the exact information retrieved from the web crawlers. Our CRAHID crawler software is described in the following sections.

7.1 Proposed CRAHID Crawling Flowchart

Our proposed CRAHID crawler software can be described using the following flowchart as shown in figure (2). From the flowchart, crawler reads input from URL list (queue) then if there is a URL, it starts processing by detecting the type of URL source file. This operation is done by using text processing for reading file extension and MIME type information from the page. By this information, the crawler decides the strategy of crawling this URL and saves extracted text information with this URL in a database for the indexing operation. In this case of an HTML file, the crawler extracts all hyperlink URLs and adds it to the queue of URL. Then removes all unwanted HTML tags and saves the raw text in the database with its URL. In the case of a PDF file, the crawler extracts all texts from the PDF file and saves it in the database with its URL. In the case of document file, the crawler reads and extracts the text from the file and saves it in the database. Also this procedure executes in the case of a text file. In the case of image file and the remaining types, the CRAHID reads the status byte in an image file (the byte, tells the CRAHID crawler about information hidden in the image or not). If there's information, the CRAHID crawler reads this information using (LSB) Least Significant Bit and saves the resulting text in a database with the URL. The information hidden in a multimedia file can be saved as (Arabic or English) language. By the way, multimedia file searching can be in Arabic, English or any other language.

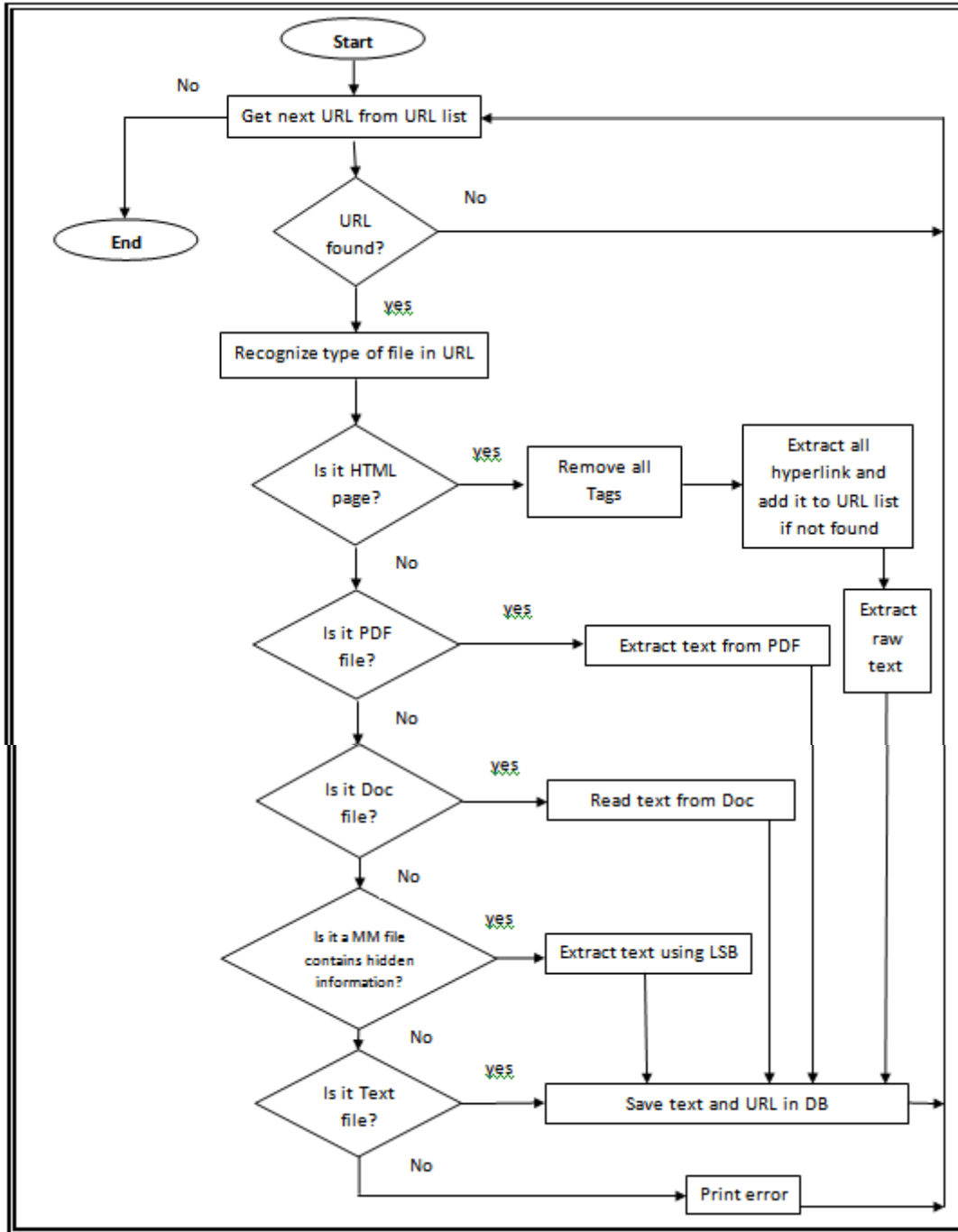


Figure (2): The CRAHID flowchart

7.2 The CRAHID Algorithm

In this section, we explain the algorithm used in our CRAHID software for crawling multimedia files using a proposed algorithm depending on information hiding technique LSB to extract information that describes the multimedia file. This algorithm is shown in figure (3) below.

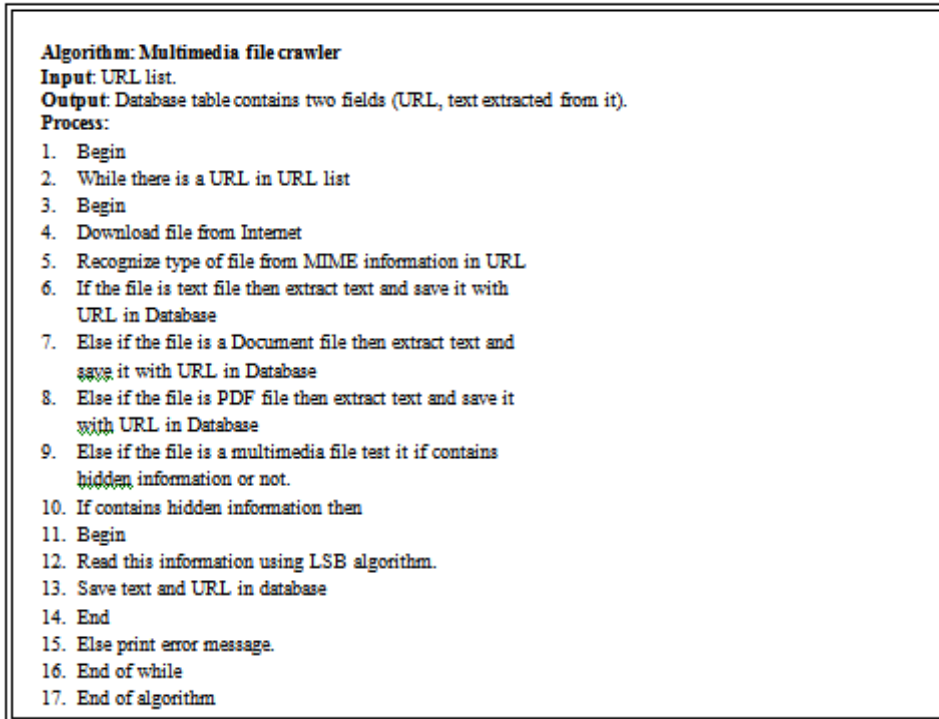
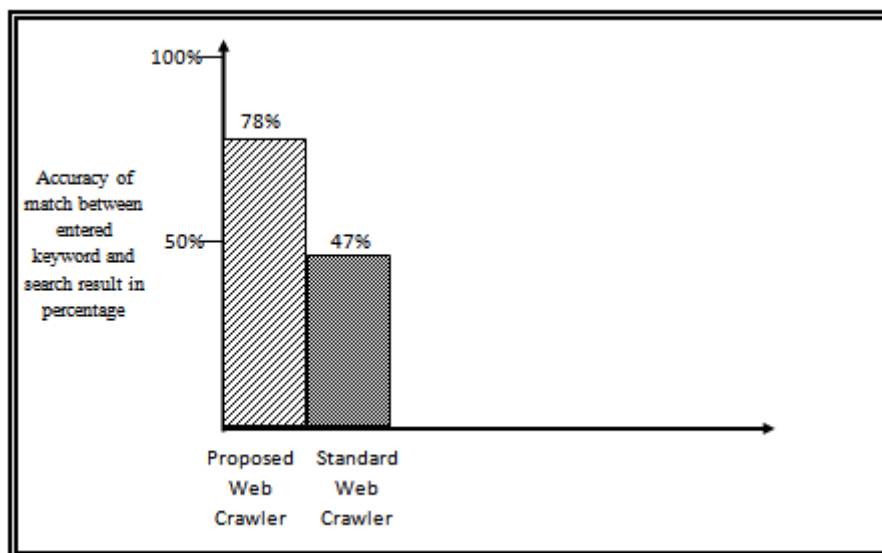


Figure (3): The CRAHID new crawling algorithm.

VIII. RESULTS

We tested our proposed CRAHID web crawler software in an Intranet with about 100 sample of URLs of web sites containing different types of files (HTML, Doc., PDF, Text and Multimedia). We got the following results. The results are shown in figures (4) and (5) below.



IX. CONCLUSIONS

From this paper, one can conclude the following:

- [1] The proposed Web crawler is the first crawler that crawls multimedia files depending on an information hiding technique.
- [2] The text hidden in a multimedia file is very useful to describe this file content. This means that the searching operation is to find the exact file when searching the hidden text information in it.
- [3] The process of extracting information is done separately from the searching operation. This job is executed in a scheduler way.

- [4] The information hidden in a multimedia file can be saved as (Arabic or English) language. By the way, multimedia file searching can be in Arabic, English or any other language.
- [5] This crawling technique is useful not only for the web site search engine, but also for any program that searches for local files in a PC computer.
- [6] We tested our CRAHID new crawler software in an intranet with a sample of 100 web sites containing different types of media. We found that it is more accurate than the normal crawler and we got an accurate crawling result (information) from the new crawling process.

FUTURE WORK

We suggest to use another information hiding technique to crawl the exact information from search engines and compare its results in maintaining time and effort with our CRAHID software.

REFERENCES

- [1] Christine Pichler, Thomas Holzmann, Benedict Wright, "Crawler Approaches and Technology", Information Search and Retrieval, WS 2011 LV-Nr.: 506.418, Group 02.
- [2] Pavalam S M, S V Kashmir Raja, Felix K Akorli and Jawahar M , "A Survey of Web Crawler Algorithms", IJCSI International Journal of Computer Science Issues, Vol. 8, Issue 6, No 1, November 2011 , ISSN (Online): 1694-0814 , www.ijcsi.org.
- [3] Carlos Castillo, " Effective Web Crawling", Submitted to the University of Chile in fulfillment of the thesis requirement to obtain the degree of Ph.D. in Computer Science , 2004.
- [4] Vladislav Shkapenyuk and Torsten Suel. "Design and implementation of a high-performance distributed web crawler", In Proceedings of the 18th International Conference on Data Engineering (ICDE), pages 357 – 368, San Jose, California, February 2002. IEEE CS Press.
- [5] Sandhya, M. Q. Rafiq, "Performance Evaluation of Web Crawler ", Proceedings published by International Journal of Computer applications (IJCA), International Conference on Emerging Technology Trends (ICETT) 2011.

ANALYSIS OF WAVELET AND CURVELET IMAGE DENOISING FOR DIFFERENT KINDS OF ADDITIVE NOISES

¹Miss Monika Shukla , ²Dr.Soni Changlani , ³Mr.Tejinder Singh Marwah

¹Dep.of Electronics & telecommunication Lakshmi Narain College of Technology & Science

ABSTRACT : This paper describes approximate digital implementations of two new mathematical transforms, namely; the wavelet transform and curvelet transform. Our implementation offers exact reconstruction, stability against perturbation, ease of implementation, low computational complexity and our main implementation is that, at a time we can use a different type of additive noise like additive Gaussian noise, speckle noise, poisson noise and salt & pepper noise etc. to get a different PSNR and MSE values. We can easily analyse our result or we can easily compare between wavelet and curvelet image denoising. A central tool is Fourier domain computation of an approximate digital Radon transform. The Radon transform in two dimensions is the integral transform consisting of the integral of a function over straight lines. In the experiments we reported here, simple thresholding of the curvelet coefficient is very competitive with “state of art” techniques based on wavelets, including threshold estimators for wavelet and curvelet transform also. Different threshold estimators are used for filtering the noisy images. Moreover, the curvelet reconstruction, offering visually sharper images and in particular, higher quality recovery of edges and of faint linear and curvilinear features. The empirical results reported here are in encouraging agreement.

KEYWORDS: Wavelet transform, Curvelet transform, Face recognition, Sparse representation, Feature extraction, Thresholding rules.

I. INTRODUCTION

Image denoising refers to the recovery of a digital image that has been contaminated by Additive White Gaussian Noise (AWGN). AWGN is a channel model in which the only impairment to communication is a linear addition of wideband or white noise with a constant spectral density (expressed as watts/ Hz of bandwidth) and a Gaussian distribution of amplitude. On a daily basis, hospitals are witnessing a large inflow of digital medical images and related clinical data. The main hindrance is that an image gets often corrupted by noise in its acquisition and transmission [1]. Image denoising is one of the classical problems in digital image processing, and has been studied for nearly half a century due to its important role as a pre – processing step in various electronic imaging applications. Its main aim is to recover the best estimate of the original image from its noisy versions [2]. Wavelet transform enables us to represent signals with a high degree of sparsity. This is the principle behind a non-linear wavelet based signal estimation technique known as wavelet denoising. In this paper we explore wavelet denoising of images using several thresholding techniques such as SURE SHRINK, VISU SHRINK and BAYES SHRINK. Further, we use a Gaussian based model to perform combined denoising and compression for natural images and compare the performance of wave transform methods [3].

In this paper, we also describe approximate of new mathematical transforms, namely as curvelet transform for image denoising [4] and wavelet transform for image denoising. Our implementations offer exact reconstruction, stability against perturbations, ease of implementations and low computational complexity. A central tool is Fourier domain computation of an approximate digital random transform. In a curvelet transform, we will use sparsity and its applications [5]. In the past, we have proposed a work on novel image denoising method which is based on DCT basis and sparse representation [6]. To achieve a good performance in these aspects, a denoising procedure should adopt to image discontinuities. Therefore, a comparative study on mammographic image denoising technique using wavelet, and curvelet transform [7]. Therefore, multi resolution analysis [8] is preferred to enhance the image originality. The transform domain denoising typically assumes that the true image can be well approximated by a linear combination of few basis elements. That is, the image is sparsely represented in the transform domain. Hence, by preserving the few high magnitude

transform coefficients that convey mostly the original image property and discarding the rest which are mainly due to noise, the original image can be effectively estimated [9]. The sparsity of the representation are critical for compression of images, estimation of images and its inverse problems. A sparse representation for images with geometrical structure depends on both the transform and the original image property.

In the recent years, there has been a fair amount of research on various denoising methods like wavelet, curvelet contourlet and various other multi resolution analysis tools. Expectation - Maximization (EM) algorithm introduced by Figueirodo and Robert [10] for image restoration based on penalized likelihood formulized in wavelet domain. State-of-art Gaussian Scale Mixture (GSM) algorithms employs modelling of images according to the activity within neighbourhoods of wavelet coefficients and attaching coefficients heavily in inactive regions [11]. Coif man and Donoho [12] pioneered in wavelet thresholding pointed out that wavelet algorithm exhibits visual artefacts'. Curvelet transform is a multi scale transform with strong directional character in which elements are highly anisotropic at fine Scales. The developing theory of curvelets predict that, in recovering images which are smooth away from edges, curvelets obtain smaller asymptotic mean square error of reconstruction than wavelet methods [13].The fundamental quality of curvelet transform is that it can easily converge for high frequency component due to which in curvelet transform we get a better performance as compare to wavelet transform.

MULTIRESOLUTION TECHNIQUES: An image can be represented at different scales by multi resolution analysis. It preserves an image according to certain levels of resolution or blurring in images and also improves the effectiveness of any diagnosis system [14].

A. WAVELET: Wavelet transform can achieve good scarcity for spatially localized details, such as edges and singularities. For typical natural images, most of the wavelet coefficients have very small magnitudes, except for a few large ones that represent high frequency features of the image such as edges. The DWT (Discrete wavelet transforms) is identical to a hierarchical sub band system. In DWT,the original image is transformed into four pieces which is normally labelled as A1,H1,V1 and D1 as the schematic depicted in fig.1.The A1 sub-band called the approximation, can be further decomposed into four sub-bands. The remaining bands are called detailed components. To obtain the next level of decomposition, sub-band A1 is further decomposed.

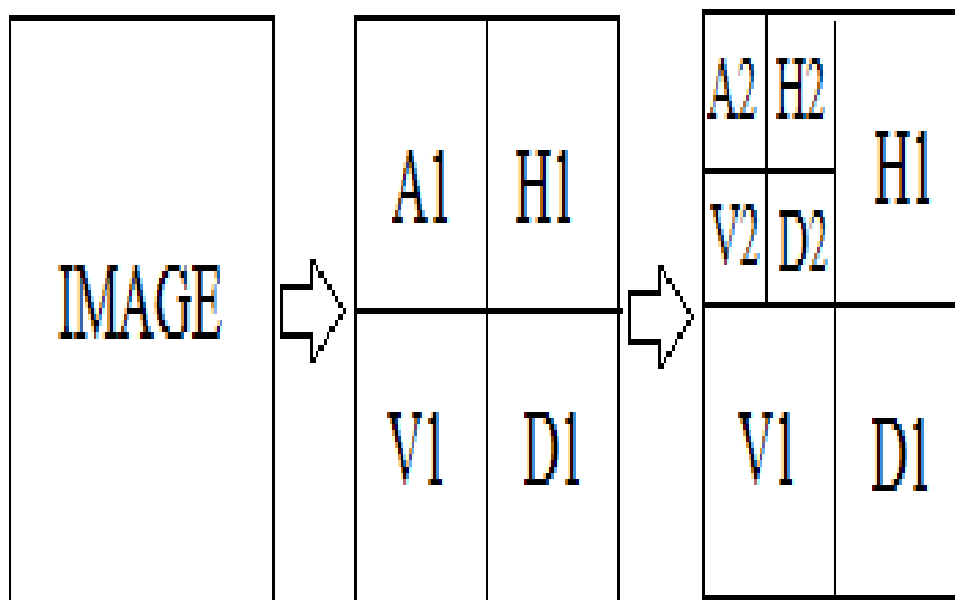


Figure 1. DWT based Wavelet decomposition to various levels

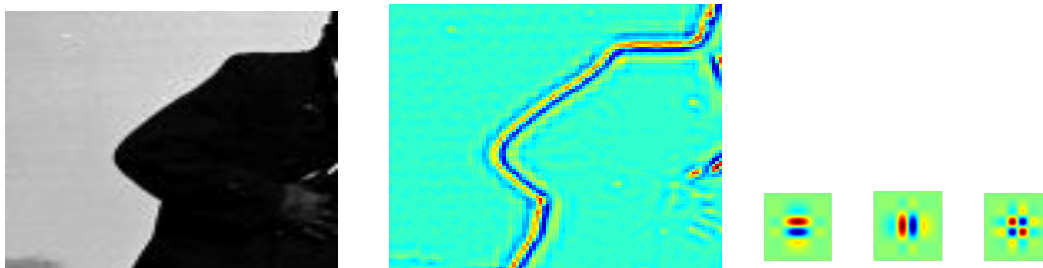
Many wavelet's are needed to represent an edge(number depends on the length of the edge,not the smoothness).In this,m-term approximation error would be occur.

$$(\|f-f_m\|_2)^2 \approx m^{-1}$$

ORIGINAL: 1% OF WAVELET COEFFS: 10% OF WAVELET COEFFS:



Wavelets and its Geometry: The basis function of wavelets is isotropic. They cannot “adapt” to geometrical structure. In this we need more refined scaling concepts.



B.CURVELET: Curvelets are a non-adaptive technique for multi-scale object representation. Being an extension of the wavelet concepts, they are becoming popular in similar fields, namely in image processing and scientific computing. Curvelet transform is a multi-scale geometric wavelet transforms, can represent edges and curves singularities much more efficiently than traditional wavelet. Curvelet combines multiscale analysis and geometrical ideas to achieve the optimal rate of convergence by simple thresholding. Multi-scale decomposition captures point discontinuities into linear structures. Curvelets in addition to a variable width have a variable length and so a variable anisotropy. The length and width of a curvelet at fine scale due to its directional characteristics is related by the parabolic scaling law:

$$\text{Width} \sim (\text{length})^2$$

Curvelets partition the frequency plan into dyadic coronaes that are sub partitioned into angular wedges displaying the parabolic aspect ratio as shown in fig.2. Curvelets at scale 2^{-k} , are of rapid decay away from a ‘ridge’ of length $2^{-k/2}$ and width 2^{-k} and this ridge is the effective support. The discrete translation of curvelet transform is achieved using wrapping algorithm[15]. The curvelet coefficients C_k for each scale and angle is defined in Fourier domain by

$$C_k(r, \theta) = 2^{-3k/4} R(2^{-k}r) A(2^{(k/2)}/2\pi, \theta)$$

Where C_k in this equation represents polar wedge supported by the radial(R) and angular (A) windows.

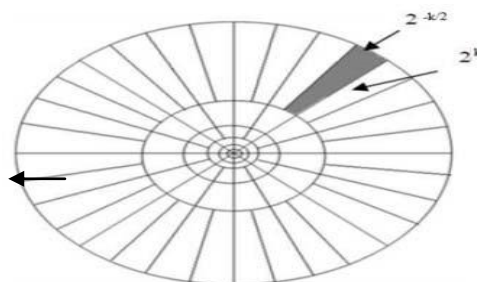


Figure 2. Curvelets in Frequency Domain

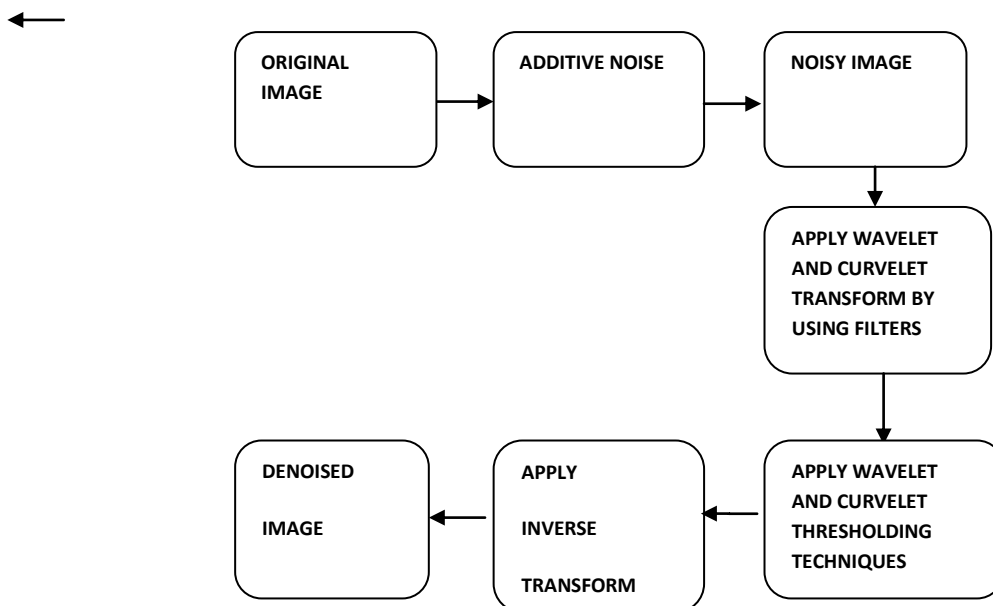
Digital Curvelet Transform can be implemented in two ways (FDCT via USFFT and FDCT via wrapping), which differ by spatial grid used to translate curvelets at each scale and angle.[16].

II. PROPOSED WORK

In this paper, we report initial efforts at image denoising based on a recently introduced family of transforms- Wavelet transform and Curvelet transform. In this paper, we compare the results from wavelet transform and curvelet transform and we will see which transform is better for the image denoising. Our main objective is to decrease a mean square error (MSE) and to increase a peak signal to noise ratio (PSNR) in db. by adding a white noise like Gaussian noise, Poisson noise and Speckle noise. During this configuration, we will use Threshold estimator like heursure, rigrsure, sqtwolog, and minimaxi. We can adjust decomposition level from 1 to 5 and we use Thresholding [17]. Thresholding is the simplest method of image segmentation. From a greyscale image, thresholding can be used to create binary images. Thresholding is a simple non-linear technique, which operates on one wavelet coefficient at a time. In its most basic form, each coefficient is threshold by comparing against threshold. If the coefficient is smaller than threshold, set to zero, otherwise it is kept or modified. On replacing the small noisy coefficients by zero and inverse wavelet transform. In both case (Soft thresholding and Hard thresholding) the coefficients that are below a certain threshold are set to zero. In hard thresholding, the remaining coefficients are left unchanged. In soft thresholding, the magnitudes of the coefficients above threshold are reduced by an amount equal to the value of the threshold. In both cases, each wavelet coefficient is multiplied by a given shrinkage factor, which is a function of the magnitude of the coefficient. In our thesis, we will use a curvelet transform as well as wavelet transform for removing a additive noise which is present in our images.

III. MATERIALS & METHODS

Image from MIAS database was denoised using wavelet and curvelet transforms. Various types of noise like the Random noise, Gaussian noise, Salt&Pepper and speckle noise were added to this image.



A. Algorithm

Denoising procedure followed here is performed by taking wavelet/curvelet transform of the noisy image (Random, Salt and Pepper, Poisson, Speckle and Gaussian noises) and then applying hard thresholding technique to eliminate noisy coefficients. The algorithm is as follows:

Step1: Computation of threshold

Step2: Apply wavelet/curvelet/contourlet transform to image

Step3: Apply computed thresholds on noisy image

Step4: Apply inverse transform on the noisy image to transform image from transform domain to spatial domain.

IV. EXPERIMENTAL RESULTS

The Experiment was done on several natural images like lena,Barbara,baboon,cameraman etc.using multiple denoising procedures for several noises. In our experiment, we have considered a image of A cricketer Mahendra Singh dhoni.In this image we have used a different additive noises like Gaussian noise, poisson noise, and speckle noise with different noise levels $\sigma=10,15,20,25,30,35$ etc. And before adding a noise,mean value is always be 0.

NOISES	NOISY IMAGES PSNR/db	WAVELET PSNR/db	CURVELET PSNR/db
Poisson	27.7344	28.0602	33.8397
Gaussian	24.9825	26.2889	32.4896
Speckle	30.2455	32.4944	38.8447
Salt & pepper	33.2355	34.7823	35.8442

TABLE.A: COMPARISON OF WAVELET AND CURVELET WITH DIFFERENT NOISE IN PSNR.



Fig.A: Graph indicating comparative results of the PSNR values of wavelet and curvelet based thresholding for image denoising

Table A. shows the comparison of wavelet and curvelet with different noises like poisson noise,Gaussian noise,speckle noise,and salt & pepper noise. and we measures the peak signal to noise ratio(in Db) and Fig.A shows a graph which indicates a comparative results of the PSNR values of wavelet and curvelet based thresholding(soft/hard) for image denoising and there is,we apply a different types of threshold estimators like rigrsure,heursure,sqtwolog,mini-maxi. And different decomposition levels like 1,2,3,4,5 & so on.

NOISES	NOISY IMAGES MSE	WAVELET MSE	CURVELET MSE
Poisson	109.5562	88.9571	26.8605
Gaussian	207.5685	152.8252	36.6541
Speckle	61.4507	25.7913	23.3111
Salt & Pepper	81.4220	22.5612	20.2213

TABLE.B: COMPARISON OF WAVELET AND CURVELET WITH DIFFERENT NOISE IN MSE.

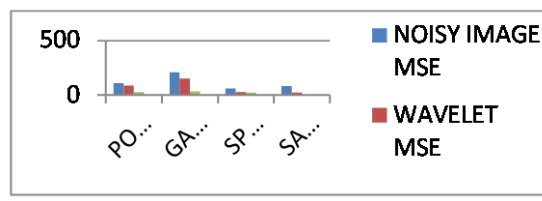
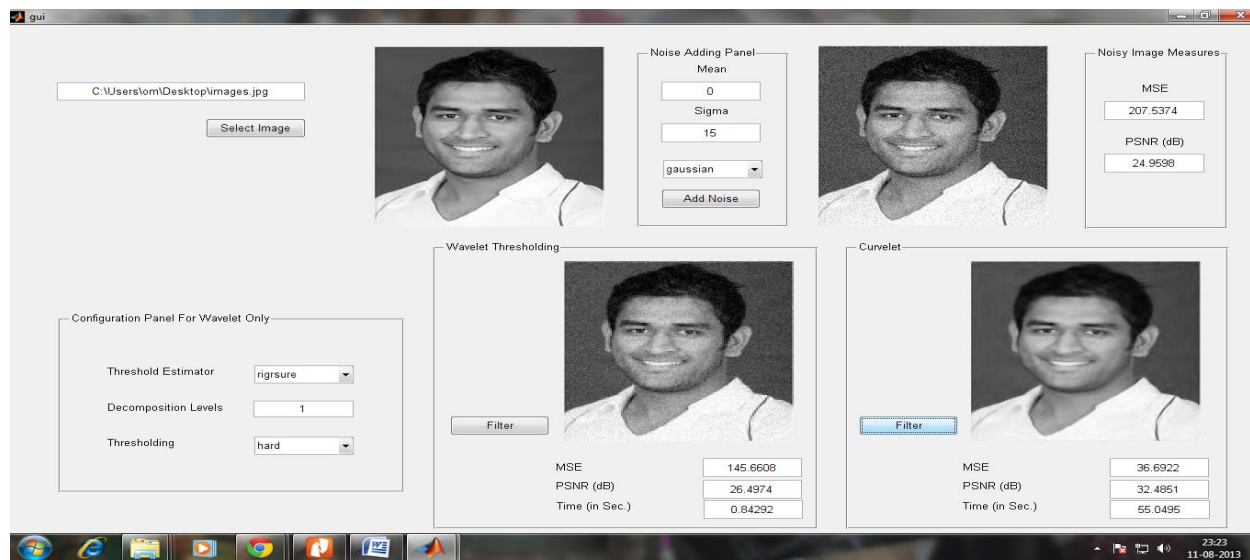


Fig.B: Graph indicating comparative results o the MSE values of wavelet and curvelet based thresholding for image denoising

Table B. shows the comparison of wavelet and curvelet with different noises like poisson noise, Gaussian noise, speckle noise, and salt & pepper noise and we measure the mean square error (MSE) and Fig. B shows a graph which indicates a comparative result of the MSE values of wavelet and curvelet based thresholding (soft/hard) for image denoising and there is, we apply different types of threshold estimators like rigsure, heursure, sqtwlog, mini-maxi. And different decomposition levels like 1, 2, 3, 4, 5 & so on.



V. CONCLUSION

The comparison of wavelet transform and curvelet transform technique is rather a new approach. The fundamental quantity of curvelet transform is that it can easily and fastly converged for high frequency components. It has a big advantages over the other techniques that it less distorts spectral characteristics of the image denoising. The experimental results show that the curvelet transform gives better results/performance than wavelet transform method. That's why the curvelet transform is more efficient or better technique for image denoising for different additive noises.

ACKNOWLEDGEMENT

The Author would like to thank The Rajiv Gandhi Pradyogiki Vishwavidyalaya, BHOPAL. For its generous support, and the Lakshmi Narain College Of Technology and Science, BHOPAL. For their hospitality, during my academic period 2011-2013. She wishes to thank Dr. Soni Changlani and Mr. Tejinder Singh for their help and encouragement.

REFERENCES

- [1] R.C. Gonzalez and R.E. Woods, digital image processing 2nd edition; Pearson Education.
- [2] D. Ghandurai and V. Sadasivam, "An effective adaptive thresholding technique for wavelet based image denoising." World Academy of Science, Engg. & Technology, 2008.
- [3] Raghuram Rangarajan, Ramji Venkataramanan, Siddharth Shah, Image denoising using wavelet; Dec 16, 2002.
- [4] Jean-luc Starck, Emmanuel J. Candès, and David L. Donoho; The curvelet transform for image denoising; IEEE Transactions on Image Processing, vol. 11, no. 6, June 2002.
- [5] Emmanuel Candès; California Institute of Technology.
- [6] Zhang Fen, Xiekai; College of Information & Mechanical Engineering; Beijing Institute of Graphic Communication, Beijing, China.
- [7] E. Malar, Akhandaswamy, S.S. Kirthana, D. Nivedhitha; Department of Bio Medical Engg. PSG College of Technology, Coimbatore, India.
- [8] J.L. Starck, M. Elad, and D. Donoho "Redundant Multiscale Transforms and their Application for Morphological Component Separation," Advances in Imaging and Electron Physics, Vol. 132, pp. 287-348, 2004.
- [9] H. Rabbani, "Image Denoising in Steerable Pyramid Domain Based on a Local Laplace Prior," Pattern Recognition, vol. 42, no. 9, September 2009, pp. 2181-2193.
- [10] M. Figueiredo and R. Nowak, "An EM Algorithm for Wavelet Based Image Restoration," IEEE Transactions on Image Processing, vol. 12, no. 8, pp. 906-916, August 2003.
- [11] J. Portilla, V. Strela, M.J. Wainwright and E.P. Simoncelli, "Image Denoising using Gaussian Scale Mixtures in the Wavelet Domain," IEEE Transactions on Image Processing.
- [12] R.R. Coifman and D.L. Donoho, "Translation-Invariant Denoising."
- [13] E. Candès and D. Donoho, "New Tight Frames of Curvelets and Optimal Representations of Objects with Piecewise Singularities."
- [14] S. Liu, C.F. Babbs and E.J. Delp, "Multiresolution Detection of Speculated Lesions in Digital Mammograms," IEEE Transactions on Image Processing.
- [15] E. Malar, A. Kandaswamy; PSG College of Technology, Coimbatore; India.
- [16] A. Patil & Jyoti Singhai, COE, Malegaon, Pune; India.
- [17] From Wikipedia. The Free Encyclopedia, Gonzalez, Rafael C. & Woods, Richard E. (2002). Thresholding in digital image processing, Pearson Edition.

A More Effective Realization Of BCD Adder By Using A New Reversible Logic BBCDC

Shefali Mamataj¹, Biswajit Das², Anurima Rahaman³

¹ Assistant Professor, Department of ECE Murshidabad College of Engineering & Technology, Berhampore,

² Assistant Professor, Department of CSE, Murshidabad College of Engineering & Technology, Berhampore

³ B.Tech Student, Department of AEIE, Future Institute of Engineering and Management, Sonarpur

Abstract:

Reversible logic is one of the emerging technologies having promising applications in quantum computing nanotechnology, and low power CMOS design. The main purposes of designing reversible logic are to decrease quantum cost, depth of the circuits and the number of garbage outputs. With the advent of quantum computer and reversible logic, design and implementation of all devices has received more attention. BCD digit adder is the basic unit of the more precise decimal computer arithmetic. This paper represents a new reversible logic BBCDC and also a more effective realization of BCD adder by using the proposed reversible logic. A comparative result is presented which shows that the proposed design is more effective in terms of number of gates and number of garbage outputs than the existing designs.

KEYWORDS: Reversible logic, Basic Reversible Gates, BCD adder, Reversible full adder, Constant input, Garbage, Quantum cost.

I. INTRODUCTION

In electronics hardware designing energy dissipation is one of the most important factor. Researchers like Landauer have shown that for irreversible logic computations, each bit of information lost, generates $kT \ln 2$ joules of heat energy, where k is Boltzmann's constant and T the absolute temperature at which computation is performed [1]. Bennett showed that $kT \ln 2$ energy dissipation would not occur, if a computation is carried out in a reversible way, since the amount of energy dissipated in a system bears a direct relationship to the number of bits erased during computation [2]. Reversible circuits are those circuits that do not lose information and reversible computation in a system can be performed only when the system comprises of reversible gates. These circuits can generate unique output vector from each input vector, and vice versa, that is, there is a one-to-one mapping between input and output vectors According to Moore's law the numbers of transistors will double every 18 months. Thus energy conservative devices are the need of the day. The amount of energy dissipated in a system bears a direct relationship to the number of bits erased during computation. Reversible circuits are those circuits that do not lose information A circuit will be reversible if input vector can be specifically retrieved from output vectors and here is one to one correspondence between input and output [3]. A reversible logic circuit should have the following features [5]:

- Use minimum number of reversible gates.
- Use minimum number of garbage outputs.
- Use minimum constant inputs.

Decimal arithmetic has found promising uses in the financial and commercial applications. This is due to the precise calculations required in these applications as oppose to binary arithmetic where some of decimal fractions can't be represented precisely [16]. In the hardware design, binary computing is preferred over decimal computing because of ease in building hardware based on binary number system. In spite of ease in building binary hardware, most of the fractional decimal numbers such as 0.110 cannot be exactly represented in binary, thus their approximate values are used for performing computations in binary hardware. Because the financial, commercial, and Internet-based applications cannot tolerate errors generated by conversion between decimal and binary formats, the decimal arithmetic is receiving significant attention and efforts are being accelerated to build dedicated hardware based on decimal arithmetic [4].

II. BASIC REVERSIBLE LOGIC GATE

2.1.Reversible logic Function:

It is an n-input n-output logic function in which there is a one-to-one correspondence between the inputs and the outputs. The reversible logic circuits must be constructed under two main constraints. They are

- Fan-out is not permitted.
- Loops or feedbacks are not permitted.

In the proposed design these two constraints along with the other parameters are optimized effectively . The important parameters which play a major role in the design of an optimized reversible logic circuit are [17-19] ,

Constants: This refers to the number of inputs that are to be maintained constant at either 0 or 1 in order to synthesize the given logical function.

Garbage: This refers to the number of outputs which are not used in the synthesis of a given function. These are very essential without which reversibility cannot be achieved.

Gate count: The number of reversible gates used to realize the function.

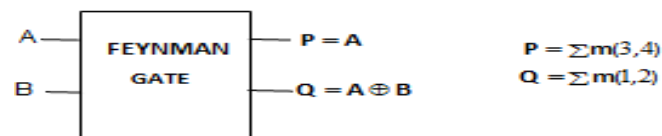
Flexibility: This refers to the universality of a reversible logic gate in realizing more functions.

Quantum cost: This refers to the cost of the circuit in terms of the cost of a primitive gate. It is calculated knowing the number of primitive reversible logic gates (1X1 or 2X2) required to realize the circuit.

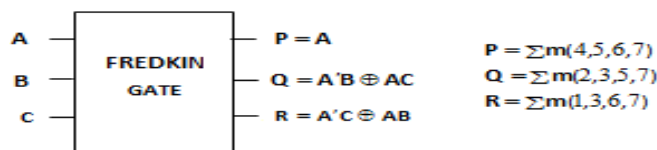
Gate levels: This refers to the number of levels in the circuit which are required to realize the given logic functions.

2.2. Basic Reversible logic Gates

The important basic reversible logic gates are, Feynman gate [6] which is the only 2X2 reversible gate which is as shown in the figure.(1a)and it is used most popularly by the designers for fan-out purposes. There is also a double Feynman gate [7], Fredkin gate [8] and Toffoli gate [9],New Gate[10] , Peres gate[11] , all of which can be used to realize important combinational functions and all are 3X3 reversible gates and are as shown in the figure.(1b) to figure.(1e) .The figures also shows the switching functions for terminals.



Figure(1a) Feynman gate – 2X2 gate



Figure(1b) Fredkin gate – 3X3 gate

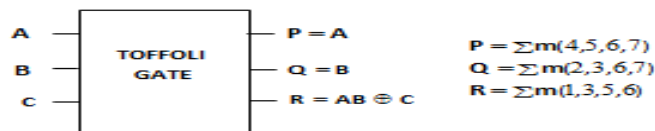


Figure.(1c) Toffoli gate – 3X 3 gate

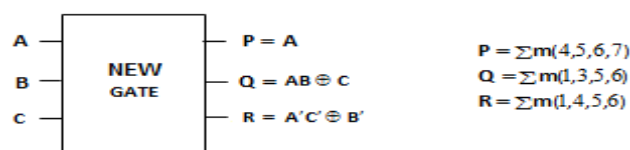
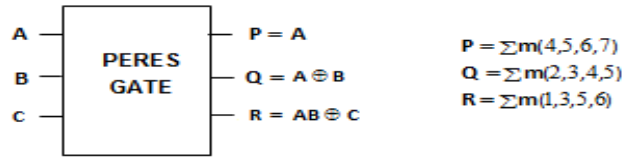
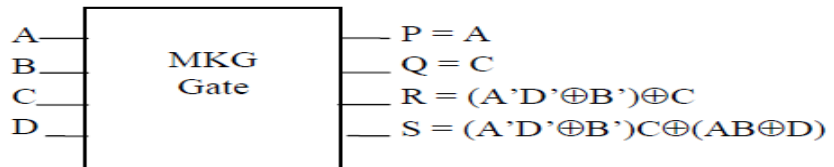


Figure.(1d) New gate – 3X 3 gate

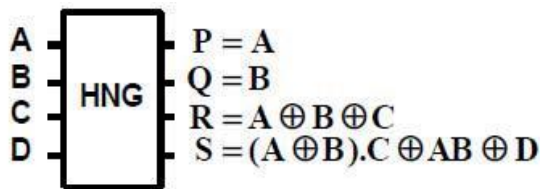


Figure(1e) Peres gate – 3X 3 gate

There are other 4X4 gates some of which are specially designed for the realization of important combinational circuit functions in addition to some basic functions. Some of the important 4X4 gates are, TSG gate [13],MKG gate [12],HNG gate [14]etc, shown in figure(2a,2b,2c) all of which are very useful for the construction of important reversible adders.



Figure(2a) Block diagram of MKG Gate



Figure(2b) Block diagram of HNG Gate diagram

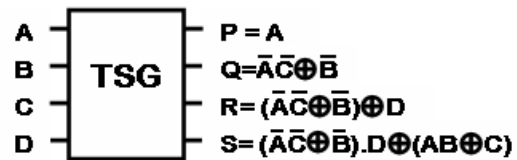
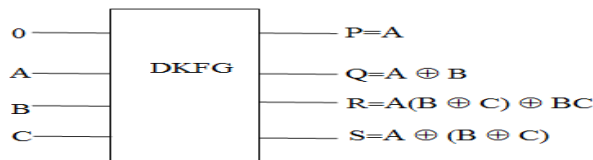


Figure (2c): TSG Gate Block

2.3.Reversible logic DKFG gate

A 4X4 reversible gate DKFG already had been proposed [20] shown in figure 2. In this gate the input vector is given by $I_V=(0,A,B,C)$ and the corresponding output vector is $O_V=(P,Q,R,S)$.



Figure(3a): DKFG reversible gate

We can use DKFG gate as a full-adder as shown in fig3b

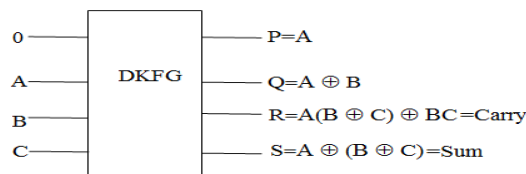


Figure (3b): DKFG gate implemented as Full adder

III. PROPOSED 5 X 5 REVERSIBLE GATE

A 5X5 reversible gate BBCDC (Binary to BCD conversion) logic has been proposed in this paper (See Figure 4) for BCD adder circuit application. The Truth table for the corresponding gate is shown in TABLE I . A closer look at the Truth Table reveals that the input pattern corresponding to a specific output pattern can be uniquely determined and thereby maintaining that there is a one-to-one correspondence between the input vector and the output vector. In this gate the input vector is given by $IV=(A,B,C,D,E)$ and the corresponding output vector is $OV=(P,Q,R,S,T)$

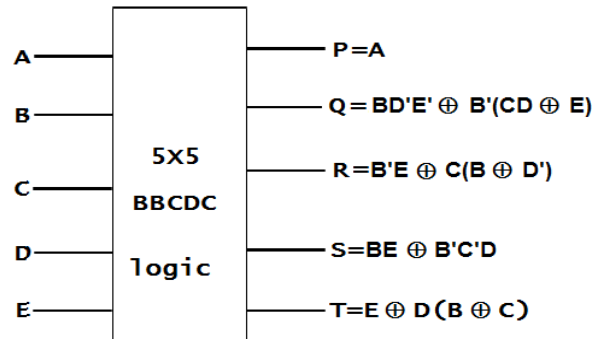


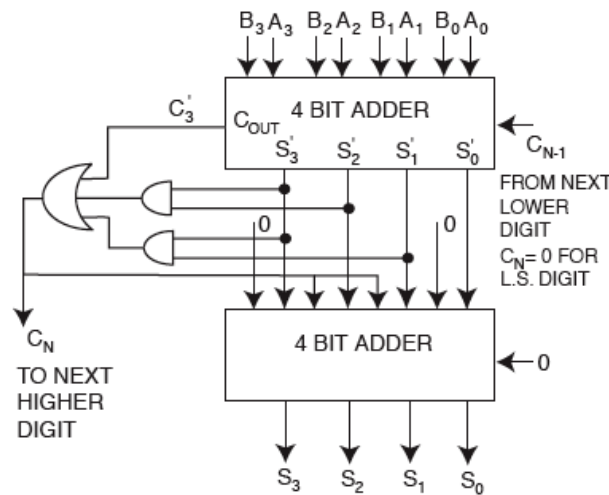
Figure 4: BBCDC reversible gate

TABLE I TRUTH TABLE OF BBCDC

INPUTS					OUTPUTS				
E	D	C	B	A	T	S	R	Q	P
0	0	0	0	0	0	0	0	0	0
0	0	0	0	1	0	0	0	0	1
0	0	0	1	0	0	0	0	1	0
0	0	0	1	1	0	0	0	1	1
0	0	1	0	0	0	0	1	0	0
0	0	1	0	1	0	0	1	0	1
0	0	1	1	0	0	0	1	1	0
0	0	1	1	1	0	0	1	1	1
0	1	0	0	0	0	1	0	0	0
0	1	0	0	1	0	1	0	0	1
0	1	0	1	0	1	0	0	0	0
0	1	0	1	1	1	0	0	0	1
0	1	1	0	0	1	0	0	1	0
0	1	1	0	1	1	0	0	1	1
0	1	1	1	0	1	0	1	0	0
0	1	1	1	1	1	0	1	0	1
1	0	0	0	0	1	0	1	1	0
1	0	0	0	1	1	0	1	1	1
1	0	0	1	0	1	1	0	0	0
1	0	0	1	1	1	1	0	0	1

IV. CONVENTIONAL BCD ADDER CIRCUIT

A Binary Coded Decimal (BCD) adder is a circuit which adds two 4-bit BCD numbers in parallel and produces a 4-bit BCD result. Fig. 5 shows the block diagram of conventional BCD adder. The circuit must include the correction logic to produce valid BCD output. Two 4-bit BCD numbers $A(A_3A_2A_1A_0)$ and $B(B_3B_2B_1B_0)$ along with carry input is added using conventional 4-bit parallel adder, 4-bit sum and a carry is taken out. If the carry output is set or if the result is greater than nine, binary 0110 is added to the intermediate sum output with the help of second stage 4-bit parallel adder circuit shown in figure 5. In a BCD adder, the correction logic which generates the C_{out} is given by, $C_{out} = S_3S_2 + S_3S_1 + C_4$



- ADD 0110 WHEN $C_N=1$
- ADD 0000 WHEN $C_N=0$

Figure 5: Conventional BCD adder circuit

V. PROPOSED BCD ADDER CIRCUIT

A BCD adder can be realized by using two parts, first part represents a four bit parallel adder and the second part gives us the appropriate addition result in the form of BCD number. The 4-bit parallel adder can be constructed using HNG gates or DKG gates or TSG gates or MKG gates. But we have designed the adder circuit by using DKFG reversible gate as a full adder. The proposed BCD adder circuit is shown in figure 6. Here two BCD numbers $A(A_3A_2A_1A_0)$ and $B(B_3B_2B_1B_0)$ are to be added and we got the result of the BCD addition as $S'_3 S'_2 S'_1 S'_0$ and final carry output K from the adder circuit. The minimum value of the one bit BCD addition is 0(0000) and the maximum value should be 19(10011).

The BCD sum cannot be greater than 19 because the range of a one bit BCD number is 0-9. Now if carry = 1, then the maximum BCD sum will be $9+9+1=19$. So in our proposed circuit we will get the maximum BCD sum (19) in binary form as $S'_3=0, S'_2=0, S'_1=1, S'_0=1$ and $K=1$. But this is not the correct BCD form. We will get the result in binary form (10011). So for getting the corrected form of BCD sum we have to convert this binary sum into BCD form by using appropriate logic. So for this we have used here a new BBCDC logic for this conversion. If we follow the truth table of BBCDC, we can see that we can get the appropriate BCD form 11001 instead of 10011. So here $S_3S_2S_1S_0$ is the corrected form of BCD sum and the minimum value is $C_{out}S_3S_2S_1S_0=00000$ and the maximum value will be $C_{out}S_3S_2S_1S_0=11001$ which is the appropriate form of BCD sum.

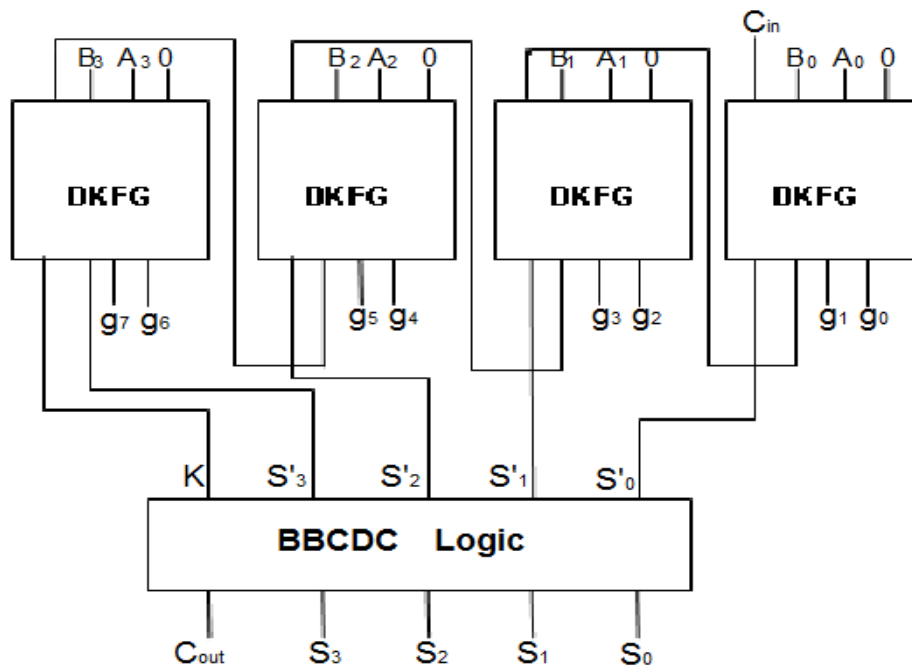


Figure 6: Proposed BCD adder circuit

TABLE III COMPARISON OF EXISTING BCD ADDERS AND PROPOSED BCD ADDER

Name of circuit	I. Different parameters		
	No. of Garbage output	No. of Constant input	No. of reversible gates
BCD adder[21]	22	17	23
BCD adder[22]	22	17	14
BCD adder[23]	22	11	11
BCD adder[24]	11	7	10
BCD adder[25]	10	6	8
BCD adder[26]	11	7	9
PROPOSED BCD adder	8	8	5

VI. CONCLUSION

We have realized BCD adder circuit by using DKFG and BBCDC reversible gates and made comparisons in TABLE II. The analysis of various implementations discussed is tabulated in TABLE II. It gives the comparisons of the different designs in terms of the important design parameters like number of reversible gates, number of garbage outputs, and number of constant inputs parameter. From the table it is observed that the present proposal uses least number of gates producing least number of garbage outputs. The efficient design of the BCD adder depends on the design methodology used for designing the reversible ripple carry adder and the reversible binary to BCD converter. Thus for future research, efficient design schemes for reversible ripple carry adder and the reversible binary to BCD converter is an interesting area to investigate. Alternate optimization methods are under investigation as a future work.

REFERENCES

- [1] R. Landauer, -Irreversibility and Heat Generation in the computational Process, IBM Journal of Research and Development, 5, pp. 183-191, 1961.
- [2] C.H. Bennett, Logical Reversibility of Computation, IBM J. Research and Development, pp. 525-532, November 1973.
- [3] Pradeep singla and Naveen kr. Malik " A Cost - Effective Design of Reversible programmable logic array" International Journal Of Computer Application , volume 41 – no. 15, march- 2012.
- [4] L. Wang, M. Erle, C. Tsen, E. M. Schwarz, and M. J. Schulte, "A survey of hardware designs for decimal arithmetic," IBM J. Research and Development, vol. 54, no. 2, pp. 8:1 – 8:15, 2010.
- [5] Perkowski, M. and P. Kerntopf, "Reversible Logic. Invited tutorial", Proc. EURO-MICRO, Sept 2001, Warsaw, Poland.
- [6] R. Feynman, "Quantum Mechanical Computers", Optical News, 1985, pp. 11-20.
- [7] B. Parhami; "Fault Tolerant Reversible Circuits" Proc. 40th Asilomar Conf. Signals, Systems, and Computers, Pacific Grove, CA, Oct. 2006.
- [8] E. Fredkin, T. Toffoli, "Conservative Logic", International Journal of Theor. Physics, 21, 1982, pp. 219-253.
- [9] T. Toffoli, "Reversible Computing", Tech memo MIT/LCS/TM-151, MIT Lab for Computer Science (1980).
- [10] Md. M. H Azad Khan, "Design of Full-adder With Reversible Gates", International Conference on Computer and Information Technology, Dhaka, Bangladesh, 2002, pp. 515-519.
- [11] Peres, A., 1985. Reversible logic and quantum computers, Physical Review: A, 32 (6): 3266-3276.
- [12] Haghparast, M. and K. Navi, 2007. A Novel Reversible Full Adder Circuit for Nanotechnology Based Systems. J. Applied Sci., 7 (24): 3995-4000.
- [13] Thapliyal H., S. Kotiyal, M. B. Srinivas, 2006. Novel BCD adders and their reversible logic implementation for IEEE 754r format. Proceedings of the 19th International Conference on VLSI Design, 3-7 Jan 2006.
- [14] Haghparast M. and K. Navi, 2008. A Novel reversible BCD adder for nanotechnology based systems. Am. J. Applied Sci., 5(3): 282-288.
- [15] "Optimal design of a reversible full adder" in International Journal of unconventional computing by Yvan Van Rentergen and Alexis De Vos.
- [16] Cowlishaw, M.F., 2003. Decimal Floating-Point: Algorithm for Computers. Proceedings of the 16th IEEE Symposium on Computer Arithmetic, pp: 104-111.
- [17] Kerntopf, P., M.A. Perkowski and M.H.A. Khan, 2004. On universality of general reversible multiple valued logic gates, IEEE proceeding of the 34th international symposium on multiple valued logic (ISMVL'04), pp: 68-73.
- [18] Perkowski, M., A. Al-Rabadi, P. Kerntopf, A. Buller, M. Chrzanowska -Jeske, A. Mishchenko, M. Azad Khan, A. Coppola, S. Yanushkevich, V. Shmerko and L. Jozwiak, 2001. "A general decomposition for reversible logic", Proc. RM'2001, Starkville, pp: 119-138.
- [19] Perkowski, M. and P. Kerntopf, 2001. Reversible Logic. Invited tutorial, Proc. EURO- MICRO, Sept 2001, Warsaw, Poland.
- [20] An Approach for Realization of 2's Complement Adder Subtractor Using DKG Reversible gate " Shefali Mamataj, Biswajit Das, Anurima Rahaman" International Journal of Emerging Technology and Advanced Engineering", Vol-3, Issue 12, December 2013.
- [21] Hafiz Md. Hasan Babu and A. R. Chowdhury, Design of a Reversible Binary Coded Decimal Adder by Using Reversible 4-bit Parallel adder", VLSI Design 2005, pp-255-260, Kolkata, India, January 2005.
- [22] M. Haghparast and K. Navi, 2008. A Novel reversible BCD adder for nanotechnology based systems. Am. J. Applied Sci., 5(3): 282-288.
- [23] Thapliyal H., S. Kotiyal, M. B. Srinivas, 2006. Novel BCD adders and their reversible logic implementation for IEEE 754r format. Proceedings of the 19th International Conference on VLSI Design, 7 Jan 2006 .
- [24] K. Biswas, et al., "Efficient approaches for designing reversible Binary Coded Decimal adders" Microelectron, J(2008) doi 10.10.16/j.mejo.2008.04.003
- [25] H R Bhagyalakshmi, M K Venkatesh "Optimized reversible BCD adder using new reversible logic gates" journal of computing Vol- 2, Issue- 2, February 2010.
- [26] James.R.K; Shahana, T.K.; Jacob, K.P.; Sasi, S. "A New Look at Reversible Logic Implementation of Decimal Adder", System on-Chip, 2007, The International Symposium on System-on-Chip Tampere, Finland Nov 20-22, 2007 Year 2007.

Effect of Chemical Reaction on Mass Transfer over a Stretching Surface Embedded In a Porous Medium

¹E. M. A. Elbashbeshy , ² A. M. Sedki

¹,Mathematics Department, Faculty of science, Ain Shams University, Abbassia, Cairo, Egypt, ²Mathematics Department, Faculty of science Jazan University, Jazan, KSA

ABSTRACT

An analysis is made to investigate the mass transfer over a stretching surface embedded in a porous medium in the presence of first order chemical reaction. Using similarity transformation, the governing partial differential equations are transformed into a set of ordinary differential equations which solved by shooting method. Comparisons with previously published work on special cases of the problem are performed and the results are found to be in excellent agreement. It is observed that the local mass transfer and concentration profile are very sensitive to change in the values of reaction rate parameter, permeability parameter and Schmidt number.

KEYWORDS: Mass transfer – Stretching surface – Porous medium- Chemical reaction.

I. INTRODUCTION

The boundary layer flows due to stretching surface in porous medium are relevant to many engineering problems such as paper production, preparing plastic and metal sheets etc. The dynamics of the boundary layer flow over a stretching surface originated from the pioneering work of Sakiadis [1, 2] who initiated the study of boundary layer flow over a continuous solid surface moving with constant speed. Crane [3] extended it to analyze the steady two dimensional boundary layer flow caused by the stretching of elastic flat surface which moves in its plane with velocity varying linearly with distance from a fixed point. Many authors presented some mathematical results, and good amount of references can be found in the papers by Ali [4] and [5], Elbashbeshy [6], Ishak et al. [7] and Elbashbeshy and Bazid [8]. The studies carried out in these papers in the case steady state flow. The unsteady state problem over a stretching surface, which is stretched with a velocity that depends on time is considered by Anderson et al. [9], Elbashbeshy and Bazid [10] and Ishak et al. [11]. The effects of chemically reactive solute distribution on fluid flow due to a stretching surface also bear equal importance in engineering researches. The chemical reaction effects were studied by many researchers on several physical aspects. The diffusion of a chemically reactive species in a laminar boundary layer flow over a flat plate was demonstrated by Chambre and Young [12]. The effect of transfer of chemically reactive species in the laminar flow over a stretching sheet explained by Andersson et al. [13]. Takhar et al. [14] analyzed the flow and mass transfer on a stretching sheet with a magnetic field and chemically reactive species with n-th order reaction.

The mass transfer in boundary layer flow due to a stretching surface in porous medium also has important applications in many industrial problems. The effect of mass transfer in laminar flow over a stretching surface was investigated by Radwan and Elbashbeshy [15]. Radwan and Elbashbeshy [15] analyzed the flow and mass transfer on a stretching surface with a magnetic field. Akyildiz et al. [16] reported a solution for diffusion of chemically reactive species in a flow of a non-Newtonian fluid over a stretching sheet immersed in a porous medium. El-Aziz [17] explained unsteady flow due to a stretching sheet with mass and heat transfer. Recently, Krishnendu [18] studied the boundary layer flow with first order chemical reaction over a porous flat plate. Krishnendu [19] studied the mass transfer on a continuous flat plate moving in a parallel or reversely to a free stream in the presence of a chemical reaction. Ferdows et al. [20] investigated the effects of order of chemical reaction on mass transfer over a linearly stretching surface. Based on the above-mentioned investigations and applications, this paper is concerned with two-dimensional steady, incompressible, laminar boundary layer flow of a fluid over a linearly stretching surface.

In this paper we investigate numerically the effects of chemical reaction on the steady laminar two-dimensional boundary layer flow and mass transfer over a stretching surface embedded in porous medium. The method of solutions based on the well-known similarity analysis together with shooting method.

II. Formulation of the problem

Consider two dimensional steady, laminar boundary layer flow of a fluid over a linearly stretching surface (i.e. stretched with a velocity proportional to x) embedded in porous medium with velocity u_w and concentration C_w moving axially through a stationary fluid. The fluid is viscous incompressible with constant physical properties. We assume that the fluid far away from the surface is at rest and at concentration C_∞ . The x – axis runs along the continuous surface in the direction of motion and y – axis is perpendicular to it. The continuity, momentum and reactive concentration equations for governing the flow and concentration distribution in the boundary layer region along the stretching surface may be written as

$$\frac{\partial u}{\partial x} + \frac{\partial v}{\partial y} = 0 \quad (1)$$

$$u \frac{\partial u}{\partial x} + v \frac{\partial u}{\partial y} = \nu \frac{\partial^2 u}{\partial y^2} - \frac{\nu}{k} u \quad (2)$$

$$u \frac{\partial C}{\partial x} + v \frac{\partial C}{\partial y} = D \frac{\partial^2 C}{\partial y^2} - R(C - C_\infty) \quad (3)$$

The boundary conditions are given by

$$y = 0 : u = \lambda x, v = 0, C = C_\infty + Ax^n \quad (4)$$

$$y \rightarrow \infty : u = 0, C = C_\infty$$

where u and v are the velocity components in the x and y directions, respectively, k is the permeability of porous medium. C is the concentration of the fluid, ν is the kinematic viscosity, R is a constant of first-order chemical reaction rate, n is a power-law exponent, which signifies the change of amount of solute in the x -direction, D is the effective diffusion coefficients and A and λ are constants. The equation of continuity is satisfied if we choose a dimensionless stream function $\psi(x, y)$ such that

$$u = \frac{\partial \psi}{\partial y}, \quad v = -\frac{\partial \psi}{\partial x}.$$

In order to solve Equations (1)-(4), we introduce the following similarity transformation and dimensionless concentration.

$$\eta = y \sqrt{\frac{n}{\nu}}, \quad f(\eta) = \frac{\psi(x, y)}{x \sqrt{n \nu}}, \quad \theta(\eta) = \frac{C - C_\infty}{C_w - C_\infty}$$

where η is the similarity variable, $\psi(x, y)$ is the dimensionless stream function, $\theta(\eta)$ is the dimensionless concentration. Consequently, equations (2)-(3) and the boundary conditions (4) can be written in the following form

$$f''' + ff'' - f'^2 - Kf' = 0 \quad (5)$$

$$\theta'' + Sc(f\theta' - n f' \theta) - ScR_c \theta = 0 \quad (6)$$

$$\eta = 0 : f = 0, f' = 1, \theta = 1 \quad (7)$$

$$\eta \rightarrow \infty : f' = 0, \theta = 0$$

Where prime denotes differentiation with respect to η . $K = \frac{v}{nk}$ is a permeability parameter, $R_c = \frac{R}{n}$ is a reaction rate parameter of the solute and $Sc = \frac{v}{D}$ is Schmidt parameter.

The mass transfer coefficient in terms of the Sherwood number Sh is given by

$$Sh = -\frac{x\left(\frac{\partial C}{\partial y}\right)}{C_w - C_\infty} = -x\sqrt{\frac{n}{v}}\theta'(0)$$

$$\frac{Sh}{\sqrt{R_e}} = -\theta'(0)$$

where $R_e = \frac{u_w x}{v}$ is the local Reynolds number.

III. Numerical method

The above Eqs. (5) and (6) along with boundary conditions (7) are solved by converting them to an initial value problem. We set

$$f' = z, \quad z' = p, \quad \theta' = q$$

$$p' = Kz + z^2 - fp \tag{8}$$

$$q' = Sc [R\theta + nz\theta - fq] \tag{9}$$

with the boundary conditions

$$f(0) = 0, \quad f'(0) = 1, \quad \theta(0) = 1 \tag{10}$$

In order to integrate (8) and (9) as an initial value problem we require a value for $p(0)$ i.e. $f''(0)$ and $\theta'(0)$ but no such values are given in the boundary. The most important factor of shooting method is to choose the appropriate finite values of η_∞ . In order to determine η_∞ for the boundary value problem stated by Eqs. (8)– (9), we start with some initial guess value for some particular set of physical parameters to obtain $f''(0)$ and $\theta'(0)$. The solution procedure is repeated with another large value of η_∞ until two successive values of $f''(0)$ and $\theta'(0)$ differ only by the specified significant digit. The last value of η_∞ is finally chosen to be the most appropriate value of the limit η_∞ for that particular set of parameters. The value of η_∞ may change for another set of physical parameters. Once the finite value of η_∞ is determined then the integration is carried out. We compare the calculated values for f' and θ at $\eta = 10$ (say) with the given boundary conditions $f'(10) = 0$ and $\theta(10) = 0$ and adjust the estimated values, $f''(0)$ and $\theta'(0)$, to give a better approximation for the solution. We take the series of values for $f''(0)$ and $\theta'(0)$, and apply the fourth order classical Runge–Kutta method with step-size $h = 0.01$. The above procedure is repeated until we get the results up to the desired degree of accuracy, 10^{-5} .

IV. RESULTS AND DISCUSSION

The set of non-linear ordinary differential equations (5) and (6) satisfying the boundary conditions (7) have been solved numerically using the Mathematica method for several values of the involved parameters, namely permeability parameter, power-law exponent, reaction rate parameter of the solute and Schmidt parameter. In case $n=0$ and $K = 0$ our results are very similar to those considered by Uddin et al. [21], Takhar et al. [14] and Andersson et al. [13]. To validate the numerical method used in this study, the case $n=0$ and $K = 0$, was considered and the results for concentration gradient are compared with the numerical solution which reported in Uddin et al. [21], Takhar et al. [14] and Andersson et al. [13]. The quantitative comparison is shown in Table 1, and found to be in excellent agreement.

Table1 Comparison of the values of $-\theta'(0)$ with that of Takhar et al. [14], Andersson et al. [13] and Uddin et al. [21] for $n=0$ and $K = 0$.

Sc	R_c	Present Study	Takhar et al. [14]	Andersson et al. [13]	Uddin et al.[21]
0.1	0.1	0.149083	0.15042	0.14900	0.15057
1	0.1	0.668754	0.67044	0.66900	0.66873
1	1	1.176401	1.17761	1.17700	1.17679
10	1	3.871327	3.87469	3.88000	3.87347
10	10	10.241185	10.24283	10.25000	10.24535

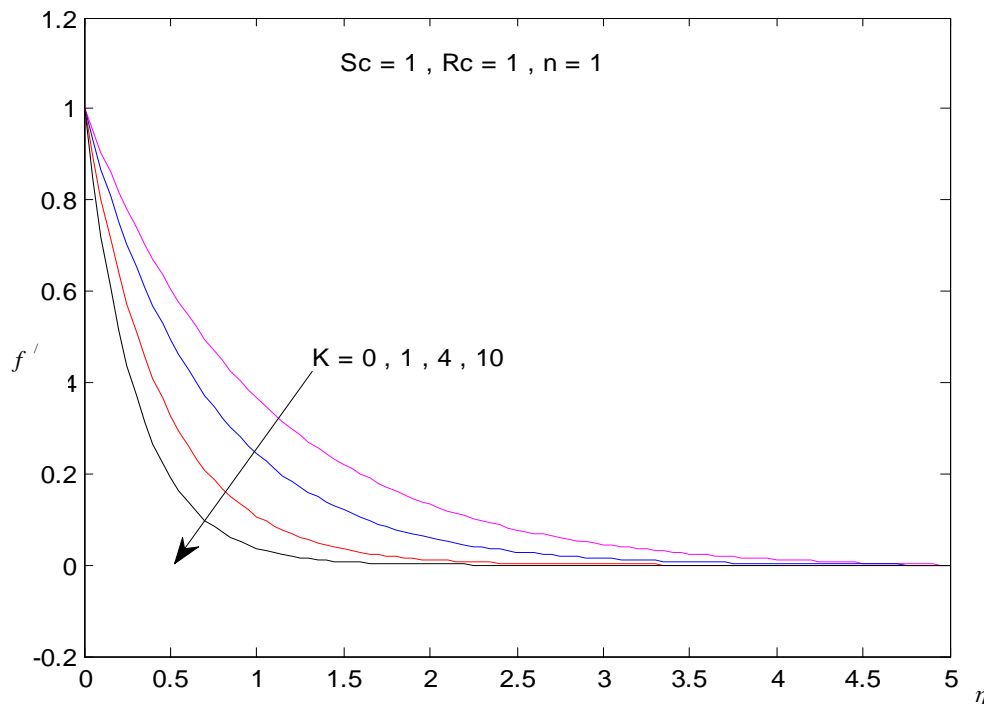


Fig. 1: Velocity profiles $f'(\eta)$ for various values of K

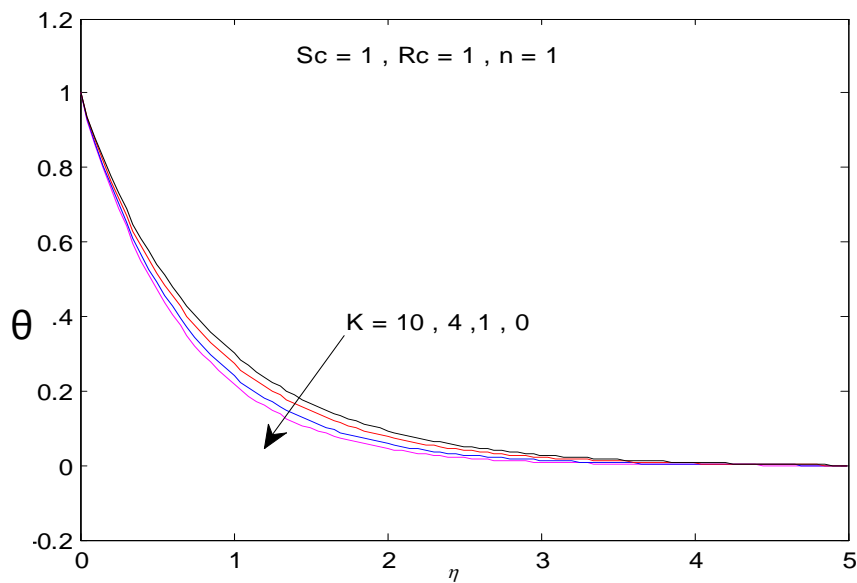


Fig.2: Concentration profiles $\theta(\eta)$ for various values of K

The numerical solution of velocity has presented for various values of the permeability parameter K . The reactant solute equation is solved numerically and the results are shown graphically. The velocity profiles for various values of the permeability parameter K have been plotted in Fig. 1. From the figure it is noted that with increase of K , the velocity for any fixed value of η decreases.

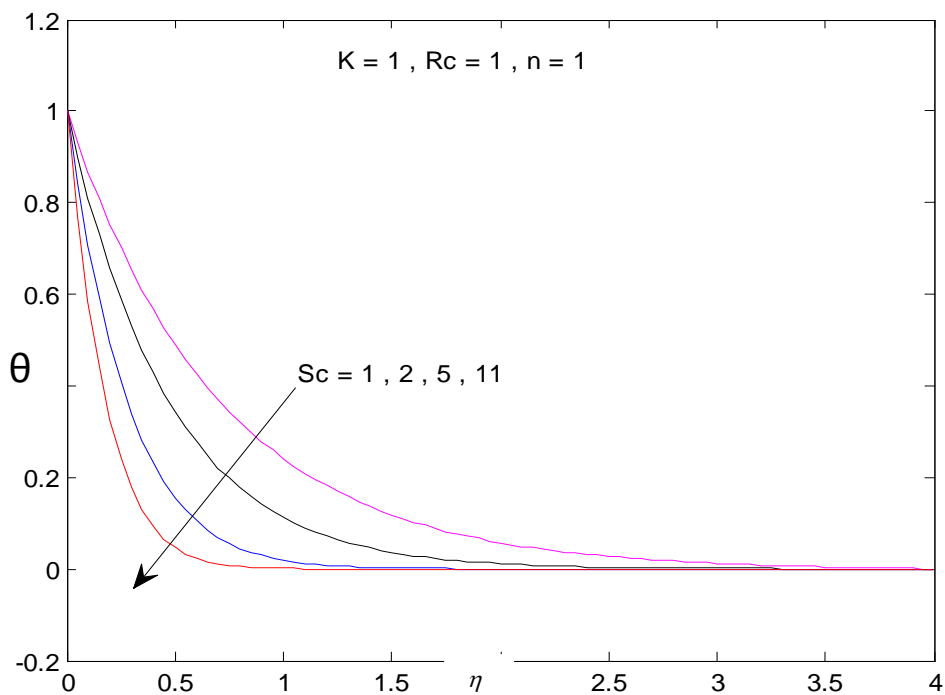


Fig. 3. Concentration profiles $\theta(\eta)$ for various values of Sc

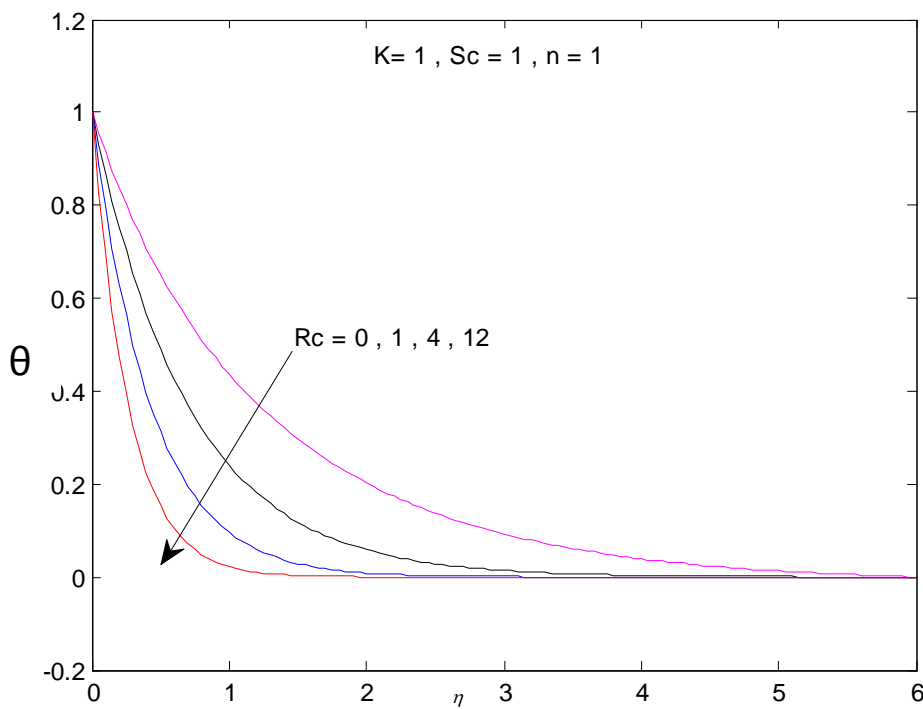


Fig4. Concentration profiles $\theta(\eta)$ for various values of R_c

Thus it is clear that the permeability parameter K opposes motion. Consequently, the momentum boundary layer thickness reduces with the increase K in and this fact is also seen from wall shear stress behaviour. Exhibits concentration profiles for various values of K . The value of contaminate solute at particular value of η increases with the increase of the permeability parameter K and also the concentration boundary layer thickness increases. This implies that the permeability parameter acts to enhance the distribution of the reaction solute on the stretching surface. This result may be useful, in the situation where the enhancement of solute transfer from the surface is the prime important.

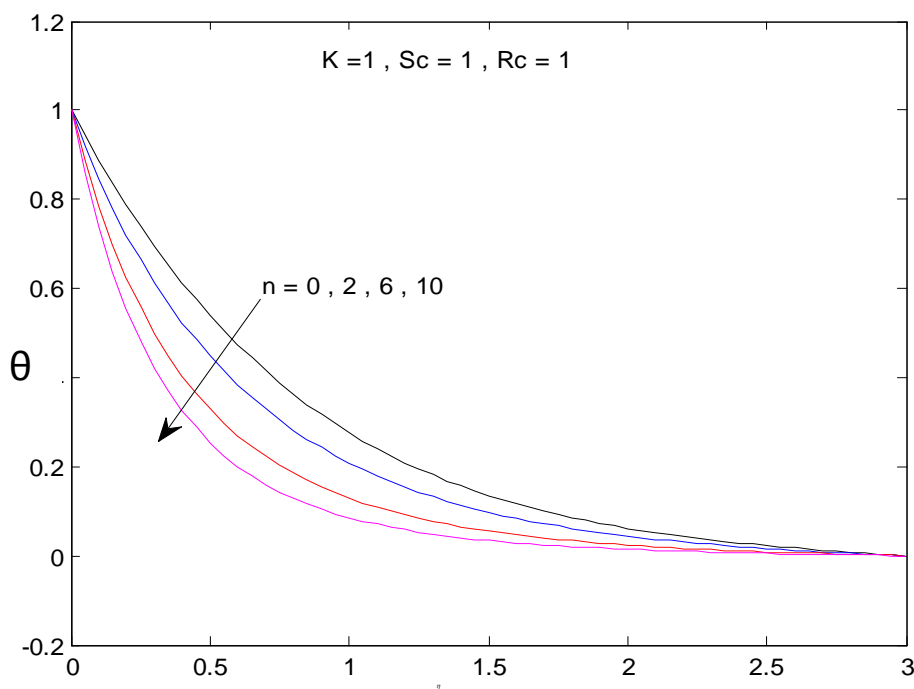


Fig. 5. Concentration profiles $\theta(\eta)$ for various values of $n(\geq 0)$. with $K=Sc=R_c = 1$

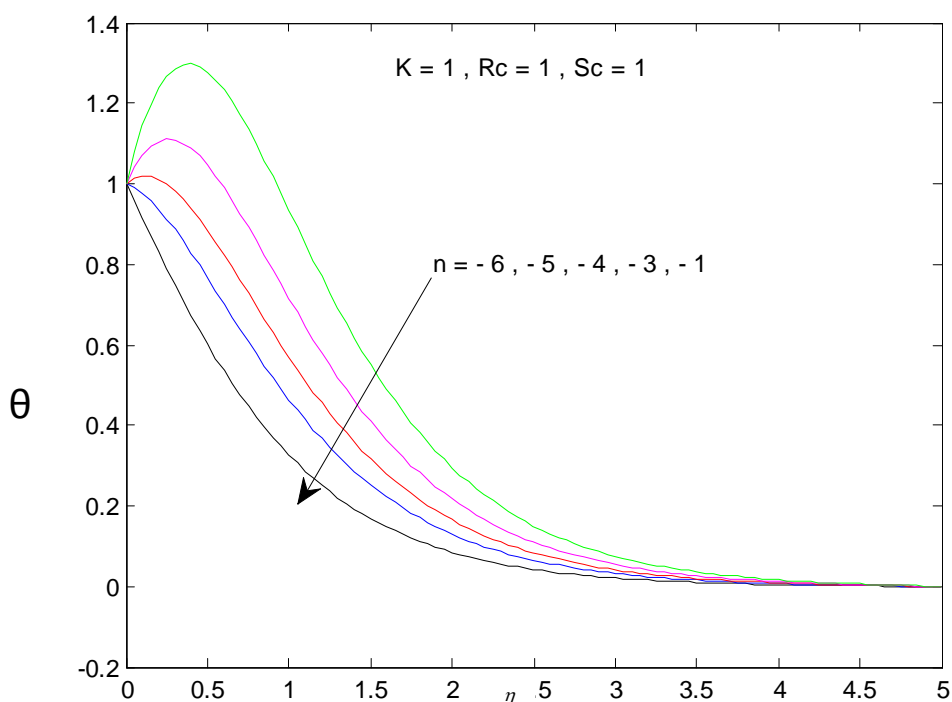


Fig. 6. Concentration profiles $\theta(\eta)$ for various values of $n(<0)$. with $K=Sc=R_c=1$

Now, we concentrate on variation the solute curves for different values of Schmidt number Sc . The curves are drawn in the Fig. 3. The Schmidt number has major effects on the distribution of solute. The concentration boundary layer thickness as well as the concentration at a fixed point decreases quickly with increasing values of Sc . This is due to the fact that the rate of solute transfer from the surface increases when the Schmidt number increases. Figure 4 is the graphical representation of concentration profiles for various values of reaction rate parameter R_c . It has been found that the reaction rate parameter affect the solute profiles in similar way as that of the Schmidt number i.e., the increase of R_c reduces both the solute boundary layer thickness and value of the solute at fixed η . So, in case of the distribution of reactive solute, the reaction rate parameter is a decelerating agent.

Finally, Figs. 5 and 6 exhibit the concentration profiles in the boundary layer flow region for different values of power-law exponent n . It is noticed from Fig. 5 that for the increasing values of n with $n>0$, the curve representing the distribution of solute for specific value of η decreases. While, in Fig. 6 the concentration profile increases with increase in the magnitude of n with $n<0$ and for large negative values of n , the overshoot of solute is observed near the surface. Thus, the effect of increase of n when the surface concentration is $C_w = C_\infty + Ax^n$ is completely opposite to the effect of increase n when the surface concentration is $C_w = C_\infty + A/x^n$ where A is constant positive. Note that, the wall concentration is constant when $n=0$.

Table 2

Values of skin-friction coefficient $f''(0)$ and $-\theta'(0)$ for various values of permeability parameter K .

K	$f''(0)$	$-\theta'(0)$
0	-1.00000	1.45942
1	-1.414214	1.414214
4	-2.236068	1.3433
10	-3.316625	1.2781

Table 3: Values of $-\theta'(0)$ for various values of Schmidt number Sc

Sc	$-\theta'(0)$
1	1.414214
2	2.063933
5	3.366092
11	5.085476

Table 4: Values of $-\theta'(0)$ for various values of reaction rate parameter R_c

R_c	$-\theta'(0)$
0	0.892503
1	1.414214
4	2.2692285
12	3.641534

Table 5: Values of $-\theta'(0)$ for various values of n

n	$-\theta'(0)$
0	1.154956
2	1.649948
6	2.434269
10	3.061963

Tables 2-5 summarize the calculated values of local skin friction coefficient $f''(0)$ and rate of mass transfer $-\theta'(0)$ for $1 \leq Sc \leq 11$, $0 \leq n \leq 10$ and $0 \leq R_c \leq 12$. These tables indicate that $-\theta'(0)$ increasing as permeability parameter K increases. Since K does not occur explicitly in the diffusion equation, its effect on mass transfer $-\theta'(0)$ is small. Also, these tables indicate that $-\theta'(0)$ increasing as n , R_c and Sc increases.

V. CONCLUSIONS

In this investigation, an analysis is made to find the behaviour of the distribution of reactive solute undergo a first order reaction in steady boundary layer flow incompressible fluid over a stretching surface embedded in porous medium with variable surface concentration. Using the similarity transformation a set of ordinary differential equations is obtained from the governing equations. The momentum equation and the equation of reactive solute are solved numerically. The results show that the permeability parameter tends to reduce the rate of flow from the wall and is broadening the solute layer. The Schmidt number and the reaction rate parameter reduce the solute boundary layer thickness. Most, importantly, the effects of initial variable solute distribution over a stretching surface is interesting i.e. for the increase in magnitude of n , the concentration decreases when $n > 0$ whereas increases when $n < 0$.

VI. REFERENCES

- [1] Sakiadis B.C., Boundary layer behavior on continuous solid surfaces: I. Boundary layer equations for two dimensional and axisymmetric flow, *AIChE J*, 7(1), 26-28, 1961.
- [2] Sakiadis B.C., Boundary layer behavior on continuous solid surfaces: II. Boundary layer equations on a continuous flat surface, *AIChE J*, 7(1), 221-225, 1961.
- [3] Crane L.J., Flow past a stretching plane, *Z. Amgew Math. Phys.*, 21, 645-647, 1970.
- [4] Ali M.E., Heat transfer characteristics of a continuous stretching surface, *Warme-Und Stoffubertragung*, 29, 227-234, 1994.
- [5] Ali M.E., On thermal boundary layer on a power law stretched surface with suction or injection, *Int. J. Heat Mass Flow*, 16, 280-290, 1995.
- [6] Elbashaeshy E.M.A., Heat transfer over a stretching surface with variable heat flux, *J. Phys.D:Appl. Phys.*, 31, 1951-1955, 1998.
- [7] -Ishak A., Nazar R. and Pop I., unsteady mixed convection boundary layer flow due to a stretching vertical surface, *Arabian J.Sce. Engng.*, 31, 165-182, 2006.
- [8] Elbashaeshy E.M.A and Bazid M.A.A., Heat transfer over a continuously moving plate embedded in non-Darcian porous medium, *Int. J. Heat and Mass Transfer*, 43, 3087-3092, 2000.
- [9] Andersson H.T., Aarseth J.B. and Dandapat B.S., Heat transfer in a liquid film on an unsteady stretching surface, *Int. J. Heat Transfer*, 43, 69-74, 2000.
- [10] Elbashaeshy E.M.A and Bazid M.A.A., Heat transfer over an unsteady stretching surface, *Heat Mass Transfer*, 41, 1-4, 2004.

- [11] Ishak A., Nazar R. and Pop I, Heat transfer over an unsteady stretching surface with prescribed heat flux, *Can. J. of Phys.*86, 853-855 ,2008 .
- [12] Chambre, P.L. and Young J.D., On diffusion of a chemically reactive species in a laminar boundary layer flow, *Physics of Fluids*, 1, 48-54, 1958.
- [13] Andersson, H.I., Hansen O.R. and Holmedal B., Diffusion of a chemically reactive species from a stretching sheet. *International Journal of Heat and Mass Transfer*, 37, 659-664, 1994.
- [14] Takhar, H.S., Chamkha A.J., Nath G., Flow and mass transfer on a stretching sheet with a magnetic field and chemically reactive species. *International Journal of Engineering Science*, 38, 1303-1314, 2000.
- [15] Radwan A.E. and Elbashbeshy E.M.A. Mass transfer over a stretching surface with variable concentration in a transverse magnetic field *IL NUOVO CIMENTO*, 105B (6), 1990.
- [16] Akyildiz, F.T., H. Bellout and K. Vajravelu, Diffusion of chemically reactive species in a porous medium over a stretching sheet. *Journal of Mathematical Analysis and Application* 320, 322-339, (2006).
- [17] El-Aziz, M.A., Unsteady fluid and heat flow induced by a stretching sheet with mass transfer and chemical reaction, *Chemical Engineering Communications* 197, 1261-1272, (2010).
- [18] Krishnendu Bhattacharyya, Boundary layer flow with diffusion and first order chemical reaction over a porous flat plate subject to suction/injection and with variable wall concentration, *Chemical Engineering Bulletin*, 15, 6-11, 2011.
- [19] Krishnendu Bhattacharyya, mass transfer on a continuous flat plate moving in a parallel or reversely to a free stream in the presence of a chemical reaction, *International Journal of Heat and Mass Transfer*, 55, 3483-3487, 2012.
- [20] Ferdows M. and Qasem M. Al-Mdallal, Effects of Order of Chemical Reaction on a Boundary Layer Flow with Heat and Mass Transfer Over a Linearly Stretching Sheet, *American Journal of Fluid Dynamics*, 2(6), 89-94, 2012.
- [21] Uddin M.S., Bhattacharyya K., Layek G.C. and Pk W.A. , Chemically Reactive Solute Distribution in a Steady MHD Boundary Layer Flow over a Stretching Surface, *Journal of Applied Fluid Mechanics*, Vol. 4, No. 4, pp. 53-58, 2011.

Development and Performance Evaluation of a Recirculatory System Fish Incubator

¹ Diabana P.D; ² Fakunmoju F.A; ¹ Adesina B.S

¹ Lagos State Polytechnic, School of Engineering, Department of Agricultural and Bio – Environmental Engineering

Lagos State Polytechnic, School of Agric, Department of Fisheries Technology

ABSTRACT

Hatching of fish eggs during the raining season is more or less difficult and time consuming in terms of heat provision for the eggs which results in a high cost of production. Consequently there is need to design and construct an effective recirculatory system fish incubator which operates under a controlled environment. An incubator with an hatching unit of (306mm x 303mm x 207mm) dimension was designed and constructed using locally available materials to reduce cost. The recirculatory system incubator has three units: the Incubating unit, the Sedimentation unit and Bio-tower system unit, The incubating unit was constructed using angular bars of dimension 3mm x 50mm which were joined together to form a rectangular shape and lined up at the back with pipe to supply water from the bio-tower system. Inside are four metal trays made from metal plate to form the hatching units. Four bulbs (60watt) each generating heat for each tray were used as heat source. The sedimentation tank was constructed using angular bar of 840mm x 307mm x 900mm dimension and covered up with metal plates and then connected to an overhead tank (Bio-tower). The flow of water from the sedimentation tank to the bio- tower is powered by a 0.5hp electric motor. The bio-tower system is made up of a plastic bowl to contain a bio filter which breaks down the nitrogenous waste of the water and allow a mixed up with atmospheric oxygen before sending it to the incubator. Also, oyster shell and larve stones were included in the bio-tower to control the pH. Two hundred grams (200gm) weight of *clarias gariepius* egg was set in the incubator under a normal temperature range of between $\pm 21^{\circ}\text{C}$ with PH range of 7 and Do_2 of 9mg/L; about 63% of hatchability was obtained after about 24hours of set-up. The experiment was replicated thrice giving a mean value of 61.25%(T1), 63.75%(T2), 67.5%(T3) and 60%(T4) and when subjected to statistical analysis shows a significant difference ($p < 0.05$) in the treatment means. The estimated cost of constructing the incubator is N87,150 which is an equivalent of \$544.69. Therefore this device is cheap, affordable and very easy to maintain as compared to the imported counterpart that sell for between \$2500 - \$4500.

KEY WORDS: Re-circulatory, Bio-tower, Sedimentation tank, Incubator, Hatchability

I. INTRODUCTION

Bulk of the domestic fish produce in Nigerian homes are from the in land capture fishes, dominated by the artisanal fishery sub-sector. Eyo and Ahmed (2005) reported that out of the 511,720 tons of fish produce in 2002. The art and fisheries sub sector accounted for 88.13% of the total production in that year. Hence the need has arisen to populate the wild fish to prevent extinction of the existing species. Incubator had been the most important source of hatching in the world. It has been in use in the southern California and China as far back 350BC till date. Push tray type, mats and a conical type are commonly used worldwide. Imported incubators are very expensive, difficult to repair and maintained. Owen (1991).The cost of buying an imported incubator has seriously restricted hatching operations by fish farmers during the raining season as the temperature is unfavorable for hatching at that period. In Africa, the traditional method of hatching the eggs is practice which involves the spawning of the eggs from the female fish through stripping and mixing the eggs thoroughly with sperm from the male fish. It is then spread on a small piece of net in a bath of water allowing sprinkle of water to flow into it under atmospheric temperature of 28-31 $^{\circ}\text{C}$.

Tray type incubator consists of a container that is screened or perforated through which a flow of water permeate to supply the egg with oxygen and flush away waste productions. Tray type incubator is used for fish egg that can be injured by the flow of water during incubation. Conical shaped tank that are not adhesive are used for fish eggs and they require constant flow of water from constant tumble in the lower portion of the jar. This type of incubator, is made of net materials and requires structural support and must be suspended inside a layer tank or placed inside the rearing tank. The flowing water must be of good quality and also well oxygenated water. The larvae is poured out of the incubator into the rearing tank as they are hatch into a soft materials shaped into a cone and used as an incubator. It is advantageous to use a screen because greater surface area is provided for water to flow out, thus preventing the egg yolk and larvae from been crush. During incubation constant flow of water is essential to prevent accumulation of a waste product and also allowing gas exchange between the egg and the surrounding water. Developmental embryos and newly hatched larvae (fry) are very sensitive and delicate at this stage of their life, so great care must be taken to provide them with the proper incubating and hatching environment. Water temperatures, water quality, size of the egg are very important factors to be considered in the design of incubator. Artificial incubation of egg is hatching a practice that will increase the economic efficiency of a commercial fish culture operation, hatching rate and survival will increase using artificial incubator. The removal of the eggs from the parent may increase egg production by shortening the time for another spawning. Ellis et. al (1996). Therefore, the aim of this work is to reduce the problem of hatching during the raining season by maintaining the temperature which will enable hatchability, and also to evaluate the performance efficiency of the recirculatory system fish incubator in order to meet the need of the farmer.

II. MATERIALS AND METHOD

CONSTRUCTION:

The recirculatory system incubator is made up of three units namely the hatching unit, sedimentation unit, and the bio-tower system.

[1] HATCHING UNIT

The hatching unit consists of a four hatching trays made from galvanized iron with a dimension of 306mm x 303mm x 207mm, which acts as a holding tank or tray for the eggs to be hatch. The trays are linked together with a pipe of 20mm diameter which transmits water from the hatching unit to the sedimentation unit.

Inside the hatching unit, there is a thermometer to measure the temperature reading of the incubator. Four bulbs were placed inside the incubator as the source of heat supply. The recirculatory system incubator temperature is controlled to the required temperature degree for hatching with the help of a regulator.

[2] SEDIMENTATION TANK

The sedimentation unit is made up of galvanized iron with a dimension of 840mm x 307mm x 900mm. The sedimentation unit consists of three chambers. The metal is welded together to form a rectangular box shape and each chamber consist of a net. The first chamber purifies the water coming from the incubator, while the second chamber consist of two nets in layers, which filters the sediments or dirt from the water before sending it to the pumping unit. The third chamber, the water that has been purified is being pumped back to the bio- tower tank with the aid of 0.5Hp pumping machine

[3] BIO-TOWER TANK UNIT

The bio-filter tank unit is made of a plastic tank of 100liters in volume. This tank serves as water reservoir and contains of a bio-filter, control valve, oyster shell and larvae stones.

The tank is connected to the 0.5Hp pumping machine which brings water into it, through a 2mm pipe from the sedimentation tank. The bio- tower is also connected to the incubator/ hatching chamber with the same size of pipe and regulated by a control valve. The valve connected to the pipe is used in the controlling water passage from the tank to the incubator and also used in regulating the pressure of flow to the tank and trays in the incubator.

The bio-filter is situated inside the bio-filter tank. This breaks down the nitrogenous waste in the incoming water. The oyster shell and the larva stone were also placed inside the tank to control the pH level of the water to 6.0 – 6.5 range which is suitable for the hatching and survivability of the eggs.

III. WORKING PRINCIPLE

The recirculatory system incubator that is made of three compartment unit namely the hatching unit, sedimentation unit, overhead tank or the bio-tower system unit with 0.5hp pumping engine.

Water from the bio-tower tank system which is free nitrogenous waste as a result of the mixing dissolved oxygen with the water flows to the hatching unit through a connecting pipe of 2mm and the pressure of flow is controlled by the tap. The dissolve oxygenated water is then released into the incubator in form of shower or spray which fills the hatching box and escapes through an opening into an outlet pipe. The four bulbs inside the hatching unit are regulated to produce the required heat which is monitored with the help of the thermometer. The water from the hatching unit flows down to the sedimentation tank where the dirt from the water settles down and later moves to the filtration tank through an opening at the base. It is then filtered before being sent to the pumping tank, where the filtered water is then pumped the bio-tower tank with the help of 0.5Hp electric motor.

IV. DETERMINATION CALCULATIONS

Design for flow of water in the recirculatory incubator

To calculate the rate of water flow in the incubator with an equation based pressure formula:

$$V = A \times h \quad \dots (1)$$

Where,

V = volume of water in the overhead tank (m³)

A = area of overhead tank (m²)

h = height or depth of the reservoir tanks (m)

$$V = \pi D^2 \times h \quad \dots (2)$$

Where,

D = Diameter of the overhead (m)

The volume of water shield of discharge Q in m³/sec was calculated

$$Q = \frac{\text{volume discharged}}{\text{time taken}} \quad \dots (3)$$

$$\text{Volume of discharge} = \text{Area} \times \text{Velocity of Discharge Pipe} \quad \dots (4)$$

$$\text{Area of Discharge Pipe} = \frac{\pi D^2}{4} \quad \dots (5)$$

The energy possessed by the moving fluid (water) at an attitude above datum (ground surface) also given by Bernoulli's equation

$$\text{Pressure head} + \text{Velocity head} + \text{Potential head} = \text{Total Head} \quad \dots (6)$$

$$\text{Pressure head from the overhead tank} = \frac{P}{\rho gh} \quad \dots (7)$$

Where,

ρ = density of water flowing in the incubator (kg/m³)

P = potential head above datum (reference point) $\frac{N}{m^2}$

g = acceleration due to gravity

Therefore

$$\text{Velocity head} = \frac{v^2}{2g} \quad \square(8)$$

$$\text{The fluid pressure due to depth \& weight} = \rho gh \quad \dots (9)$$

Where,

ρ = water density

H = height of the overhead tank

Fluid pressure was given as 21582 $\frac{N}{m^2}$

Atmospheric pressure was given as 1.01325 $\frac{N}{m^2}$

Total pressure was reservoir before discharge in from as

$$P1 + \text{Atmospheric Pressure} \quad \dots(10)$$

V. METHODOLOGY

Matured male and female broodstocks were purchased and their weight was 1kg each when measured. The female broodstocks was injected with 0.5ml of ovaprim (injection). The female broodstock was left to rest for 8-10hrs, so as to activate the release of eggs. After 10hrs of injection the female broodstock was stripped to release the eggs. The released eggs was weighted to determine the weight so as to be able to calculate the hatching percentage which was calculated as weight of egg x % hatchability, in which 50g of eggs is equivalent to 35,000 pcs of eggs. The male broodstock is cut open to remove the male semen sac and the semen sac is cut

opened to released the content into the eggs mass. The content is then mixed properly by shaking the mixture thoroughly to allow for proper mix up of the content and for easy fertilization process.

The mixture of the fertilized eggs were then removed with the help of a tablespoon and spread on a net inserted into water in the incubating trays. Water was allowed to run at a speed of 0.02ppm/sec, and the heat inside the incubator was regulated to a temperature of between $\pm 21^{\circ}\text{C}$. The pH of the water was tested and regulated to a pH of between 6.5-7, while dissolved (DO_2) oxygen level of the water coming into the incubator is between 7.0 – 9.0mg/L and ammonia level of the incubator was also controlled by removing the water from the sedimentation tank and replacing it with clean fresh water. The eggs were monitored and the hatching began at exactly 18hrs after the setting of the eggs. The net from the hatchery trays were remove and the shell waste from the water were siphoned using 5mm diameter hose. The velocity of the water dropping into the incubator is then increased to 0.05ppm/sec to allow for fast and proper evacuation of the water. Then the water level of the incubator was reduced through the bio tower system to a minimal and fresh water added to it to reduce the ammonia concentration level of the water. After the second day the larva were siphoned into the larva rearing tanks for further managerial activities.

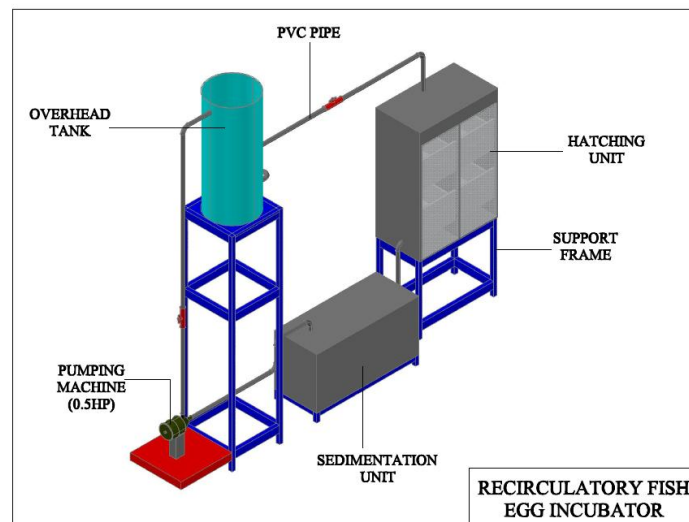


Figure 1. Recirculatory fish incubator

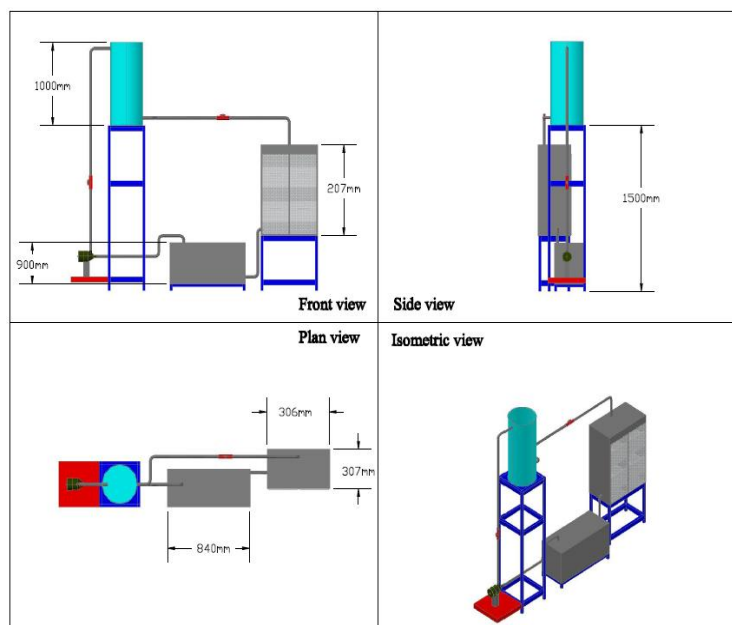


Figure 2. Recirculatory fish incubator

Figure 3 Showing the True picture of the constructed re-circulatory hatching incubator.



Table1: showing percentage hatchability when tested.

Test/wk	T1	T2	T3	T4	TEMP	PH LEVEL	(DO ₂) mg/L
1	60%	70%	75%	65%	± 21 °C	6.8	7.00
2	65%	65%	70%	60%	± 21 °C	6.5	7.20
3	60%	60%	65%	60%	± 21 °C	6.9	8.50
4	60%	60%	60%	55%	± 21 °C	7.0	9.00
MEAN	61.25%	63.75%	67.5%	60%	± 21 °C	6.8	7.9

Table 2: showing the cost analysis of constructing the recirculatory hatchery incubator.

S/NO	ITEM	QTY	UNIT COST	TOTAL COST
1	Angle Iron 50x50x60mm	5	2,900	14,500
2	Bio-filter	1 bundle	1,500	1,500
3	Control valve	6	300	1,800
4	Heat regulator	1	500	500
5	Overhead tank(100 litres)	1	3000	3,000
6	Thermometer	2	800	1,600
7	Lagging materials(fiber)		10,000	10,000
8	Galvanised sheet	4	3,500	14,000
9	Pumping machine(0.5hp)	1	4,000	4,000
10	lamp holder	4	50	200
11	Bulbs	4	50	200
12	1.5mm coil wire	15yds	70	1,050
13	Pvc pipe(20mm)	6	300	1,800
14	Pipe connector	30	50	1,500
15	Plastic glass	3	1,500	4,500
16	Larvae stone	2	100	200
17	Net (screen)	1yd	100	100
18	Paint(silver/green)	4cups	400	1,600
19	Topgit gum	2	250	500
	Workmanship			25,000
	TOTAL			N 87,150
	\$ 544.69			

VI. RESULT AND DISCUSSION

Figure 1.shows the details of the component that constitute the re-circulatory hatchery incubator. The result of the test for percentage hatchability is presented in Table 1. The mean hatchability percentage obtained for the 4 treatments were put at 61.3% (T_1), 63.75(T₂), 67.5% (T₃), 60% (T₄). The result obtained was subjected to statistical analysis and it reveals that there were significant differences ($P<0.05$) in the treatment means and that T3 had the highest hatchability percentage(%) of 67.5%.And as such proves that the hatching incubator is very effective for hatching at any period of the year. The hatching Temperature, PH and the Do₂ level were favourable for the hatching FAO(2004).Table 2. reveals the cost analysis of the construction which proves that it is affordable by the hatchery farmer at #87,150 which is an equivalent of \$544.69 as compared to that of imported counterpart whose cost ranges between \$2500 -\$4500.The size and operation of the incubator is very simple as compared to the imported incubator which looks so cumbersome in structure and maintenance.

VII. CONCLUSION AND RECOMMENDATION

Devices of simple technology with low cost of production as compared to the imported devices, easy maintenance conveniently Less space occupying like this will go a long way to reduce the problem of hatching during the cold weather and thereby increasing the production of high quality fries from hatchery production.The device can easily be operated by a 0.5 HP machine which is fixed at the base of the bio-tower system on a frame. It is therefore necessary that more equipment trials be carried out so as to achieve perfection of the device. It is also recommended that the extension agent should try to enlighten the hatchery operators on this latest technology of re-circulatory hatchery incubator

REFERENCES

- [1] Ellism.m, B.Weotfall, and ManionD.Ellis (1996). Determination of water quality. U.S fish and Wildin.serv, Res Rept, Vol (9) Pp 1-122
- [2] Eyo A.A. and Ahmed Y.B. (2005). Management of inland capture fisheries and challenges of fish production in Nigeria. In P.A Araoyeled proceedings of the 19th Annual conference of fison 29th – 3rd Dec 2004. Ilorin. Nigeria PP 624-636.
- [3] Okeke.P.N. Anyakola.M.W (1987) senior secondary physics revised edition 190 -191
- [4] Owan,J; (1991). Principles Problem and incubator design chapter 13, Pp B 205-226 in : Avian incubation. S.G. Tuttle, ed butter worth-Heinenmam London, U.K.
- [5] Food and Agricultural Organization (FAO, 1996): FOOD FOR ALL POOR issued on the occasion Of the World Food Summit in Rome. FAO Rome, p.64.
- [6] Food and Agricultural Organization (FAO, 2004): The state of World Fisheries and Aquaculture. Food and Agriculture Organization, United Nations.Rome. p 33
- [7] Food and Agricultural Organization (FAO, 2006): State of World aquaculture FAO Fisheries Technical paper, No. 500. Rome, 134pp

Fractional Derivative Associated With the Generalized M-Series and Multivariable Polynomials

¹Ashok Singh Shekhawat , ²Jyoti Shaktawat

¹Department of Mathematics Arya College of Engineering and Information Technology, Jaipur, Rajasthan

²Department of Mathematics Kautilya Institute of Technology and Engineering, Jaipur, Rajasthan

ABSTRACT

The aim of present paper is to derive a fractional derivative of the multivariable H-function of Srivastava and Panda [9], associated with a general class of multivariable polynomials of Srivastava [6] and the generalized Lauricella functions of Srivastava and Daoust [11] the generalized M-series. Certain special cases have also been discussed. The results derived here are of a very general nature and hence encompass several cases of interest hitherto scattered in the literature.

I. INTRODUCTION

In this paper the H-function of several complex variables introduced and studied by Srivastava and Panda [9] is an extension of the multivariable G-function and includes Fox's H-function, Meijer's G-function of one and two variables, the generalized Lauricella functions of Srivastava and Daoust [11], Appell functions etc. In this note we derive a fractional derivative of H-function of several complex variables of Srivastava and Panda [9], associated with a general polynomials (multivariable) of Srivastava [6] and the generalized Lauricella functions of Srivastava and Daoust [11]. Generalized M-series extension of the both Mittag-Laffler function and generalized hypergeometric functions.

II. DEFINITIONS AND NOTATIONS

By Oldham and Spanner [4] and Srivastava and Goyal [7] the fractional derivative of a function f(t) of complex order γ

$${}_a D_t^\gamma \{f(t)\} = \begin{cases} \frac{1}{\Gamma(-\gamma)} \int_0^t (t-x)^{-\gamma-1} f(x) dx, & \text{Re}(\gamma) < 0 \\ \frac{d^m}{dt^m} {}_a D_t^{\gamma-m} \{f(t)\} & 0 \leq \text{Re}(\gamma) < m \end{cases} \quad \dots(2.1)$$

Where m is positive integer.

The multivariable H-function is defined by Srivastava and Panda [9] in the following manner

$$H[z_1, \dots, z_r] = H_{A, C : [B', D'] ; \dots ; (B^{(r)}, D^{(r)})}^{0, \lambda : (u', v') ; \dots ; (u^{(r)}, v^{(r)})} \left[\begin{matrix} z_1 \\ \vdots \\ z_r \end{matrix} \middle| \begin{matrix} [(a) : \theta', \dots, \theta^{(r)}] : [(b') : \phi'] ; \dots ; [b^{(r)} : \phi^{(r)}] \\ [(c) : \psi', \dots, \psi^{(r)}] : [(d') : \delta'] ; \dots ; [d^{(r)} : \delta^{(r)}] \end{matrix} \right]$$

$$= \frac{1}{(2\pi i)^r} \int_{L_1} \dots \int_{L_r} \psi_1(\xi_1, \dots, \xi_r) \dots \phi_1(\xi_1) \dots \phi_r(\xi_r) z_1^{\xi_1} \dots z_r^{\xi_r} d\xi_1 \dots d\xi_r, \quad \dots(2.2)$$

where $(i = \sqrt{-1})$.

The general class of multivariable polynomials defined by Srivastava [6] defined as

$$S_{q_1, \dots, q_s}^{p_1, \dots, p_s} [x_1 \dots x_s] = \sum_{k_1=0}^{(q_1/p_1)} \dots \sum_{k_s=0}^{(q_s/p_s)} \frac{(-q_1)_{p_1 k_1}}{k_1!} \dots \frac{(-q_s)_{p_s k_s}}{k_s!}$$

$$\times A [q_1, k_1, \dots; q_s, k_s] x_1^{k_1} \dots x_s^{k_s} \dots(2.3)$$

where $q_j = 0, 1, 2, \dots; p_j \neq 0 (j = 1, \dots, s)$ are non-zero arbitrary positive integer the coefficients

$A [q_1, k_1, \dots; q_s, k_s]$ being arbitrary constants, real or complex.

The following known result of Srivastava and Panda [10]

Lemma. If $(\lambda \geq 0), 0 < x < 1, \text{Re}(1+p) > 0, \text{Re}(q) > -1, \lambda_i > 0$ and $\Delta_i > 0$ or $\Delta_i = 0$ and $|z_i| < \sigma, i = 1, 2, \dots, r$ then

$$x^\lambda F \begin{pmatrix} z_1 x^{\lambda_1} \\ \vdots \\ z_r x^{\lambda_r} \end{pmatrix} = \sum_{M=0}^{\infty} \frac{(1+p+q+2M)(-\lambda)_M (1+p)_\lambda}{M!(1+p+q+M)_{\lambda+1}} \cdot F_M [z_1, \dots, z_r] {}_2F_1 \left[\begin{matrix} -M, 1+p+q+M \\ 1+p \end{matrix}; x \right] \dots(2.4)$$

where

$$F_M [z_1, \dots, z_r] = F_{p+2:V'; \dots; V^{(r)}}^{E+2:U'; \dots; U^{(r)}} \left[\begin{matrix} [(e):\eta'; \dots; \eta^{(r)}] [1+p+\lambda: \lambda_1, \dots, \lambda_r], \\ [(g):\xi'; \dots; \xi^{(r)}] [2+p+q+M+\lambda: \lambda_1, \dots, \lambda_r] \\ [\lambda+1; \dots; \lambda_r]: [(w'):x']; \dots; [(w^{(r)}):x^{(r)}]; \\ [\lambda-M+1; \lambda_1, \dots, \lambda_r]: [(v'):t']; \dots; [(v^{(r)}):t^{(r)}]; \end{matrix} z_1, \dots, z_r \right] \dots(2.5)$$

where $M \geq 0$,

In this paper, we also use short notations as given

$$F_{p:V'; \dots; V^{(r)}}^{E:U'; \dots; U^{(r)}} \begin{pmatrix} \gamma_1 \\ \vdots \\ \gamma_t \end{pmatrix} \equiv F \begin{pmatrix} \gamma_1 \\ \vdots \\ \gamma_r \end{pmatrix} \dots(2.6)$$

denote the generalized Lauricella function of several complex variable. The special case of the fractional derivative of Oldham and Spanier [4] is

$$D_t^\gamma (t^\mu) = \frac{\Gamma(\mu+1)}{\Gamma(\mu-\gamma+1)} t^{\mu-\gamma} \quad \text{Re}(\mu) > -1 \dots(2.7)$$

The generalized M-series is the extension of the both Mittag-Leffler function and generalized hypergeometric function.

It represent as following

$$M_{p,q}^{\lambda, \mu} (c_1, \dots, c_p; d_1, \dots, d_q; z) = M_{p,q}^{\lambda, \mu} (z) = \sum_{k=0}^{\infty} \frac{(c_1)_k \dots (c_p)_k}{(d_1)_k \dots (d_q)_k} \frac{z^k}{\Gamma(\lambda k + \mu)} z, \lambda, \mu \in \mathbb{C}, \text{Re}(\lambda) > 0 \dots(2.8)$$

III. THE MAIN RESULT

Our main result of this paper is the fractional derivative formula involving the Lauricella functions, generalized polynomials and the multivariable H-function and generalized M-series as given

$$\begin{aligned}
 & D_{\ell}^{\gamma} \left\{ (\ell - x)^{\sigma} \eta^{\sigma} (y - \ell)^{\sigma + \rho} F \left[\begin{matrix} z_1 \{\eta(y\ell)\}^{\sigma_1} \\ \vdots \\ z_r \{\eta(y-\ell)\}^{\sigma_r} \end{matrix} \right] S_{N_1, \dots, N_s}^{M_1, \dots, M_s} \left[\begin{matrix} (\ell - x)^{a_1} (y - \ell)^{b_1} \\ \vdots \\ (\ell - x)^{a_s} (y - \ell)^{b_s} \end{matrix} \right] \right. \\
 & \times M_{\ell, m}^{\lambda, \mu} \{ (\ell - x)^{\lambda_1} (y - \ell)^{\lambda_2} \} H \left[\begin{matrix} w_1 \{\ell(\ell - x)\}^{\sigma_1} \{\ell(y - \ell)\}^{\rho_1} \\ \vdots \\ w_r \{\ell(\ell - x)\}^{\sigma_r} \{\ell(y - \ell)\}^{\rho_r} \end{matrix} \right] \\
 & = \sum_{\alpha, \beta=0}^{\infty} \sum_{k, M=0}^{\infty} \sum_{k_1=0}^{(N_1/M_1)} \dots \sum_{k_s=0}^{(N_s/M_s)} \frac{(-N_1)_{M_1 k_1}}{k_1!} \dots \frac{(-N_s)_{M_s k_s}}{k_s!} A[N_1, k_1, \dots, N_s, k_s] \\
 & \Delta H_{A+3, C+3; [B', D']; \dots; [B^{(r)}, D^{(r)}]}^{0, \lambda+3; \dots; (u', v'); \dots; (u^{(r)}, v^{(r)})} \left[\begin{matrix} w_1(-x)^{\sigma_1} y^{\rho_1} \ell^{\rho_1 + \sigma_1} \\ \vdots \\ w_r(-x)^{\sigma_r} y^{\rho_r} \ell^{\rho_r + \sigma_r} \end{matrix} \right] \left[\begin{matrix} (-\alpha - \beta; \rho_1 + \sigma_1, \dots, \rho_r + \sigma_r), \\ \left(\alpha - \sigma - \sum_{i=1}^s a_i k_i - \lambda_1 k; \sigma_1, \dots, \sigma_r \right) \end{matrix} \right] \\
 & \left. \left[\begin{matrix} \left(-\sigma - \sum_{i=1}^s a_i k_i - \lambda_1 k; \sigma_1, \dots, \sigma_r \right) \right] \left[\begin{matrix} \left(-\rho - k - \sum_{i=1}^s b_i k_i - \lambda_2 k; \rho_1, \dots, \rho_r \right) \right] : [(a): \theta'; \dots, \theta^{(r)}] : [(b'): \phi'; \dots, (b^{(r)}): \phi^{(r)}] \\ \left(\beta - \rho - k - \sum_{i=1}^s b_i k_i - \lambda_2 k; \rho_1, \dots, \rho_r \right) : (\gamma - \alpha - \beta; \rho_1 + \sigma_1, \dots, \rho_r + \sigma_r) : [(c): \psi'; \dots, \psi^{(r)}] : [(d'): \delta'; \dots, (d^{(r)}): \delta^{(r)}] \end{matrix} \right] \dots (3.1)
 \end{aligned}$$

where

$$\begin{aligned}
 \Delta & = \frac{(-1)^{\beta} (1 + \rho + q + 2M) (1 + p + q + M)_k (-M)_k (-\sigma)_M (1 + p)_{\sigma}}{k! M! (1 + p + q + M)_{\sigma+1} \Gamma(\lambda k + \mu) (1 + p)_k \Gamma \alpha + 1 \Gamma \beta + 1} \\
 & \cdot \eta^k (-x)^{\sigma - \alpha + \lambda_1 k + \sum_{i=1}^s a_i k_i} (y)^{\rho + \lambda_2 k - \beta + \sum_{i=1}^s b_i k_i} t^{\alpha + \beta - \gamma} \\
 & \cdot F_M(z_1, \dots, z_r) \frac{(c_1)_R \dots (c_r)_R}{(d_1)_R \dots (d_m)_R} \sigma_i > 0, s_i > 0, i = 1, 2, \dots, r
 \end{aligned}$$

and

$$\begin{aligned}
 \operatorname{Re}(\sigma) + \sum_{i=1}^r \sigma_i \left(\frac{d_j^{(i)}}{\delta_j^{(i)}} \right) & > -1 \\
 \operatorname{Re}(\rho) + \sum_{i=1}^r \rho_i \left(\frac{d_j^{(i)}}{\delta_j^{(i)}} \right) & > -1
 \end{aligned}$$

Proof. In order to prove (3.1) express the Lauricella function by (2.4) and the multivariable H-function in terms of Mellin-Barnes type of contour integrals by (2.2) and generalized polynomials given by (2.3) respectively and generalized M-series (2.8) and collecting the power of $(\ell - x)$ and $(y - \ell)$. Finally making use of the result (2.7), we get (3.1).

IV. PARTICULAR CASES

With $\lambda = A = C = 0$, the multivariable H-function breaks into product of Fox's H-function and consequently there holds the following result

$$\begin{aligned}
 & D_{\ell}^{\gamma} \left\{ (\ell - x)^{\sigma} \eta^{\sigma} (y - \ell)^{\sigma + \rho} F \left[\begin{matrix} z_1 \{\eta(y - \ell)\}^{\sigma_1} \\ \vdots \\ z_r \{\eta(y - \ell)\}^{\sigma_r} \end{matrix} \right] S_{\substack{M_1, \dots, M_s \\ N_1, \dots, N_s}} \left[\begin{matrix} (\ell - x)^{a_1} (y - \ell)^{b_1} \\ \vdots \\ (\ell - x)^{a_s} (y - \ell)^{b_s} \end{matrix} \right] \right. \\
 & \quad \times M_{\ell, m}^{\lambda, \mu} \{ (\ell - x)^{\lambda_1} (y - \ell)^{\lambda_2} \} \prod_{i=1}^r H_{B^{(i)}, D^{(i)}}^{u^{(i)}, v^{(i)}} \left[w_i \{ \ell(\ell - x) \}^{\sigma_i} \{ \ell(y - \ell) \}^{\rho_i} \left| \begin{matrix} [b^{(i)} : \phi^{(i)}] \\ [d^{(i)} : \delta^{(i)}] \end{matrix} \right. \right] \\
 & = \sum_{\alpha, \beta=0}^{\infty} \sum_{k, M=0}^{\infty} \sum_{k_1=0}^{(N_1/M_1)} \dots \sum_{k_s=0}^{(N_s/M_s)} \frac{(-N_1)_{M_1 k_1}}{k_1!} \dots \frac{(-N_s)_{M_s k_s}}{k_s!} A[N_1, k_1, \dots, N_s, k_s] \\
 & \quad \Delta H_{\substack{0,3:(u',v') \dots; (u^{(r)}, v^{(r)}) \\ 3,3:[B',D'] \dots; [B^{(r)}, D^{(r)}]}} \left[\begin{matrix} w_1(-x)^{\sigma_1} y^{\rho_1} \ell^{\rho_1 + \sigma_1} \\ \vdots \\ w_r(-x)^{\sigma_r} y^{\rho_r} \ell^{\rho_r + \sigma_r} \end{matrix} \right] \left[\begin{matrix} (-\alpha - \beta : \rho_1 + \sigma_1, \dots, \rho_r + \sigma_r), \\ \left(\begin{matrix} s \\ \alpha - \sigma - \sum_{i=1}^s a_i k_i - \lambda_1 k : \sigma_1, \dots, \sigma_r \end{matrix} \right) \end{matrix} \right] \\
 & \quad \left[\begin{matrix} \left(-\sigma - \sum_{i=1}^s a_i k_i - \lambda_1 k : \sigma_1, \dots, \sigma_r \right) \\ \left(-\rho - k - \sum_{i=1}^s b_i k_i - \lambda_2 k : \rho_1, \dots, \rho_r \right) \end{matrix} \right], [(b') : \phi'] \dots; [(b^{(r)}) : \phi^{(r)}] \\
 & \quad \left[\begin{matrix} \left(\beta - \rho - k - \sum_{i=1}^s b_i k_i - \lambda_2 k : \rho_1, \dots, \rho_r \right) \\ (\gamma - \alpha - \beta : \rho_1 + \sigma_1, \dots, \rho_r + \sigma_r) \end{matrix} \right] : [(d') : \delta'] \dots, [d^{(r)} : \delta^{(r)}] \quad \dots(4.1)
 \end{aligned}$$

valid under the conditions surrounding (3.1).

II. If $\phi^{(i)} = \delta^{(i)} = 1$, ($i = 1, 2, \dots$) equation (4.1) reduces to

$$\begin{aligned}
 & D_{\ell}^{\gamma} \left\{ (\ell - x)^{\sigma} \eta^{\sigma} (y - \ell)^{\sigma + \rho} F \left[\begin{matrix} z_1 \{\eta(y - \ell)\}^{\sigma_1} \\ \vdots \\ z_r \{\eta(y - \ell)\}^{\sigma_r} \end{matrix} \right] S_{\substack{M_1, \dots, M_s \\ N_1, \dots, N_s}} \left[\begin{matrix} (\ell - x)^{a_1} (y - \ell)^{b_1} \\ \vdots \\ (\ell - x)^{a_s} (y - \ell)^{b_s} \end{matrix} \right] \right. \\
 & \quad \times M_{\ell, m}^{\lambda, \mu} \{ (\ell - x)^{\lambda_1} (y - \ell)^{\lambda_2} \} \prod_{i=1}^r G_{B^{(i)}, D^{(i)}}^{u^{(i)}, v^{(i)}} \left[w_i \{ \ell(\ell - x) \}^{\sigma_i} \{ \ell(y - \ell) \}^{\rho_i} \left| \begin{matrix} [b^{(i)}] \\ [d^{(i)}] \end{matrix} \right. \right] \\
 & = \sum_{\alpha, \beta=0}^{\infty} \sum_{k, M=0}^{\infty} \sum_{k_1=0}^{(N_1/M_1)} \dots \sum_{k_s=0}^{(N_s/M_s)} \frac{(-N_1)_{M_1 k_1}}{k_1!} \dots \frac{(-N_s)_{M_s k_s}}{k_s!} A[N_1, k_1, \dots, N_s, k_s] \\
 & \quad \Delta H_{\substack{0,3:(u',v') \dots; (u^{(r)}, v^{(r)}) \\ 3,3:[B',D'] \dots; [B^{(r)}, D^{(r)}]}} \left[\begin{matrix} w_1(-x)^{\sigma_1} y^{\rho_1} \ell^{\rho_1 + \sigma_1} \\ \vdots \\ w_r(-x)^{\sigma_r} (y)^{\rho_r} \ell^{\rho_r + \sigma_r} \end{matrix} \right] \left[\begin{matrix} (-\alpha - \beta : \rho_1 + \sigma_1, \dots, \rho_r + \sigma_r), \\ \left(\begin{matrix} s \\ \alpha - \sigma - \sum_{i=1}^s a_i k_i - \lambda_1 k : \sigma_1, \dots, \sigma_r \end{matrix} \right) \end{matrix} \right]
 \end{aligned}$$

$$\left[\begin{array}{l} \left(-\sigma - \sum_{i=1}^s a_i k_i - \lambda_1 k : \sigma_1, \dots, \sigma_r \right) \left(-\rho - k - \sum_{i=1}^s b_i k_i - \lambda_2 k : \rho_1, \dots, \rho_r \right) : [(b') : \dots; [b^{(r)}]] \\ \left(\beta - \rho - k - \sum_{i=1}^s b_i k_i - \lambda_2 k : \rho_1, \dots, \rho_r \right) : (\gamma - \alpha - \beta : \rho_1 + \sigma_1, \dots, \rho_r + \sigma_r) : [(d') : \dots; [d^{(r)}]] \end{array} \right] \dots(4.2)$$

valid under the conditions as obtainable from (3.1).

III. Let $N_i = 0$ ($i = 1, \dots, s$), the result in (3.1) reduces to the known result given by Sharma and Singh [], after a little simplification.

IV. Replacing N_1, \dots, N_s by N in (3.1) we have a known result recently obtained by Chaurasia and Singh [].

V. ACKNOWLEDGEMENT

The authors are grateful to Professor H.M. Srivastava, University of Victoria, Canada for his kind help and valuable suggestions in the preparation of this paper.

REFERENCES

- [1] V.B.L. Chaurasia and V.K Singhal, Fractional derivative of the multivariable polynomials, Bull. Malaysian Math. Sc. Soc. (Second Series), 26 (2003), 1-8.
- [2] M. Sharma, Fractional integration and fractional differentiation of the M-series, J. Fract. Calc. and Appl. Anal., Vol.11, No.2 (2008), 187-191.
- [3] M. Sharma and Jain, R., A note on a generalized series as a special function, n of fractional calculus. J. Fract. Calc. and Appl. Anal., Vol.12, No. 4 (2009), 449-452.
- [4] K.B. Oldham and J. Spanier, The Fractional Calculus, Academic Press, New York, 1974.
- [5] C.K. Sharma and Singh Indra Jeet, Fractional derivatives of the Lauricella functions and the multivariable H-function, Jñānābha, 1(1991), 165-170.
- [6] H.M. Srivastava, A multilinear generating function for the Konhauser sets of biorthogonal polynomials suggested by the Laguerre polynomials, Pacific J. Math., 117 (1985), 157-191.
- [7] H.M. Srivastava and S.P. Goyal, Fractional derivatives of the H-function of several variables, J.Math. Anal. Appl., 112 (1985), 641-651.
- [8] H.M. Srivastava, K.C. Gupta and S.P. Goyal, The H-Functions of One and Two Variables with Applications, South Asian Publishers, New Delhi-Madras, 1982.
- [9] H.M. Srivastava and R. Panda, Some bilateral generating functions for a class of generalized hypergeometric polynomials, J. Reine Angew. Math. 283/284 (1976), 265-274.
- [10] H.M. Srivastava and R. Panda, Certain expansion formulas involving the generalized Lauricella functions, II Comment. Math.Univ. St. Paul., 24 (1974), 7-14.
- [11] H.M. Srivastava and M.C. Daoust, Certain generalized Neuman expansions associated with the Kampé de Fériet function, Nederl. Akad. Wetensch Indag. Math., 31 (1969), 449-457.

DMZ: A trusted honeypot for secure transmission

¹M.Buvaswari , ²M.P. Loganathan

Postal Address:6/16 Mohan Street, East Tambaram, Chennai-600059

ABSTRACT:

In general, denial of service is nothing but flooding of unrelated information over the network. This causes, overload of network and higher bandwidth consumption. Therefore particular service requested by authorized user cannot receive at particular time. Thus causes larger security threat in network. When these system get distributed (distributed network), the mitigation becomes very complex. In existing technique the DoS has been mitigated using many filtering technique. In order to reduce the effect of DDoS attack we had introduced the concept of ihoneycol[1], which includes the collaboration of firecol(intrusion prevention system) these forms a virtual mitigation shield around the destination and safe guard from the source and honey pot(intrusion detection system). To improve these security, we are going to introduce "trusted honey pot". These can be done using honey token and honey sign.

KEYWORDS: Denial of service, ihoneycol, honey pot, honey token, honey sign.

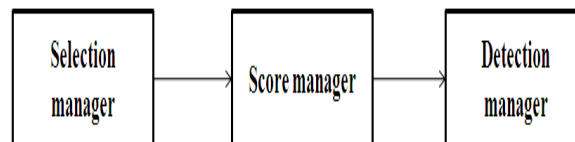
I. INTRODUCTION:

Denial of service or otherwise generally known as packet flooding over the network. This leads to exploitation of OS and causes major security threats[2]. Worms and viruses are also poses security issues which are not related to denial of service attack. Denial of Service detection algorithm are located near the vulnerability and victim vicinity around them. Here the detection of threat is made as flexible as possible. The major trade off is that, the local response is made ineffective and the bandwidth occupies the upstream path. The most coupling problem is that "IP traceback"[3] and "IP pushback"[4]. These aim to identify the attack and move on to counter measures which lies near the source of threat. To deal with this problem "Fire Collaborator" has been introduced which deals with the problem at ISP level. It takes the advantage of various IPS rules[5]. It is detection and alert information sharing system that makes the IPS rules that mitigate the effect of denial of service attack which is far from the victim destination. Honeypot is a trap set to detect unauthorized traffic pattern for detection.

II. RELATED WORKS:

Firecol" is either a hardware or software helps in reducing the effect of denial of service using many IPS rules. Initially all the customer in the network register at ISP level. Each customer receives an UID(unique identity) number. When more than one nodes use the same UID number then it is detected as a malicious or unauthorized node. Firecol contains various IPS rules according to the detection of various traffic each rules will be activated.

Fig 1.Firecol functions.



As we already seen that firecol contains many rules and these rules will be activated in the following manner. The selection manager will determine the rules according to the attack and absorb the various malicious traffic over the network. The score manager assigns the scores according to the belief traffic and the rules designed. These scores can be exchanged as a token of trust within the neighbors in the network. The detection manager reads and detect the various traffic among the authorized and unauthorized traffic from the clients. The following are existing solution for denial of service attack:

- [1] Attack prevention and pre-emption:
The attacks are prevented at the client side itself and the mode of mitigation done from far clients. Pre-emption is done when the authorized clients itself wanted to send the malicious data. To achieve this they swap with neighbor network devices.
- [2] Attack detection and filtering:
Here the attack is detected and filtered according to various network traffic monitored by the detection system. These traffic are registered as patterns. These filtering technique can be integrated in to firewall. It can be either software or hardware.
- [3] Attack source and identification:
Once the attack is identified the main source of attack is detected and its IP address has been moved to blacklist and stored in honeypot server.

Traditionally denial of service mitigation takes place in two major phases:

1. deployment phase: Here the deployment of many compromised nodes take place in network.
2. Attack phase: Here the attack mitigation and prevention takes place.

Reduction of Denial of Service include techniques like spoofing, prevention technique(Ingress and RPF filtering[6]). The other includes manually employed countermeasures (firewall filtering, rate limiting or route black holes[7]). Various abrupt traffic patterns are absorbed in multiple network domains[8]. These leads to very accurate detections and communication overheads. Group testing is performed to identify the denial of service at backend server[9]. Here various malicious traffic are distinguished. Denial of service also distinguish various network traffic and quantify network[10]. This reduces false alarm rate over the network. In order to achieve effective result, this honeypot should be integrated with any IPS system like firewall hardware or softwares[11].

III. PROPOSED WORK:

In general, the client system will be arranged in form of network. The trusted transmission occur among them using authentication and authorization procedures. The client forward the information via firecol routers. These routers are made up of set of IPS rules(intrusion prevention system). They check the traffic according to the rules embedded in it. Later the data get forwarded to load balancer in network. Here we use "Non-cooperative scheme with communication" for attaining higher performance. The traffic here are classified accordingly normal and abrupt traffic. Normal traffic are forwarded to original server or the destination. Abnormal traffic patterns are detected and monitored by set of honeypot system called honeycomb.

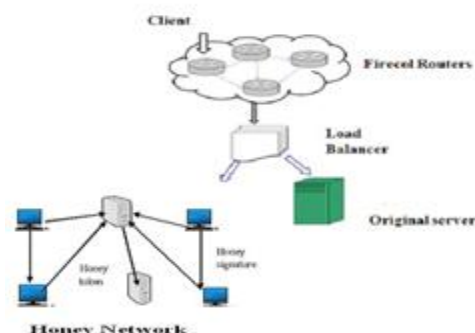


Fig 1.2 Proposed Network

Honeycomb is defined as set of interconnected mesh network. They are multiprocessor system. The group of honeypot performs similar task known as honeycomb.

IV. HYBRID LOAD BALANCER:

Load balancing in general used to attain higher performance in transmission. Initially all the node get registered with the server using their own IP address and load status of an individual node in network. According to load(also trace the historical pattern and sends the maximum load it can take) the load balancer allots a specific weights to all nodes. If the weight crosses the threshold value then that node is called as high weight node, other called as light weight node. These weights are assigned within the fuzzy value interval of [0,1]. The transmission takes place using all the light weight node irrespective of shortest path to attain higher performance. Since we are taking the calculation of individual node we call it as "Non-cooperative scheme with communication".

V. TRUSTED HONEYCOMB:

Honeycomb contains the set of interconnecting mesh network computers. Each honeycomb contains set of honeypot systems and honey servers. Honeypot are computer system whose values can be lied and can be easily compromised. Each honeypot will be exchanging the trusted note by passing honey signatures. Honey signatures are unique signature generated by each system and get stored in honey server. Each honey servers can be recognized using honey token which was made initially while forming the network. Honeytokens are trusted token exchanged among the various honey servers during regular interval of time dynamically. This honey comb environment separately forms an de-militarized zone where it is invisible for authorized users.

VI. CONCLUSION:

By considering the above technique as an effective way we can solve many network security threats. In future I have planned to apply this for four various threat. The usage of signatures and tokens can be extended to original servers using various algorithms.

REFERENCES

- [1]. C.Siaterlis,B.Maglaris."Detecting DDoS attacks with passive measurement based heuristics",IEEE conference publication 2004.
- [2]. S.Savage, D.Wetherall, A.Karlin, T.Anderson. Practical network support for IP traceback", proceedings of 2000ACM SIGCOMM conference.
- [3]. J.Ioannidis and M.Bellovin. "Implementing pushback,router based defense against DDoS attack", proceeding of NDSS, Feb2002.The internet society.
- [4]. J.Francois,Adel,E.Atawy,E.Al-Shaee, R.Boutaba,"A collaborative approach for proactive detection of DDoS attack",IEEE transaction 2012.
- [5]. CISCO.Remote triggered blackhole filtering.ftp://ftp_eng.cisco.com/cons/isp/security/.
- [6]. Kai Hwang and Wei-Shinn Ku," A collaborative detection of DDoS attack over multiple domain", IEEE journal 2007.
- [7]. Yin Xuan, Incheol Shin, My T.Thai,Taieb Znati, "Detecting application Denial of Service attack: A group testing based approach", IEEE publication 2009.
- [8]. Yan Xiang,Ke LI,Wanlei Zhou,"Low rate DDoS attackdetection and traceback by using new information metrics",IEEE publication 2011.
- [9]. Nathalie Weiler,"Honey pots for DDoS attack",IEEE conference publication 2002.
- [10]. Satish.P and A.T.Chronopoulos, "Dynamic multi user load balancing in distributed system", IEEE publication 2007.
- [11]. Christian K and Jon Crowcroft "Honeycomb- creating intrusion detection signature using honeypot" <http://nms.lcs.mit.edu/HotNets-II/papers/honeycomb.pdf>.

Efficient Cluster Head Selection Method For Wireless Sensor Network

Manjusha M S¹, K E Kannammal²

¹ PG Scholar, Department Of Computing Science, Sri Shakthi Institute Of Engineering And Technology
Tamilnadu, India,

² Associate Professor, Department Of Computing Science, Sri Shakthi Institute Of Engineering And Technology
Tamilnadu, India

ABSTRACT:

A WSN (Wireless Sensor Network) consists of over hundreds of sensor nodes which have limited energy, process capability and memory. The applications of WSN in some extreme environment make sensor nodes difficult to replace once they use up the battery resource. Since the wireless transmission is the most energy consuming operation, how to design an energy efficient routing protocol becomes the main goal for the wireless sensor network. LEACH is considered as the most popular routing protocol which has better performance in saving the energy consumption. However, the selecting formula neglecting the change of nodes' energy will make the nodes acting as cluster heads too many times which leads to the death of the cluster head early by consuming excessive amount of energy. Also, the frequent reclustering wastes certain amount of energy. This paper presents a new version of LEACH protocol referred to as VLEACH which aims to reduce energy consumption within the wireless network.

KEYWORDS: Clustering, Cluster Head, LEACH protocol, Routing, V-LEACH, Vice Cluster Head, Wireless sensor networks

I. INTRODUCTION

Wireless sensor network consists of hundreds and even thousands of small tiny devices called sensor nodes distributed autonomously to observe physical or environmental conditions like temperature, pressure, vibration and motion at different locations such as landslides [5]. Every node in a sensor network usually equipped with one sensor, a wireless communications device like radio transceiver, a small microcontroller, and an energy supply, a battery. Since the nodes are battery operated energy plays a vital role. The application of the WSN involves several fields, like military battleground, fire detection, and other extreme environments. In these situations, it is troublesome to replace the dead nodes caused by energy's depletion with new ones to provide energy for the system. Therefore, making sensor nodes operating as long as possible is the main method to maximize the lifespan of the sensor network. Because the energy's consumption of sensor node primarily originates from the long distance transmission of data, an efficient routing protocol can have a good impact on the energy's consumption. Thus how to design an energy efficient routing protocol becomes the main goal for the wireless sensor network [6].

The basic objective on any routing protocol is to make the network useful and efficient. A cluster based routing protocol group sensor nodes where each group of nodes has a Cluster Head (CH). Sensed data is sent to the CH rather than send it to the BS; CH performs some aggregation function on data it receives then sends it to the BS where these data is needed. LEACH [7] is considered as the most popular routing protocol that use cluster based routing in order to minimize the energy consumption. Leach divides the communication process into rounds with each round including a set-up phase and a steady-state phase. In the setup phase, some sensor nodes are selected as CHs according to certain rules and other nodes join in the clusters as member nodes. Within the steady-state phase, the CHs collect the data coming from their own cluster members and aggregate them before transmitting to the BS [4]. However, due to the inherent characteristic of LEACH, the unnecessary energy consumption caused by the

unreasonable choosing formula and the high frequency of reclustering among sensor nodes will cause the uneven energy distribution and waste a certain amount of energy in the whole network. Supported the ideology of traditional LEACH, we modify the selecting formula by considering the dynamic change of sensor nodes' energy and establish a Vice cluster head for every cluster during the communication process, that aims to diminish the energy consumption spent on the reclustering and prolong the time of being in a steady-state phase.[2]

II. LEACH PROTOCOL

Low Energy Adaptive Clustering Hierarchy (LEACH) [3, 8] is the first hierarchical cluster-based routing protocol for wireless sensor network that partitions the nodes into clusters, in each cluster a special node with extra privileges referred to as Cluster Head (CH) is responsible for creating and manipulating a TDMA (Time division multiple access) schedule and sending aggregated data from nodes to the BS where these data is needed using CDMA (Code division multiple access). Remaining nodes are cluster members. Figure 1 shows the LEACH protocol. LEACH is divided into rounds; each round consists of two phases.

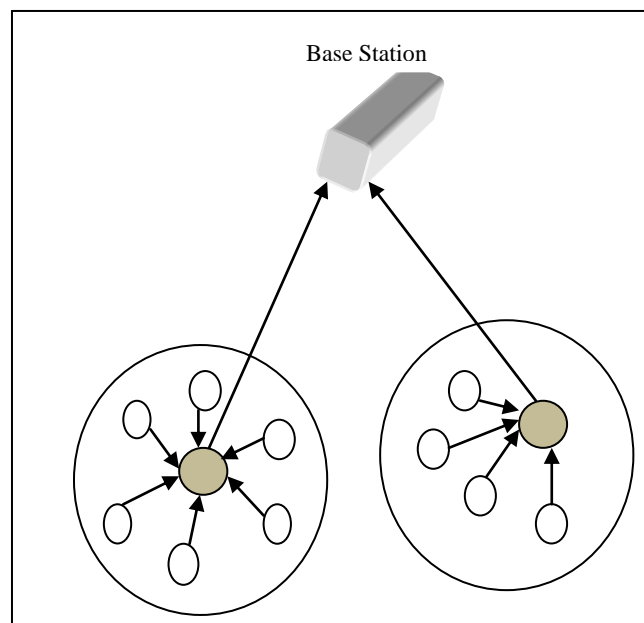


Figure 1. LEACH Protocol

2.1. Set-Up Phase. After finishing the deployment of sensor nodes, each node within the monitor field decides independently of other nodes whether or not it can become a cluster head in the current round. Throughout the phase, every node generates a random number between zero and one [1] and then compares it with the threshold value $T(n)$.

$$T(n) = \begin{cases} \frac{p}{1-p \cdot [r \bmod (\frac{1}{p})]}, & n \in G \\ 0, & n \notin G \end{cases} \quad (1)$$

Where p is that the percentage of cluster heads over all nodes within the network, r is the number of rounds of selection, and G is that the set of nodes that haven't been selected as cluster heads in round $1/p$. The node whose number is larger than the threshold can choose itself as a cluster head so broadcasts the message to its surround sensor nodes. During this phase, a node could receive more than one broadcast message from completely different cluster heads, however the node will decide its distance to a cluster from the strength of received broadcast signal; the stronger the signal, the nearer to a cluster. So the node whose number is smaller than threshold will only send request message containing its ID to the cluster that has the strongest signal strength for saving energy spent on the transmission distance. Once the cluster head receives request message returning from one node, it records the node's ID and decides it as its member node. Once the message exchanges between cluster heads and normal nodes, every CH gets its own member nodes' information regarding IDs and every normal node gets that cluster that it belongs to. Based on the message it records, a

TDMA schedule is created by the CH and broadcasts it to the cluster members. So all the member nodes of that CH gets their idle slots for data transmission. Then the steady-state phase starts.

2.2. Steady-State Phase. The establishment of a cluster head in every cluster during the set-up phase provides a guarantee for the data transmission in the steady-state phase. In normal cases, member nodes can put off their radio till they sense the required surrounding environment data. If there are some data in need for transmission, they will send the data to CH during the idle slots recorded within the TDMA schedule table. As for the CHs, they need to keep up communication status at all times so as to receive the data from different member nodes. Once receiving all the data from their members, CHs will aggregate these data's and then send them to BS. As a result of some sensor nodes may sense similar environment data, the aggregation on the cluster head will diminish excess bandwidth cost and communication traffic that includes a positive reflection to the energy's consumption. Also, the transmission distance becomes shorter comparing with transmitting to BS on an individual basis for each member node, which can save energy for the member nodes. However, the heavy tasks on CH will result in an excessive amount of energy consumption. So as to avoid making the CHs die early and cause the cascade result within the network, a new round begins and new clusters are going to be rebuilt in the whole network.

Although the LEACH protocol acts in a very sensible manner, they also suffer from several drawbacks just like the following:

- [1] CHs' selection is random, that doesn't consider the residual energy of every node or want the support of BS.
- [2] The high frequency of reclustering wastes a certain quantity of energy.
- [3] It can't cover a large area.
- [4] CHs aren't uniformly distributed, where CH may be settled at the edges of the clusters.

III. PROPOSED SYSTEM -VLEACH

Motivated by the initial LEACH and different improvement protocols [2, 3] we tend to propose a modification to the cluster head selection method to reduce energy consumption. For a small sensor network, we make the following assumptions.

- [1] The base station (BS) is located at a fixed location which is far from the sensors and is immobile.
- [2] All nodes within the network have limited energy with an identify ID.
- [3] All the nodes are able to reach BS and can communicate with one another.
- [4] CH perform data compression and aggregation function.

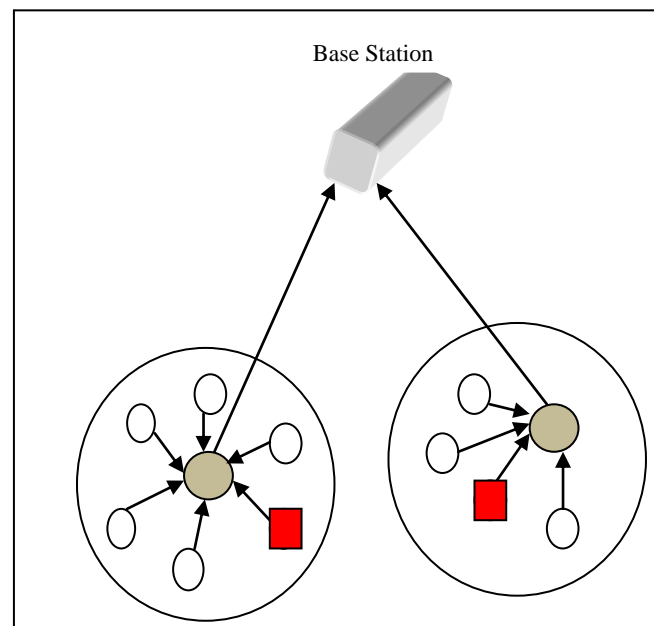


Figure 2. Proposed VLEACH

In the improvement, we also make use of the hierarchical clustering ideology and divide a round into a set-up phase and steady-state phase. The set-up phase will use a modified formula for selecting the appropriate

CHs which are responsible for collecting data from their member nodes and transmitting them to BS. CHs will consume more energy than member nodes because of the heavy tasks so in order to avoid making the CHs die early, LEACH take the measure of beginning a new round and rebuilding the clusters. However, in the proposed system we will make use of the information about the member node which is achieved dynamically by cluster heads in the steady phase to choose the vice cluster heads (VCHs). VCH take over the role of cluster heads in the later period of steady state phase. Figure 2 shows the VLEACH protocol. Comparing with the normal LEACH, the VCHs proposed will diminish the frequency of reclustering in the same interval and extend the time of being in steady-state phase, which is able to prolong the lifecycle of the whole network.

3.1. Selecting Cluster Heads (CHs) in the Set-Up Phase. Based on the fact that LEACH does not take into account the residual energy of the nodes during the selection of cluster heads in the set-up phase, we tend to develop the present energy and also the times being selected as CH or VCH. We first consider about the threshold $T(n)$ and are modified to the following equation:

$$T(n) = \begin{cases} \frac{p}{1-p \cdot [r \bmod (\frac{1}{p})]} \times \left[\frac{E_{n_{current}}}{E_{n_{init}}} + \left(1 - \frac{E_{n_{curr}}}{E_{n_{ini}}} \right) \right], & n \in \\ \times \frac{p}{(CH_{times} + VCH_{times} + 1)}, & n \notin \\ 0, & n \notin \end{cases} \quad (2)$$

Where p is that the percentage of cluster heads over all the nodes within the network, R is the number of round of selection in current time. G is that the set of nodes that haven't been selected as cluster heads in round $1/p$. $E_{n_{curr}}$ is the residual energy of the node and E_n is the initial energy of each node. CH times (VCH times) is that the times of being selected CH (VCH times) once. Deducing from (2), we can able to get that the larger the $E_{n_{curr}}$ larger the $T(n)$. So we can infer that the node that has lot of energy will have a much bigger probability to become the cluster head within the current round. But at the same time, if a node acts as CH or VCH for an excessive amount of time, the energy it consumes are going to be larger than other sensor nodes. However, the improved equation can lower the probability of a node acting as CH or VCH too many times to become CH again. We are able to observe that the improved formula adds some useful determinacy factors within the choice of cluster heads that is helpful to the stabilization of clusters. If there are too many selected cluster heads in the deployed area then it will cause some unnecessary energy consumption. For limiting the cluster heads' number to a reasonable range, we tend to develop the simulated annealing algorithm to form appropriate numbers of cluster heads which is about 4%-5% of the overall sensor nodes. Once finishing the choice of cluster heads within the set-up phase by using the improved equation and simulated annealing algorithm, begin the steady-state phase of a round.

3.2. Establishment of Vice Cluster Heads' (VCHs') during the Steady-State Phase. In the steady-state phase of LEACH protocol, the cluster heads will consume more energy than member nodes. As a result they need to take the responsibility of aggregating and relaying data to remote BS for their member nodes. So as to avoid making the cluster heads die early when undergoing certain amount of communication time, a new replacement round begins to reorganize the nodes into clusters and reselect the cluster heads. So, all the nodes go to judge themselves and rebuild the cluster heads so as to campaign for new cluster heads. So, it consumes some energy spent on recompleting the cluster heads and shortens the full time of being in steady-state phase. Thus we propose a new scheme to extend the time of being in steady phase and diminish the frequency of recluster. The new scheme works as follows. During the data communication in steady-state phase, as a result of all member nodes send the data sensed from environment to their own cluster head, the cluster head will have the chance to find out the status information of its members. Based on this, the cluster head will record the information of various member nodes dynamically in the format like $\langle id, E \rangle$, which refers the member node id has residual energy E . Through this fashion, the CH can have global energy information about its member nodes. So as to extend the time of being in steady-state phase and delay a new round's coming; CH can appoint a member node which has the utmost energy in cluster to take over the role of it if it consumes too much energy in the later steady-state phase of current round. Thus we can call the member node which is appointed by the CH as a vice cluster (VCH). So as to make the rest of member nodes get the VCH's id , the CH broadcast this message containing the VCHs id to various other member nodes. Then from that, the CH itself will become a standard member node because of the too much energy consumption and the establishment of VCH in a cluster. Since then, all the member nodes can send their data to VCH, which send the compressed data to the BS. We are able to observe that the establishment of VCH in cluster can prolong the communication time of being in steady-state phase and it also delay the coming of a new round. But the problem is that after a certain time,

VCH also consumes more energy than the member nodes due to the heavy tasks undertaken as previous CH. To avoid the chances of being the VCH die early, start a new round for selecting CHs among all the sensor nodes in the set-up phase. So we can call the whole communication in our improved protocol as the cycle of “CH-VCH-CH.” It can be described using the Figure 3.

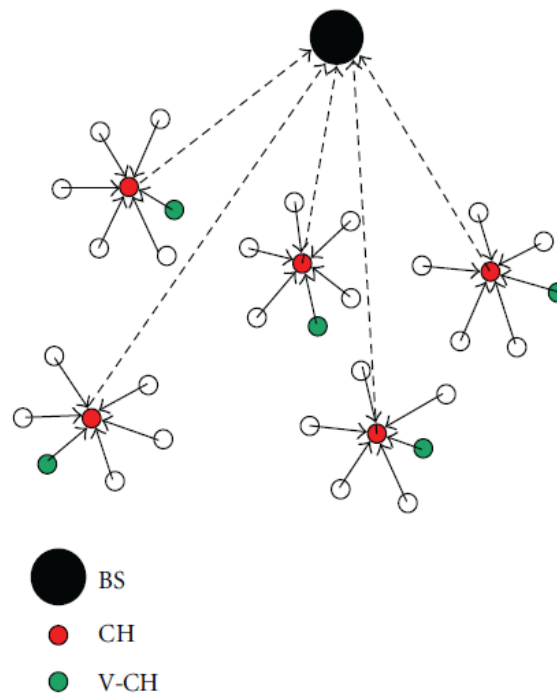


Figure 3. Improved hierarchical protocol working process

In the proposed protocol, we have taken the measure of choosing a VCH for every cluster in the later period of the steady-state phase in a round by using the energy information achieved by CH, which may diminish the frequency of reclustering and extend the time of being in steady-state phase. Within the whole communication phase of a round, CH and VCH have similar roles such as collecting data from member nodes and relaying the aggregated data to the BS. The distinction is that the CH takes the responsibility within the earlier stage of the steady-state phase, while VCH replaces the CH and works in the later stage of the steady phase of the current round. Also, the CHs choice originates the competition among all the nodes within the set-up phase. However, CH directly establishes the VCH within the later stage of the steady-state phase in a round. We are able to get that the method of establishing VCH is easy and speedy comparing with the generation and cooperation of random numbers within the set-up phase. Thus all of them have a good benefit to the saving of energy in the whole network.

IV. SIMULATION RESULT

We examine the improved protocol through simulations in matlab. A network consists of 100 nodes is deployed in an area of $100\text{m} \times 100\text{m}$ with BS at (50, 50). For comparing the advantages of the improved VLEACH protocol we use the number of dead nodes as simulation parameter. The simulation results are shown in Figure 4. From the simulation we can observe that in our proposed VLEACH node starts to dead earlier than the normal LEACH protocol.

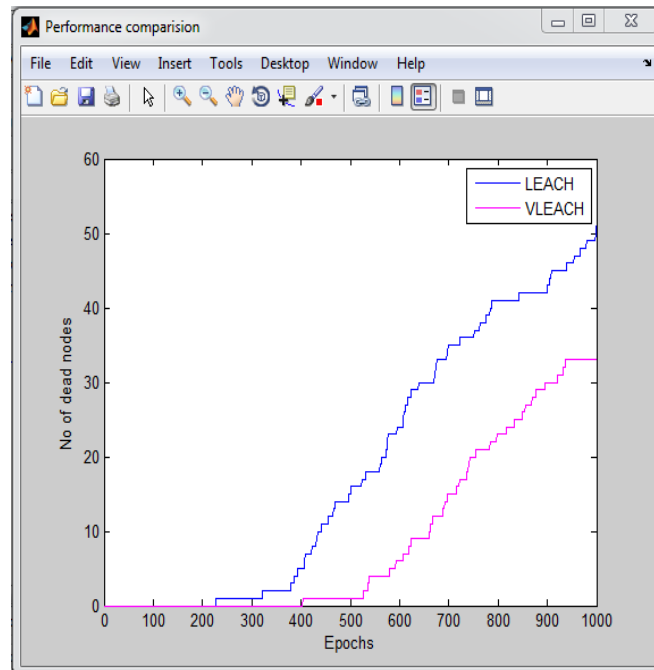


Figure 4: LEACH and VLEACH with 100 nodes

We also compare the LEACH and VLEACH with 200 nodes for showing that our proposed protocol also works in the case of dense networks also. The simulation result with 200 nodes is shown in Figure 5.

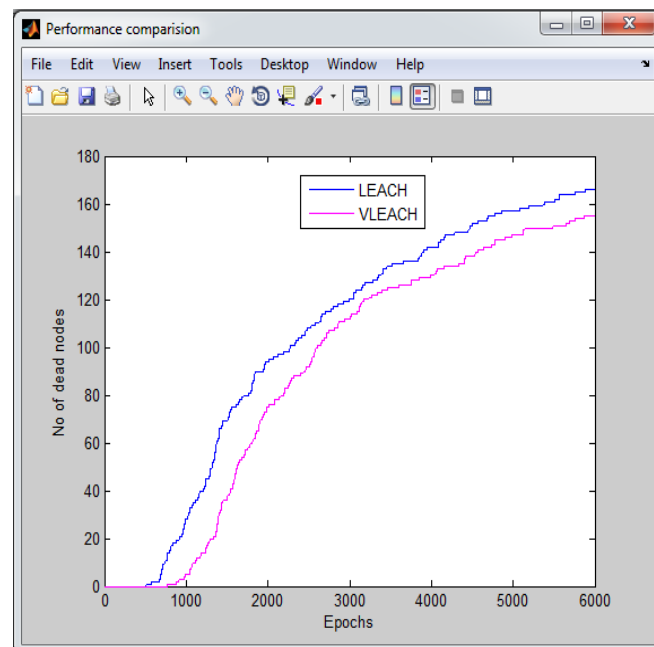


Figure 5: LEACH and VLEACH with 200 nodes

By the introduction of VCH, certain amount of energy spent on the reclustering and recomputing among different nodes gets reduced. From Figure 4 and 5, we can obtain that the number of dead nodes is reduced in our improved routing protocol than LEACH over the simulation rounds. This shows that our improved protocol consumes less energy. Also due to our modification to the steady-state phase, the times for selecting the cluster heads to each member node in the whole network become reduced. This results the remaining energy of the network using our improved protocol exceeds that of the original LEACH protocol.

V. CONCLUSION

In this paper, an outline of the original LEACH protocol is presented and proposed a new version of hierarchical protocol referred to as VLEACH. The proposed protocol obtains energy efficiency by the modification for selecting the cluster head formula and the steady-state phase. The modification to the choosing of cluster heads formula makes the CH or VCH have more opportunity to act as CHs. So the total energy of the whole network has more even distribution among different nodes. Thus the VCH introduction makes the frequency of reclustering more lowly and prolongs the time of being in steady-state phase; thus the energy used for calculating the formula on every node reduces.

REFERENCES

- [1] B. Deosarkar, N. Yadav, and R. P. Yadav, "Cluster head selection in clustering algorithms for wireless sensor networks: a survey," in *Proceedings of the International Conference on Computing Communication and Networking*, Tamilnadu, India, December 2008.
- [2] Fuzhe Zhao, You Xu, and Ru Li, "Improved LEACH Routing Communication Protocol for a Wireless Sensor Network", Hindawi Publishing Corporation, International Journal of Distributed Sensor Networks, Volume 2012, Article ID 649609.
- [3] G. Ran, H. Zhang, and S. Gong, "Improving on LEACH protocol of wireless sensor networks using fuzzy logic," *Journal of Information and Computational Science*, vol. 7, no. 3, pp. 767–775, 2010.
- [4] Heinzelman W.R, Chandrakasan A., and Balakrishnan H.: "Energy-Efficient Communication Protocol for Wireless Micro sensor Networks".2000.
- [5] http://en.wikipedia.org/wiki/Low_Energy_Adaptive_Clustering_Hierarchy [Online].
- [6] J. Li and H. Gao, "Research advances in wireless sensor networks," *Journal of Computer Research and Advances*, vol. 45, no. 1, pp. 1–15, 2008.
- [7] K. Khamforoosh and H. Khamforoush, "A new routing algorithm for energy reduction in wireless sensor networks," in *Proceedings of the 2nd IEEE International Conference on Computer Science and Information Technology (ICCSIT '09)*, pp. 505–509, August 2009.
- [8] M. Bani Yassein, A. Al-zou'bi, Y. Khamayseh, W. "Improvement on LEACH protocol of Wireless Sensor Network (VLEACH)".

Optimal Synthesis of a Single-Dwell 6-Bar Planar Linkage

Galal A. Hassaan

Mechanical Design & Production Department, Faculty of Engineering, Cairo University, Giza, Egypt

ABSTRACT

Six-bar linkage of single or double dwell linkage are used to overcome the problems of cam-follower mechanisms. Optimal synthesis of dwell mechanisms provides accurate synthesis fulfilling most of the functional constraints imposed to satisfy the mechanism specifications for proper operation. In the present work, the synthesis problem is formulated in the form of an objective function and three functional constraints. The synthesis problem incorporates seven parameters to be optimally evaluated covering all the links of the mechanism. The transmission angle of the 4-bar linkage and at the output slider are both considered to control the performance quality of the synthesized mechanism. In an application on the methodology presented, it was possible to synthesize 6-bar planar linkage for a single dwell across 60 degrees of crank rotation with a maximum error of 0.229 %.

KEYWORDS: optimal mechanism design – 6-bar planar linkage – single-dwell mechanism.

I. INTRODUCTION

It is difficult to synthesize 6-bar planar dwell mechanisms using the geometrical-graphical analysis approach. This simply because this approach requires exactly circular parts of the coupler point within a specific crank angle. Optimal mechanism synthesis is the proper solution which provides accurate and straight forward synthesis. Some approaches are available in the literature in this concern.

Sandgren (1985) applied the nonlinear programming technique to a class of 6-bar linkage to produce single and multi-dwell mechanisms [1]. Kota, Erdman and

Riley (1987) studied the 4-bar linkage generating straight line, arc and symmetrical curves [2]. In a second part of their work they explained the development of an expert system for designing linkage-type dwell mechanisms [3].

Danian, Yuanji and Shaowei (1988) studied the synthesis of 6-bar long dwell mechanisms [4]. **Iyer (1996)** developed a computer-aided design approach to design both circular-arc and straight line dwell mechanisms [5].

Ogot (1996) developed a design tool to support the design of a linkage-type dwell mechanism required for a vertical filler. He presented single and double dwell examples [6].

Chen and Yang (2005) proposed a procedure to synthesize optimal mechanisms using the multi-level decomposition approach. They applied their approach to design a 4-bar linkage and 6-bar dwell mechanisms [7].

Shiakolas, Koladiya and Kebrle (2005) presented a methodology for the synthesis of 6-bar linkages dwell and dual-dwell mechanisms with prescribed timing and transmission angle constraints [8].

Sonmez (2007) introduced new classes of compliant long dwell mechanism designs incorporating the buckling motion of flexible links [9].

Jagannath (2011) introduced an approach for the design of planar 6-bar linkage with rotating joints producing two dwells. He used a genetic algorithm-based optimization scheme for solving the resulting optimization problem [10].

II. ANALYSIS

A 6-bar single-dwell planar mechanism with translational output has the structure shown in Fig.1 [11].

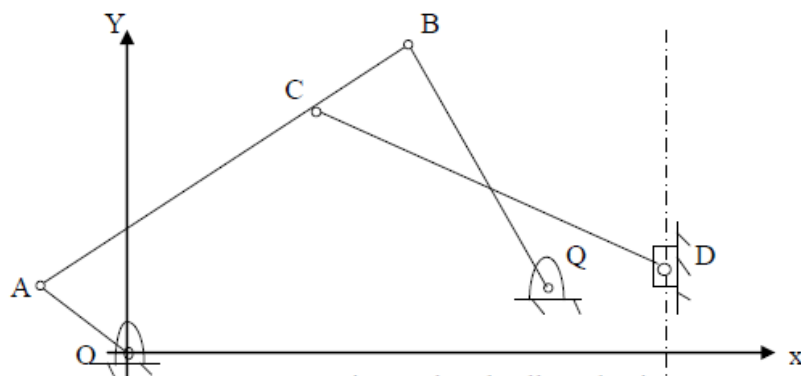


Fig.1: 6-bar dwell mechanism.

Mathematical models are build for the whole mechanism using two displacement polygons as shown in

Fig.2.

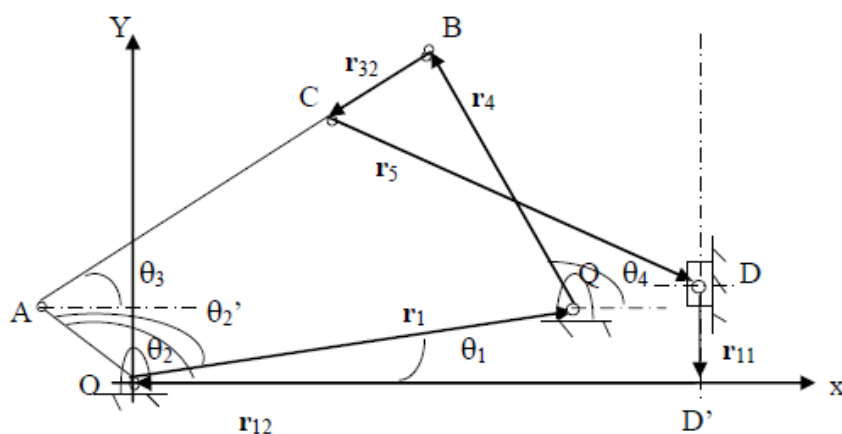


Fig.2: Displacement analysis of the 6-bar dwell mechanism.

Polygon 1: OABQO

This polygon reveals two kinematical equations relating the orientation of vectors AB and BQ [12]. Those equations are nonlinear and can be solved numerically or using MATLAB through its command “fsolve”. To avoid solving nonlinear equations, geometrical relationships can be used revealing θ_3 (orientation of AB) and θ_4 (orientation of QB) as [13]:

$$\theta_3 = \mu - \beta - \theta_1$$

where:

$$\mu = \tan^{-1} \{r_4 \sin \gamma / (r_3 - r_4 \cos \gamma)\}$$

$$\beta = \tan^{-1} \{r_2 \sin \theta_2' / (r_1 - r_2 \cos \theta_2')\}$$

$$\theta_2' = \theta_2 - \theta_1$$

$$\gamma = \cos^{-1} (A_1 + B_1)$$

$$A_1 = (r_3^2 + r_4^2 - r_1^2 - r_2^2) / (2r_3r_4)$$

$$B_1 = [r_1 r_2 / (r_3 r_4)] \cos \theta_2'$$

And $\theta_4 = \square - \beta - \sigma + \theta_1$

Where $\sigma = \square - \mu - \gamma$

Polygon: *OQBCDD'O*

The displacement analysis vector equation across this polygon is (see Fig.2):

$$\mathbf{r}_1 + \mathbf{r}_4 + \mathbf{r}_{32} + \mathbf{r}_5 + \mathbf{r}_{11} + \mathbf{r}_{12} = 0$$

Resolving in the x- direction gives:

$$r_{1x} + r_{4x} + r_{32x} + r_{5x} + r_{11x} + r_{12x} = 0 \tag{1}$$

where: $r_{1x} = r_1 \cos \theta_1$, $r_{4x} = r_4 \cos \theta_4$

$$r_{32x} = r_{32} \cos \theta_{32} , r_{11x} = 0$$

$$r_{12x} = r_{12}$$

Resolving in the y-direction gives:

$$r_{1y} + r_{4y} + r_{32y} + r_{5y} + r_{11y} + r_{12y} = 0 \tag{2}$$

where: $r_{1y} = r_1 \sin \theta_1$, $r_{4y} = r_4 \sin \theta_4$

$$r_{32y} = r_{32} \sin \theta_{32} , r_{11y} = r_{11}$$

$$r_{12y} = 0$$

The orientation θ_{32} is related to θ_3 through:

$$\theta_{32} = \theta_3 + \square$$

The vector component r_{5x} is given from Eq. 1 by:

$$r_{5x} = - r_{1x} - r_{4x} - r_{32x} - r_{11x} - r_{12x}$$

As r_5 is the length of link 5, the component r_{5y} is given by (Fig.2):

$$r_{5y} = - \sqrt{\{r_5^2 - r_{5x}^2\}}$$

Now, Eq. 2 gives r_{11} as:

$$r_{11} = - r_{1y} - r_{4y} - r_{32y} - r_{5y} \tag{3}$$

Eq.3 gives the output slider displacement, y_D as:

$$y_D = - r_{11} \tag{4}$$

Mechanism transmission angle: Any mechanism has to be synthesized such that its transmission angle is not far away from an optimal value [14]. In the present 6-bar mechanism, transmission angle can be considered in 2- locations in the mechanism:

- [1] Transmission angle between the coupler and rocker of the 4-bar linkage (OABQ).
- [2] Transmission angle between link 5 and the slider D (output link).

4-bar linkage transmission angle:

This is angle ABQ in Fig.1. It has a minimum and maximum values ($TA_{4barmin}$ and $TA_{4barmax}$) when the crank is co-linear with the coupler. That is [15]:

$$TA_{4barmin} = \cos^{-1} \{ [r_3^2 + r_4^2 - (r_1 - r_2)^2] / (2r_3r_4) \} \quad (5)$$

$$\text{And } TA_{4barmax} = \cos^{-1} \{ [r_3^2 + r_4^2 - (r_1 + r_2)^2] / (2r_3r_4) \} \quad (6)$$

Output link transmission angle: This transmission angle, TA_{out} , is related to the orientation of the position vector r_5 (θ_5) through:

$$TA_{out} = 2\theta_5 - \theta_5$$

III. REQUIREMENTS

It is required that:

- [1] The mechanism output, y_D dwells once during the rotation of the crank for one revolutions.
- [2] The dwell motion of the slider is through a specific crank angle θ_2 .
- [3] The transmission angle of the 4-bar linkage OABQ and at the output slider are within the recommended range (between 45 and 135 degrees [12]).

IV. OPTIMAL MECHANISM SYNTHESIS

(a) Objective function

An error function is used to define the objective function of the optimization process. The error, e in this case is between the slider displacement y_D and the desired slider displacement, y_{Ddes} at specific crank angles. That is:

$$e = y_D - y_{Ddes} \quad (8)$$

The objective function F is the integral of absolute error (IAE). That is:

$$F = \int |e| dt \quad (9)$$

(b) Functional constraints

The performance of the 6-bar planar dwell mechanism is controlled using a three functional constraints:

(i) The minimum transmission angle of the 4-bar linkage, $TA_{4barmin}$:

$$C_1 = (45^\circ - TA_{4barmin}) \quad (10)$$

(ii) The maximum transmission angle of the 4-bar linkage, $TA_{4barmax}$:

$$C_2 = TA_{4barmax} - 135^\circ \quad (11)$$

(iii) The minimum transmission angle of the output slider, TA_{outmin} :

$$C_3 = (45^\circ - TA_{outmin}) \quad (12)$$

(c) Design parameters

The design parameters of the 6-bar planar dwell mechanism are:

- Ground orientation: θ_1 .
- Ground link: r_1 .
- Crank: r_2 .
- Coupler: r_3 .
- Rocker: r_4 .
- Mini-coupler: r_{32} .
- Output coupler: r_5 .

(d) Optimazation technique

MATLAB optimization toolbox is used to provide the optimal design of the mechanism under study [16,17].

APPLICATION

Suppose that it is required to synthesise a 6-bar planar single dwell mechanism having:

- Slider line of action at 800 mm from the fixed origin O.
- Slider dwells at 100 mm during a crank angle from 300 to 360 degrees.

A MATLAB code is written using the methodology presented in this paper. The code results are as follows:

- Ground orientation: $\theta_1 = 100$ degrees
- Ground link: $r_1 = 617.9$ mm
- Crank: $r_2 = 100$ mm
- Coupler: $r_3 = 698.805$ mm
- Rocker: $r_4 = 511.840$ mm
- Mini-coupler: $r_{32} = 0$
- Output coupler: $r_5 = 347.180$ mm

The output slider displacement for one revolution of the crank of the optimally synthesized mechanism is shown in Fig.3.

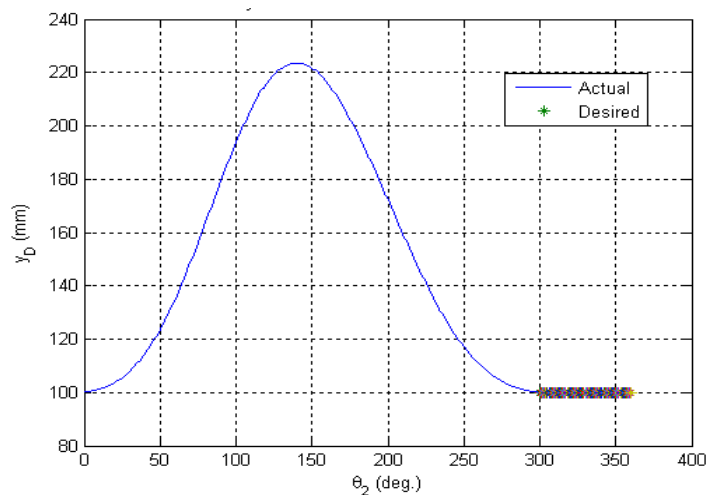


Fig.3 Output slider displacement.

Characteristics of the optimally synthesized mechanism:

- 4-bar minimum transmission angle: 47.63 degrees
- 4-bar maximum transmission angle: 70.83 degrees
- Output slider minimum transmission angle: 123.0 degrees
- Output slider maximum transmission angle: 144.5 degrees
- The 4- bar linkage is a Grashof crank-rocker one allowing complete rotation of the crank (shortest link).
- The transmission angle of the 4-bar linkage against the crank angle is shown in Fig.4.
- The transmission angle at the output slider against the crank angle is shown in Fig.5.

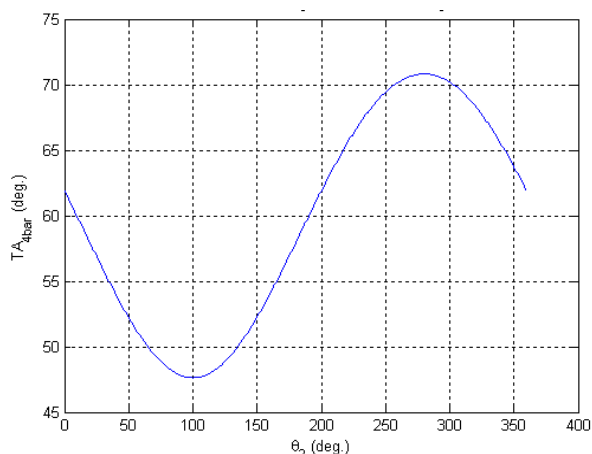


Fig.4: The 4-bar linkage transmission angle.

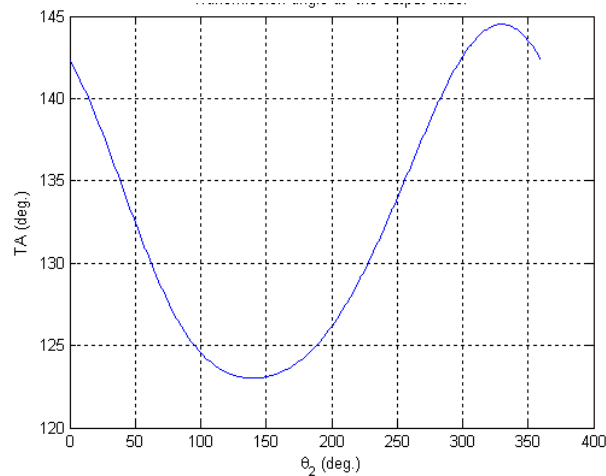


Fig.5: The mechanism transmission angle at the output slider.

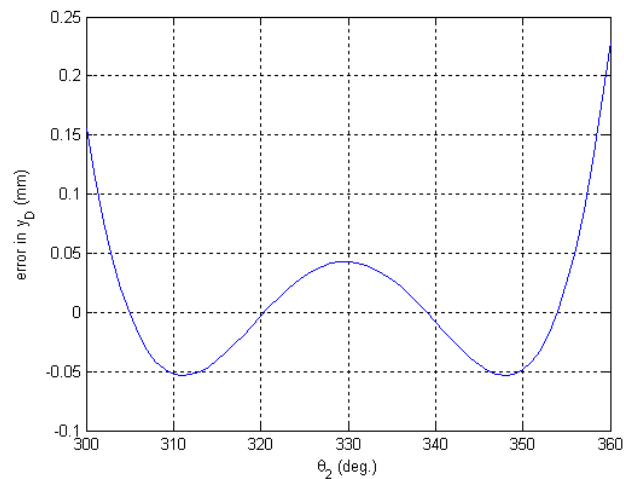


Fig.6: Error in the slider displacement.

V. DISCUSSIONS

- It is possible to synthesize accurately a 6-bar planar single dwell mechanism using nonlinear optimization.
- The proposed approach relied on defining an IAE objective function and three functional constraints.
- Constrains were set on the transmission angles of the 4-bar linkage of the mechanism and on its output slider transmission angle.
- All the values of the transmission angle during operation of the optimally synthesized mechanism were within the recommended range.
- It was possible in the application presented to attain a single dwell motion over 60 degrees of the crank rotation with a maximum error of 0.229 %.

REFERENCES:

- [1] Sandgren E. , "Design of single and multiple-dwell 6-bar mechanisms through design optimization", Mechanism and Machine Theory, Vol.20, No.6, 1985, pp.483-490.
- [2] Kota S. , A. Erdman and D. Riley, "Development of knowledge base for designing linkage-type dwell mechanisms: Part 1-Theory", J. of Mech. Trans., September 1987, Vol.109, No.3, pp.308-315.
- [3] Kota S., A. Erdman and D. Riley, "Development of knowledge base for designing linkage-type dwell mechanisms: Part 2-Application", J. of Mech. Trans., September 1987, Vol.109, No.3, pp.316-321.
- [4] Danian H. , M. Yuanji and M. Yuanji, "The classification and kinematic synthesis of the 6-bar long-dwell mechanism", J. of China Textile University, Vol.4, 1988, pp.1-6.
- [5] Iyer V. , "RECDWELL- Computer-aided design of 6-link planar dwell mechanisms", Mechanism and Machine Theory, Vol.31, No.8, 1996, pp.1185-1194.
- [6] Ogot M. , "Alternate filling of MRE placeables", Report No.CRAMTD STP15-FTR 13.0, February 1996.
- [7] Chen T. and C. Yang, "Multi disciplinary design optimization of mechanisms", Advances in Engineering Software, Vol.36, 2005, pp.301-311.
- [8] Shiakolas P., D. Koladira and J. Kebrle, "On the optimum synthesis of 6-bar linkages using differential evolution and the geometric centroid of precision positions technique", Mechanism and Machine Theory, Vol.40, 2005, pp.319-335.

- [9] Sonmez U., "Introduction to compliant long dwell mechanism design using buckling beams and arcs", J. of Mechanism Design, Vol.129, No.8, August 2007, pp.831-843.
- [10] Jagannath M., "Optimization design of 6-bar double dwell mechanisms: a new approach", Applied Mechanics and Materials, Vol.110-116, 2011, pp.110-116.
- [11] Norton R., "Design of Machinery", McGraw Hill, 2011.
- [12] Wilson C. and J. Sadler, "Kinematics and dynamics of machinery", Prentice Hall, 2003.
- [13] Erdman A. and G. Sandor, "Mechanism design: analysis and synthesis", Prentice Hall, Vol.1, 1984.
- [14] Shijie F. and L. Li, "Novel method of realizing the optimal transmission of the crank-and-rocker mechanism", Chinese J. of Mechanical Engineering, No.1, 2003.
- [15] Waldron K. and G. Kinzel, "Kinematics, dynamics and design of machinery", J. Wiley & Sons, 1999.
- [16] -----, "Global optimization toolbox: Users guide", The Math Works Inc., 2004 – 2012.
- Bjorkman M. and K. Holmstrom, "Global optimization using direct algorithm in matlab", Advanced Modeling and Optimization, Vo.1, No.2, 1999, pp.17-3

Vehicles Weight Ratio V. Initial Velocity of Vehicle in Chain Accidents on Highways

Robert M Brooks¹, Mehmet Cetin²

¹ College of Engineering, Temple University, USA (Corresponding Author)

² College of Engineering, Temple University, USA

ABSTRACT:

The objective of this study is to determine the influence of vehicles weight ratio on the initial velocity of the first vehicle in a chain accident on highways involving three vehicles. Regression analysis on the results of these variables was conducted. Excellent correlation coefficient was found for the relationship at $\alpha = 0.05$ significance level. The influence of Vehicles Weight Ratio on the Initial Velocity is shown by a quadratic equation (Initial velocity = 9.4313 Vehicles Weight Ratio ² - 45.94 Vehicles Weight Ratio + 143.52) with $R = 0.91$.

KEYWORDS: Accident Reconstruction, Chain Accidents, Highways, Initial Velocity, Regression Analysis, Reconstruction engineering, Vehicles Weight Ratio.

I. INTRODUCTION

Accident reconstructing engineering is the planning, surveying, measuring, investigating, analyzing, and report making process on the intricate engineering details of how accidents occurred. The analysis and conclusions are based on the extensive application of fundamental principles of physics and engineering including Newton's Laws of Motion [1] and First Law of Thermodynamics [2]. The first law of thermodynamics when applied to accidents states that the total energy before and after the accident will be the same. The input variables include roadway, vehicle, driver and environmental conditions. Accident reconstruction engineering studies can be utilized by the industry, city and state governments for modifying the structural facilities such as roads. The modifications may include obtaining improved friction factors, increased number of lanes and lane widths and better site distances. Vehicle manufacturers use the results of the studies for developing better designs of vehicles. Some of the recent vehicles may use event data recorder containing information on the speed of the vehicle before and at the time of the accident. Some manufacturers, such as GM and Ford, allow downloading the information from these boxes after an accident [3]. The results of the accident reconstruction studies are also used for producing better navigations aids to assist the drivers. In this study the guidelines of Accreditation Commission for Traffic Accident Reconstruction (ACTAR) [4] are used. There are many research studies on the application of accident reconstruction engineering principles. One of the most important one is that of Hurt's [5]. Hurt found that motorcyclists needed to develop their capabilities on controlling skids and proper use of helmets significantly reduced head injuries. Hurt further found that out of all the turning movements, the left turners were the most involved ones in the accidents while turning in front of the oncoming motorcycles.

II. SCOPE OF THE STUDY

The study is limited to the accidents caused by negligent drivers of cars hitting the parked cars [6,7,8]. All the accidents caused elastic deformations only [9,10]. There are no significant plastic deformations [11,12,13].

III. METHODOLOGY

C1 was travelling at certain speed, feet per second and skidded s feet before hitting C2. One half of the energy was transmitted from C1 to C2. C2 was travelling at certain speed, feet per second before the accident. C2 picked up the energy from C1 and hit C3. The weight ratios of C1/C2 and C2/C3 are noted. Again one half of the energy of C2 was transmitted to C3.

The following equations were used.

- [1] The total product of mass and velocity of Car2 is equal to that of Car 3 as shown in the following equation.
 [2] $M_2u_2 = m_3 u_3$ (2)
 Where, m_2 = mass of vehicle C2 and u_2 is the velocity of C2. M_3 = mass of C3 and u_3 = velocity of C3.

- [3] Deceleration was calculated by using Equation1.
 a. Final velocity was calculated by the following equation.

$$u = \sqrt{v^2 - 2as} \tag{3}$$

Where, u = initial velocity of the vehicle, ft/sec
 v =final velocity, ft/sec
 a = deceleration of the vehicle, ft/sec²
 s = skidded distance, feet

IV. RESULTS AND DISCUSSION

The following assumptions were made in this study

- [1] The energy lost in sound produced by the accident is negligible.
 [2] The energy lost in causing the slight angular movement of the vehicle is negligible.

Professional engineering principles allow the application of the above two assumptions in the appropriate engineering calculations.

Table I shows the Engineering Calculations for Mixed Variables for Case 1 through Case 5 for Determininig the Initial Velocity while Table II gives the Engineering Calculations for Mixed Variables for Case 6 thurough 10 for Determininig the Initial Velocity.

Engineering Calculations for Case 1 through Case 5; Case 6 through Case 10; and Case 11 through Case 15 for Determininig the influence of Vehicles Weight Ratio on the Initial Velocity are given in Tables III, IV, and V respectively.

The following regression relationship was found with statistically significant correlation coefficient for predicting the performance of the engineering variables. The relationship was significant at $\alpha = 0.05$ significance level [14,15,16].

Fig. 1 shows the influence of Vehicles Weight Ratio on the Initial Velocity. This relationship is described by a quadratic equation (Initial velocity = 9.4313 Vehicles Weight Ratio ² – 45.94 Vehicles Weight Ratio +143.52) with R = 0.91.

Table I. Engineering Calculations for Mixed Variables for Case 1 through Case 5 for Determininig the Initial Velocity.

	Case 1	Case 2	Case 3	Case 4	Case 5
Car3					
Velocity after the second accident, ft/sec	123.71	121.83	126.35	117.46	116.09
Weight Ratio, C3/C2	0.48	0.60	0.68	0.78	0.92
Velocity before the second accident, ft/sec	70	75	80	72	74
Weight, pounds	3000	3500	3800	4200	4800
Car2					
Weight, Pounds	6200	5800	5600	5400	5200
Weight Ratio, C2/C1	3.10	2.32	1.87	1.54	1.30

Velocity after the first accident, ft/sec	51.98	56.52	62.90	70.71	77.70
Velocity before the first accident, ft/sec	42	44	48	50	52
Car1					
Weight, pounds	2000	2500	3000	3500	4000
Final Velocity (after skidding, and before first accident) ft/sec	61.87	58.10	55.63	63.90	66.81
Skidded Distance, ft	22	26	28	30	32
Pavement Friction	0.28	0.28	0.28	0.28	0.28
Deceleration, ft/sec ²	9.02	9.02	9.02	9.02	9.02
Initial Velocity, ft/sec	65	62	60	68	71

Table II. Engineering Calculations for Mixed Variables for Case 6 through Case 10 for Determining the Initial Velocity.

	Case 6	Case 7	Case 8	Case 9	Case 10
Car3					
Velocity after the second accident, ft/sec	117.41	101.18	103.05	107.60	104.28
Weight Ratio, C3/C2	1.10	1.17	1.32	1.50	1.74
Velocity before the second accident, ft/sec	78	60	63	68	65
Weight, pounds	5300	5400	5800	6000	6100
Car2					
Weight, Pounds	4800	4600	4400	4000	3500
Weight Ratio, C2/C1	1.07	0.92	0.80	0.67	0.54
Velocity after the first accident, ft/sec	87.04	96.69	105.58	118.80	136.91
Velocity before the first accident, ft/sec	54	56	58	60	62
Car1					
Weight, pounds	4500	5000	5500	6000	6500
Final Velocity (after skidding, and before first accident) ft/sec	70.49	74.86	76.13	78.41	80.67
Skidded Distance, ft	20	18	16	14	12
Pavement Friction	0.28	0.28	0.28	0.28	0.28
Deceleration, ft/sec ²	9.02	9.02	9.02	9.02	9.02
Initial Velocity, ft/sec	73	77	78	80	82

Table III. Engineering Calculations for Case 1 through Case 5 for Determininig the Relationship between Vehicles Weight Ratio and Initial Velocity.

	Case 1	Case 2	Case 3	Case 4	Case 5
Car3					
Velocity after the second accident, ft/sec	140.89	133.62	121.33	113.74	106.08
Weight Ratio, C3/C2	1.00	1.00	1.00	1.00	1.00
Velocity before the second accident, ft/sec	60	60	60	60	60
Weight, pounds	1800	2000	2400	2800	3500
Car2					
Weight, Pounds	1800	2000	2400	2800	3500
Weight Ratio, C2/C1	0.30	0.34	0.46	0.58	0.80
Velocity after the first accident, ft/sec	161.77	147.24	122.65	107.48	92.15
Velocity before the first accident, ft/sec	50	50	50	50	50
Car1					
Weight, pounds	6000	5800	5200	4800	4400
Final Velocity (after skidding, and before first accident) ft/sec	67.06	67.06	67.06	67.06	67.06
Skidded Distance, ft	25	25	25	25	25
Pavement Friction	0.25	0.25	0.25	0.25	0.25
Deceleration, ft/sec ²	8.05	8.05	8.05	8.05	8.05
Initial Velocity, ft/sec	70	70	70	70	70

Table IV. Engineering Calculations for Case 6 through Case 10 for Determininig the Relationship between Vehicles Weight Ratio and Initial Velocity.

	Case 6	Case 7	Case 8	Case 9	Case 10
Car3					
Velocity after the second accident, ft/sec	100.97	98.62	97.07	96.51	95.44
Weight Ratio, C3/C2	1.00	1.00	1.00	1.00	1.00
Velocity before the second accident, ft/sec	60	60	60	60	60
Weight, pounds	4200	4800	5000	5100	5300
Car2					

Weight, Pounds	4200	4800	5000	5100	5300
Weight Ratio, C2/C1	1.05	1.23	1.39	1.46	1.61
Velocity after the first accident, ft/sec	81.93	77.24	74.14	73.01	70.88
Velocity before the first accident, ft/sec	50	50	50	50	50
Car1					
Weight, pounds	4000	3900	3600	3500	3300
Final Velocity (after skidding, and before first accident) ft/sec	67.06	67.06	67.06	67.06	67.06
Skidded Distance, ft	25	25	25	25	25
Pavement Friction	0.25	0.25	0.25	0.25	0.25
Deceleration, ft/sec ²	8.05	8.05	8.05	8.05	8.05
Initial Velocity, ft/sec	70	70	70	70	70

Table V. Engineering Calculations for Case 11 through Case 15 for Determining the Relationship between Vehicles Weight Ratio and Initial Velocity.

	Case 11	Case 12	Case 13	Case 14	Case 15
Car3					
Velocity after the second accident, ft/sec	93.54	92.35	91.65	90.68	90.03
Weight Ratio, C3/C2	1.00	1.00	1.00	1.00	1.00
Velocity before the second accident, ft/sec	60	60	60	60	60
Weight, pounds	5500	5700	5800	5900	6000
Car2					
Weight, Pounds	5500	5700	5800	5900	6000
Weight Ratio, C2/C1	1.96	2.28	2.52	2.95	3.33
Velocity after the first accident, ft/sec	67.07	64.71	63.30	61.37	60.06
Velocity before the first accident, ft/sec	50	50	50	50	50
Car1					
Weight, pounds	2800	2500	2300	2000	1800
Final Velocity (after skidding, and before first accident) ft/sec	67.06	67.06	67.06	67.06	67.06
Skidded Distance, ft	25	25	25	25	25
Pavement Friction	0.25	0.25	0.25	0.25	0.25
Deceleration, ft/sec ²	8.05	8.05	8.05	8.05	8.05
Initial Velocity, ft/sec	70	70	70	70	70

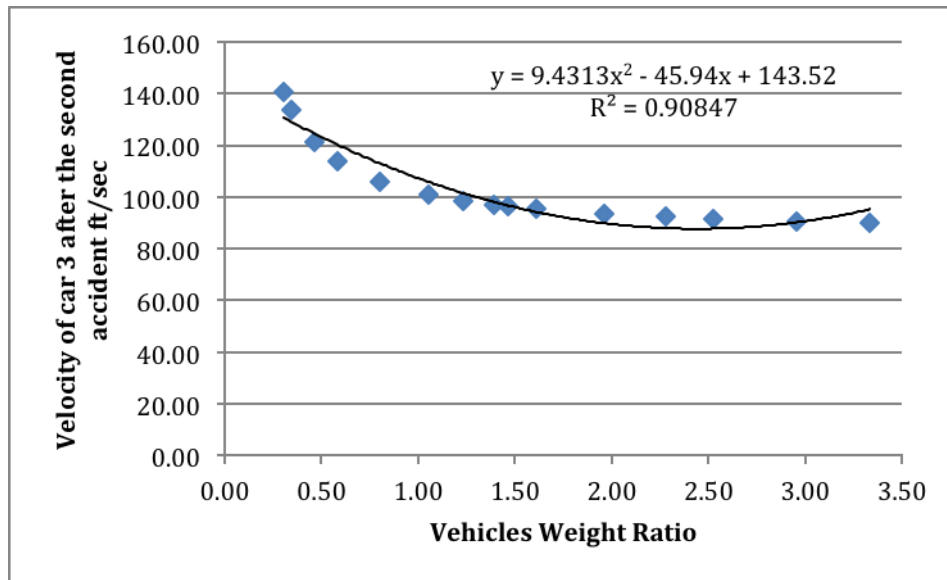


Figure 1 Influence of Vehicles Weight Ratio on the Initial Velocity

V. CONCLUSIONS

The following regression relationship was found with statistically significant correlation coefficient for predicting the performance of the engineering variables. The influence of Vehicles Weight Ratio on the Initial Velocity is shown by a quadratic equation (Initial velocity = 9.4313 Vehicles Weight Ratio ² – 45.94 Vehicles Weight Ratio +143.52) with R = 0.91.

VI. ACKNOWLEDGMENTS

The Republic Of Turkey, Ministry Of National Education Scholarships Is Duly Acknowledged For Providing Scholarship.

REFERENCES

- [1] Newton's Three Laws of Motion. <http://csep10.phys.utk.edu/astr161/lect/history/newton3laws.html>
- [2] First Law of Thermodynamics. <http://hyperphysics.phy-astr.gsu.edu/hbase/thermo/firlaw.html>
- [3] Engber, D. The Ferrari That Split in Half. 2006. http://www.slate.com/articles/news_and_politics/explainer/2006/04/the_ferrari_that_split_in_half.html
- [4] Accreditation Commission for Traffic Accident Reconstruction (ACTAR). <http://www.actar.org/>
- [5] Hurt, H. Jr. AMA Motorcycle Hall of Fame. <http://www.motorcyclemuseum.org/halloffame/detail.aspx?RacerID=398>
- [6] Brooks R. M.; Cetin M. Determination of the Influence of Vehicles Weight Ratio on the Initial Velocity Using the Accident Reconstruction Engineering Principles. International Journal of Emerging Technology and Advanced Engineering, Volume 3, Issue 3, ISSN: 2250-2459, S. No: 159, March 2013, pp. 927-931.
- [7] Brooks R. M.; Cetin M. Determination of the Influence of Pavement Friction on the Initial Velocity Using the Accident Reconstruction Engineering Principles. International Journal of Engineering Inventions, Volume 2, Issue 6, e-ISSN: 2278-7461, p-ISSN: 2319-6491, S. No: 9, April 2013, pp. 63-68.
- [8] Brooks R. M.; Cetin M. Determination of the Influence of Skidded Distance on the Initial Velocity Using the Accident Reconstruction Engineering Principles. International Journal of Research and Reviews in Applied Sciences, Volume 15, Issue 3, EISSN: 2076-7366, ISSN: 2076-734X, S. No: 3, June 2013, pp. 225-229.
- [9] Brooks R. M.; Cetin M. Pavement Friction V. Initial Velocity of Vehicle in Chain Accidents on Highways. International Journal of Engineering Inventions, Volume 3, Issue 2, S. No: 5, e-ISSN: 2278-7461, September 2013, pp. 27-31.
- [10] Brooks R. M.; Cetin M. Skidded Distance V. Initial Velocity of Vehicle in Chain Accidents on Highways. International Journal of Engineering and Science, Volume 3, Issue 1, Version 3, ISSN(e): 2319-1813, January 2014, pp. 10-14.
- [11] Brooks R. M.; Cetin M. Influence of Skidded Distance on the Initial Velocity of Vehicle in Chain Accidents at Intersections. International Journal of Modern Engineering Research, Volume 3, Issue 5, S. No:5 5, ISSN: 2249-6645, September-October 2013, pp. 2939-2943.
- [12] Brooks R. M.; Cetin M. Influence of Pavement Friction on the Initial Velocity of Vehicle in Chain Accidents at Intersections. International Journal of Emerging Technology and Advanced Engineering, Volume 3, Issue 7, S. No: 2, ISSN 2250-2459, July 2013, page 10-15.
- [13] Brooks R. M.; Cetin M. Influence of Vehicles Weight Ratio on the Initial Velocity of Vehicle in Chain Accidents at Intersections. International Journal of Research and Reviews in Applied Sciences, Volume 17, Issue 2, S. No: 9, ISSN 2076-734X, EISSN: 2076-7366, November 2013, pp. 212-217.

- [14] Moore D. S., McCabe G. P., and Craig, B. A., Introduction to the practice of statistics (W H Freeman & Co (Sd), 7th Edition, New York, 2005).
- [15] Devore J. L., and Farnum N. R., Applied statistics for engineers and scientists (Duxbury Press. ISBN 05435601X, 1st edition, 2004).
- [16] Montgomery, D.C., Design and analysis of experiments (John Wiley & Sons Inc. 7th edition, 2008).

To Study and Analyze To Foresee Market Using Data Mining Technique

¹Amit Khedkar, ²Prof. Rajendra Argiddi

^{1,2}Department of Computer Science & Engineering Walchand Institute of Technology, Solapur, India

ABSTRACT

In every field there is huge growth and demand in knowledge and information over the internet. The automation using data mining and predictive technologies are doing an advance amount of deals in the markets. Data mining is all based on the theory that the historic data holds the essential memory for predicting the future direction. This technology is designed to help shareholders to discover hidden patterns from the historic data that have probable predictive capability in their investment decisions. The prediction of stock markets is regarded as a challenging task of financial time series prediction. Data analysis is one way of predicting if future stocks prices will increase or decrease. There are some methods of analyzing stocks which were combined to predict if the day's closing price would increase or decrease. These methods include study of Price, Index, and Average. (For e.g. Typical Price (TP), Bands, Relative Strength Index (RSI), CMI and Moving Average (MA)).

KEYWORDS :Data mining, Stock prediction, Historical data

I. INTRODUCTION

Data mining means 'making better use of data'. Every human being is increasingly faced with unmanageable amounts of data; hence, data mining or knowledge discovery apparently affects all of us. It is therefore recognized as one of the key research areas. Ideally, we would like to develop techniques for "making better use of any kind of data for any purpose". However, we argue that this goal is too demanding yet. Over the last three decades, increasingly large amounts of historical data have been stored electronically and this volume is expected to continue to grow considerably in the future. Yet despite this wealth of data, many fund managers have been unable to fully capitalize on their value. This paper attempts to determine if it is possible to predict if the closing price of stocks will increase or decrease on the following day. The approach taken in this paper was to combine six methods of analyzing stocks and use them to automatically generate a prediction of whether or not stock prices will go up or go down. After the predictions were made they were tested with the following day's closing price. If the following day's closing price can be predicted to increase or decrease 70% of the time at the 0.07 confidence level, then this analysis would be an easy and useful aid in financial investing. Furthermore, the results would show that the results are better than random at a reasonable level of significance. Many fund management firms have invested heavily in information technology to help them manage their financial portfolios.

Over the last three decades, increasingly large amounts of historical data have been stored electronically and this volume is expected to continue to grow considerably in the future. Yet despite this wealth of data, many fund managers have been unable to fully capitalize on their value. This is because information that is implicit in the data for the purpose of investment is not easy to discern. For example, a fund manager may keep detailed information about each stock and its historic data but still it is difficult to pinpoint the subtle buying patterns until systematic explorative studies are conducted. The automated computer programs using data mining and predictive technologies do a fare amount of trades in the markets. Data mining is well founded on the theory that the historic data holds the essential memory for predicting the future direction. This technology is designed to help investors discover hidden patterns from the historic data that have probable predictive capability in their investment decisions. This is an attempt, made to maximize the prediction of financial stock markets using data mining techniques. Predictive patterns from quantitative time series analysis will be invented fortunately, a field known as data mining using quantitative analytical techniques is helping to discover previously undetected patterns present in the historic data to determine the buying and selling points of equities. When market beating strategies are discovered via data mining, there are a number of potential problems in making the leap from a back-tested strategy to successfully investing in future real world conditions.

The first problem is determining the probability that the relationships are not random at all market conditions. This is done using large historic market data to represent varying conditions and confirming that the time series patterns have statistically significant predictive power for high probability of profitable trades and high profitable.

II. PROBLEM STATEMENT

The aim is to propose a model which can calculate and tell the user about the investment in the stock market. Market analysis is the basis for the prediction.

III. SYSTEM DESIGN

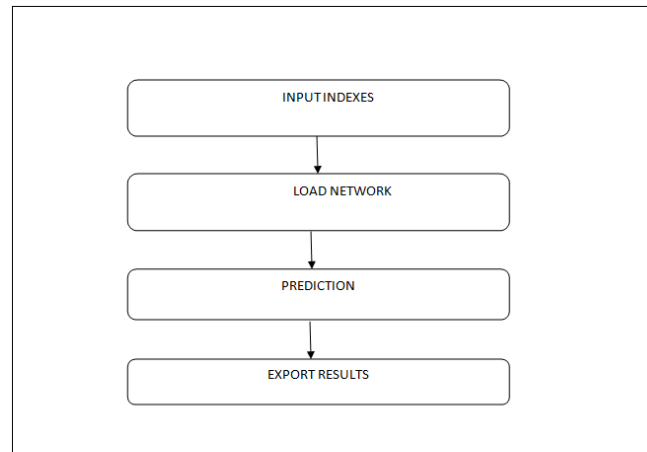


Fig. System Design

Indexes are the basic inputs for the network. Network is trained on provision of the input. It is possible to predict the future depending on the analysis. Design flow works on the same principal. At last whatever the results we got we save it for the prediction.

IV. METHODOLOGY

Five methods of analyzing stocks were combined to predict if the following day's closing price would increase or decrease. All five methods needed to be in agreement for the algorithm to predict a stock price increase or decrease. The five methods were Typical Price (TP), Chaikin Money Flow indicator (CMI), Stochastic Momentum Index (SMI), Relative Strength Index (RSI), Moving Average (MA) and Bollinger Signal.

Algorithm:

1. Give High, Low, Close values of the daily share as the input
2. Take an output array and add the values of H, L, and C
3. Divide the total by 3

$$(TP - [H + L + C]/3)$$

Where, H=High; L=Low; C=Close. Where the TP greater than the bench mark we have to sell or to buy.

Chaikin Money Flow Indicator

Chaikin's money flow is based on Chaikin's accumulation/distribution. Accumulation/distribution in turn, is based on the premise that if the stock closes above its midpoint $[(high+low)/2]$ for the day, then there was accumulation that day, and if it closes below its midpoint, then there was distribution that day. Chaikin's money flow is calculated by summing the values of accumulation/distribution for 13 periods and then dividing by the 13-period sum of the volume. It is based upon the assumption that a bullish stock will have a relatively high close price within its daily range and have increasing volume. However, if a stock consistently closed with a relatively low close price within its daily range with high volume, this would be indicative of a weak security. There is pressure to buy when a stock closes in the upper half of a period's range and there is selling pressure when a stock closes in the lower half of the period's trading range. Of course, the exact number of periods for the indicator should be varied according to the sensitivity sought and the time horizon of individual investor. An obvious bearish signal is when Chaikin Money Flow is less than zero.

A reading of less than zero indicates that a security is under selling pressure or experiencing distribution. An obvious bearish signal is when Chaikin Money Flow is less than zero. A reading of less than zero indicates that a security is under selling pressure or experiencing distribution. A second potentially bearish signal is the length of time that Chaikin Money Flow has remained less than zero. The longer it remains negative, the greater the evidence of sustained selling pressure or distribution. Extended periods below zero can indicate bearish sentiment towards the underlying security and downward pressure on the price is likely. The third potentially bearish signal is the degree of selling pressure. This can be determined by the oscillator's absolute level. Readings on either side of the zero line or plus or minus 0.10 are usually not considered strong enough to warrant either a bullish or bearish signal. Once the indicator moves below -0.10, the degree selling pressure begins to warrant a bearish signal. Likewise, a move above +0.10 would be significant enough to warrant a bullish signal. Marc Chaikin considers a reading below -0.25 to be indicative of strong selling pressure. Conversely, a reading above +0.25 is considered to be indicative of strong buying pressure. The Chaikin Money Flow is based upon the assumption that a bullish stock will have a relatively high close price within its daily range and have increasing volume. This condition would be indicative of a strong security. However, if it consistently closed with a relatively low close price within its daily range and high volume, this would be indicative of a weak security.

The Following formula was used to calculate CMI.

$$\text{CMI} = \frac{\sum(\text{AD},n)}{\sum(\text{VOL},n)} ;$$
$$\text{AD} = \text{VOL} \left[\frac{\text{CL} - \text{OP}}{\text{HL} - \text{LO}} \right]$$

Where, AD stands for Accumulation Distribution, n=Period, CL=today's close price; OP=today's open price, HI=High Value; LO=Low value

Stochastic Momentum Index

The Stochastic Momentum Index (SMI) is based on the Stochastic Oscillator. The difference is that the Stochastic Oscillator calculates where the close is relative to the high/low range, while the SMI calculates where the close is relative to the midpoint of the high/low range. The values of the SMI range from +100 to -100. When the close is greater than the midpoint, the SMI is above zero, when the close is less than the midpoint, the SMI is below zero. The SMI is interpreted the same way as the Stochastic Oscillator. Extreme high/low SMI values indicate overbought/oversold conditions. A buy signal is generated when the SMI rises above -50, or when it crosses above the signal line. A sell signal is generated when the SMI falls below +50, or when it crosses below the signal line. Also look for divergence with the price to signal the end of a trend or indicate a false trend.

Relative Strength Index

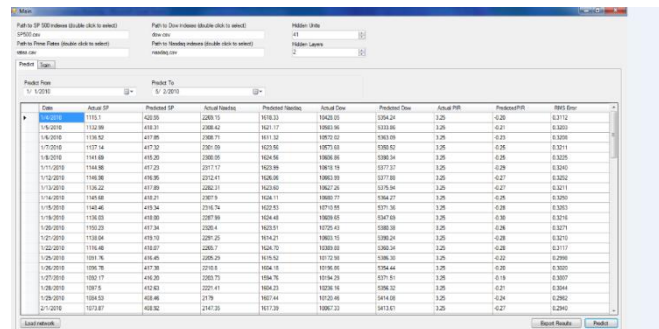
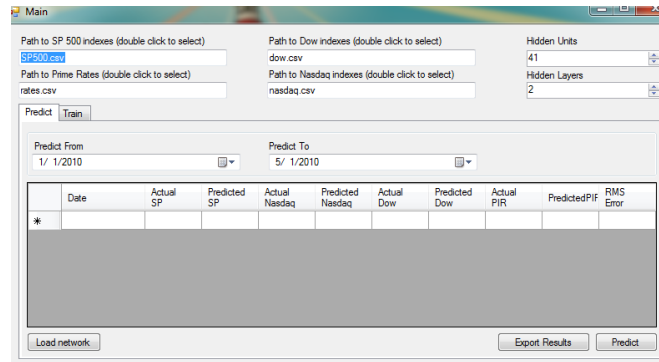
This indicator compares the number of days a stock finishes up with the number of days it finishes down. It is calculated for a certain time span usually between 9 and 15 days. The average number of up days is divided by the average number of down days. This number is added to one and the result is used to divide 100. This number is subtracted from 100. The RSI has a range between 0 and 100. A RSI of 70 or above can indicate a stock which is overbought and due for a fall in price. When the RSI falls below 30 the stock may be oversold and is a good they can vary depending on whether the market is bullish or bearish. RSI charted over longer periods tend to show less extremes of movement. Looking at historical charts over a period of a year or so can give a good indicator of how a stock price moves in relation to its RSI.

Moving Average

The most popular indicator is the moving average. This shows the average price over a period of time. For a 30 day moving average you add the closing prices for each of the 30 days and divide by 30. The most common averages are 20, 30, 50, 100, and 200 days. Longer time spans are less affected by daily price fluctuations. A moving average is plotted as a line on a graph of price changes. When prices fall below the moving average they have a tendency to keep on falling.

V. RESULTS AND ANALYSIS

The Output is best located on a web page given below in snapshots. The GUI for the application will look and seems much user friendly. The numerical data that will be retrieved are located in a systematic fashion.



Other information related to the results such as total no. of results retrieved and time to of retrieval is easy & shown in a simple but effective manner.

VI. CONCLUSION AND FINDINGS

The results show that this work is able to predict that the day's closing price would increase or decrease better than chance (50%) with some level of significance. Furthermore, this shows that there is some validity to technical analysis of stocks. These efforts may be useful for trading analysis.

REFERENCES

- [1] Financial Stock Market Forecast using Data Mining Techniques (K. Senthamarai Kannan, P. Sailapathi Sekar, M.Mohamed Sathik and P. Arumugam) (IMECS International Multiconference of Engineers and Computer Scientists, 2010, Hong Kong)
- [2] Hunter, (2007). Hedge Funds Do About 60% Of Bond Trading, Study Says, The Wall Street Journal.
- [3] Durbin Hunte, (2007). "Hedge Funds Do About 60% Of Bond Trading, Study Says", The Wall Street Journal.
- [4] Hossein Nikooa, Mahdi Azarpeikanb, Mohammad Reza Yousefiba,c, Reza Ebrahimpourb,c, and Abolfazl Shahrabadi,d (2007). "Using A Trainable Neural Ntwork Ensemble for Trend Prediction of Tehran Stock Exchange" IJCSNS International Journal of Computer Science and Network Security, VOL.7 No.12.
- [5] Jiarui Ni and Chengqi Zhang (2006). A Human-Friendly MAS for Mining Stock Data IEEE / WIC / ACM International onference on Web Intelligence and Intelligent Agent Technology.
- [6] Amaury Lendasse, Francesco Corona, Antti Sorjamaa, Elia Liitiäinen, Tuomas Kärnä, Yu Qi, Emil Eirola, Yoan Mich'e, Yongnang Ji, Olli Simula, (2006). "Time series prediction".
- [7] Juliana Yim , Heather Mitchell (2005). A comparison of corporate distress prediction models in Brazil, nova Economia_Belo Horizonte, 15 (1), 73-93.
- [8] Eamonn Keogh, Stefano Lonardi, (2004). Chotirat Ann Ratanamahatana Towards Parameter-Free Data Mining, KDD '04.
- [9] Garth Garner, Prediction of Closing Stock Prices, (2004). This work was completed as part of a course project for Engineering Data Analysis and Modeling at Portland State University.

Multiple Single Input Change Vectors for Built-In Self Test (MSIC-BIST)

¹Praveenkumar.J ²Danesh.K

^{1,2}M.E VLSI Design ARM CET Maraimalainagar, India.
ARM CET

ABSTRACT:

Digital circuit's complexity and density are increasing while, at the same time, more quality and reliability are required. These trends, together with high test costs, make the validation of VLSI circuits more and more difficult. In this project we introduce the automatic test pattern generator with multiple single input change (SIC) vectors for post silicon validation schemes. Choosing a best device leads to challenges in various factors, In this paper performs a novel test pattern generator (TPG) for built-in self-test. Our method generates multiple single input change (MSIC) vectors in a pattern, i.e., each vector applied to a scan chain is an SIC vector. A reconfigurable Johnson counter and a scalable SIC counter are developed to generate a class of minimum transition sequences. The designed TPG is flexible to both the test-per-clock and the test-per-scan schemes. A theory is also developed to represent and analyze the sequences and to extract a class of MSIC sequences. Analysis results show that the produced MSIC sequences have the favorable features of uniform distribution and low input transition density. The performances of the designed TPGs and the circuits under test with 45 nm are evaluated. Simulation results with ISCAS benchmarks demonstrate that MSIC can save test power and impose no more than 7.5% overhead for a scan design. It also achieves the target fault coverage without increasing the test length.

INDEX TERMS: Built in self test, single input change vectors, test pattern generator, Johnson counter.

I. INTRODUCTION

Built-In Self-Test (BIST) techniques used in the VLSI testing. It can be reduce the difficulty and complexity of VLSI testing. The conventional BIST architectures, the linear feedback shift register (LFSR) is commonly used in the test pattern generators (TPGs) and output response analyzers. The major drawback of these architectures is that the pseudorandom patterns generated by the LFSR lead to significantly high switching activities in the CUT [1], which can cause excessive power dissipation. Several advanced BIST techniques have been studied and applied. The first class is the LFSR tuning. Girard et al. analyzed the impact of an LFSR's polynomial and seed selection on the CUT's switching activity, and proposed a method to select the LFSR seed for energy reduction. The second class is low-power TPGs. One approach is to design low-transition TPGs. Wang and Gupta used two LFSRs of different speeds to control those inputs that have elevated transition densities [5]. Corno *et al.* provided a low power TPG based on the cellular automata to reduce the test power in combinational circuits [6]. Another approach focuses on modifying LFSRs. The scheme in [7] reduces the power in the CUT in general and clock tree in particular. In [8], a low-power BIST for data path architecture is proposed, which is circuit dependent. However, this dependency implies that non detecting subsequences must be determined for each circuit test sequence. Bonhomme *et al.* [9] used a clock gating technique where two non overlapping clocks control the odd and even scan cells of the scan chain so that the shift power dissipation is reduced by a factor of two. The ring generator [10] can generate a single-input change (SIC) sequence which can effectively reduce test power. The third approach aims to reduce the dynamic power dissipation during scan shift through gating of the outputs of a portion of the scan cells. Bhunia *et al.* [11] inserted blocking logic into the stimulus path of the scan flip-flops to prevent the propagation of the scan ripple effect to logic gates. The need for transistors insertion, however, makes it difficult to use with standard cell libraries that do not have power-gated cells. In [12], the efficient selection of the most suitable subset of scan cells for gating along with their gating values is studied.

Existing System:-

In the existing design a Test Pattern Generator is flexible to both the test-per-clock and the test-per-scan schemes were realized. A theory is also developed to represent and analyze the sequences and to extract a class of MSIC sequences. Analysis results show that the produced MSIC sequences have the favorable features of uniform distribution and low input transition density. The performances of the designed TPGs and the circuits under test with 45 nm are evaluated.

Proposed System:-

In the proposed system a sample module is created to do the Built in self test algorithm using automatic test pattern generation also user defined test pattern generation option also we design, The entire hardware is realized as digital circuits and the test results are simulated in Modelsim.

II MSIC-TPG SCHEME

A TPG scheme that can convert an SIC vector to unique low transition vectors for multiple scan chains. First, the SIC vector is decompressed to its multiple code words.

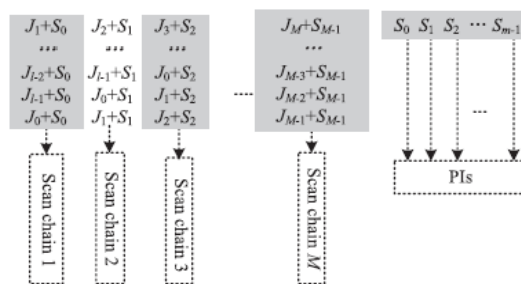


Fig.1 Symbolic representation of an MSIC pattern.

Meanwhile, the generated code words will bit-XOR with a same seed vector in turn. Hence, a test pattern with similar test vectors will be applied to all scan chains. The proposed MSIC-TPG consists of an SIC generator, a seed generator, an XOR gate network, and a clock and control block.

A. Test Pattern Generation Method

There are m primary inputs (PIs) and M scan chains in a full scan design, and each scan chain has scan cells. Fig. 1(a) shows the symbolic simulation for one generated pattern. The vector generated by an m-bit LFSR with the primitive polynomial can be expressed as $S(t) = S_0(t)S_1(t)S_2(t), \dots, S_{m-1}(t)$ (hereinafter referred to as the seed), and the vector generated by an l-bit Johnson counter can be expressed as $J(t) = J_0(t)J_1(t)J_2(t), \dots, J_{l-1}(t)$. The first clock cycle, $J = J_0 J_1 J_2, \dots, J_{l-1}$ will bit-XOR with $S = S_0S_1S_2, \dots, S_{m-1}$, and the results $X_1X_{l+1}X_{2l+1}, \dots, X_{(M-1)l+1}$ will be shifted into M scan chains, respectively. In the second clock cycle, $J = J_0 J_1 J_2, \dots, J_{l-1}$ will be circularly shifted as $J = J_{l-1} J_0 J_1, \dots, J_{l-2}$, which will also bit-XOR with the seed $S = S_0S_1S_2, \dots, S_{m-1}$. The resulting $X_2X_{l+2}X_{2l+2}, \dots, X_{(M-1)l+2}$ will be shifted into M scan chains, respectively. After l clocks, each scan chain will be fully loaded with a unique Johnson codeword, and seed $S_0S_1S_2, \dots, S_{m-1}$ will be applied to m PIs. Therefore circular Johnson counter can generate l unique Johnson code words through circular shifting a Johnson vector, the circular Johnson counter and XOR gates in Fig. 1 actually constitute a linear sequential de compressor.

B. Reconfigurable Johnson Counter

The different scenarios of scan length, this paper develops two kinds of SIC generators to generate Johnson vectors and Johnson code words, i.e., the reconfigurable Johnson counter and the scalable SIC counter.

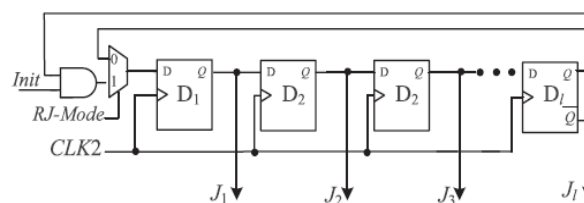


Fig.2 Reconfigurable Johnson counter.

III MSIC SEQUENCES

The proposed algorithm is to reduce the switching activity. In order to reduce the hardware overhead, the linear relations are selected with consecutive vectors or within a pattern, which can generate a sequence with a sequential de compressor, facilitating hardware implementation. Another requirement is that the MSIC sequence should not contain any repeated test patterns, because repeated patterns could prolong the test time and reduce test efficiency.

Scalable SIC Counter: The maximal scan chain length l is much larger than the scan chain number M , we develop an SIC counter named the “scalable SIC counter.” As shown in Fig. 2(b), it contains a k -bit adder clocked by the rising SE signal, a k -bit subtract or clocked by test clock $CLK2$, an M -bit shift register clocked by test clock $CLK2$, and k multiplexers. The value of k is the integer of $\log_2(l - M)$. The waveforms of the scalable SIC counter are shown in Fig. 2(c). The k -bit adder is clocked by the falling SE signal, and generates a new count that is the number of 1s (0s) to fill into the shift register. As shown in Fig. 2(b), it can operate in three modes.

- 1) If $SE = 0$, the count from the adder is stored to the k -bit subtract or. During $SE = 1$, the contents of the k -bit subtract or will be decreased from the stored count to all zeros gradually.
- 2) If $SE = 1$ and the contents of the k -bit subtract or are not all zeros, M -Johnson will be kept at logic 1 (0).
- 3) Otherwise, it will be kept at logic 0 (1). Thus, the needed 1s (0s) will be shifted into the M -bit shift register by clocking $CLK2$ l times, and unique Johnson code words will be applied into different scan chains.

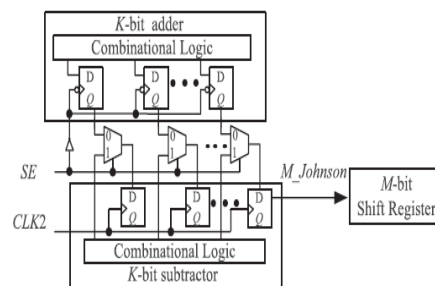


Fig.3 Scalable SIC counter.

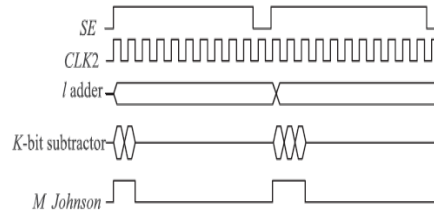


Fig.4 Waveforms of the scalable SIC counter

MSIC-TPGs for Test-per-Clock Schemes: The CUT's PIs $X1 - X_{mn}$ are arranged as an $n \times m$ SRAM-like grid structure. Each grid has a two-input XOR gate whose inputs are tapped from a seed output and an output of the Johnson counter. The outputs of the XOR gates are applied to the CUT's PIs. A seed generator is an m -stage conventional LFSR, and operates at low frequency $CLK1$. The test procedure is as follows.

- 1) The seed generator generates a new seed by clocking $CLK1$ one time.
- 2) The Johnson counter generates a new vector by clocking $CLK2$ one time.
- 3) Repeat 2 until 21 Johnson vectors are generated.
- 4) Repeat 1–3 until the expected fault coverage or test length is achieved.

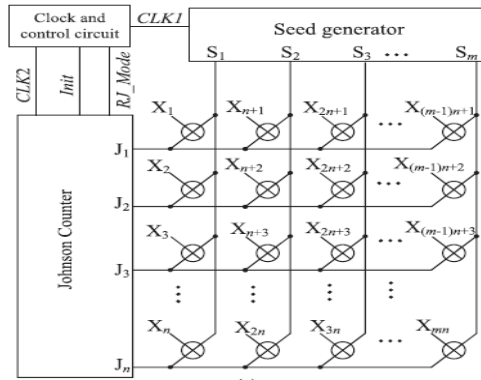


Fig.5 Test-Per-Clock

MSIC-TPGs for Test-per-Scan Schemes: The MSIC-TPG for test-per-scan schemes is illustrated in Fig. 3(b). The stage of the SIC generator is the same as the maximum scan length, and the width of a seed generator is not smaller than the scan chain number. The inputs of the XOR gates come from the seed generator and the SIC counter, and their outputs are applied to M scan chains, respectively. The outputs of the seed generator and XOR gates are applied to the CUT's PIs, respectively. The test procedure is as follows.

- 1) The seed circuit generates a new seed by clocking CLK1 one time.
- 2) RJ_Mode is set to "0". The reconfigurable Johnson counter will operate in the Johnson counter mode and generate a Johnson vector by clocking CLK2 one time.
- 3) After a new Johnson vector is generated, RJ_Mode and Init are set to 1. The reconfigurable Johnson counter operates as a circular shift register, and generates l code words by clocking CLK2 l times. Then, a capture operation is inserted.
- 4) Repeat 2–3 until $2l$ Johnson vectors are generated.
- 5) Repeat 1–4 until the expected fault coverage or test length is achieved.

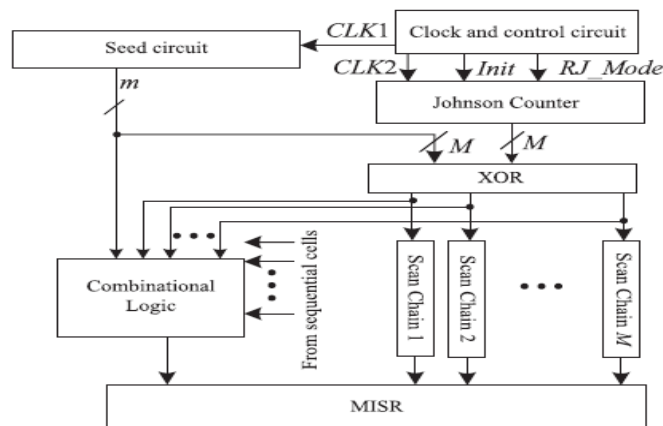


Fig.6 Test-Per-Scan

IV RESULTS

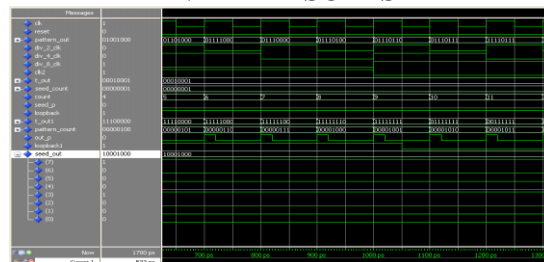


Fig.7 Output For Test Per Clock

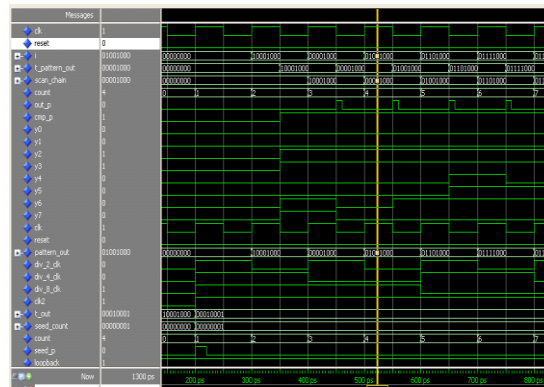


Fig.8 Output for Test per Scan

V CONCLUSION

This paper proposed a low-power test pattern generation method for giving the patterns to the device under test. In this we generate the multiple single input change vectors from the seed produced by conventional 8_bit pseudo random number generator. The power consumption of our proposed system has low because of low transaction behavior of the system. Analysis results showed that an MSIC sequence had the favorable features of uniform distribution, low input transition density, and low dependency relationship between the test length and the TPG's initial states. Combined with the proposed reconfigurable Johnson counter or scalable SIC counter, the MSIC-TPG can be easily implemented, and is flexible to test-per-clock schemes and test-per-scan schemes. Experimental results and analysis results demonstrate that the MSIC-TPG is scalable to scan length, and has negligible impact on the test overhead. After the generating the MSIC, in this we conduct the validation process on the combinational logic circuit and verified the output.

REFERENCES

- [1] Y. Zorian, "A distributed BIST control scheme for complex VLSI devices," in 11th Annu. IEEE VLSI Test Symp. Dig. Papers, Apr. 1993, pp. 4–9.
- [2] P. Girard, "Survey of low-power testing of VLSI circuits," IEEE Design Test Comput., vol. 19, no. 3, pp. 80–90, May–Jun. 2002.
- [3] A. Abu-Issa and S. Quigley, "Bit-swapping LFSR and scan-chain ordering: A novel technique for peak- and average-power reduction in scan-based BIST," IEEE Trans. Comput.-Aided Design Integr. Circuits Syst., vol. 28, no. 5, pp. 755–759, May 2009.
- [4] P. Girard, L. Guiller, C. Landrault, S. Pravossoudovitch, J. Figueras, S. Manich, P. Teixeira, and M. Santos, "Low-energy BIST design: Impact of the LFSR TPG parameters on the weighted switching activity," in Proc. IEEE Int. Symp. Circuits Syst., vol. 1, Jul. 1999, pp. 110–113.
- [5] S. Wang and S. Gupta, "DS-LFSR: A BIST TPG for low switching activity," IEEE Trans. Comput.-Aided Design Integr. Circuits Syst., vol. 21, no. 7, pp. 842–851, Jul. 2002.
- [6] F. Corno, M. Rebaudengo, M. Reorda, G. Squillero, and M. Violante, "Low power BIST via non-linear hybrid cellular automata," in Proc. 18th IEEE VLSI Test Symp., Apr.–May 2000, pp. 29–34.
- [7] P. Girard, L. Guiller, C. Landrault, S. Pravossoudovitch, and H. Wunderlich, "A modified clock scheme for a low power BIST test pattern generator," in Proc. 19th IEEE VTS VLSI Test Symp., Mar.–Apr. 2001, pp. 306–311.
- [8] D. Gizopoulos, N. Krantitis, A. Paschalis, M. Psarakis, and Y. Zorian, "Low power/energy BIST scheme for datapaths," in Proc. 18th IEEE VLSI Test Symp., Apr.–May 2000, pp. 23–28.
- [9] Y. Bonhomme, P. Girard, L. Guiller, C. Landrault, and S. Pravossoudovitch, "A gated clock scheme for low power scan testing of logic ICs or embedded cores," in Proc. 10th Asian Test Symp., Nov. 2001, pp. 253–258.
- [10] C. Laoudias and D. Nikolos, "A new test pattern generator for high defect coverage in a BIST environment," in Proc. 14th ACM Great Lakes Symp. VLSI, Apr. 2004, pp. 417–420.
- [11] S. Bhunia, H. Mahmoodi, D. Ghosh, S. Mukhopadhyay, and K. Roy, "Low-power scan design using first-level supply gating," IEEE Trans. Very Large Scale Integr. (VLSI) Syst., vol. 13, no. 3, pp. 384–395, Mar. 2005.
- [12] X. Kavousianos, D. Bakalis, and D. Nikolos, "Efficient partial scan cell gating for low-power scan-based testing," ACM Trans. Design Autom. Electron. Syst., vol. 14, no. 2, pp. 28–1–28–15, Mar. 2009.
- [13] P. Girard, L. Guiller, C. Landrault, and S. Pravossoudovitch, "A test vector inhibiting technique for low energy BIST design," in Proc. 17th IEEE VLSI Test Symp., Apr. 1999, pp. 407–412.
- [14] S. Manich, A. Gabarro, M. Lopez, J. Figueras, P. Girard, L. Guiller, C. Landrault, S. Pravossoudovitch, P. Teixeira, and M. Santos, "Low power BIST by filtering non-detecting vectors," J. Electron. Test.-Theory Appl., vol. 16, no. 3, pp. 193–202, Jun. 2000.
- [15] F. Corno, M. Rebaudengo, M. Reorda, and M. Violante, "A new BIST architecture for low power circuits," in Proc. Eur. Test Workshop, May 1999, pp. 160–164.

Design and Implementation of Testable Reversible Sequential Circuits Optimized Power

¹, Manikandan.B, ², Vijayaprabhu.A

¹ M.E. VLSI Design Svcet, Tiruvallur

² Assistant Professor Ece Dept Svcet, Tiruvallur

ABSTRACT:

The conservative reversible gates are used to designed reversible sequential circuits. The sequential circuits are flip flops and latches. The conservative logic gates are Feynman, Toffoli, and Fredkin. The design of two vectors testable sequential circuits based on conservative logic gates. All sequential circuit based on conservative logic gates can be tested for classical unidirectional stuck-at faults using only two test vectors. The two test vectors are all 1s, and all 0s. The designs of two vectors testable latches, master-slave flip-flops and double edge triggered (DET) flip-flops are presented. We also showed the application of the proposed approach toward 100% fault coverage for single missing/additional cell defect in the quantum-dot cellular automata (QCA) layout of the Fredkin gate. The conservative logic gates are in terms of complexity, speed and area.

I. INTRODUCTION

Reversible sequential circuits are considered as significant memory block for their ultra-low power consumption. Conservative logic is called reversible conservative logic when there is a one-to-one mapping between the inputs and the outputs vectors along with the property that there are equal numbers of 1s in the outputs as in the inputs.

Conservative logic can be reversible in nature or may not be reversible in nature. Reversibility is the property of circuits in which there is one to- one mapping between the inputs and the output vectors that is for each input vector there is a unique output vector and vice-versa.

QCA is one of the emerging nanotechnologies in which it is possible to implement reversible logic gates. QCA makes it possible to achieve circuit densities and clock frequencies beyond the limits of existing CMOS technology. In QCA, computing logic states of 1 and 0 are represented by the position of the electrons inside the QCA cell. Thus, when the bit is flipped from 1 to 0 there is no actual discharging of the capacitor as in conventional CMOS. Hence, QCA does not have to dissipate all its signal energy during transition. Further, propagation of the polarization from one cell to another is because of interaction of the electrons in adjacent QCA cells. As there is no movement of electrons from one QCA cell to the other, there is no current flow. Therefore, QCA has significant advantage compared to CMOS technology in terms of power dissipation. Due to high error rates in nano-scale manufacturing, QCA and other nanotechnologies target reducing device error rates.

This paper is organized as follows. Section II presents the conservative logic gates, Section III presents design of testable reversible latches, Section IV describes QCA, Section V presents design of testable reversible flip-flop, Section VI discusses the application of the proposed two vectors, all 0s and all 1s, Section VII provides some discussions and conclusions.

II. CONSERVATIVE LOGIC GATES

In order to design the sequential circuits, the conventional logic gates are appropriately designed from the reversible gates. The reversible gates used to design the conventional logic are so chosen to minimize the number of reversible gates used and garbage outputs produced. The design of AND function using Fredkin gate. The design of NAND and NOR function using New Gate respectively. Feynman Gates can be used for copying the outputs and to avoid the fan out problem in reversible logic. In the Feynman gate, there are exactly two outputs corresponding to the inputs and a '0' in the second input will copy the first input to both the outputs of that gate. Hence it can be concluded that Feynman gate is the most suitable gate for single copy of bit since it does not produces any garbage output. The Feynman gate as copying output and NOT function respectively. May stuck at 0 or 1 leading to accessing wrong address, no address, or multiple addresses.

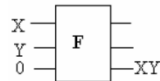


Fig.1 Fredkin Gate as AND Gate

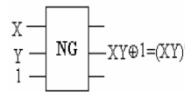


Fig.2 New Gate As NAND Gate

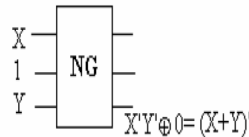


Fig.3 New Gate As NOR Gate

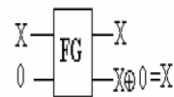


Fig.4 Feynman Gate As Copying Output

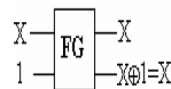


Fig.5 Feynman Gate As Not Gate

Novel Reversible Flip Flops are designed using Feynman Gate, New gate and Fredkin Gate. The designed FFs are highly optimized in terms of number of reversible gates and garbage outputs.

Gate Type	Functionality
1*1 Not	$x^+ = \bar{x}$
2*2 Feynman [4]	$x^+ = x$ $y^+ = x \oplus y$
3*3 Toffoli [19]	$x^+ = x$ $y^+ = y$ $z^+ = xy \oplus z$
3*3 Fredkin [5]	$x^+ = x$ $y^+ = \bar{x}y \oplus xz$ $z^+ = \bar{x}z \oplus xy$

Table.1 Gate functionality

Reversible logic elements, both with and without the property of conservatism, can be defined in many different logic systems. For the purposes of this paper, the class of reversible elements that can be modeled as binary-valued logic circuits will be called classical reversible logic elements. Much work has been done in defining and characterizing classical reversible logic and applying the concepts toward power conservation and specific technology implementations. This section will briefly define basic results in classical reversible logic.

III. DESIGN REVERSIBLE LATCHES

The characteristic equation of the D latch can be written as $Q+ = D \cdot E + .E \cdot Q$. In the proposed work, enable (E) refers to the clock and is used interchangeably in place of clock. When the enable signal (clock) is 1, the value of the input D is reflected at the output that is $Q+ = D$. While, when $E = 0$ the latch maintains its previous state, that is $Q+ = Q$. The reversible Fredkin gate has two of its outputs working as 2:1 MUXes, thus the characteristic equation of the D latch can be mapped to the Fredkin gate (F). The realization of the reversible D latch using the Fredkin gate. But FO is not allowed in conservative reversible logic. Moreover, the design cannot be tested by two input vectors all 0s and all 1s because of feedback, as the output Q would latch 1 when the inputs are toggled from all 1s to all 0s and could be misinterpreted as stuck-at-1 fault.

In this paper, we propose to cascade another Fredkin gate to output Q as shown in Fig. The design has two control signals, $C1$ and $C2$. The design can work in two modes: normal mode and test mode.

A. NORMAL MODE

The normal mode is shown in Fig. in which we will have $C1C2 = 01$ and we will have the design working as a D latch without any fan-out problem.

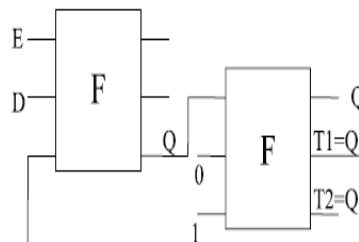


Fig.6 Fredkin gate based D Latch in normal mode: $C1 = 0$ and $C2 = 1$

B. TEST MODE

In test mode, when $C1C2 = 00$ as shown in Fig. it will make the design testable with all 0s input vectors as output $T1$ will become 0 resulting in making it testable with all 0s input vectors. Thus, any stuck-at-1 fault can be detected. When $C1C2 = 11$ as shown in Fig. the output $T1$ will become 1 and the design will become testable with all 1s input vectors for any stuck-at-0 fault. It can be seen from above that $C1$ and $C2$ will disrupt the feedback in test mode, and in normal mode will take care of the fan-out. Thus, our proposed design works as a reversible D latch and can be tested with only two test vectors, all 0s and all 1s, for any stuck-at fault by utilizing the inherent property of conservative reversible logic.

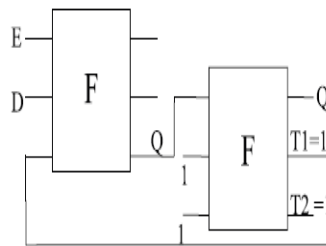


Fig.7 Fredkin gate based D latch in test mode for stuck-at-0 fault: $C1 = 1$ and $C2 = 1$.

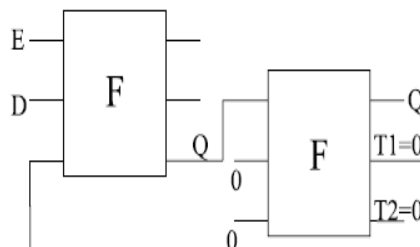


Fig.8 Fredkin gate based D latch in test mode for stuck-at-1 fault: $C1 = 0$ and $C2 = 0$.

IV. QUANTUM-DOT CELLULAR AUTOMATA

Quantum-dot cellular automata (QCA) is a nanotechnology that has recently been recognized as one of the top six emerging technologies with potential applications in future computers. Several studies have reported that QCA can be used to design general-purpose computational and memory circuits. First proposed in 1993 by Lent et al., and experimentally verified in 1997, QCA is expected to achieve high device density, extremely low power consumption, and very high switching speed. The fundamental QCA logic primitives are the three-input majority gate, wire, and inverter. Each of these can be considered as a separate QCA locally interconnected structure, where QCA digital architectures are combinations of these cellular automata structures. Traditional logic reduction methods, such as Karnaugh maps (K-maps), always produce simplified expressions in the two standard forms: sum of products (SOP) or product of sums (POS). However, we will encounter difficulties in converting these two forms into majority expressions due to the complexity of multilevel majority gates. In CMOS/silicon design, the logic circuits are usually implemented using AND, OR gates based on SOP or POS formats. However, since QCA logic is based on a majority gate primitive, it is critical that an efficient technique be established for designing with this primitive. In this paper, we develop a Boolean algebra based on a geometrical interpretation of three-variable Boolean functions to facilitate the conversion of sum-of-products expressions into reduced majority logic. Thirteen standard functions are introduced, which represent all possible three-variable Boolean functions. For each of these standard functions, we present the reduced majority expression. As an example of this technique, we present a QCA adder design, and show that the proposed method is able to reduce the total hardware, as compared to previously published designs.

A. QCA LOGIC DEVICES

The fundamental QCA logic primitives include a QCA wire, QCA inverter, and QCA majority gate, as described below.

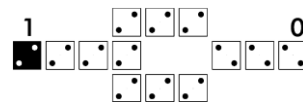


Fig.9 QCA Inverter

B. QCA Clock

A QCA clock consists of four phases which are called Switch, Hold, Release, and Relax as shown in Fig. During the Switch phase, the inter dot barriers are slowly raised and the QCA cells become polarized according to the state of their drivers (that is, their input cells). During the Hold phase, the interdot barriers are kept high and the QCA cells

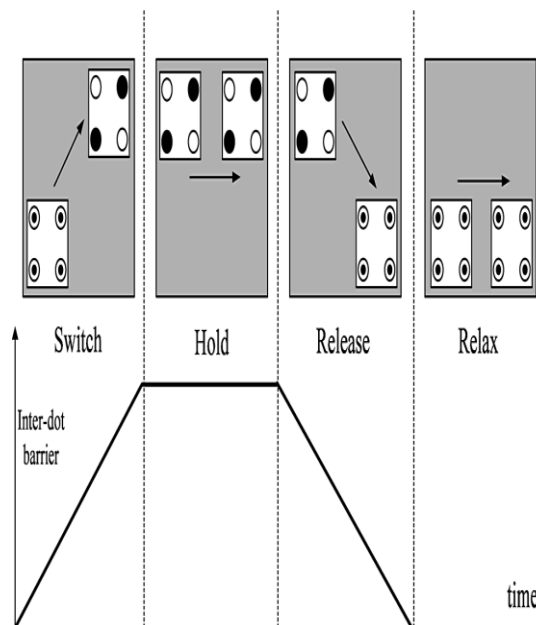


Fig.10 Four phases of a QCA clock.

retain their states. In the Release phase, the barriers are lowered and the cells are allowed to relax to an unpolarized state. Finally, in the Relax phase, the barriers are kept low and the cells remain unpolarized. A QCA circuit is partitioned into serial zones. These zones can be of irregular shape, but their size must be within certain limits imposed by fabrication and dissipation concerns. All cells in the same zone are controlled by the common clock signal. The scheme of clock zones permits an array of QCA cells to make a certain calculation and then have its state frozen, and finally, have its output serve as the input to the next clock zone.

V. REVERSIBLE FLIP-FLOP

The D flip flop is a modification of the clocked RS flip flop. In the D flip flop, the D input goes directly to the S input and its complement is applied as an R input. The D flip flop designed from irreversible gates. The D flip flop designed from the reversible equivalent gates.

The proposed circuit of the flip flop is evaluated in terms of number of reversible gates used and garbage outputs produced.

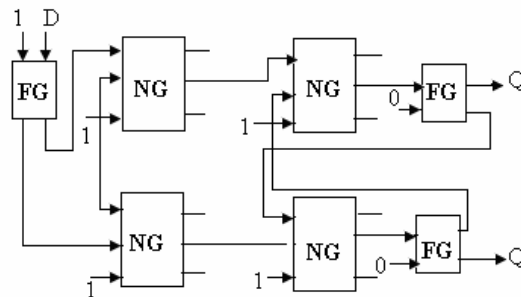


Fig.11 Reversible D Flip Flop

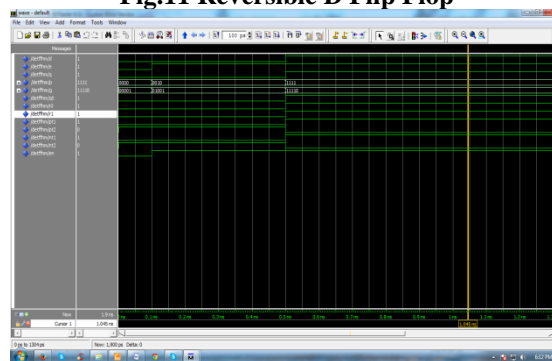


Fig.12 Output for reversible D Flip Flop

s

I. TESTING APPROACH TO QCA COMPUTING

QCA computing provides a promising technology to implement reversible logic gates. The QCA design of Fredkin gate using the four-phase clocking scheme in which the clocking zone is shown by the number next to D (D0 means clock 0 zone, D1 means clock 1 zone, and so on). It can be seen that the Fredkin gate has two level MV implementation, and it requires 6 MVs and four clocking zones for implementation. The number of clocking zones in a QCA circuit represents the delay of the circuit (delay between the inputs and the outputs). Higher the number of clocking zones, lower the operating speed of the circuit. In QCA manufacturing, defects can occur during the synthesis and deposition phases, although defects are most likely to take place during the deposition phase. Researchers have shown that QCA cells are more susceptible to missing and additional QCA cell defects. The additional cell defect is because of the deposition of an additional cell on the substrate. The missing cell defect is due to the missing of a particular cell. Researchers have been addressing the design and test of QCA circuits assuming the single missing/additional cell defect model.

VI. CONCLUSION

Therefore conservative reversible logic gates are used to designed sequential circuits. The proposed system is used in the Feynman gate. This paper proposed reversible sequential circuits based on conservative logic that is testable for any unidirectional stuck-at faults using only two test vectors, all 0s and all 1s. The proposed sequential circuits based on conservative logic gates outperform the sequential circuit implemented in classical gates in terms of testability. The sequential circuits implemented using conventional classic gates do not provide inherited support for testability. Hence, a conventional sequential circuit needs modification in the original circuitry to provide the testing capability. Also as the complexity of a sequential circuit increases the number of test vector required to test the sequential circuit also increases. For example, to test a complex sequential circuit thousand of test vectors are required to test all stuck-at-faults, while if the same sequential circuit is build using proposed reversible sequential building blocks it can be tested by only two test vectors, all 0s and all 1s. Thus, the main advantage of the proposed conservative reversible sequential circuits compared to the conventional sequential circuit is the need of only two test vectors to test any sequential circuit irrespective of its complexity. The reduction in number of test vectors minimizes the overhead of test time for a reversible sequential circuit. The proposed work has the limitation that it cannot detect multiple stuck-at-faults as well as multiple missing/additional cell defects. In conclusion, this paper advances the state-of-the-art by minimizing the number of test vectors needed to detect stuck-at-faults as well as single missing/additional cell defects.

REFERENCES

- [1] J. Ren and V. K. Semenov, "Progress with physically and logically reversible superconducting digital circuits," *IEEE Trans. Appl. Super- conduct.*, vol. 21, no. 3, pp. 780–786, Jun. 2011.
- [2] S. F. Murphy, M. Ottavi, M. Frank, and E. DeBenedictis, "On the design of reversible QDCA systems," Sandia National Laboratories, Albuquerque, NM, Tech. Rep. SAND2006-5990, 2006.
- [3] H. Thapliyal and N. Ranganathan, "Reversible logic-based concurrently testable latches for molecular QCA," *IEEE Trans. Nanotechnol.*, vol. 9, no. 1, pp. 62–69, Jan. 2010.
- [4] P. Tougaw and C. Lent, "Logical devices implemented using quantum cellular automata," *J. Appl. Phys.*, vol. 75, no. 3, pp. 1818–1825, Nov. 1994.
- [5] P. Tougaw and C. Lent, "Dynamic behavior of quantum cellular automata," *J. Appl. Phys.*, vol. 80, no. 8, pp. 4722–4736, Oct. 1996. [6] M. B. Tahoori, J. Huang, M. Momenzadeh, and F. Lombardi, "Testing of quantum cellular automata," *IEEE Trans. Nanotechnol.*, vol. 3, no. 4, pp. 432–442, Dec. 2004.
- [7] G. Swaminathan, J. Aylor, and B. Johnson, "Concurrent testing of VLSI circuits using conservative logic," in *Proc. Int. Conf. Comput. Design*, Cambridge, MA, Sep. 1990, pp. 60–65.
- [8] E. Fredkin and T. Toffoli, "Conservative logic," *Int. J. Theor. Phys.*, vol. 21, nos. 3–4, pp. 219–253, 1982.
- [9] P. Kartschoke, "Implementation issues in conservative logic networks," M.S. thesis, Dept. Electr. Eng., Univ. Virginia, Charlottesville, 1992. [10] G. Swaminathan, "Concurrent error detection techniques using parity," M.S. thesis, Dept. Electr. Eng., Univ. Virginia, Charlottesville, 1989.
- [11] H. Thapliyal, M. B. Srinivas, and M. Zwolinski, "A beginning in the reversible logic synthesis of sequential circuits," in *Proc. Int. Conf. Military Aerosp. Program. Logic Devices*, Washington, DC, Sep. 2005, pp. 1–5.
- [12] S. Mahammad and K. Veezhinathan, "Constructing online testable circuits using reversible logic," *IEEE Trans. Instrum. Meas.*, vol. 59, no. 1, pp. 101–109, Jan. 2010.
- [13] H. Thapliyal and N. Ranganathan, "Design of reversible sequential circuits optimizing quantum cost, delay and garbage outputs," *ACM J. Emerg. Technol. Comput. Syst.*, vol. 6, no. 4, pp. 14:1–14:35, Dec. 2010.
- [14] M. Hasan, A. Islam, and A. Chowdhury, "Design and analysis of online testability of reversible sequential circuits," in *Proc. Int. Conf. Comput. Inf. Technol.*, Dec. 2009, pp. 180–185.
- [15] M. Pedram, Q. Wu, and X. Wu, "A new design for double edge triggered flip-flops," in *Proc. Asia South Pacific Design Autom. Conf.*, 1998, pp. 417–421.

Mathematical Methods in Medical Image Processing and Magnetic Resonance Imaging

Joyjit patra¹, Himadri Nath Moulick², Arun Kanti Manna³, Rajarshi Roy⁴

¹(C.S.E, Aryabhatta Institute Of Engineering And Management,Durgapur,West Bengal,India)

²(C.S.E, Aryabhatta Institute Of Engineering And Management,Durgapur,West Bengal,India)

³(Persuing Ph.D. from Techno India University,W.B.India)

⁴(B.Tech 4th year Student,CSE Dept,Aryabhatta Institute of Engineering and Mangement,Durgapur,W.B,India)

ABSTRACT:

In this paper,we describe some central mathematical problems in medical imaging.The subject has been undergoing rapid changes driven by better hardware and software.Much of the software is based on novel methods utilizing geometric partial differential equations in conjunction with standard signal/image processing techniques as well as computer graphics facilitating man/machine interactions.As part of this enterprise,researchers have been trying to base biomedical engineering principles on rigorous mathematical foundations for the development of software methods to be integrated into complete therapy delivery systems.These systems support the more effective delivery of many image-guided procedures such as radiation therapy,biopsy,and minimally invasive surgery.We will show how mathematics may impact some of the main problems in this area including image enhancement,registration,and segmentation.This paper[1] describes image processing techniques for Diffusion Tensor Magnetic Resonance.In Diffusion Tensor MRI,a tensor describing local water diffusion is acquired for each voxel. The geometric nature of the diffusion tensors can quantitatively characterize the local structure in tissues such as bone,muscles,and white matter of the brain.The close relationship between local image structure and apparent diffusion makes this image modality very interesting for medical image analysis.We present a decomposition of the diffusion tensor based on its symmetry properties resulting in useful measures describing the geometry of the diffusion ellipsoid. A simple anisotropy measure follows naturally from this analysis.We describe how the geometry,or shape,of the tensor can be visualized using a coloring scheme based on the derived shape measures.We show how filtering of the tensor data of a human brain can provide a description of macrostructural diffusion which can be used for measures of fiber-tract organization.We also describe how tracking of white matter tracts can be implemented using the introduced methods.

Keywords: Medical imaging, artificial vision, smoothing, registration, segmentation, image-guided therapy (IGT) and image guided surgery (IGS).

I. INTRODUCTION

Medical imaging has been undergoing a revolution in the past decade with the advent of faster, more accurate,and less invasive devices.This has driven the need for corresponding software development which in turn has provided a major impetus for new algorithms in signal and image processing. Many of these algorithms are based on partial differential equations and curvature driven flows which will be the main topics of this survey paper.Mathematical models are the foundation of biomedical computing.Basing those models on data extracted from images continues to be a fundamental technique for achieving scientific progress in experimental,clinical,biomedical,and behavioral research.Today,medical images are acquired by a range of techniques across all biological scales,which go far beyond the visible light photographs and microscope images of the early 20th century.Modern medical images may be considered to be geometrically arranged arrays of data samples which quantify such diverse physical phenomena as the time variation of hemoglobin deoxygenation during neuronal metabolism,or the diffusion of water molecules through and within tissue.The broadening scope of imaging as a way to organize our observations of the biophysical world has led to a dramatic increase in our ability to apply new processing techniques and to combine multiple channels of data into sophisticated and complex mathematical models of physiological function and dysfunction.A key research area is the formulation of biomedical engineering principles based on rigorous mathematical foundations in order to develop general-purpose software methods that can be integrated into complete therapy delivery systems.Such systems support the more effective delivery of many image-guided procedures such as biopsy,minimally invasive surgery,and radiation therapy.In order to understand the extensive role of imaging in the therapeutic process, and to appreciate the current usage of images before,during,and after treatment,we focus our analysis on four main components of image-guided therapy (IGT) and image guided surgery (IGS): localization, targeting, monitoring, and control.Specifically, in medical imaging we have four key problems:

(1) Segmentation- automated methods that create patient-specific models of relevant anatomy from images; (2) Registration - automated methods that align multiple data sets with each other; (3) Visualization - the technological environment in which image-guided procedures can be displayed; (4) Simulation - softwares that can be used to rehearse and plan procedures, evaluate access strategies, and simulate planned treatments. In this paper, we will only consider the first two problem areas. However, it is essential to note that in modern medical imaging, we need to integrate these technologies into complete and coherent image guided therapy delivery systems and validate these integrated systems using performance measures established in particular application areas. We should note that in this survey we touch only upon those aspects of the mathematics of medical imaging reflecting the personal tastes (and prejudices) of the authors. Indeed, we do not discuss a number of very important techniques such as wavelets, which have had a significant impact on imaging and signal processing; see [60] and the references therein. Several articles and books are available which describe various mathematical aspects of imaging processing such as [67] (segmentation), [83] (curve evolution), and [71, 87] (level set methods). Finally, it is extremely important to note that all the mathematical algorithms which we sketch lead to interactive procedures. This means that in each case there is a human user in the loop (typically a clinical radiologist) who is the ultimate judge of the utility of the procedure, and who tunes the parameters either on or off-line. Nevertheless, there is a major need for further mathematical techniques which lead to more automatic and easier to use medical procedures. We hope that this paper may facilitate a dialogue between the mathematical and medical imaging communities.

Diffusion Tensor Magnetic Resonance Imaging (DT-MRI) is a recent MR imaging modality. In Diffusion Tensor MRI, a tensor describing local water diffusion is acquired for each voxel. Diffusion in tissue can be anisotropic depending on the characteristics of the tissue. For example in the white matter fiber tracts the diffusion is mainly in the direction of the fibers. In areas with fluid, such in the CSF filled ventricles, the diffusion is spherical, i.e. isotropic. The advent of robust diffusion tensor imaging techniques has prompted the development of quantitative measures for describing the diffusion anisotropy. A good review by Basser and Pierpaoli can be found in [1]. Since MRI methods in general always obtain a macroscopic measure of a microscopic quantity which necessarily entails intravoxel averaging, the voxel dimensions influence the measured diffusion tensor at any particular location in the brain. Factors which would affect the shape of the apparent diffusion tensor (shape of the diffusion ellipsoid) in the white matter include the density of fibers, the degree of myelination, the average fiber diameter and the directional similarity of the fibers in the voxel. The geometric nature of the measured diffusion tensor within a voxel is thus a meaningful measure of fiber tract organization. With current conventional proton magnetic resonance imaging (MRI) techniques, the white matter of the brain appears to be a remarkably homogeneous tissue without any suggestion of the complex arrangement of fiber tracts. Although the individual axons and the surrounding myelin sheaths cannot be revealed with the limited spatial resolution of in vivo imaging, distinct bands of white matter fibers with parallel orientation may be distinguished from others running in different directions if MRI techniques are sensitized to water diffusion and the preferred direction of diffusion is determined. Water diffusion in tissue due to Brownian motion is random but some structural characteristics of tissues may limit diffusion. In the white matter, the mobility of the water is restricted in the directions perpendicular to the axons which are oriented along the fiber tracts. This anisotropic diffusion is due to the presence of tightly packed multiple myelin membranes encompassing the axon. Myelination is not essential for diffusion anisotropy of nerves as shown in studies of nonmyelinated garfish olfactory nerves [3] and anisotropy exists in brains of neonates before the histological appearance of myelin [16] but myelin is widely assumed to be the major barrier to diffusion in myelinated fiber tracts. Therefore the demonstration of anisotropic diffusion in brain by magnetic resonance has opened the way to explore noninvasively the structural anatomy of the white matter in vivo [8, 4, 1, 10].

II. MEDICAL IMAGING

2.1. Generalities

In 1895, Roentgen discovered X-rays and pioneered medical imaging. His initial publication [82] contained a radiograph (i.e. an X-ray generated photograph) of Mrs. Roentgen's hand; see Figure 1(a). For the first time, it was possible to visualize non-invasively (i.e., not through surgery) the interior of the human body. The discovery was widely publicized in the popular press and an "Xray mania" immediately seized Europe and the United States [30, 47]. Within only a few months, public demonstrations were organized, commercial ventures created and innumerable medical applications investigated; The field of radiography was born with a bang! Today, medical imaging is a routine and essential part of medicine. Pathologies can be observed directly rather than inferred from symptoms. For example, a physician can non-invasively monitor the healing of damaged tissue or the growth of a brain tumor, and determine an appropriate medical response. Medical imaging techniques can also be used when planning or even while performing surgery. For



(a) First radiograph of Mrs. Roentgen's hand.
Fig:1. X-ray radiography at the end of the 19th century.

example, a neurosurgeon can determine the “best” path in which to insert a needle, and then verify in real time its position as it is being inserted.

III. MAGNETIC RESONANCE IMAGING

This technique relies on the relaxation properties of magnetically-excited hydrogen nuclei of water molecules in the body. The patient under study is briefly exposed to a burst of radio-frequency energy, which, in the presence of a magnetic field, puts the nuclei in an elevated energy state. As the molecules undergo their normal, microscopic tumbling, they shed this energy into their surroundings, in a process referred to as relaxation. Images are created from the difference in relaxation rates in different tissues. This technique was initially known as nuclear magnetic resonance (NMR) but the term “nuclear” was removed to avoid any association with nuclear radiation. MRI utilizes strong magnetic fields and non-ionizing radiation in the radio frequency range, and according to current medical knowledge, is harmless to patients. Another advantage of MRI is that soft tissue contrast is much better than with X-rays leading to higher-quality images, especially in brain and spinal cord scans. See Figure 2(a). Refinements have been developed such as functional MRI (fMRI) that measures temporal variations (e.g., for detection of neural activity), and diffusion MRI that measures the diffusion of water molecules in anisotropic tissues such as white matter in the brain.

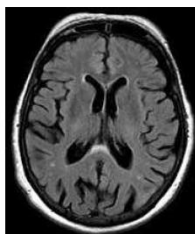


Fig: 2(a). Magnetic Resonance Image (brain, 2D axial slice).

IV. POSITRON EMISSION TOMOGRAPHY

The patient is injected with radioactive isotopes that emit particles called positrons (anti-electrons). When a positron meets an electron, the collision produces a pair of gamma ray photons having the same energy but moving in opposite directions. From the position and delay between the photon pair on a receptor, the origin of the photons can be determined. While MRI and CT can only detect anatomical changes, PET is a functional modality that can be used to visualize pathologies at the much finer molecular level. This is achieved by employing radioisotopes that have different rates of intake for different tissues. For example, the change of regional blood flow in various anatomical structures (as a measure of the injected positron emitter) can be visualized and relatively quantified. Since the patient has to be injected with radioactive material, PET is relatively invasive. The radiation dose however is similar to a CT scan. Image resolution may be poor and major preprocessing may be necessary. See Figure 3(a).



Figure 3(a). Positron Emission Tomography (brain, 2D axial slice).

V. ALGORITHMS & PDES

Many mathematical approaches have been investigated for applications in artificial vision(e.g.,fractals and self-similarity,wavelets,pattern theory,stochastic point process,random graph theory; see [42]).In particular,methods based on partial differential equations (PDEs) have been extremely popular in the past few years [20, 35].Here we briefly outline the major concepts involved in using PDEs for image processing.As explained in detail in [17], one can think of an image as a map $I : D \rightarrow C$, i.e., to any point x in the domain D , I associates a “color” $I(x)$ in a color space C . For ease of presentation we will mainly restrict ourselves to the case of a twodimensional gray scale image which we can think of as a function from a domain $D = [0, 1] \times [0, 1]$ to the unit interval $C = [0, 1]$.The algorithms all involve solving the initial value problem for some PDE for a given amount of time. The solution to this PDE can be either the image itself at different stages of modification, or some other object (such as a closed curve delineating object boundaries) whose evolution is driven by the image. For example, introducing an artificial time t , the image can be deformed according to

$$\frac{\partial I}{\partial t} = \mathcal{F}[I], \dots\dots\dots(1)$$

where $I(x, t) : D \times [0, T) \rightarrow C$ is the evolving image, \mathcal{F} is an operator which characterizes the given algorithm, and the initial condition is the input image I_0 .The processed image is the solution $I(x, t)$ of the differential equation at time t .The operator \mathcal{F} usually is a differential operator, although its dependence on I may also be nonlocal.Similarly,one can evolve a closed curve representing the boundaries of some planar shape (Γ need not be connected and could have several components).In this case, the operator \mathcal{F} specifies the normal velocity of the curve that it deforms. In many cases this normal velocity is a function of the curvature κ of Γ ,and of the image I evaluated on Γ .A flow of the form

$$\frac{\partial \Gamma}{\partial t} = \mathcal{F}(I, \kappa)\mathbf{N} \dots\dots\dots(2)$$

is obtained,where \mathbf{N} is the unit normal to the curve Γ .Very often,the deformation is obtained as the steepest descent for some energy functional.For example,the energy

$$\mathcal{E}(I) = \frac{1}{2} \int \|\nabla I\|^2 dx dy \dots\dots\dots(3)$$

and its associated steepest descent, the heat equation,

$$\frac{\partial I}{\partial t} = \Delta I \dots\dots\dots(4)$$

correspond to the classical Gaussian smoothing.The use of PDEs allows for the modelling of the crucial but poorly understood interactions between top-down and bottom-up vision 5.In a variational framework, for example, an energy \mathcal{E} is defined globally while the corresponding operator \mathcal{F} will influence the image locally.Algorithms defined in terms of PDEs treat images as continuous rather than discrete objects.This simplifies the formalism,which becomes grid independent.On the other hand models based on nonlinear PDEs may be much harder to analyze and implement rigorously.

VI. IMAGING PROBLEMS

Medical images typically suffer from one or more of the following imperfections:

- low resolution (in the spatial and spectral domains);
- high level of noise;
- low contrast;
- geometric deformations;
- presence of imaging artifacts.

These imperfections can be inherent to the imaging modality (e.g., X-rays offer low contrast for soft tissues, ultrasound produces very noisy images, and metallic implants will cause imaging artifacts in MRI) or the result of a deliberate trade-off during acquisition. For example, finer spatial sampling may be obtained through a longer acquisition time. However that would also increase the probability of patient movement and thus blurring. In this paper, we will only be interested in the processing and analysis of images and we will not be concerned with the challenging problem of designing optimal procedures for their acquisition. Several tasks can be performed (semi)-automatically to support the eye-brain system of medical practitioners. Smoothing is the problem of simplifying the image while retaining important information. Registration is the problem of fusing images of the same region acquired from different modalities or putting in correspondence images of one patient at different times or of different patients. Finally, segmentation is the problem of isolating anatomical structures for quantitative shape analysis or visualization. The ideal clinical application should be fast, robust with regards to image imperfections, simple to use, and as automatic as possible. The ultimate goal of artificial vision is to imitate human vision, which is intrinsically subjective. The technique we present below are applied to two-dimensional grayscale images. The majority of them, however, can be extended to higher dimensions (e.g., vector-valued volumetric images).

6.1. Image Segmentation

When looking at an image, a human observer cannot help seeing structures which often may be identified with objects. However, digital images as the raw retinal input of local intensities are not structured. Segmentation is the process of creating a structured visual representation from an unstructured one. The problem was first studied in the 1920's by psychologists of the Gestalt school (see Kohler [54] and the references therein), and later by psychophysicists [49, 95]. In its modern formulation, image segmentation is the problem of partitioning an image into homogeneous regions that are semantically meaningful, i.e., that correspond to objects we can identify. Segmentation is not concerned with actually determining what the partitions are. In that sense, it is a lower level problem than object recognition. In the context of medical imaging, these regions have to be anatomically meaningful. A typical example is partitioning a MRI image of the brain into the white and gray matter. Since it replaces continuous intensities with discrete labels, segmentation can be seen as an extreme form of smoothing/information reduction. Segmentation is also related to registration in the sense that if an atlas can be perfectly registered to a dataset at hand, then the registered atlas labels are the segmentation. Segmentation is useful for visualization, it allows for quantitative shape analysis, and provides an indispensable anatomical framework for virtually any subsequent automatic analysis. Indeed, segmentation is perhaps the central problem of artificial vision, and accordingly many approaches have been proposed (for a nice survey of modern segmentation methods, see the monograph [67]). There are basically two dual approaches. In the first, one can start by considering the whole image to be the object of interest, and then refine this initial guess. These "split and merge" techniques can be thought of as somewhat analogous to the top-down processes of human vision. In the other approach, one starts from one point assumed to be inside the object, and adds other points until the region encompasses the object. Those are the "region growing" techniques and bear some resemblance to the bottom-up processes of biological vision. The dual problem to segmentation is that of determining the boundaries of the segmented homogeneous regions. This approach has been popular for some time since it allows one to build upon the well-investigated problem of edge detection (Section 6.2). Difficulties arise with this approach because noise can be responsible for spurious edges. Another major difficulty is that local edges need to be connected into topologically correct region boundaries. To address these issues, it was proposed to set the topology of the boundary to that of a sphere and then deform the geometry in a variational framework to match the edges. In 2D, the boundary is a closed curve and this approach was named snakes. Improvements of the technique include geometric active contours and conformal active contours. All these techniques are generically referred to as active contours. Finally, as described in [67], most segmentation methods can be set in the elegant mathematical framework proposed by Mumford and Shah [69].

6.2. Edge Detectors

Consider the ideal case of a bright object \mathcal{O} on a dark background. The physical object is represented by its projections on the image I . The characteristic function $1_{\mathcal{O}}$ of the object is the ideal segmentation, and since the object is contrasted on the background, the variations of the intensity I are large on the boundary $\partial\mathcal{O}$. It is therefore natural to characterize the boundary $\partial\mathcal{O}$ as the locus of points where the norm of the gradient $\|I\|$ is large. In fact, if $\partial\mathcal{O}$ is piecewise smooth then $\|I\|$ is a singular measure whose support is exactly $\partial\mathcal{O}$. This is the approach taken in the 60's and 70's by Roberts [81] and Sobel [91] who proposed slightly different discrete convolution masks to approximate the gradient of digital images. Disadvantages with these approaches are that edges are not precisely localized, and may be corrupted by noise. See Figure 4(b) is the result of a Sobel edge detector on a medical image. Note the thickness of the boundary of the heart ventricle as well as the presence of "spurious edges" due to noise. Canny [14] proposed to add a smoothing pre-processing step (to reduce the influence of the noise) as well as a thinning post-processing phase (to ensure that the edges are uniquely localized). See [26] for a survey and evaluation of edge detectors using gradient techniques. A slightly different approach initially motivated by psychophysics was proposed by Marr and Hildreth [62, 61] where edges are defined as the zeros of $\Delta G_{\sigma} * I$, the Laplacian of a smooth version of the image. One can give a heuristic justification by assuming that the edges are smooth curves; more precisely, assume that near

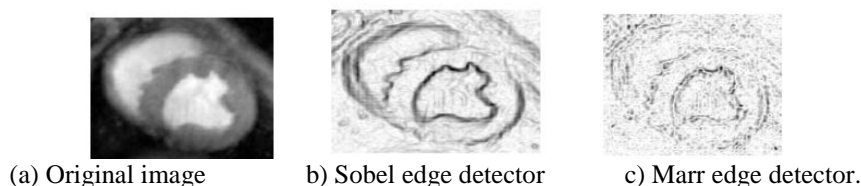


Fig.4 Result of two edge detectors on a heart MRI image.

an edge the image is of the form

$$I(\mathbf{x}) = \varphi\left(\frac{S(\mathbf{x})}{\varepsilon}\right), \dots\dots(5)$$

where S is a smooth function which vanishes on the edge, ε is a small parameter proportional to the width of the edge, and R → [0, 1] is a smooth increasing function with limits.

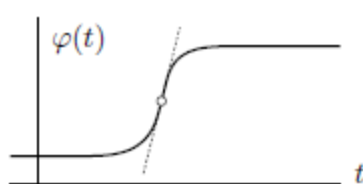


Fig. 4.1.

VII. MATERIALS AND METHODS

In this work we applied a modified version of the recently proposed Line Scan Diffusion Imaging (LSDI) technique. This method, like the commonly used diffusion-sensitized, ultrafast, echo-planar imaging (EPI) technique [12] is relatively insensitive to bulk motion and physiologic pulsations of vascular origin. But unlike EPI, LSDI exhibits minimal image distortion, does not require cardiac gating, head restraints or post-processing image correction, and can be implemented without specialized hardware on all standard MRI scanners. Here, we present a quantitative characterization of the geometric nature of the diffusion tensors, a method for characterization of macrostructural diffusion properties, and a display method for showing clear and detailed in vivo images of human white matter tracts. The orientation and distribution of most of the known major fiber tracts can be identified using these methods.

7.1. Imaging Parameters

Suppose, some data were acquired at a hospital on a GE Signa 1.5 Tesla, Horizon Echospeed 5.6 system with standard 2.2 Gauss/cm field gradients. The time required for acquisition of the diffusion tensor data for one slice was 1 min; no averaging was performed. Imaging parameters were: effective TR=2.4 s, TE=65 ms, $b_{high}=750$ s/mm², $b_{low}=5$ s/mm², field of view 22 cm, effective voxel size 4.8_1.6_1.5 mm³, 3.6 kHz readout bandwidth, acquisition matrix 128_128. The gradient cycle in the LSDI interleaving scheme was modified to provide acquisition of more gradient directions and to allow elimination of the crusher gradients. Instead of alternating merely between high and low gradient strengths, the modified sequence cycled through eight configurations of the diffusion gradients. In all other respects it was identical to the sequence described in [7].

7.2. Calculation of Tensors

For each slice, eight images are collected with different diffusion weightings and noncollinear gradient directions. If S_0 represents the signal intensity in the absence of a diffusion-sensitizing field gradient and S the signal intensity in the presence of gradient $\mathbf{g} = (g_x, g_y, g_z)$, the equation for the loss in signal intensity due to diffusion is given by the Stejskal-Tanner formula:

$$\ln(S) = \ln(S_0) - \gamma^2 \delta^2 (\Delta - \delta/3) \mathbf{g}^T \mathbf{D} \mathbf{g}, \quad \dots\dots\dots(6)$$

where γ is the gyromagnetic ratio of hydrogen 1H (protons), δ is the duration of the diffusion sensitizing gradient pulses and Δ is the time between the centers of the two gradient pulses. The eight images provide eight equations for S in each voxel which are solved in a least-squares sense for the 6+1 unknowns: the six independent components of the symmetric diffusion tensor, \mathbf{D} , and S_0 . In the LSDI sequence, it is easy to show that cross terms between the slice select gradient for the 180 pulse and the diffusion sensitizing gradients account for less than 0.1% of the diffusion weighting, and have therefore been neglected here. Diffusion attenuation due to imaging gradients is already factored into S_0 , as is T2 weighting.

7.3. Geometrical Measures of Diffusion

In order to relate the measure of diffusion anisotropy to the structural geometry of the tissue a mathematical description of diffusion tensors and their quantification is necessary. First, a complete diffusion tensor, \mathbf{D} , is calculated for each voxel. Using the symmetry properties of the diffusion ellipsoid we decomposed the diffusion tensor, and from the tensor basis assigned scalar measures, describing the linearity and the anisotropy, to each voxel. The diffusion tensor can be visualized using an ellipsoid where the principal axes correspond to the directions of the eigenvector system. Let $\lambda_1 \geq \lambda_2 \geq \lambda_3 \geq 0$ be the eigenvalues of the symmetric tensor \mathbf{D}

$$\mathbf{D} = \lambda_1 \hat{\mathbf{e}}_1 \hat{\mathbf{e}}_1^T + \lambda_2 \hat{\mathbf{e}}_2 \hat{\mathbf{e}}_2^T + \lambda_3 \hat{\mathbf{e}}_3 \hat{\mathbf{e}}_3^T \quad \dots\dots\dots(7)$$

Diffusion can be divided into three basic cases depending on the rank, of the representation tensor:

1) Linear case ($\lambda_1 \gg \lambda_2 \simeq \lambda_3$): diffusion is mainly in the direction corresponding to the largest eigenvalue.

$$\mathbf{D} \simeq \lambda_1 \mathbf{D}_l = \lambda_1 \hat{\mathbf{e}}_1 \hat{\mathbf{e}}_1^T. \quad \dots\dots\dots(8)$$

2) Planar case ($\lambda_1 \simeq \lambda_2 \gg \lambda_3$): diffusion is restricted to a plane spanned by the two eigenvectors corresponding to the two largest eigenvalues.

$$\mathbf{D} \simeq 2\lambda_1 \mathbf{D}_p = \lambda_1 (\hat{\mathbf{e}}_1 \hat{\mathbf{e}}_1^T + \hat{\mathbf{e}}_2 \hat{\mathbf{e}}_2^T). \quad \dots\dots\dots(9)$$

3) Spherical case ($\lambda_1 \simeq \lambda_2 \simeq \lambda_3$): isotropic diffusion:

$$\mathbf{D} \simeq 3\lambda_1 \mathbf{D}_s = \lambda_1 (\hat{\mathbf{e}}_1 \hat{\mathbf{e}}_1^T + \hat{\mathbf{e}}_2 \hat{\mathbf{e}}_2^T + \hat{\mathbf{e}}_3 \hat{\mathbf{e}}_3^T). \quad \dots\dots\dots(10)$$

In general, the diffusion tensor \mathbf{D} will be a combination of these cases. Expanding the diffusion tensor using these cases as a basis gives:

$$\begin{aligned} \mathbf{D} &= \lambda_1 \hat{\mathbf{e}}_1 \hat{\mathbf{e}}_1^T + \lambda_2 \hat{\mathbf{e}}_2 \hat{\mathbf{e}}_2^T + \lambda_3 \hat{\mathbf{e}}_3 \hat{\mathbf{e}}_3^T \\ &= (\lambda_1 - \lambda_2) \hat{\mathbf{e}}_1 \hat{\mathbf{e}}_1^T + (\lambda_2 - \lambda_3) (\hat{\mathbf{e}}_1 \hat{\mathbf{e}}_1^T + \hat{\mathbf{e}}_2 \hat{\mathbf{e}}_2^T) \\ &\quad + \lambda_3 (\hat{\mathbf{e}}_1 \hat{\mathbf{e}}_1^T + \hat{\mathbf{e}}_2 \hat{\mathbf{e}}_2^T + \hat{\mathbf{e}}_3 \hat{\mathbf{e}}_3^T) \\ &= (\lambda_1 - \lambda_2) \mathbf{D}_l + (\lambda_2 - \lambda_3) \mathbf{D}_p + \lambda_3 \mathbf{D}_s \quad \dots\dots\dots(11) \end{aligned}$$

where $(\lambda_1 - \lambda_2)$, $(\lambda_2 - \lambda_3)$ and λ_3 are the coordinates of D in the tensor basis $\{D_t, D_p, D_s\}$. A similar tensor shape analysis has proven to be useful in a number of computer vision applications. As described, the relationships between the eigenvalues of the diffusion tensor can be used for classification of the diffusion tensor according to geometrically meaningful criteria. By using the coordinates of the tensor in our new basis measures are obtained of how close the diffusion tensor is to the generic cases of line, plane and sphere. The generic shape of a tensor is obtained by normalizing with a magnitude measure of the diffusion. Here we define this magnitude as the largest eigenvalues of the tensor. This gives for the linear, planar and spherical measures:

$$\begin{aligned} c_t &= \frac{\lambda_1 - \lambda_2}{\lambda_1} \\ c_p &= \frac{\lambda_2 - \lambda_3}{\lambda_1} \\ c_s &= \frac{\lambda_3}{\lambda_1} \\ c_t + c_p + c_s &= 1 \end{aligned} \quad \dots\dots(12)$$

An anisotropy measure describing the deviation from the spherical case is achieved as follows:

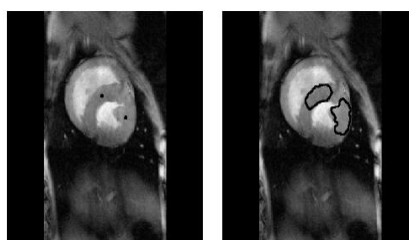
$$c_a = c_t + c_p = 1 - c_s = 1 - \frac{\lambda_3}{\lambda_1} \quad \dots\dots(13)$$

7.4. Visualization of Diffusion Tensors

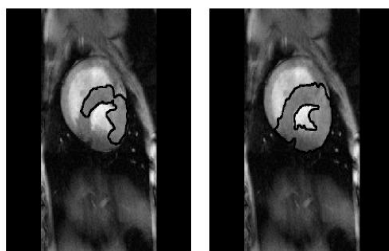
A 3D diffusion tensor can be visualized using an ellipsoid where the principal axes correspond to the tensor’s eigenvector system. However, it is difficult to distinguish between an edge-on, flat ellipsoid and an oblong one using the surface shading information. Similar ambiguity exists between a face-on, flat ellipsoid and a sphere. We propose two techniques for the visualization of tensor fields that overcome the problems with ellipsoids. We compare the ellipsoidal representation of a tensor with a composite shape whose linear, planar, and spherical components are scaled according to c_t , c_p , and c_s (c_l , c_p , and c_s). Additionally, coloring based on the shape measures c_t , c_p , and c_s can be used for visualization of shape.

VIII. CONCLUSION

In this paper, we sketched some of the fundamental concepts of medical image processing. It is important to emphasize that none of these problem areas has been satisfactorily solved, and all of the algorithms we have described are open to considerable improvement. In particular, segmentation remains a rather ad hoc procedure with the best results being obtained via interactive programs with considerable input from the user. Nevertheless, progress has been made in the field of automatic analysis of medical images over the last few years thanks to improvements in hardware, acquisition methods, signal processing techniques, and of course mathematics. Curvature driven flows have proven to be an excellent tool for a number of image processing tasks and have definitely had a major impact on the technology base. Several algorithms based on partial differential equation methods have been incorporated into clinical software and are available in open software packages such as the National Library of Medicine Insight Segmentation and Registration Toolkit (ITK), and the 3D Slicer of the Harvard Medical School [90]. These projects are very important in disseminating both standard and new mathematical methods in medical imaging to the broader community.



(a) Two initial bubbles. (b) Evolving active contours



(c) Merging of active contours. (d) Steady state.

Fig.5 Myocardium segmentation in MRI heart image with two merging expanding conformal active contours.

The mathematical challenges in medical imaging are still considerable and the necessary techniques touch just about every major branch of mathematics. In summary, we can use all the help we can get! We have proposed measures classifying diffusion tensors into three generic cases based on a tensor basis expansion. When applied to white matter the linear index shows uniformity of tract direction within a voxel while the anisotropic index quantifies the deviation from spatial homogeneity. The non-orthogonal tensor basis chosen is intuitively appealing since it is based on three simple, yet descriptive, geometrically meaningful cases. We have described how tensor diffusion data can be processed without reverting to the use of only scalar measures of the tensor data. By staying in the tensor domain, cleaning up of the data can be done meaningfully with simple methods such as smoothing. We discuss addition of tensors geometrically and argue that adding tensors and vectors are different in that tensor summation gives more than the "mean" event due to more degrees of freedom. By using the geometric diffusion measures on locally averaged tensors local directionality consistency can be determined (e.g. existence of larger fiber tracts). We have proposed that this averaging approach can be used to derive a tensor field that can be used to describe macrostructural features in the tensor diffusion data. The linear measure cl derived from the averaged tensor field can for example be used for quantitative evaluation of fiber tract organization. We also have described how non-linear operations can be used to remap the eigenvalues of the diffusion tensors and given a sketch of how this can be used for tracking white matter tracts.

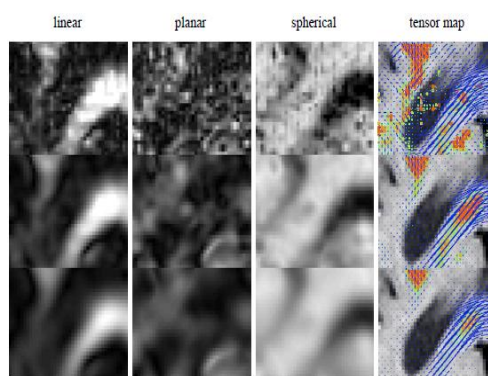


Fig.6. Axial brain images showing the three geometrical measures and diffusion tensor maps with three different smoothing parameters.

Top: shows the geometrical measures and the tensor map derived from the original data.

Middle: shows the same measures derived from data that has been averaged with $9 \times 9 \times 3$ Gaussian kernel.

Bottom: from data averaged with a $15 \times 15 \times 5$ Gaussian kernel. The rightmost column shows the tensors. The blue headless arrows represent the in-plane components of $c_l \hat{e}_1$. The out-of-plane components of $c_l \hat{e}_1$ ($c_l \hat{e}_1$) are shown in colors ranging from green through yellow to red, with red indicating the highest value for this component.

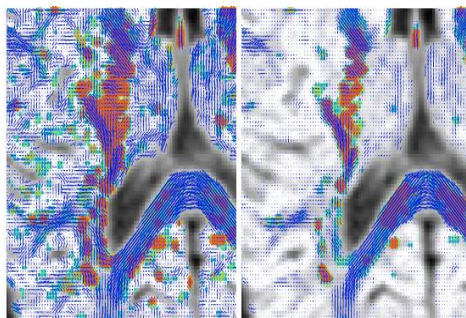


Figure 8.3. Left: Diffusion tensors, weighted with their linear measure $cl_{\mathbf{c}_l}$, from an axial slice of a human brain. Right: Averaged diffusion tensors using a $5 \times 5 \times 3$ Gaussian kernel weighted with their linear measure $cl_{\mathbf{c}_l}$.

REFERENCES

- [1] Alvarez, F. Guichard, P. L. Lions, and J. M. Morel, Axiomes et ´equations fondamentales du traitement d’images, C. R. Acad. Sci. Paris 315 (1992), 135–138.
- [2] Axioms and fundamental equations of image processing, Arch. Rat. Mech. Anal. 123 (1993), no. 3, 199–257.
- [3] Alvarez, P. L. Lions, and J. M. Morel, Image selective smoothing and edge detection by nonlinear diffusion, SIAM J. Numer. Anal. 29 (1992), 845–866.
- [4] Alvarez and J-M. Morel, Formalization and computational aspects of image analysis, Acta Numerica 3 (1994), 1–59.
- [5] Ambrosio, A compactness theorem for a special class of functions of bounded variation, Boll. Un. Math. It. 3-B (1989), 857–881.
- [6] Lecture notes on optimal transport theory, Euro Summer School, Mathematical Aspects of Evolving Interfaces, CIME Series of Springer Lecture Notes, Springer, July 2000.
- [7] S. Ando, Consistent gradient operators, IEEE Transactions on Pattern Analysis and Machine Intelligence 22 (2000), no. 3, 252–265.
- [8] S. Angenent, S. Haker, and A. Tannenbaum, Minimizing flows for the Monge Kantorovich problem, SIAM J. Math. Anal. 35 (2003), no. 1, 61–97 (electronic).
- [9] S. Angenent, G. Sapiro, and A. Tannenbaum, On the affine heat flow for non-convex curves, J. Amer. Math. Soc. 11 (1998), no. 3, 601–634.
- [10] J.-D. Benamou and Y. Brenier, A computational fluid mechanics solution to the Monge- Kantorovich mass transfer problem, Numerische Mathematik 84 (2000), 375–393.
- [11] Mixed l2/wasserstein optimal mapping between prescribed density functions, J. Optimization Theory Applications 111 (2001), 255–271.
- [12] Y. Brenier, Polar factorization and monotone rearrangement of vector-valued functions, Comm. Pure Appl. Math. 64 (1991), 375–417.
- [13] D. Brooks, Emerging medical imaging modalities, IEEE Signal Processing Magazine 18 (2001), no. 6, 12–13.
- [14] J. Canny, Computational approach to edge detection, IEEE Transactions on Pattern Analysis and Machine Intelligence 8 (1986), no. 6, 679–698.
- [15] C-F. Westin, S. Peled, H. Gudbjartsson, R. Kikinis, and F.A. Jolesz. Geometrical diffusion measures for MRI from tensor basis analysis. In ISMRM ’97, Vancouver, Canada, April 1997.
- [16] D. M. Wimberger, T. P. Roberts, A. J. Barkovich, L. M. Prayer, M. E. Moseley, and J. Kucharczyk. Identification of “premyelination” by diffusion-weighted MRI. J. Comp. Assist. Tomogr, 19(1):28–33, 1995.
- [17] H. Gudbjartsson, S. E. Maier, R. V. Mulkern, I. A. ´. Mo´roc, S. Patz, and F. A. Jolesz. Line scan diffusion imaging. Magn. Reson. Med., 36:509–519, 1996.
- [18] M. E. Moseley, Y. Cohen, J. Kucharczyk, J. Mintorovitch, H. S. Asgari, M. F. Wendland, J. Tsuruda, and D. Norman. Diffusion-weighted MR imaging of anisotropic water diffusion in the central nervous system. Radiology, 176:439–445, 1990.
- [19] S. Peled, H. Gudbjartsson, C-F. Westin, R. Kikinis, and F.A. Jolesz. Magnetic Resonance Imaging shows Orientation and Asymmetry of White Matter Tracts. Brain Research, 780(1):27–33, January 1998.
- [20] C. Pierpaoli, P. Jezzard, P. J. Basser, A. Barnett, and G. Di Chiro. Diffusion tensor MR imaging of the human brain. Radiology, 201:637, 1996.
- [21] C. Poupon, J.-F. Mangin, F. Frouin, J. R´egis, F. Poupon, M. Pachot-Clouard, D. Le Bihan, and I. Bloch. Regularization of mr diffusion tensor maps for tracking brain white matter bundles. In Proceedings of MICCAI’98, number ISSN 0302-9743 in Lecture Notes in Computer Science 1496. Springer Verlag, 1998.
- [22] R. Turner, D. le Bihan, J. Maier, R. Vavrek, L. K. Hedges, and J. Pekar. Echo planar imaging of intravoxel incoherent motions. Radiology, 177:407–414, 1990.
- [23] C-F. Westin and H. Knutsson. Extraction of local symmetries using tensor field filtering. In Proceedings of 2nd Singapore International Conference on Image Processing. IEEE Singapore Section, September 1992.
- [24] C-F. Westin and H. Knutsson. Estimation of Motion Vector Fields using Tensor Field Filtering. In Proceedings of IEEE International Conference on Image Processing, Austin, Texas, November 1994. IEEE
- [25] L. C. Evans and J. Spruck, Motion of level sets by mean curvature, I, J. Differential Geometry 33 (1991), no. 3, 635–681.
- [26] J.R. Fram and E.S. Deutsch, On the quantitative evaluation of edge detection schemes and their comparisons with human performance, IEEE Transaction on Computers 24 (1975), no. 6, 616–627.
- [27] D. Fry, Shape recognition using metrics on the space of shapes, Ph.D. thesis, Harvard University, 1993.
- [28] M. Gage and R. S. Hamilton, The heat equation shrinking convex plane curves, J. Differential Geometry 23 (1986), 69–96.
- [29] W. Gangbo and R. McCann, The geometry of optimal transportation, Acta Math. 177 (1996), 113–161.
- [30] E.S. Gerson, Scenes from the past: X-Ray mania, the X-Ray in advertising, circa 1895, Radiographics 24 (2004), 544–551.
- [31] E. Giusti, Minimal surfaces and functions of bounded variation, Birkh’auser Verlag, 1984.
- [32] R. Gonzalez and R. Woods, Digital image processing, Prentice Hall, 2001.
- [33] M. Grayson, The heat equation shrinks embedded plane curves to round points, J. Differential Geometry 26 (1987), 285–314.
- [34] Shortening embedded curves, Annals of Mathematics 129 (1989), 71–111.

- [35] F. Guichard, L. Moisan, and J.M. Morel, A review of PDE models in image processing and image analysis, *Journal de Physique IV* (2002), no. 12, 137–154.
- [36] S.R. Gunn, On the discrete representation of the Laplacian of Gaussian, *Pattern Recognition* 32 (1999), no. 8, 1463–1472.
- [37] J. Hajnal, D.J. Hawkes, D. Hill, and J.V. Hajnal (eds.), *Medical image registration*, CRC Press, 2001.
- [38] S. Haker, L. Zhu, A. Tannenbaum, and S. Angenent, Optimal mass transport for registration and warping, *Int. Journal Computer Vision* 60 (2004), no. 3, 225–240.
- [39] R. Haralick and L. Shapiro, *Computer and robot vision*, Addison-Wesley, 1992.
- [40] S. Helgason, *The Radon transform*, Birkh'auser, Boston, MA, 1980.
- [41] W. Hendee and R. Ritenour, *Medical imaging physics*, 4 ed., Wiley-Liss, 2002.
- [42] A.O. Hero and H. Krim, *Mathematical methods in imaging*, *IEEE Signal Processing Magazine* 19 (2002), no. 5, 13–14.
- [43] R. Hobbie, *Intermediate physics for medicine and biology* (third edition), Springer, New York, 1997.
- [44] B.K.P. Horn, *Robot vision*, MIT Press, 1986.
- [45] G. Huisken, Flow by mean curvature of convex surfaces into spheres, *J. Differential Geometry* 20 (1984), 237–266.
- [46] R. Hummel, Representations based on zero-crossings in scale-space, *IEEE Computer Vision and Pattern Recognition*, 1986, pp. 204–209.
- [47] Radiology Centennial Inc., A century of radiology, <http://www.xray.hmc.psu.edu/rci/centennial.html>.
- [48] Insight Segmentation and Registration Toolkit, <http://itk.org>.
- [49] B. Julesz, Textons, the elements of texture perception, and their interactions, *Nature* 12 (1981), no. 290, 91–97.
- [50] L. V. Kantorovich, On a problem of Monge, *Uspekhi Mat. Nauk.* 3 (1948), 225–226.
- [51] S. Kichenassamy, A. Kumar, P. Olver, A. Tannenbaum, and A. Yezzi, Conformal curvature flows: from phase transitions to active vision, *Arch. Rational Mech. Anal.* 134 (1996), no. 3, 275–301.
- [52] M. Knott and C. Smith, On the optimal mapping of distributions, *J. Optim. Theory* 43 (1984), 39–49.
- [53] J. J. Koenderink, The structure of images, *Biological Cybernetics* 50 (1984), 363–370.
- [54] W. K'ohler, Gestalt psychology today, *American Psychologist* 14 (1959), 727–734.
- [55] S. Osher L. I. Rudin and E. Fatemi, Nonlinear total variation based noise removal algorithms, *Physica D* 60 (1992), 259–268.
- [56] H. Ishii M. G. Crandall and P. L. Lions, User's guide to viscosity solutions of second order partial differential equations, *Bulletin of the American Mathematical Society* 27 (1992), 1–67.
- [57] A. Witkin M. Kass and D. Terzopoulos, Snakes: active contour models, *Int. Journal of Computer Vision* 1 (1987), 321–331.
- [58] F. Maes, A. Collignon, D. Vandermeulen, G. Marchal, and P. Suetens, Multimodality image registration by maximization of mutual information, *IEEE Transactions on Medical Imaging* 16 (1997), no. 2, 187 – 198.
- [59] J. Maintz and M. Viergever, A survey of medical image registration, *Medical Image Analysis* 2 (1998), no. 1, 1–36.
- [60] S. Mallat, A wavelet tour of signal processing, Elsevier, UK, 1999.
- [61] D. Marr, *Vision*, Freeman, san Francisco, 1982.
- [62] D. Marr and E. Hildreth, Theory of edge detection, *Proc. R. Soc. Lond. B* (1980), no. 207, 187–217.
- [63] R. McCann, A convexity theory for interacting gases and equilibrium crystals, Ph.D. Thesis, Princeton University, 1994.
- [64] T. McInerney and D. Terzopoulos, Topologically adaptable snakes, *Int. Conf. on Computer Vision* (Cambridge, Mass), June 1995, pp. 840–845.
- [65] Deformable models in medical image analysis: a survey, *Medical Image Analysis* 1(1996), no. 2, 91–108.
- [66] J. Milnor, *Morse theory*, Princeton University Press, 1963.
- [67] J-M. Morel and S. Solimini, *Variational methods in image segmentation*, Birkh'auser, Boston, 1994.
- [68] D. Mumford, Geometry-driven diffusion in computer vision, ch. *The Bayesian Rationale for Energy Functionals*, pp. 141–153, Kluwer Academic Publisher, 1994.
- [69] D. Mumford and J. Shah, Boundary detection by minimizing functionals, *IEEE Conference on Computer Vision and Pattern Recognition*, 1985, pp. 22–26.
- [70] Optimal approximations by piecewise smooth functions and associated variation problems, *Comm. Pure Appl. Math.* 42 (1989), no. 5, 577–685.
- [71] S. Osher and R. P. Fedkiw, Level set methods: An overview and some recent results, *Journal of Computational Physics* 169 (2001), 463–502.
- [72] S. J. Osher and J. A. Sethian, Front propagation with curvature dependent speed: Algorithms based on hamilton-jacobi formulations, *Journal of Computational Physics* 79 (1988), 12–49.
- [73] Jacob Palis, Jr. and Welington de Melo, *Geometric theory of dynamical systems*, Springer- Verlag, New York, 1982, An introduction, Translated from the Portuguese by A. K. Manning.
- [74] G.P. Penney, J. Weese, J.A. J.A. Little, P. Desmedt, D.L.O Hill, and D.J. Hawkes, A comparison of similarity measures for use in 2-D-3-D medical image registration, *IEEE Transactions on Medical Imaging* 17 (1998), no. 4, 586–595.
- [75] P. Perona and J. Malik, Scale-space and edge detection using anisotropic diffusion, *IEEE Trans. Pattern Anal. Machine Intel.* 12 (1990), 629–639.
- [76] E. Pichon, A. Tannenbaum, and R. Kikinis, Statistically based flow for image segmentation, *Medical Imaging Analysis* 8 (2004), 267–274.
- [77] J.P.W Pluim and J.M. Fitzpatrick (Editors), Special issue on image registration, *IEEE Transactions on Medical Imaging* 22 (2003), no. 11.
- [78] J.P.W Pluim, J.B.A. Maintz, and M.A. Viergever, Mutual-information-based registration of medical images: a survey, *IEEE Transactions on Medical Imaging* 22 (2003), no. 8, 986–1004.
- [79] J. Sethian R. Malladi and B. Vemuri, Shape modeling with front propagation: a level set approach, *IEEE Trans. Pattern Anal. Machine Intell.* 17 (1995), 158–175.
- [80] S. Rachev and L. R'uschendorf, *Mass transportation problems*, Springer, 1998.
- [81] L. Roberts, Optical and electro-optical information processing, ch. *Machine perception of 3-D solids*, MIT Press, 1965.
- [82] W.C. Roentgen, Ueber eine neue Art von Strahlen, *Annalen der Physik* 64 (1898), 1–37.
- [83] G. Sapiro, *Geometric partial differential equations and image processing*, Cambridge University Press, Cambridge, 2001.
- [84] G. Sapiro and A. Tannenbaum, Affine invariant scale-space, *International Journal of Computer Vision* 11 (1993), no. 1, 25–44.
- [85] On invariant curve evolution and image analysis, *Indiana Univ. Math. J.* 42 (1993),no. 3, 985–1009.
- [86] On affine plane curve evolution, *Journal of Functional Analysis* 119 (1994), no. 1,79–120.
- [87] J.A. Sethian, *Levelset methods and fast marching methods*, Cambridge University Press, 1999.
- [88] K. Siddiqi, Y. Lauziere, A. Tannenbaum, and S. Zucker, Area and length minimizing flows for shape segmentation, *IEEE TMI* 7 (1998), 433–443.

- [89] L. Simon, Lectures on geometric measure theory, Proceedings of the Centre for Mathematical Analysis, Australian National University, Canberra, 1983.
- [90] 3D Slicer, <http://slicer.org>.
- [91] I.E. Sobel, Camera models and machine perception, Ph.D. thesis, Stanford Univ., 1970.
- [92] M. Sonka, V. Hlavac, and R. Boyle, Image processing: Analysis and machine vision, 2 ed. Brooks Cole, 1998.
- [93] A. Toga, Brain warping, Academic Press, San Diego, 1999.
- [94] A. Tsai, A. Yezzi, and A. Willsky, A curve evolution approach to smoothing and segmentation using the Mumford-Shah functional, CVPR (2000), 1119–1124.
- [95] R. von de Heydt and E. Peterhans, Illusory contours and cortical neuron responses, Science 224 (1984), no. 4654, 1260–2.
- [96] B. White, Some recent developments in differential geometry, Mathematical Intelligencer 11 (1989), 41–47.
- [97] A. P. Witkin, Scale-space filtering, Int. Joint. Conf. Artificial Intelligence (1983), 1019–1021.
- [98] L. Zhu, On visualizing branched surfaces: An angle/area preserving approach, Ph.D. thesis, Department of Biomedical Engineering, Georgia Institute of Technology, 2004.

Erbil Guide Application

*Roojwan Scddeek.Esmael, *Shahab WahabKareem, *Rami S. Youail.

*Department of Information System Engineering-Erbil Technical Engineering College- Hawler Polytechnic University (previously FTE- Erbil), Iraq.

ABSTRACT:

In this paper, a mobile application for navigation system via GSM has been designed. This application is used to search for hotels, restaurants and tourism places in Kurdistan-Iraq. This application help users to find any information about tourist attractions and archaeological and their geographical locations and how to reach them as well as information about hotels, their geographical location and how reach them, the same case for restaurants. In the past it wasn't easy to get this information, and even now, without the use of such applications, it will be difficult for tourists to get such information. The advantage of using this application it helps the users to develop a plan and budget for their trip or visit. The second advantage backs to the hotels and restaurants in which they get an advertisement with low prices throughout the year.

KEYWORDS: mobile technology, Global system for mobile (GSM), geographical location, smart phone, mobile application, windows phone,

I. INTRODUCTION

We now live in the digital age and the information revolution age, what we know to some extent this moment that the technological development and the information revolution brought about great strides in the lives of the people , it has become very easy to get information, by push a button we can get any information at any time we want, the impact of these developments on the field of communication between humans are very big, it has become very easy to communicate with anyone by audio, image, and video even if we live in two different places and away from each other in two different cities or countries, or even continents , Since the invention of the computer at the end of the forties and early fifties of the last century brought about changes and developments are significant in different areas of human life, and one of these fields are mobile phones or cellular. The first mobile phone was produced in the beginning of the seventies The goal of it is the possibility of make a communication of any location in the world to any location in the world without wires, but after thirty years and at the present time mobile phones have become more than just a means of communication it has evolved in the fields of hardware and software, in terms of hardware it has become a great potential of great ability on photography and high accuracy.[1]

technology Development in wireless communication offer the users to access any information and network resource at any time and at any where access to any information and any network resources without restricting them to the fixed network infrastructure. Mobility introduces new challenges as several assumptions made regarding distributed networks that are no longer valid. Many of the research issues regarding wireless networks and mobile computing are not new, for they have been discussed in the context of distributed systems.[2]

II. MOBILE OPERATING SYSTEM.

Referred to as mobile OS, it is the operating system that operates a smart phone, tablet, PDA, or other digital mobile devices. Modern mobile operating systems combine the features of a personal computer operating system with a touch screen, cellular, Bluetooth, Wi-Fi, GPS mobile navigation, camera, video camera, speech recognition, voice recorder, music player, near field communication, Infrared Blaster, and other features.[3]

2-1 Windows Phone Operating System (abbreviated as WP)

It is a series of mobile operating systems developed by Microsoft, and is the successor to its Windows Mobile platform although incompatible with it. Unlike its predecessor, it is primarily aimed at the consumer market rather than the enterprise market. It was first launched in October 2010, with a release in Asia following in early 2011. The latest release of Windows Phone is Windows Phone 8, which has been available to consumers since October 29, 2012. For Windows Phone,

Microsoft created a new user interface, featuring its design language called the Modern design language. Additionally, the software is integrated with third party services, Microsoft services, and sets minimum requirements for the hardware on which it runs. Microsoft is currently developing the next version of Windows Phone, codenamed "Windows Phone Blue" (previously "Windows Phone Apollo Plus") which will either be named Windows Phone 8.1 or Windows Phone 9. [3]

2-2 mobile application (or mobile app)

Is a software application designed to run on smart phones, tablet computers and other mobile devices. They are usually available through application distribution platforms, which are typically operated by the owner of the mobile operating system, such as the Apple App Store, Google Play, Windows Phone Store, and BlackBerry App World. Some apps are free, while others must be bought. Usually, they are downloaded from the platform to a target device, such as an iPhone, BlackBerry, Android phone or Windows Phone, but sometimes they can be downloaded to laptops or desktops. For apps with a price, generally a percentage, 20-30%, goes to the distribution provider (such as iTunes), and the rest goes to the producer of the app. [3]

III. THE TOOLS OF THIS APPLICATION

- [1] Environment Visual Studio 2010 for Windows Mobile iPhone developed by Microsoft Corporation [4]: Visual Studio Express 2010 for Windows Phone is a complete development environment for creating Windows Phone apps. Visual Studio Express 2010 for Windows Phone includes development features such as Windows Phone project templates, a code editor, a Windows Phone-based visual designer, and a Toolbox that contains Windows Phone controls. It also includes integrated testing features such as simulation, monitoring and profiling, and the Windows Phone Store Test Kit. With Visual Studio Express 2010 for Windows Phone, you can debug and deploy your apps on Windows Phone Emulator or a Windows Phone device.
- [2] C Sharp programming language developed by Microsoft Corporation [3]: is a multi-paradigm programming language encompassing strong typing, imperative, declarative, functional, procedural, generic, object-oriented (class-based), and component-oriented programming disciplines. It was developed by Microsoft within its .NET initiative and later approved as a standard by Ecma (ECMA-334) and ISO (ISO/IEC 23270:2006). C# is one of the programming languages designed for the Common Language Infrastructure. C# is intended to be a simple, modern, general purpose, object-oriented programming language. Its development team is led by Anders Hejlsberg.
- [3] Database MySQL [3]: the world's most widely used open source relational database management system (RDBMS) that runs as a server providing multi-user access to a number of databases. It is named after co-founder Michael Widenius' daughter, my. The SQL phrase stands for Structured Query Language.
- [4] Local the server and Wampserver [5]: WampServer is a Windows web development environment. It allows you to create web applications with Apache2, PHP and a MySQL database. Alongside, PhpMyAdmin allows you to manage easily your databases.
- [5] Google Maps [3]: is a web mapping service application and technology provided by Google, that powers many map-based services, including the Google Maps website, Google Ride Finder, Google Transit, and maps embedded on third-party websites via the Google Maps API [3]. It offers street maps, a route planner for traveling by foot, car, bike (beta), or with public transportation and a locator for urban businesses in numerous countries around the world. Google Maps satellite images are not updated in real time, but rather they are several months or years old.

IV. PROPOSED SYSTEM

The application consists of five sections that shown in the figure 1

- a) The hotels department.
- b) The restaurants department.
- c) The tourist areas in the city of Erbil department.
- d) The archeological sites in the city of Erbil department.
- e) The service department.

There is important note to be mention here is that this application that is available to the users has access to the Internet in order to be able to linked to the application database that consist of the names of hotels and restaurants and information available to them and also he could occupy Google maps that need the availability of the Internet. figure (1) represent all the sections of the application. In the following we will explain the function of each section of the application with some details..



Figure-1- Home

- a) Hotels Department : This section of the application dedicated to finding hotels within the city of Erbil, depending on the prices of hotels, which gives the information needed by anyone who wants to book at any hotel when the user presses the (hotels) icon.



Figure-2- Hotels Icon

By selecting the hotel icon it will move the application to the next page for looking about Hotels as shown in figure-3-The application user writes the price of hotel per night in the text box then click search, the system list the name of all hotels that price are less or equal to the price that the user entered . In the same page the user can list the names of all hotel in erbil city by selecting the (list of Hotels in Erbil) button.



Figure-3- search for hotel

when the user presses the button is induction will move the application to the Next page which show the names of all the hotels as shown in figure -4- ,and then the user choose and click on the name of hotel he want, then the system will move to the next page of the application, which gives all the information needed about the selected hotel by the user as in figure-5-



Figure-4- list of hotel



Figure-5-information of hotel

there are two information about location property , the longitude and latitude of the globe and the No. of hotel in order to help the user to contact them either for reservation or to inquire them by phone number or by e-mail address of the hotel, and also there is a Website for the on the Internet and there are also the command button (map) at the top of the application next to the image when the user presses it, it will show the location of the hotel on the map as in figure-6-

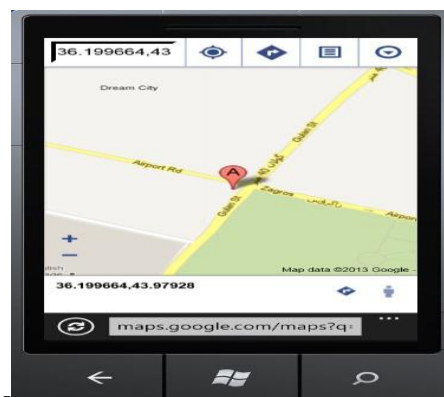


Figure-6- latitude and longitude of the hotels

b) Restaurants Department: This section of the application, dedicated to finding restaurants within the city of Erbil, depending on the number of stars that enjoyed by the restaurant .when the user clicks on the icon restaurants as in figure-7-the system gives all the information needed for the user



Figure-7- icon restaurants

- c) Tourist places in the Erbil city Department: This section of the application dedicated to show the tourist places located in the city of Erbil . when the user presses the places tourism icon as shown in figure-8- it will move the application to the next page, which shows a list of places of tourist located in the city of Erbil and all information about each place.



Figure-8- icon places tourism

- d) Archeological sites in the city of Erbil department : This section of the application dedicated to show the archaeological sites located in the city of Erbil by showing a list of all these places when the user presses the icon Archeological as in figure-9-



Figure-9- icon Archeological

Then the application move to the next page, which shows the list of all places of archaeological located in the city of Erbil that shown in figure-10-



Figure-10-list of city in Erbil

and when the user chooses the place by simply pressing on the name of the place the system will move to the next page, which gives the user a range of information about the selected place as in figure-11-



Figure-11- site archaeological

- e) Services department : This section is intended to give information on some commercial premises in the city of Erbil and also gives phone numbers of some government services as the number of police and hospital number when the user clicks on the icon services as in figure-12-



Figure-12- icon Services

V. CONCLUSION

- [1] The cost of the application is less than the navigator that produce by the tourism because it only needed to download the application and it's free.
- [2] turning Mobile both its hardware and software and systems operation and applications to become more than just a means of communication as it was before for more than a decade . At the present time it communicate between peoples and even it is entertain him and facilitate their lives in many fields of life . At the level of developer and working groups in the field of mobiles it has opened new horizons and promising opportunity to work and improve the standard of living of the lowest costs in countries where there are no use in the field of infrastructure.
- [3] The system don't need any external hardware like pc or laptop with Wi-Fi for search of any location
- [4] The system don't need any wireless coverage to connect to the internet
- [5] The speed of the proposal system is faster than using wifi or internet.

REFERENCES

- [1.] <http://www.unlimit-tech.com>
- [2.] Mazliza O.,Fakulti S. K. &Teknologi M “Mobile Computing and Communications: An Introduction” Malaysian Journal of Computer Science, Vol. 12 No.2, December 1999.
- [3.] <http://en.wikipedia.org/>
- [4.] <http://msdn.microsoft.com/>
- [5.] <http://www.wampserver.com/>

Algorithm on conditional probability on random graph using Markov Chain.

Habiba El-Zohny⁽¹⁾, Hend El- Morsy⁽²⁾

^{1,2}, Mathematics Department Faculty of science Alazhar University Cairo - Egypt

ABSTRACT:

In this paper we will illustrate the conditional probability on random graph. We will compute steady state which can be defined as limits of stationary matrix S . The steady state will be computed for some examples. After that we will illustrate algorithm of random walk in weighted and unweighted graph.

Definitions:

Markov chain, Markov model: Is a mathematical model that makes it possible to study complex systems by establishing a state of the system and then effecting a transition to a new state, such a transition being dependent only on the values of the current state, and not dependent on the previous history of the system up to that point [1].

Probability matrix P: Conditional probability concerning a discrete Markov chain giving the probabilities of change from one state to another [4].

A stationary probability vector S: Is defined as a vector that does not change under application of the transition matrix; that is, it is defined as a left eigenvector of the probability matrix, associated with eigenvalue 1: $SP = S$ [2].

Random Graph: Is a graph in which properties such as the number of graph vertices, graph edges, and connections between them are determined in some random way [3].

Main Results:

Algorithm which calculate the steady state probability of random graph:

Let P is a probability matrix (For which each row sums to 1), and let S is stationary matrix, then the distribution over states can be written as general with relation: $S^{n+1} = S^n P$.

Where (n) describe time period of the system.

Then if at time n the system is in state 2, then 3 times periods later at time $n+3$ the distribution is $S^{n+3} = S^{n+2} P = (S^{n+1} P) P = S^{n+1} P^2$ and so on.

The Algorithm:

- [1] Create associated probability matrix for a given graph.
- [2] Get stationary matrix S .
- [3] Compute $S^0 P = S^1$ which describe the initial distribution of graph.
- [4] Compute $S^{n+1} P = S^n$ until you get steady state probability which defined as :
 - a. $\gamma = \lim_{n \rightarrow \infty} (S)^n$.

Example 1: The graph shown in Fig.(1) represent the probability connects vertices with each other. According to figure, vertex A has probability of 0.9 to connect with A and 0.075 to connect with B, 0.25 to connect with C.

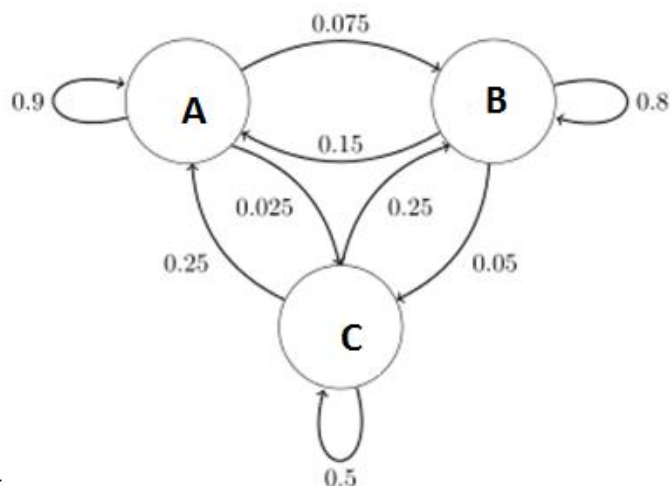


Fig.(1)

We will compute the steady state for this distribution as follows:

[1] Create associated probability matrix $P = \begin{bmatrix} 0.9 & 0.075 & 0.025 \\ 0.15 & 0.8 & 0.05 \\ 0.25 & 0.25 & 0.5 \end{bmatrix}$.

[2] Consider the stationary matrix $S = (0 \ 1 \ 0)$.

[3] Calculate :

$$S^0 P = (0 \ 1 \ 0) \begin{bmatrix} 0.9 & 0.075 & 0.025 \\ 0.15 & 0.8 & 0.05 \\ 0.25 & 0.25 & 0.5 \end{bmatrix} = (0.15 \ 0.8 \ 0.05)$$

[4] $S^1 P = (0.15 \ 0.8 \ 0.05) \begin{bmatrix} 0.9 & 0.075 & 0.025 \\ 0.15 & 0.8 & 0.05 \\ 0.25 & 0.25 & 0.5 \end{bmatrix} = (0.2675 \ 0.6637 \ 0.0687)$

[5] $S^2 P = (0.2675 \ 0.6637 \ 0.0687) \begin{bmatrix} 0.9 & 0.075 & 0.025 \\ 0.15 & 0.8 & 0.05 \\ 0.25 & 0.25 & 0.5 \end{bmatrix} = (0.3575 \ 0.56825 \ 0.0742)$

[6] $S^3 P = (0.3575 \ 0.5682 \ 0.0742) \begin{bmatrix} 0.9 & 0.075 & 0.025 \\ 0.15 & 0.8 & 0.05 \\ 0.25 & 0.25 & 0.5 \end{bmatrix} = (0.4255 \ 0.4999 \ 0.0744)$

Compute steady state distribution as follows:

$\gamma P = \gamma I = \gamma$, then

$\gamma (P - I) = 0$

$$(\gamma_1 \ \gamma_2 \ \gamma_3) \begin{bmatrix} 0.9 & 0.075 & 0.025 \\ 0.15 & 0.8 & 0.05 \\ 0.25 & 0.25 & 0.5 \end{bmatrix} - \begin{bmatrix} 1 & 0 & 0 \\ 0 & 1 & 0 \\ 0 & 0 & 1 \end{bmatrix} = (0 \ 0 \ 0)$$

$$(\gamma_1 \ \gamma_2 \ \gamma_3) \begin{bmatrix} -0.1 & 0.075 & 0.025 \\ 0.15 & -0.2 & 0.05 \\ 0.25 & 0.25 & -0.5 \end{bmatrix} = (0 \ 0 \ 0)$$

Create a system of equation then solve it:

$\gamma_1 + 0.15 \gamma_2 + 0.025 \gamma_3 = 0$

$0.075 \gamma_1 - 0.2 \gamma_2 + 0.025 \gamma_3 = 0$

$0.025 \gamma_1 + 0.5 \gamma_2 - 0.5 \gamma_3 = 0$

And $\gamma_1 + \gamma_2 + \gamma_3 = 1$

This imply that:

$(\gamma_1 \ \gamma_2 \ \gamma_3) = (0.625 \ 0.3125 \ 0.0625)$

This mean that the steady state probabilities indicated that 62.5% of vertices connected with A , 31.5% connect with B and 6.25% connect with C .

Example 2: A Simple Markov Weather Model:

The probabilities of weather conditions, given the weather on the preceding day, can be represented by a transition matrix: $P = \begin{bmatrix} 0.9 & 0.1 \\ 0.5 & 0.5 \end{bmatrix}$

The matrix P represents the weather model in which a sunny day is 90% likely to be followed by another sunny day, and a rainy day is 50% likely to be followed by another rainy day. The columns can be labelled "sunny" and "rainy" respectively, and the rows can be labelled in the same order. $(P)_{ij}$ is the probability that, if a given day is of type i , it will be followed by a day of type j . Notice that the rows of P sum to 1: this is because P is a stochastic matrix.

Predicting the weather

The weather on day 0 is known to be sunny. This is represented by a vector in which the "sunny" entry is 100%, and the "rainy" entry is 0%: $S^0 = (1 \ 0)$

The weather on day 1 can be predicted by:

$$S^1 = S^0 P = (1 \ 0) \begin{bmatrix} 0.9 & 0.1 \\ 0.5 & 0.5 \end{bmatrix} = (0.9 \ 0.1).$$

Thus, there is an 90% chance that day 1 will also be sunny. The weather on day 2 can be predicted in the same way: $S^2 = S^1 P = S^0 P^2 = (0.9 \ 0.1) \begin{bmatrix} 0.9 & 0.1 \\ 0.5 & 0.5 \end{bmatrix} = (0.86 \ 0.14).$

And so on.

Steady state of the weather

In this example, predictions for the weather on more distant days are increasingly inaccurate and tend towards a steady state vector. This vector represents the probabilities of sunny and rainy weather on all days, and is independent of the initial weather.

$\gamma P = \gamma I = \gamma$, then

$$\gamma (P - I) = 0$$

$$(\gamma_1 \ \gamma_2) \left(\begin{bmatrix} 0.9 & 0.1 \\ 0.5 & 0.5 \end{bmatrix} - \begin{bmatrix} 1 & 0 \\ 0 & 1 \end{bmatrix} \right) = (0 \ 0) .$$

$$(\gamma_1 \ \gamma_2) \begin{bmatrix} -0.1 & 0.1 \\ 0.5 & -0.5 \end{bmatrix} = (0 \ 0).$$

$$-0.1 \gamma_1 + 0.5 \gamma_2 = 0$$

$\gamma_1 + \gamma_2 = 1$ by solving these equations we have:

$$(\gamma_1 \ \gamma_2) = (0.833 \ 0.167) . \text{ In conclusion, in the long term, 83\% of days are sunny.}$$

Example 3: Consider a company has two brands A,B .10 % market share using brand A and 40% use the other brand. the transition matrix given by: $P = \begin{bmatrix} 0.8 & 0.2 \\ 0.6 & 0.4 \end{bmatrix}$ If $S^0 = (0.1 \ 0.4).$

$$S^1 = S^0 P = (0.1 \ 0.4) \begin{bmatrix} 0.8 & 0.2 \\ 0.6 & 0.4 \end{bmatrix} = (0.62 \ 0.38).$$

$$S^2 = (0.62 \ 0.38) \begin{bmatrix} 0.8 & 0.2 \\ 0.6 & 0.4 \end{bmatrix} = (0.724 \ 0.276).$$

$$S^3 = (0.724 \ 0.276) \begin{bmatrix} 0.8 & 0.2 \\ 0.6 & 0.4 \end{bmatrix} = (0.744 \ 0.255).$$

And so on ,then the steady state will be: $(\gamma_1 \ \gamma_2) \left(\begin{bmatrix} 0.8 & 0.2 \\ 0.6 & 0.4 \end{bmatrix} - \begin{bmatrix} 1 & 0 \\ 0 & 1 \end{bmatrix} \right) = (0 \ 0) .$

$$(\gamma_1 \ \gamma_2) \begin{bmatrix} -0.2 & 0.1 \\ 0.5 & -0.6 \end{bmatrix} = (0 \ 0).$$

$$-0.2 \gamma_1 + 0.6 \gamma_2 = 0$$

$\gamma_1 + \gamma_2 = 1$ by solving these equations we have:

$$(\gamma_1 \ \gamma_2) = (0.75 \ 0.25) . \text{ this means that 75\% use brand A and 25\% use brand B.}$$

Algorithm which calculate random graph:

We will illustrate the algorithm for two kinds of graph , weighted and un weighted graph.

For un weighted graph:

Input: An undirected graph $G(V,E)$ with $|V| > 1, |E| > 0$.

Steps:

- [1] Look for random pair of nodes x, y that are nonadjacent .
- [2] If no such pair of nodes x, y exists , then output G' .
Else
- [3] Add element $\{ x, y \}$ to set E' .
- [4] Return to step 1 .
End while.
- [5] Output G' .
End algorithm.

We find that output graph G' is graph with the same number of connected component as G , and has maximum possible density as a clique.

Example 1:By using the previous algorithm find the output random graph shown in Fig. (4)

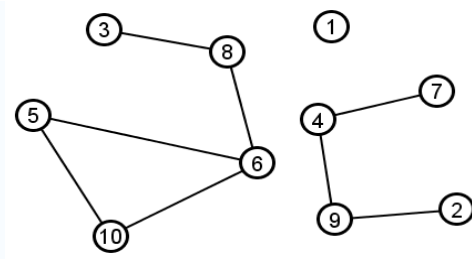


Fig.(4)

Input: Undirected graph with 10 vertices , and has 3 component , $|E| = 8$ edges.

Steps:

- [1] Start randomly with two nonadjacent nodes $\{ 8, 10 \}$
- [2] Add element $\{ 8, 10 \}$ to set E' .
- [3] Return to step 1 with another pair of nodes.
- [4] Output G' .
End algorithm.

The result graph G' shown in Fig.(5).

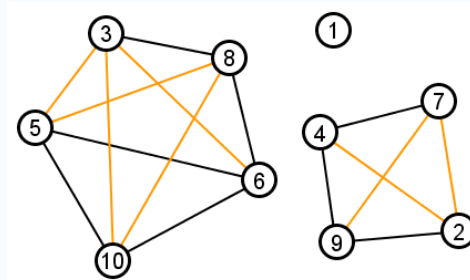


Fig.(5)

We find that the output graph is regular and complete.

Lemma 1: The output graph generating by algorithm of random graph will be regular and complete.

Example 2:For another graph shown in Fig.(6) with 10 vertices but 1 component.

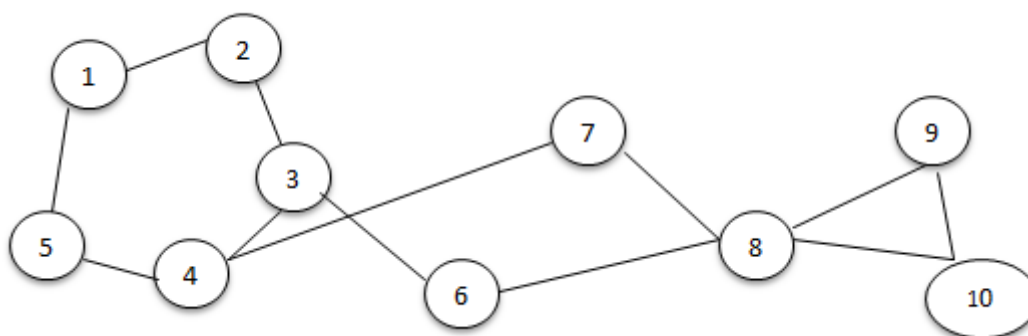


Fig.(6)

Input: Undirected graph with 10 vertices and 1 component.

Steps:

- [1] Start randomly with nonadjacent vertices s.t {1,6}.
- [2] Add element {1,6} to set E' .
- [3] Return to step 1.
- [4] Output G' .

End algorithm. Output graph shown in Fig.(7).

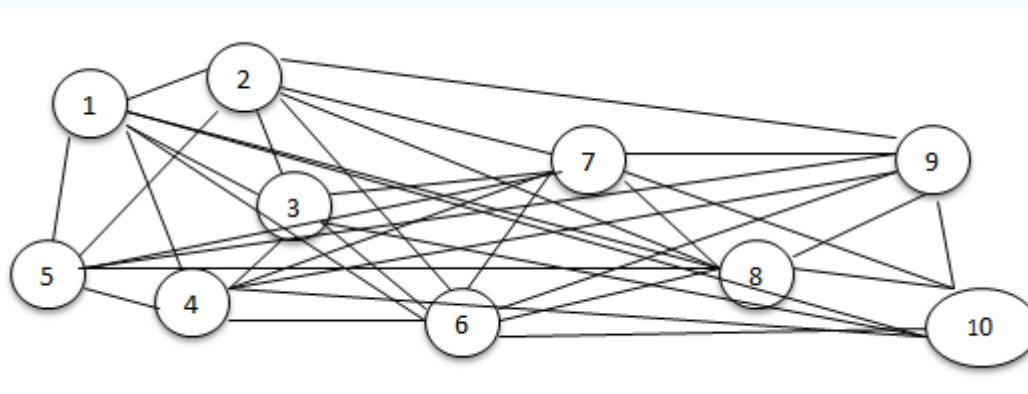


Fig.(7)

2b. For weighted graph:

Input: An undirected weighted graph $G(V, E)$ with $|V| > 1$, $|E| > 0$.

Steps:

1. Create the associated matrix .
2. Normalize this matrix.
3. Get the first transition probability matrix P .
4. Expand by taking P^{th} power of P .
5. Get stationary matrix S .
6. Compute $S^0 P = S^1$ which describe the initial distribution of graph.
7. Compute $S^{n+1} P = S^n$ until you get steady state probability which defined as :

$$\gamma = \lim_{n \rightarrow \infty} (S)^n$$

Notes: 1. When normalize matrix in this algorithm, column sums to one.
 2. Each power of P consider as possibility distribution of random graph.

Example 3: Calculate random graph for weighted graph shown in Fig.(8).

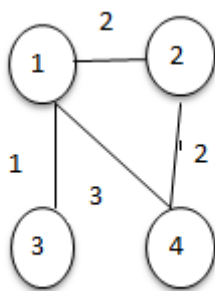


Fig.(8)

1. Associated matrix is:
$$\begin{bmatrix} 0 & 2 & 1 & 3 \\ 2 & 0 & 0 & 2 \\ 1 & 0 & 0 & 0 \end{bmatrix}$$

2. Normalize the matrix :
$$\begin{bmatrix} 0 & 1/2 & 1 & 3/5 \\ 1/3 & 0 & 0 & 2/5 \\ 1/6 & 0 & 0 & 0 \end{bmatrix}.$$

3.
$$P^2 = P \cdot P = \begin{bmatrix} 19/30 & 3/10 & 0 & 1/5 \\ 1/5 & 11/30 & 1/3 & 1/5 \\ 0 & 1/12 & 1/6 & 1/10 \end{bmatrix}$$

$$P^3 = P^2 \cdot P = \begin{bmatrix} 1/5 & 5/12 & 19/30 & 25/50 \\ 5/18 & 1/5 & 1/5 & 4/15 \\ 11/45 & 1/20 & 0 & 1/30 \end{bmatrix}$$
 And so on.

4. Get steady state :
$$\begin{pmatrix} \gamma_1 \\ \gamma_2 \\ \gamma_3 \\ \gamma_4 \end{pmatrix} \left(\begin{bmatrix} 0 & 1/2 & 1 & 3/5 \\ 1/3 & 0 & 0 & 2/5 \\ 1/6 & 0 & 0 & 0 \end{bmatrix} - \begin{bmatrix} 1 & 0 & 0 & 0 \\ 0 & 1 & 0 & 0 \\ 0 & 0 & 1 & 0 \end{bmatrix} \right) = \begin{pmatrix} 0 \\ 0 \\ 0 \\ 0 \end{pmatrix}$$

$$\begin{pmatrix} \gamma_1 \\ \gamma_2 \\ \gamma_3 \\ \gamma_4 \end{pmatrix} \begin{bmatrix} -1 & 1/2 & 1 & 3/5 \\ 1/3 & -1 & 0 & 2/5 \\ 1/6 & 0 & -1 & 0 \end{bmatrix} = \begin{pmatrix} 0 \\ 0 \\ 0 \\ 0 \end{pmatrix}$$

Then $\gamma_1 =$

$\gamma_3 =$

$\gamma_2 =$

$\gamma_4 =$

Note: We normalize the matrix by dividing the column (Which expressed a vertex V) by sums of weights of all edges coming out of this vertex.

As example, vertex 1 adjacent with 3 edges of weights 2,3,1 then we divide column1 by (2+3+1) and so on.

Example 4: For graph shown in Fig.(9) calculate two possibility distributions for random graph.

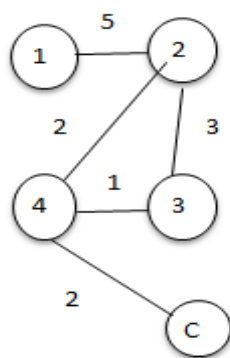


Fig.(9)

4. Associated matrix :
$$\begin{bmatrix} 0 & 5 & 0 & 0 & 0 \\ 5 & 0 & 3 & 2 & 0 \\ 0 & 3 & 0 & 1 & 0 \end{bmatrix}$$

5. Normalize matrix :
$$\begin{bmatrix} 0 & 5/10 & 0 & 0 & 0 \\ 1 & 0 & 3/4 & 2/5 & 0 \\ 0 & 3/10 & 0 & 1/5 & 0 \end{bmatrix} = P.$$

6.
$$P^2 = P \cdot P = \begin{bmatrix} 5/10 & 0 & 15/40 & 10/50 & 0 \\ 0 & 161/200 & 2/20 & 3/20 & 2/5 \\ 3/10 & 2/50 & 11/40 & 6/50 & 1/5 \end{bmatrix}$$

Application: Steady state for random bipartite graph:

Definition of random bipartite graph: Is a bipartite graph which two sets can be randomly joined with each other, such that the first set can be considered as begin then the other set consider as begin.

In random bipartite graph, we will compute steady state two times by changing the beginning set.

Example 4: Consider a bipartite graph as shown in Fig.(2) which consist of two sets : { 1,2,3 } and { A,B,C }, compute the steady state for this graph when set { 1,2,3 } is beginning set, then when { A,B,C } is beginning set.

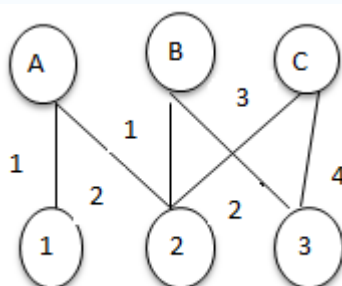


Fig.(2)

First, the incident matrix of this graph is:
$$\begin{bmatrix} 1 & 0 & 0 \\ 2 & 1 & 2 \\ 0 & 3 & 4 \end{bmatrix}$$

Normalize the matrix:
$$\begin{bmatrix} 1/3 & 0 & 0 \\ 2/3 & 1/4 & 2/6 \\ 0 & 3/4 & 4/6 \end{bmatrix}, S^0 = \begin{pmatrix} 0 \\ 1 \\ 0 \end{pmatrix}$$

$$\text{Then: } S^1 = \begin{pmatrix} 0 \\ 1 \\ 0 \end{pmatrix} \begin{bmatrix} 1/3 & 0 & 0 \\ 2/3 & 1/4 & 2/6 \\ 0 & 3/4 & 4/6 \end{bmatrix} = \begin{pmatrix} 0 \\ 1/4 \\ 3/4 \end{pmatrix}$$

$$S^2 = \begin{pmatrix} 0 \\ 1/4 \\ 3/4 \end{pmatrix} \begin{bmatrix} 1/3 & 0 & 0 \\ 2/3 & 1/4 & 2/6 \\ 0 & 3/4 & 4/6 \end{bmatrix} = \begin{pmatrix} 0 \\ 5/16 \\ 11/16 \end{pmatrix} \text{ and so on.}$$

Then the steady state can obtained as follows:

$$\begin{pmatrix} \gamma_1 \\ \gamma_2 \\ \gamma_3 \end{pmatrix} \left(\begin{bmatrix} 1/3 & 0 & 0 \\ 2/3 & 1/4 & 1/3 \\ 0 & 3/4 & 2/3 \end{bmatrix} - \begin{bmatrix} 1 & 0 & 0 \\ 0 & 1 & 0 \\ 0 & 0 & 1 \end{bmatrix} \right) = \begin{pmatrix} 0 \\ 0 \\ 0 \end{pmatrix}$$

$$\begin{pmatrix} \gamma_1 \\ \gamma_2 \\ \gamma_3 \end{pmatrix} \begin{bmatrix} -2/3 & 0 & 0 \\ 2/3 & -3/4 & 1/3 \\ 0 & 3/4 & -1/3 \end{bmatrix} = \begin{pmatrix} 0 \\ 0 \\ 0 \end{pmatrix}$$

$$-2/3 \gamma_1 = 0 \quad \gamma_1 = 0,$$

$$2/3 \gamma_1 - 3/4 \gamma_2 + 1/3 \gamma_3 = 0, \quad \gamma_1 + \gamma_2 + \gamma_3 = 1$$

By solving these equations we find that:

$$\begin{pmatrix} \gamma_1 \\ \gamma_2 \\ \gamma_3 \end{pmatrix} = \begin{pmatrix} 0 \\ 4/13 \\ 9/13 \end{pmatrix}$$

We can compute steady state for the same graph by considered the set { 1,2,3} is the beginning set as follows:

$$\text{the incident matrix of this graph will be: } \begin{bmatrix} 1 & 2 & 0 \\ 0 & 1 & 3 \\ 0 & 2 & 4 \end{bmatrix}$$

$$\text{Normalize the matrix: } \begin{bmatrix} 1 & 2/5 & 0 \\ 0 & 1/5 & 3/7 \\ 0 & 2/5 & 4/7 \end{bmatrix}, S^0 = \begin{pmatrix} 0 \\ 1 \\ 0 \end{pmatrix}$$

$$\text{Then: } S^1 = \begin{pmatrix} 0 \\ 1 \\ 0 \end{pmatrix} \begin{bmatrix} 1 & 2/5 & 0 \\ 0 & 1/5 & 3/7 \\ 0 & 2/5 & 4/7 \end{bmatrix} = \begin{pmatrix} 0 \\ 1/4 \\ 3/4 \end{pmatrix}$$

$$S^2 = \begin{pmatrix} 0 \\ 1/4 \\ 3/4 \end{pmatrix} \begin{bmatrix} 1 & 2/5 & 0 \\ 0 & 1/5 & 3/7 \\ 0 & 2/5 & 4/7 \end{bmatrix} = \begin{pmatrix} 2/5 \\ 1/5 \\ 2/5 \end{pmatrix} \text{ and so on.}$$

Then the steady state can obtained as follows:

$$\begin{pmatrix} \gamma_1 \\ \gamma_2 \\ \gamma_3 \end{pmatrix} \left(\begin{bmatrix} 1 & 2/5 & 0 \\ 0 & 1/5 & 3/7 \\ 0 & 2/5 & 4/7 \end{bmatrix} - \begin{bmatrix} 1 & 0 & 0 \\ 0 & 1 & 0 \\ 0 & 0 & 1 \end{bmatrix} \right) = \begin{pmatrix} 0 \\ 0 \\ 0 \end{pmatrix}$$

$$\begin{pmatrix} \gamma_1 \\ \gamma_2 \\ \gamma_3 \end{pmatrix} \begin{bmatrix} 0 & 2/5 & 0 \\ 0 & -4/5 & 3/7 \\ 0 & 2/5 & -3/7 \end{bmatrix} = \begin{pmatrix} 0 \\ 0 \\ 0 \end{pmatrix}$$

After Creating a system of equation and solve it we find that:

$$\begin{pmatrix} \gamma_1 \\ \gamma_2 \\ \gamma_3 \end{pmatrix} = \begin{pmatrix} 1 \\ 0 \\ 0 \end{pmatrix}.$$

by comparing the two states we find that γ_1 at first has highest steady state and lowest steady state when we consider set {1,2,3} is the beginning set, the same note for γ_2, γ_3 .

Example 2:for bipartite graph shown in Fig.(3), compute the steady state for each vertex.

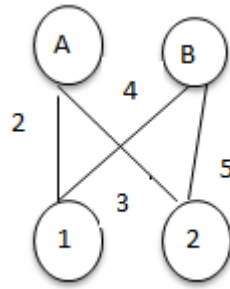


Fig.(3)

First , the incident matrix of this graph is : $\begin{bmatrix} 2 & 3 \\ 4 & 5 \end{bmatrix}$

Normalize the matrix : $\begin{bmatrix} 2/6 & 3/8 \\ 4/6 & 5/8 \end{bmatrix}$

Then the steady state can obtained as follows:

$$\begin{pmatrix} \gamma_1 \\ \gamma_2 \end{pmatrix} \left(\begin{bmatrix} 1/3 & 3/8 \\ 2/3 & 5/8 \end{bmatrix} - \begin{bmatrix} 1 & 0 \\ 0 & 1 \end{bmatrix} \right) = \begin{pmatrix} 0 \\ 0 \end{pmatrix}$$

$$\begin{pmatrix} \gamma_1 \\ \gamma_2 \end{pmatrix} \begin{bmatrix} -2/3 & 3/8 \\ 2/3 & -3/8 \end{bmatrix} = \begin{pmatrix} 0 \\ 0 \end{pmatrix}$$

since $\gamma_1 + \gamma_2 = 1$, $-2/3 \gamma_1 + \frac{3}{8\gamma_2} = 0$ then

$$\begin{pmatrix} \gamma_1 \\ \gamma_2 \end{pmatrix} = \begin{pmatrix} 9/25 \\ 16/25 \end{pmatrix}$$

We can compute steady state for the same graph by considered the set { 1,2} is the beginning set as follows:

the incident matrix of this graph will be: $\begin{bmatrix} 2 & 4 \\ 3 & 5 \end{bmatrix}$

Normalize the matrix: $\begin{bmatrix} 2/5 & 4/9 \\ 3/5 & 5/9 \end{bmatrix}$

$$\text{then : } \begin{pmatrix} \gamma_1 \\ \gamma_2 \end{pmatrix} \begin{bmatrix} -3/5 & 4/9 \\ 3/5 & -4/9 \end{bmatrix} = \begin{pmatrix} 0 \\ 0 \end{pmatrix}$$

$$-3/5 \gamma_1 + 4/9 \gamma_2 = 0$$

$$\gamma_1 + \gamma_2 = 1$$

$$\begin{pmatrix} \gamma_1 \\ \gamma_2 \end{pmatrix} = \begin{pmatrix} 28/75 \\ 47/75 \end{pmatrix}. \text{ Which change of the first state.}$$

REFERENCES:

- [1]Saunders Comprehensive Veterinary Dictionary , 3 ed , Elsevier, Inc , (2007).
- [2]G. Latouche, V. Ramaswami. Introduction to Matrix Analytic Methods in Stochastic Modeling, 1st edition. Chapter 2: PH Distributions; ASA SIAM, 1999.
- [3]Bollobás, B. Random Graphs. London: Academic Press, 1985.
- [4]<http://www.answers.com/topic/transition-probability#ixzz2VQy2siJm> .

Analysis of Activity Patterns and Design Features Relationships in Urban Public Spaces: A Case Study of the Old City Of As-Salt

Dr. Rana Almatarneh, Ph.D.

Assistant Professor of Architecture Chair, Department of Architectural Engineering College of Architecture and Design Al- Ahliyya Amman University

ABSTRACT

Urban public spaces have been considered an essential part of cities throughout history. Over the span of urban life, public spaces have continuously reflected the complexities of their cities' cultural, social, and economic contexts; whether as memorable, accessible, or meaningful places. However, recent researches on public spaces reveal that some are currently experiencing a decline in their physical design and in their use. Thus, in this period of change in using public spaces, it becomes important to investigate and evaluate the actual use of public spaces, how and why they are used, particularly in terms of their physical deterioration and improvement. Therefore, an opportunity exists to reveal and understand the interrelationship between physical patterns of public spaces and people's activity patterns within such spaces. As such, this research considers the design features of urban public space, focusing on people's activities and various forms of use. It employs a methodology that combines three major components; case study selection, data collection and management, data analysis to explore in depth the activity pattern related to the physical pattern of public spaces, within the case study. Finally, this research is expected to add insights into the application of urban design theories and practice which could lead to further studies to improve the public spaces design and planning process.

KEYWORDS: The Old City of As-Salt, Public Space, Public Square, Activity Patterns, Design Factors, Case Study

I. INTRODUCTION

Throughout the centuries, squares have been created and used for various purposes: from places to debate every-day societal issues and to exchange commodities to venues for political demonstrations or special events. Urban development would be impossible without public spaces such as squares, because they have been common exchange platforms of goods, knowledge, experience, culture, and entertainment (van Melik, 2008). Although the functions differ from square to square and from period to period, there is a common denominator: most squares function as meeting places where people spend time in. During the last decade we have been able to observe a renewed interest in urban public spaces in general, and most particularly in streets and squares both among town dwellers, theoreticians and practitioners of urbanism and architecture (Appleyard, 1981; Jacobs, 1961; Whyte, 1980). It is obvious that cities and their public spaces have a very close relationship, whereby, over the span of urban life, public spaces have continuously reflected the complexities of their cities' cultural, social, and economic contexts. Public spaces play a particular role in the life of urban areas, whether as memorable, accessible, or meaningful places (Madanipour, 2010). People may feel attached to both the social and physical aspects of public spaces. Therefore, these spaces may be places for socializing, hosting the greatest number of people's interactions (Tibbalds, 2003). Moreover, their physical attributes may indicate particular meanings to the people, having a significant impact on people's perceptions, interactions and activities (Canter, 1977).

However, recent researches on public spaces reveal that some are currently experiencing a decline in their physical design and in their use (Carmona, 2010). In his article "Contemporary public

space: critique and classification”, Carmona (2010) mentions that the critiques in this realm begin with the attitude that public spaces are facing a physical deterioration. Many writers and scholars of public spaces issues identify a general decline, for which the causes and prescriptions are different according to the context of urban planning and designing. For example, one of the critiques that Carmona discusses relates to the phenomenon of “Invaded Space”, resulting from the loss or lack of social function and experiences in urban spaces that is now over used by traffic and private cars. Thus, in this period of change in using public spaces, it becomes important to evaluate and investigate actual use of contemporary public spaces, how and why they are used, particularly in terms of their physical deterioration and/or improvement. As some scholars of urban planning and designing, including Jan Ghel (1987) and William Whyte (1980), have argued, the use of public spaces is an empirical result of the physical qualities of space.

Therefore, an opportunity exists to reveal and understand the interrelationship between physical patterns of contemporary public spaces and people’s activity patterns within these spaces. Such empirical researches on public spaces will help to find out why and how “some places work and others do not” (Whyte, 1980). Moreover, it should be possible to find out how physical settings impact the experience of activities taking place within the public spaces. As such, this paper addresses two main questions: 1) How people’s activities relate to the design features of an urban public square, and 2) How activities are influenced and encouraged by design features.

II. Overview of the urban open public space

2.1 Urban open public spaces definition and characteristics Public space is an integral part of the public realm. The physical public realm means the series of spaces and settings that support or facilitate public life and social interaction. It is considered as sites or settings of formal and informal public life that have ‘physical’ (i.e. space) and ‘social’ (i.e. activity) dimensions. The activities and events occurring within urban spaces can make it the socio – cultural public realm (Carmona, 2010, 137). For Montgomery (1998), the public realm in a city accomplishes different functions by providing meeting places, defining spaces for local traditions and identifying meaning and identity (Montgomery, 1998: 110). Public space are conceived of as an outdoor room within a neighborhood, somewhere to relax, and enjoy the urban experience, a venue for a range of different activities, from outdoor eating to street entertainment; from sport and play areas to a venue for civic or political functions; and most importantly of all a place for walking or sitting out. Public spaces work best when they establish a direct relationship between the space and the people who live and work around it” (Thompson, 2002, 61). Public space as a fundamental part of the public realm is penetrating in social sciences and humanities disciplines.

Thus, the UK government has adopted the following definition of public space (Carmona et al. 2010: 137): Public space relates to all those parts of the built and natural environment where the public have free access. It encompasses: all the streets, squares and other rights of way, whether predominantly in residential, commercial or community/civic uses; the open spaces and parks; and the “public-private” spaces where public access is unrestricted. It includes the interfaces with key internal and private spaces to which the public normally has free access. Cooper and Francis (1998) gave a definition drawn from the work of Lynch (1981) who argues that open space is open when it is accessible; “urban open spaces are defined as publicly accessible open places designed and built for human activity and enjoyment including parks and downtown plazas” (Cooper and Francis, 1998: 76). According to Carr et al. (1992), in terms of use and design, public space characterized in three main categories. Thus, these places as well as being “Meaningful” allowing people to make rich linkage and attachments with place, “Democratic” – protecting the right of user groups, and accessible to all groups and providing for freedom of action – should be “Responsive” – to address intended users’ needs (Carmona, 2010, 208-209).

2.2 Activity

Pattern Regarding the concept of place, finding potential relationships between types of place and types of activities requires identifying patterns of activity in a place. Many places have clearly defined activity patterns associated with them. Some activities are appropriate to certain places, and some places may be characterized with particular activities (Canter, 1977: 116). According to Canter (1977), the issue is that some places have very specific functions and appropriate categories of activities, while for others are more difficult to identify particular activities. Their character thus derives from the range of activities they accommodate. Therefore, most places are somewhere between these two extremes and understanding place differentiation relates to the pattern of activities taking place within them (Canter, 1977: 117). For Carmona (2010), “movement” is fundamental to understanding how places work. Pedestrian flow and movement within public spaces is necessary factor for urban experience and vitality. Where people choose to sit in public space is often based on available choices for people-watching and provides opportunities for related activities such as social and cultural interactions (Carmona, 2010: 201). Carmona (2010) stated that successful “people places” may be considered as destinations (go to places) but there are also places on the way to many other places (go through places). Therefore, there is a movement to and movement through places (Carmona, 2010: 202). Hillier et al. (1993) explored the relationship between pedestrian movement and the configuration of urban space, and thereafter the relationship with pedestrian densities and land uses. Based on this research, movement densities can be accurately predicted by analyzing spatial configuration.

The configuration of space, particularly its effect on visual permeability, is most important in determining movement densities. To encourage pedestrian movement and support a vital and viable range of uses connectivity among active places is essential. This connectedness with the surrounding thus identifies the density of use and forms the activity patterns (Carmona, 2010). Within such spaces presence of people and the number of them who chose the space to use also identifies the success level of space in terms of use. Jacobs (1961) argued that bringing people to the street will lead to vitality. Therefore, the design of successful spaces will support and facilitate the people’s activities (Carmona, 2010: 208). Urban designers, thus, need to learn how to make better people places by observing existing places and through dialogue with their users and stakeholders (Carmona, 2010: 132). Vital and peopled urban public spaces provide people’s need and desires. In other words, people need to feel psychologically comfortable or engaged enough to want to stay and play within the space (Carmona, 2010: 206).

In terms of being engaged to stay in a place, Carmona (2010) identifies two major types of engagement: Passive engagement: this type of engagement with the environment relates to a sense of relaxation which will require appropriate physical settings in a place while there is no need to become actively involved. Sitting and people watching are among the primary form of passive engagement (Carmona, 2010: 209). Whyte (1980:13), for example, found that “what attracts people is other people”, which will also bring life and activity to a place. This type of engagement often takes place next to the pedestrian flow while design features also provide sitting choices such as fountains, benches on walkways. Active engagement: this type of engagement represents an active experience within a place and will often result in social interaction among the involved people. Successful “people places” provide opportunities for different levels of engagement and the design of a space can create such opportunities. Thus, the arrangement of different design elements leads to social interaction. These elements could include small-scale components; public artworks, play equipment, street furniture, sculptures, fountains and stairways which will create places for meeting (Carmona, 2010: 211). According to Jan Gehl (1987), one of the most important attributes of public spaces is people activity.

In terms of activities typology, Gehl (1987) distinguishes three main types; necessary/functional activities, optional/recreational activities and social activities that take place based on public space characteristics. According to this typology, the optional activities reveal the relationship between design features offered by the space and people activities. It is the potential activities that defined

people places with different opportunities such as eating, sitting, playing. As the third typology, social activities are the result of other types of activities and rather depend on the involved people within the space than physical features of the space. It is worth mentioning that optional activities are most affected by the environmental qualities and often lead to “social cohesion” of space. As such, spaces become meaningful and attractive when all activities of all types occur in combination (Golicnik, 2010). 2.3 Physical Pattern Lynch (1981) offers basic design qualities in place making process: Vitality, Sense, Access, Control and Fit. Through vitality he believes that a city allows range of diverse activities within the city. For Lynch, sensible city is achieved through form and functions relationships which make it legible. Accessibility for a city allows all different groups of people to use resources and services. Lynch stated that a city with good control is organized in way that citizens have a role in spaces management as they are working and living. The fifth criterion, fit, refers to creating the relationship between activities and physical form of a place. Considering the physical pattern, fit provides the building, spaces and networks for people who are using them and activities are taking place within them. In his research, Lynch (1960) identified five key physical elements – paths, edges, districts, nodes and landmarks – that contribute to configure the image of a city: “districts are structured with nodes, defined by edges, penetrated by paths, and sprinkled with landmarks... elements regularly overlap and pierce one another” (Lynch, 1960: 47-49). Thus, these key physical elements are essential in creating relationship between physical and activity pattern. 3.

III. METHOD

3.1 Conceptual

Theoretical Framework The current study investigated the way in which built environment qualities as well as patterns of particular qualities affect people activity within the urban spaces. It discusses the actual use of urban public spaces, particularly public squares, how and why they are used in terms of their physical Setting. Therefore, it employs an empirical methodology that combines three major components; case study selection, data collection and management, data analysis. As such, this study provides a conceptual framework based on physical and functional attributes described by physical and activity principles such as population density, mixed use, accessibility, human Scale, connectivity, Imageability and legibility, landmark, enclosure, complexity, architectural style and green space (Table 1). It also investigates the inter-relationship between the physical design features of urban public space and people’s activities and various forms of use – from active to passive engagement.

Table 1. Case Study Selection Criteria

Place Components	Principles			
Activity	Types of Activity	Necessary	Active Engagement	Population density
				Pedestrian flows and movements
				Vitality and Diversity
		Optional	Passive Engagement	People attractors
				Cultural and Social events
				people watching
Social				
Physical Setting			Population density	
			Mixed use	
			Human Scale	
			Accessibility	
			Connectivity	
			Imageability and legibility	
			Landmarks	
			Enclosure	
			Complexity	
			Architectural style	
			Green/Water space	

A case study was selected and employed as the qualitative strategy of inquiry to explore in depth the *activity pattern*– from *active* to *passive engagement*– related to the *physical pattern* of public spaces (Table 2). In addition, *the detailed information* was collected, using *direct field observation*, a *questionnaire survey*, *maps* and *photos*, based on the activities of people at the selected study sites and during a certain period of time. *Field observation* was utilized to record activities in an unstructured or semi structured way and often notes were augmented with visual materials. The collected data was gathered and tailed for the activity typology and physical components based on the selected urban design principles as represented in Table 2. The percentages of each reference are then calculated to refer to each activity. This methodology contributes greatly to the understanding of the physical structure of the cases in this study.

Table 2. Activity typology and physical components based on the selected theoretical principles

Activity Component		Activity Principles
Activity Level	Activity Types	
Passive engagement	Sitting	Vitality and Density of population: Number of people using the space
	Sitting with a child	
	Sitting on a wheelchair	
	Standing	
	Standing with a child	
	Laying down on lawn or bench	
Active engagement	Cycling	People attractors
	Exercising	
	Taking photo	Diversity of space use
	Playing	
	Playing music	
	Walking	
	Walking with a child	
	Walking with a wheelchair	
Physical Component	Physical Principles	Physical Principles
Design Features		<ul style="list-style-type: none"> ▪ Design lay out ▪ Landmark ▪ Grass and water space
Paths, Edges, Furniture, Natural Features		

3.2 Case Study Selection Procedure

Case studies allow exploration of theories and provide opportunities understanding and in examining them at the ground (Baxter & Jack, 2008, p. 544). Thus, within this study, where the goal is to provide insight into how peoples’ activities relate to the physical pattern of public spaces, a case study is appropriate since it serves as laboratory for testing theoretical and methodological theories and concepts (Cresswell, 2009). The Old City of Salt was selected as the study area among other Jordanian cities due to its strategic, geographical, political and cultural position as the most historic town in Jordan. Furthermore, Old Salt is a multicultural and diverse city that has a variety of proportions of uses and needs regarding public space use. Public Squares in The Old City of Salt consist of a range of design configurations that lead to *various types of activities*. In order to understand the relationship between *physical* and *activity patterns* within a public space, Al-Ain Square, Al-Hammam Square and Al- Baladiyyah Square were selected as the study sites. The goal is to select public squares with varying levels of physical features and activity patterns.

IV. OVERVIEW OF THE URBAN PUBLIC SQUARE IN THE OLD CITY OF AS-SALT

4.1 The Old City of As-Salt

Salt lies 20 kilometers to the east of Jordan Valley at an altitude of 800 m (Fig. 1). Its foundation is based on a merchant city, developed from the towns of Middle Age. It was of great importance in the 19th and early 20th century during the Turkish rule in Jordan, where served as the chief administrative and trading center for the surrounding area. During this period of time, it became the most important trading and market Centre serving Gilead on the East Bank, with links to Nablus, Jerusalem and the Mediterranean to the west and Damascus to the north. Salt’s heyday was when traders arrived from Nablus to expand their trading network eastwards beyond the River Jordan.

As a result of the influx of newcomers this period saw the rapid expansion of Salt from a simple peasant village into a town with unique landscape, new land-uses and architectural styles. It is now the administrative Centre for the Balqa Region, only 30km north-west Amman with which it has a close inter-relationship. The present population of Salt is approximately 62,109 of whom some 15,000 live in the older central districts: "Old Salt". Old Salt developed around the spring in the Akrad Valley, on three hills- Al-Qal'a, Al-Jad'a and As-Salalem- separated by the flood plain of Wadi-Akrad and Wadi As-Salt; and composed of a web of footpaths and stairways running across the slopes and limited number of roads following the slopes where the contours allowed (Figure 2).

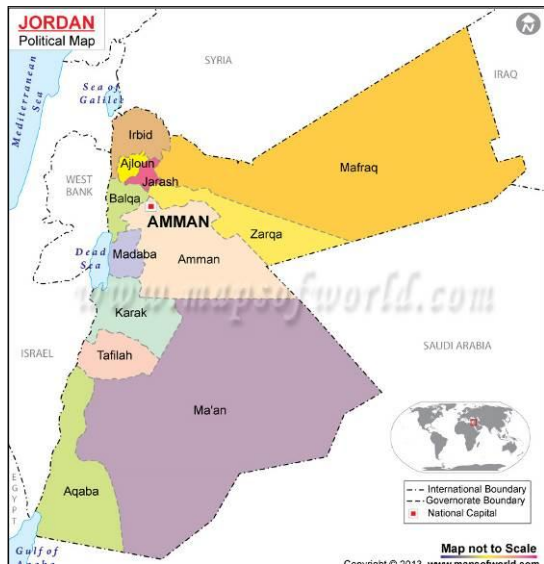
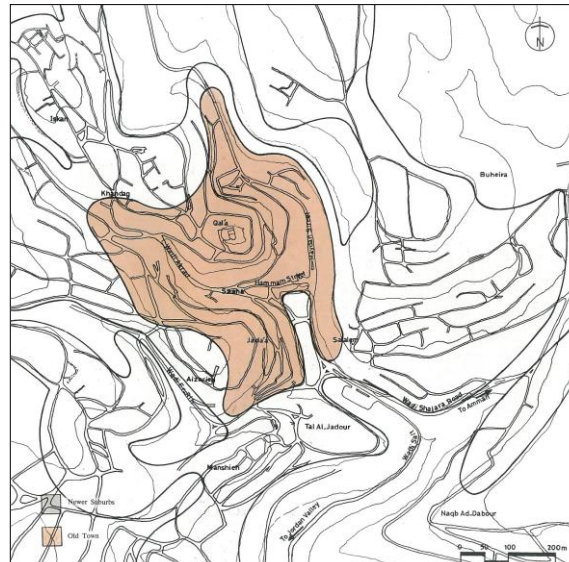


Fig. 1 Location of As-Salt, Jordan. Source: <http://www.mapsofworld.com>.



ig.2 Urban form of Old City As-Salt

The *main patterns of land use* of the old central districts: "Old Salt" focused on a *multifunctional core structure* enveloping surrounding the *central mosque* by different layers of interconnected suqs (Figure 3). As a rule, these are interspersed with a number of hammams, madrasas, and caravanserais, which constitute the support for the mosque and retail shops (Figure 4).

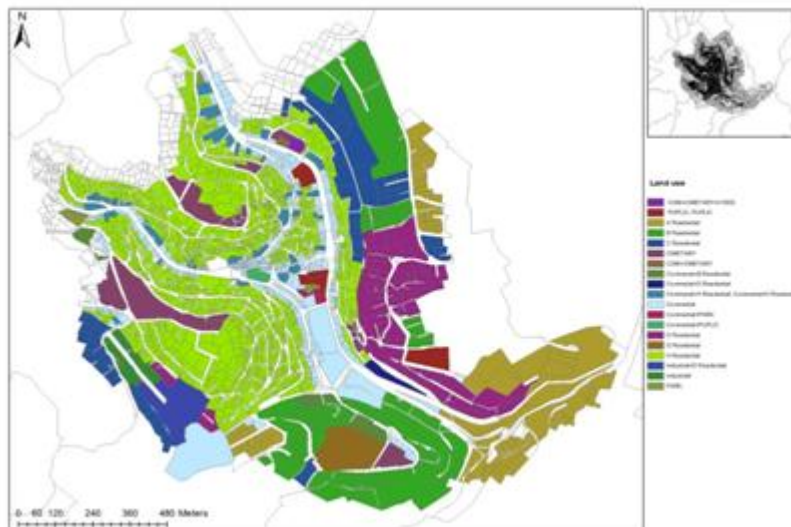


FIG .3 Land Use of the Old Salt City

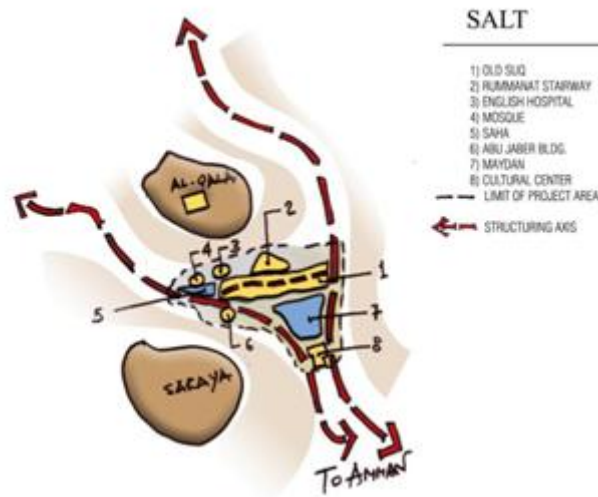


Fig. 4 Urban Structure of Old Salt City

4.2 Public Open Spaces in the Old City of As-Salt

The analysis of the traditional urban form of Arab cities can be applied, to a great extent, to the historic city of Old As-Salt and to its public open spaces. The old city of As-Salt developed without large-scale public spaces—and resisted symbolic notions of the public typical in western cities. Instead of a single, static central space, it accommodates diversity and contradiction. Urban squares in the Old City of Salt were developed during the reign of the Ottoman Empire. Three squares of a great important were developed in this period of time were *Sahat Al-Ain*, *Sahat Al-Hammam*, and *Sahat Al-Baladiyya* (Figure 5); which are distinctive at the city scale due to their *centralized position* and their association with major civic or religious buildings.

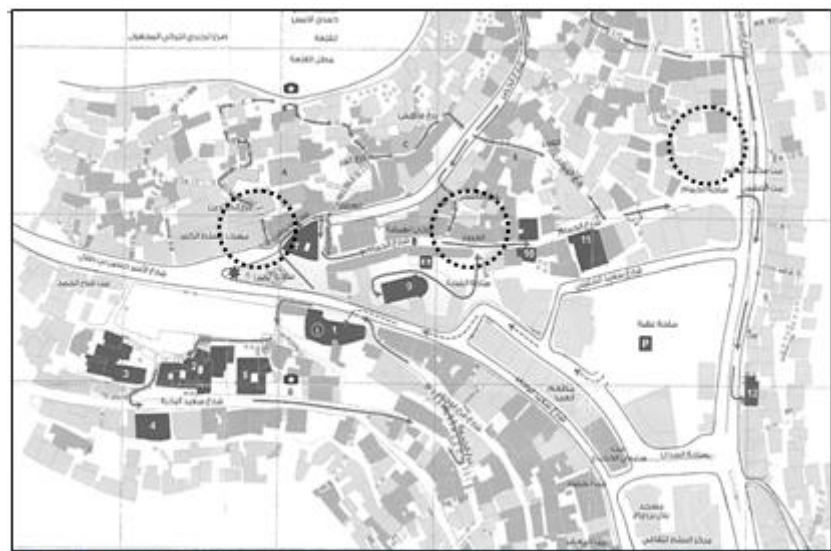


Fig. 5 The selected public Squares in the Old City of As-Salt: Al-Ain, Al-Hammam, and Al-Baladiya.
World heritage sites

Through history, they had woven together many types of public life for the city’s many publics. They played a critical social, economic, cultural, and political role. These spaces typically were used for multiple purposes, such as cultural events, military assembly, local trade, and social interaction. Names of these three squares coalesce into text and define the city on a sociological level. They tell the history of a city and act as “a system of representation through which the collective identity defines itself. *Sahat Al-Ain* referred to the name of the main water spring in this neighborhood and it has all the memory of women going to it for their daily needs. *Sahat Al-Hammam* referred to the name of Turkish founded during the Ottoman era that ruled Salt between

19th and 20th century. *Al-Baladiyya Saha* referred to the Greater Salt Municipality, which is opposite to the *Saha*. The value of such historic places resides in the complexity of their structures, which are impregnated with the record of life and human thoughts and activities.

The following sections present empirical analyses of public open spaces in the historic city of As-Salt. The questions of how ‘*Sahat Al-Ain, Sahat Al-Hammam, and Sahat Al-Baladiyya*’ as open public spaces are appropriated by the various segments of the population, what are the main components which integrate to create these squares? and 2) What procedures are available for identifying places and their attributes? are addressed here through the following sections.

4.2.1 Al- Ain Square

The Al- Ain Square was developed by Nabulsi traders in the early quarter of the 20th century. Sahet Al-Ain is a physical node of public space that has been used by its local community. Sahet Al-Ain has been subjected to many changes during the last decade. In 2004, in its first effort to rehabilitate the historic city, the Municipality of As-Salt, with funding from the Japan Government, initiated a project to provide a space for civic activities and link the surrounding mixed uses such as shops, restaurants and public transport; and to enhance the aesthetic quality of the square. The square provides an environment compatible for passive engagement such as sitting, relaxing and eating lunch. Al- Ain square is distinctive at the old Salt scale due to its centralized position, large size (with a total area of 5000m²), and association with major civic or religious buildings. Al- Ain square is located in the heart of the old Salt next to the great Mosque at the west side and along Said Abu Jaber Street, Al-Khader Street, and Al-Hammam Street that leads up to the square's eastern entrance. Thus, Al- Ain square provides an appropriate visual setting for these three historic streets in the old town (Figure 6). Ringed by religious (Deir Latin cathedral which was the first Latin Church in Jordan), governmental, administration buildings, and educational buildings and home to large markets and recreational activities, the square is in an excellent location where many potential users exist.

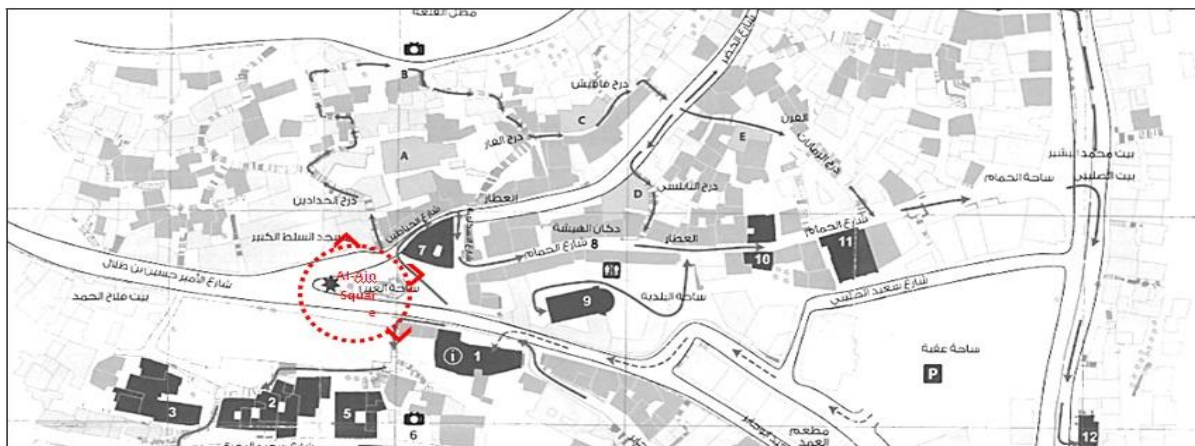


Fig.6 Al- Ain Square Map. Heritage buildings around Square: 1.Salt's Historic Museum; 7. Dawoud Building; 9. Deir Latin cathedral



Fig.7 Al- Ain Square Satellite Map



Fig.8 Al- Ain Square: a physical node of public space



4.2.1.1 Analyzing Activity Types and Design Features relationship in Al- Ain Square

To find out how design features affect people’s activity type, consideration of how many people were using the space regarding the design features throughout the all observation sessions is required. In the other words, to understand the activity type and the use of the design features relationship determining the activity frequency is needed. The Table 3 is the outcome of working with “Symbology” and using the “Frequency” tool by selecting two attribute fields of activity type and design features. Thus, the result displayed how many people were doing what (activity type) and were using what type of design features.

Table 3. Activity Type and Design Features_ Al- Ain Square

Activity Level	Activity Type	Design Features	Frequency	Percentage
Active	Cycle	Walkway	0	0
	Exercise	Grass Space	0	0
		Walkway	70	5.6
	Photo	Grass Space	0	0
		Walkway	1	0.08
	Play	Grass Space	0	0
		Walkway	24	1.92
	Play-Music	Walkway	23	1.84
	Walk	Grass Space	0	0
		Walkway	266	21.24
	Walk-Child	Walkway	21	1.72
Walk-Wheelchair	Walkway	0	0	
Total			405	32.40

Passive	Lay	Bench	4	0.32
		Grass Space	0	0
	Sit	Bench	320	26
		Edge	175	14.08
		Grass Space	0	0
		Table	210	16.8
	Sit-Child	Bench	4	0.32
		Edge	1	0.08
		Grass Space	0	0
		Table	3	0.24
	Sit-Wheelchair	Walkway	1	0.08
	Stand	Grass Space	0	0
		Walkway	120	9.6
	Stand-Child	Walkway	1	0.08
Total		840	67.6	
Total		1245	100	

As can be seen from the Table 2, for the *active level* of activities, the highest rank went for walking within walkways which in total was 23% with the frequency of 287 out of 1245 and the second rank belonged to playing at 2% and revealed that children constituted small percentage of the involved population (almost 2%). Activities such as Cycling, taking photo, and Walking-Wheelchair had no place here. It is worth mentioning that most of the observed people were adults and noticeably, almost 33% of them were seniors who were mostly sitting and playing traditional games such as "Zaher Table"; enjoying the peaceful environment (Figure 10. A). Turning to the activity level, for the passive activities, sitting on a bench with 26% took the highest rank among the other passive activities whereas sitting on a bench with a child and standing with a child took the least percentage which is less than 1%.

Sitting on a table, on an edge are among the second preferable design features that people choose to use (Table 1). Another passive activity that can be seen and is noticeable is standing on the walkway which constitutes almost 10% of the activities within the space with the frequency of 121 out of 1245. Through these comparisons and results of observations one of the major findings is beginning to shine through as "*Sittable Space*". William Whyte (1980) in his landmark book on urban public space "The Social Life of Small Urban Spaces" wrote that "people tend to sit where there are places to sit" as they do like to use "basics" within a space. Through the detailed observations of plazas and parks in New York City, Whyte (1980) found comfortable seating choices to be the primary and essential component of urban public spaces. He examined many correlations between space use and the physical environment and found that one of the major factors in space use is *sittable space* that should be designed for people to sit, not for "architectural punctuation". People are adaptable to use space in a way they feel comfortable and are able find a place to sit whether it is a bench or it is a concrete *sittable edge* if the dimensions are right. According to the timing of the activities during a regular day, morning was the most populated time (39%) whereas evening and after work hours were not as populated as lunch time (Figure 10).



A. Al-Ain Square's Entrance from Abu Jaber St.



Morning time around 10:00 AM



Morning time around 10:00 AM

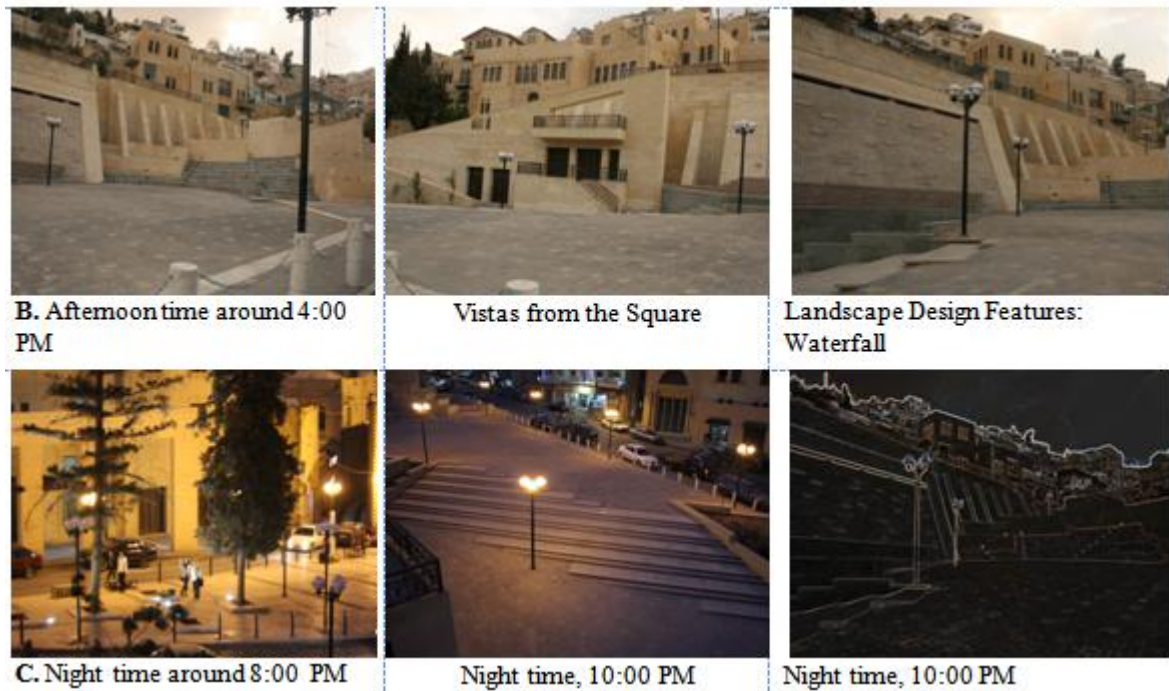


Fig.10 Activity type and Design Features at different times of a Weekday—at Al- Ain Square

Regarding the use of design features during a regular day, walkways were allocated to leisurely walking and benches had the highest rank of occupation for the sitting activity which was 29.18%. It is also worth pointing out that edges had the second rank in using for sitting at 14.72% (Table 4).

Table 4. Design Features' Frequent Use at Al- Ain Square

Design Features	No.	%
Bench	365	29.18
Edge	184	14.72
Grass Space	0	0
Table	37	3
Walkway	729	58
Total	1315	100

According to the timing during the weekend's day, it can be seen that weekend morning (around Friday pray) had the highest number of involved people (47%) whereas in the evening the lowest numbers of people were presented.

Successful features and potentials: sunny and shady sitting places, diverse use settings, water element, good maintenance with a centralized management, legibility, accessibility for disabled and other user categories with special needs, good accessibility from closest surroundings, walkability, relatively new and upgraded design of urban furnishings, mixture of user categories.

Unsuccessful features and problems: lack of adequate seating variety and orientation, protection against adverse weather conditions, lack of potential secondary seating and outdoor food services, lack of programmed events to draw the users into area, vegetation variety, access to food facilities is limited, parking areas is limited, and the square does not encompass many features encouraging use to make it a publicly accessible space. However, the positive elements that currently exist in the plaza provide an excellent base for a well-used space and the negative design aspects leave room for improvements. The recommendations below are changes that could enhance Al- Ain square and begin to attract regular users to the space.

Recommendations

Appearance

- Addition of *landscape design elements* (such as variety of vegetation, water feature, pergolas, etc.) to create a more interesting space.
- Improve *vegetation* near some benches
- Trees can contribute greatly to the attraction and character of a space by providing shade
- Encourage increased *animation and programming*
- Develop *public art* provision within public spaces and along public routes, which will attract people to visit the space. A range of event based activities to occur within the space will foster *social capital* and increase levels of activity
- Provide a *memorable icon* for the space.
- Improve *lighting coverage*

Security

- upgrade *night-time safety*

Microclimate

- Encourage greater use of public spaces in winter/colder weather. This can be achieved by providing facilities to allow people to sit in sheltered/sunny locations under partial or glazed cover.

4.2.2 Al-Hammam Square

In traditional towns such as As-Salt, the **Al-Hammam Square** forms a strong civic focus which is important in setting the town's image and identity. The Al-Hammam **Square**, with a total area of 750 m², is located on the eastern side of the old town along the first commercial street in Salt *_Al-Hammam Street_* that leads up to the western gate of the Square. This square has another entrance located along the Prince Hamzeh Ben Al-Hussein Street (Figure 11). Its location at the center of the old city made it very convenient for trade and the moving of goods to and from buildings in this area; it was thus the commercial hub for light industry. This **Square** was developed by Nabulsi traders in the last quarter of the 19th century; where the main social activities and center of government were located. Today, the **Al-Hammam Square** is a multifunctional area that, in association with the **Al-Hammam Street**, offers a continuous pedestrianized shopping area.

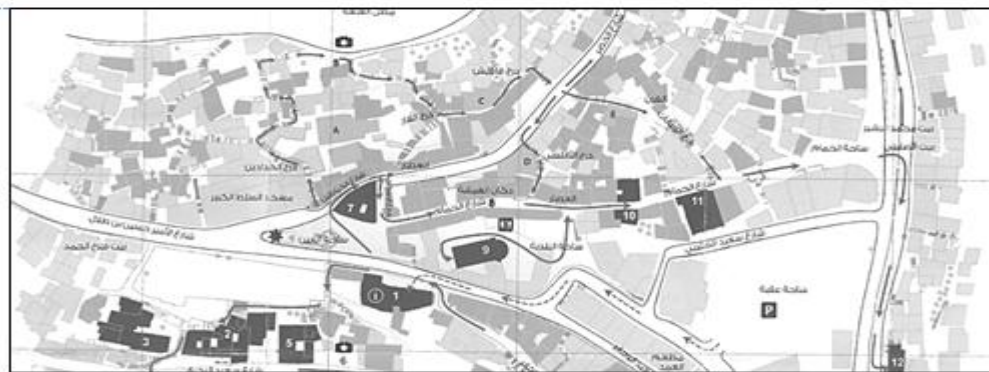


Fig 11. Al-Hammam Square Building 11. The Small Mosque.

Al-Hammam Square is a pedestrian square, integrated into a network of streets and squares which are mostly pedestrian. The square has supportive land uses that provide users to the space. However, its situation is such that a large number of trades and services are accessible to the dwellers at a short distance. At the present time it is surrounded by twenty-two trades, of which all can be considered as being necessary to fulfill every day needs; most of those trades are banks, medical centers, pharmacies, groceries and foodstuff, clothes, shoe ware and home appliances (Figure 12). Also, number of heritage buildings existed around this square such as Muhiyar building, and Toukan building. In particular, Al-Hammam Public Market and The Small Mosque at the end of this street are the major draw to this square. In addition, the adjacent cultural centre is particularly important because it provides the space with numerous weekly events that are a major draw to the square.

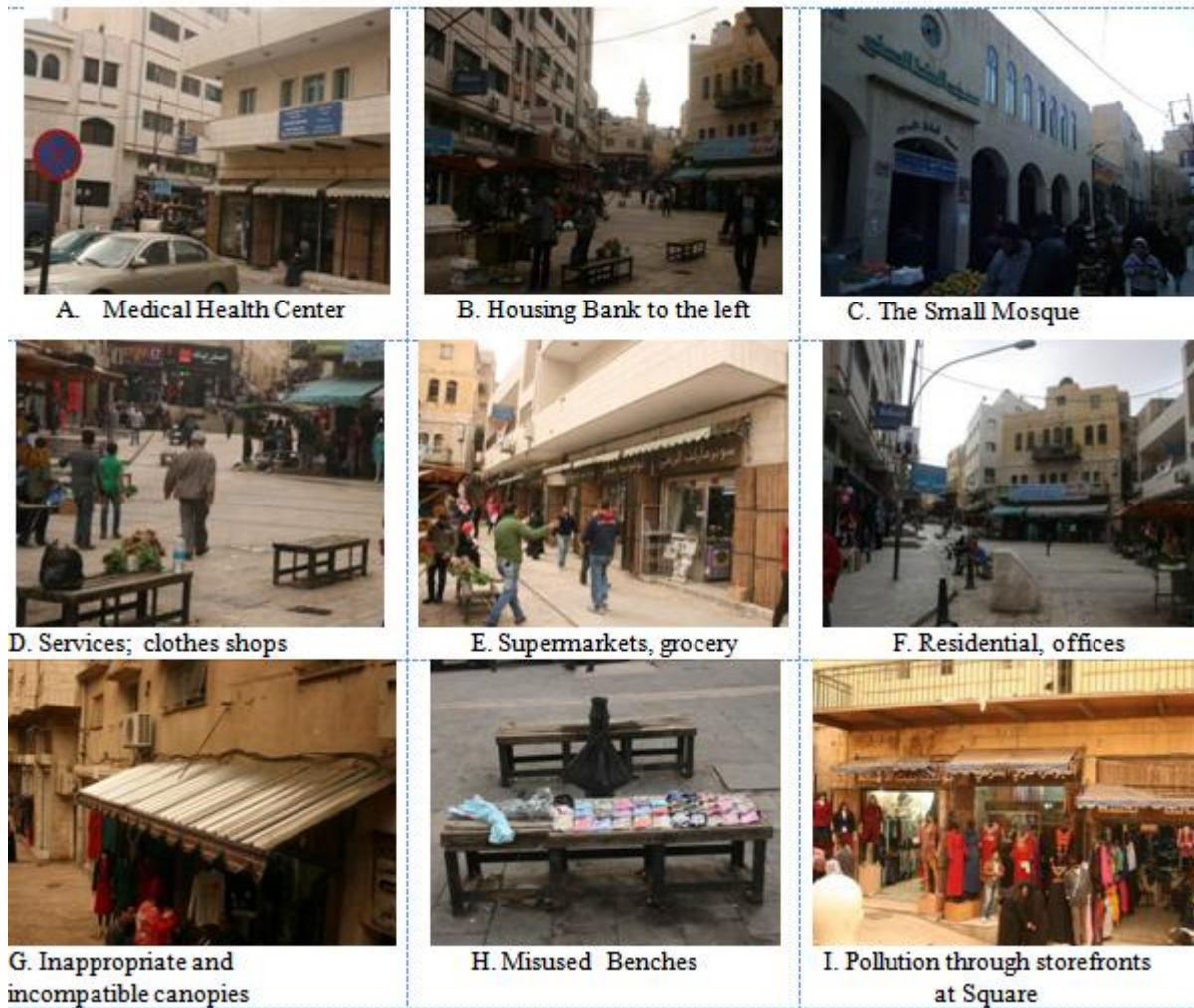


Fig.12 Al- Hammam Square: Activity types and Design Features at different times of a weekday

Analyzing Activity Types and Design Features relationship in Al- Hammam Square

Beginning with the activity level during the weekdays, as the collected data reveal, approximately 85% of activities were taking place at the *active level*. First of all it is clear that *walking* activity had the greatest percentage of activities which is almost 62% including all types of walking (Table 5). The worth pointing out results regarding the active level was that at the second place after walking playing had the highest percentage among other activities which was 2% and revealed that children constituted small percentage of the involved population (almost 2%). Similarly during weekdays the collected data revealed that approximately 15% of activities belonged to the *passive activities* (Table 5). Obviously, among passive activities, *sitting* had the rank which constituted only 10% of all activities; this is due to their dirt and misuse. Most benches are used for other activates rather than sitting such as putting bought items on.

Table 5. Al- Hammam Square: Activity Types and Design Features

Activity Level	Activity Type	Design Features	Frequency	Percentage
Active	Cycle	Walkway	0	0
		Grass Space	0	0
	Exercise	Walkway	0	0
		Grass Space	0	0
	Photo	Walkway	7	0.56
		Grass Space	0	0
	Play	Walkway	10	0.80
		Grass Space	0	0
	Play-Music	Walkway	11	0.10
Grass Space		0	0	
Walk	Walkway	765	61.23	

	Walk-Child	Walkway	11	0.77
	Walk-Wheelchair	Walkway	0	0
Total			577	84.90
Passive	Lay	Bench	1	0.08
		Grass Space	0	0
	Sit	Bench	128	10.28
		Edge	3	0.24
		Grass Space	0	0
		Table	0	0
	Sit-Child	Bench	1	0.08
		Edge	0	0
		Grass Space	0	0
		Table	0	0
	Sit-Wheelchair	Walkway	0	0
	Stand	Grass Space	0	0
		Walkway	54	4.40
	Stand-Child	Walkway	0	0
Total			187	15.10
Total			764	100

Successful features and potentials: good accessibility from closest surroundings, walkability, mixture of user categories, clear differentiation between pedestrian and vehicular traffic.

Unsuccessful features and problems: today *legibility* of traditional *Al- Hammam Square* is threatened by inappropriate and incompatible modern activities. For instance, all street-vendors remain illegally creating disturbance and pollution through bringing their storefronts to the *Square* to attract buyers; and left places along the *Square* in a state of mess. This increased illegal commercialization has resulted in loss of its legibility, identity, original symmetry and harmony in the physical environment of *Al- Hammam* square. Therefore, *Al- Hammam* square *requires a great deal of attention to land use, streetscape, and ground-floor activity (as confirmed by the Public Life public space survey; to ensure that mixed-use developments are functional, attractive, and withstand the test of time.* Other minor negative aspects are the noise levels from the cars at the adjacent intersection, limited food choices and limited lighting in the plaza after dark. Overall, lack of adequate seating variety and orientation, protection against adverse weather conditions, lack of potential secondary seating and outdoor food services, and presence of “undesirables” turns the square into a transit character where passing through is a predominant activity rather than a place where people like to spend time, perform various activities. The recommendations below are changes that could enhance the plaza and begin to attract regular users to the space.

Recommendations

Appearance: Improve the appearance and attractiveness of Al-Hammam square; and this could be achieved through:

- **Avoiding** the clutter and visual barriers that are existed in the space, which **restrict** people's enjoyment and creating unsafe blind spots.
- Limiting land use and ground-floor activity for the adjacent buildings
- Improving quality landscape treatment:
 - Create well-defined footpaths within the landscape for **passive recreation and activities.**
 - Appropriate street furniture
 - Improve lighting coverage
 - Improve signage
- Encaging positive interaction with buildings
- Improving well define edges
- Creating small scale **landmarks**
- Creating and enhance positive and memorable entrances:
 - Entrance at the west end of Al-Hammam square needs improvement

Security

- upgrade night-time safety

Condition

- Improve high levels of maintenance
- Address cleanliness

4.2.3 Al- Baladiyyah square

Al- Baladiyyah Square is distinctive at the old Salt scale due to its centralized position, and association with major civic or religious buildings. Al- Baladiyyah Square is surrounded by Al-Hammam Street to the north, the Al-Midan Street to the south, and the Deir Latin cathedral to the west and provides approximately 620m² of a space provides an appropriate visual setting for these two historic streets and number of heritage buildings such as Al-Dawoud, Mihyar and Deir Latin buildings (Figure 12). The main entrance is landmarked with a Clock Tower at the Al-Midan Street (Figure 13).

Ringed by religious, governmental (As-Salt Greater Municipality), administrative buildings, and educational buildings and home to many traditional trades such as groceries and foodstuff, clothes, shoe-ware and home



Fig.12 Al- Baladiyyah Square. 9. Deir Latin cathedral; 10. Mihyar Building

appliances, and other traditional handcrafts that are considered as basic elements of its architectural and social network (Figure 13).

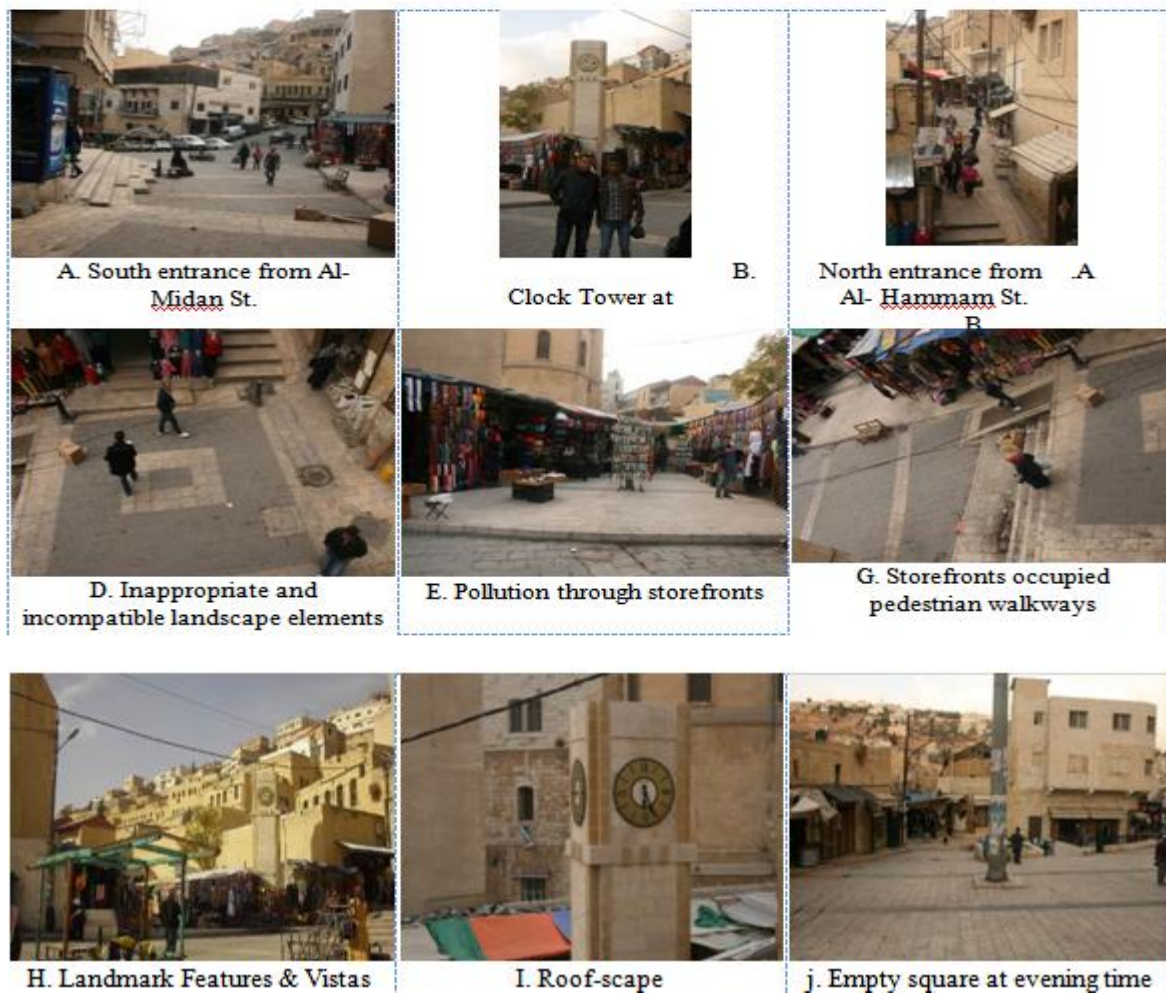


Fig.13 Activity types and Design Features at different times of a day_ Al- Baladiyyah Square

4.2.3.1 Analyzing Activity Types and Design Features relationship in Al- Baladiyyah Square

Beginning with the activity level during the weekdays, as the collected data reveal, approximately 83% of activities were taking place at the *active level*. First of all it is clear that *shopping* activity had the greatest percentage of activities which is almost 55% including all types of walking. Obviously, the observation data shows that *playing, playing music* and *taking photo* were also taking minimum place and constitute 2% of all the activities. In this observation session one fifth of activities was passive including *standing* which was most popular with more than 12% of the total. Among active level of activities, *sitting* was noticeable even though constitutes approximately 5% of the total counted people (Table 6). Approximately, 95% of the observed people were adults and noticeably, almost 33% of them were seniors who were mostly shopping. According to the collected data, with regard to the timing, Friday morning was the less populated time, 81 people were out within the space. The following table illustrates how activities vary by activity type during the observation sessions (Figure 13).

Table 6. Activity Type and Design Features _ Al- Baladiyyah Square

Activity Level	Activity Type	Design Features	Frequency	Percentage
Active	Cycle	Walkway	0	0
	Exercise (Shopping)	Grass Space	0	0
		Walkway	694	55.52
	Photo	Grass Space	0	0
		Walkway	3	0.24
	Play	Grass Space	0	0
		Walkway	2	0.16
	Play-Music	Walkway	19	1.52
	Walk	Grass Space	0	0
		Walkway	300	24
Walk-Child	Walkway	21	1.68	
Walk-Wheelchair	Walkway	0	0	
Total			1040	83.00
Passive	Lay	Bench	0	0
		Grass Space	0	0
	Sit	Bench	32	2.56
		Edge	17	1.41
		Grass Space	0	0
		Table	0	0
	Sit-Child	Bench	7	0.56
		Edge	9	0.72
		Grass Space	0	0
		Table	0	0
	Sit-Wheelchair	Walkway	0	0
	Stand	Grass Space	0	0
		Walkway	144	11.55
Stand-Child	Walkway	1	0.08	
Total			210	17.00
Total			1250	100

Successful features and potentials: commercial stores and souqs, made this square important site for residents coming from different parts of As-Salt and for people who enjoy shopping and roaming within the charm of the old city. Al-Baladiyya Square has some good features such as legibility, good accessibility from closest surroundings, walkability, mixture of user categories, clear differentiation between pedestrian and vehicular traffic.

Unsuccessful features and problems: obviously, as the main active activities are the predominant, this square is not a definite ideal square in terms of social attractivity. Moreover, unsuccessful physical features incorporate to the absence of the passive activities. Example of unsuccessful features are inappropriate use of cobblestone surface, poorer accessibility for disabled other user categories with special needs, lack of greenery elements, lack of colour and texture in vegetation, lack of adequate seating variety and orientation, protection against adverse weather conditions, lack of potential secondary seating and outdoor food services, lack of programmed events to draw the users into area, presence of “undesirables”, lack of aesthetic harmony in all urban element’s design. The analysis of factors revealed few issues which could be improved in order to encourage and increase the level of the social attractivity to even more extent.

Recommendations:

- provide food and other (shop) outdoor services of different types in the outer subarea of the square
- provide adequate primary seating variety and orientation as well as other secondary seating, support seating designed for groups
- open up and diversify the use of ground floors facades, provide mixed uses of shops, services, etc., support multifunctionality
- strengthen the identity and develop the attachment to the square (for example by organizing more programmed or traditional city events in order to draw the residents and users into the area)
- make use of available variety of flexible design, use temporary art and other attractions to activate users and to reduce presence of “undesirables”
- upgrade existing entry points and activate the edges of the square
- strengthen the relationship between the square and the city centre as whole, consider an impact of small-scale in a large-scale, reconsider the network of public spaces within the whole city centre according to users’ needs.

V. CONCLUSION

Public spaces are like humans beings. They have ups and downs; sometimes they are vivid, live and active, and sometimes they are dull, empty and dark. Also, public open spaces influenced and were influenced by the world around them. The value of such historic places resides in the complexity of their structures, which are impregnated with the record of life and human thoughts and activities: the whole is much greater than the sum of its parts. Indeed, the meaning of an urban entity draws on the interaction between the *activity patterns* and the *design features* of the urban space. Open spaces in *Old Salt* are essential components of its centre, providing a valuable contrast to the built urban environment, and afford a rich urban experience to residents. The analysis of the case study in this paper provides some insights into the strengths and shortcomings of contemporary open public squares in the "Old Salt" in terms of urban design. Design criteria that can be readily incorporated into open public squares has been demonstrated. Conversely, some entrenched barriers to certain design principles have been highlighted while areas of potential use for the planning and development industry, such as innovation incentives, have also been flagged. The analysis of *activity patterns* and *design features* revealed few issues which could be improved in order to encourage and increase the level of the social attractiveness to even more extent.

General recommendations:

- Effective public open space should not, where possible, be designed for a *single physical activity*. Rather, effective public open space should cater for a *diverse range of activities and uses*.
- The *functionality* of the open space is very important to fostering *physical activity*. Open space needs to be considered as fulfilling a range of *functions*. For example, a range of event based activities to occur within the space will foster *social capital* and increase levels of activity.
- The *attractiveness* of the open space is very important to fostering *physical activity*. Open space needs to be designed as high quality spaces with appropriate street furniture, well define edges and small scale **landmarks**
- Open space designs should take account of the *variety and intensity of potential uses*.

Users of open space need to feel *safe regardless of sex or age*. Designs should take account of safety principles to ensure security.

REFERENCES

- [1] Applyard, D., (1981), “Livable Street”, University of California Press, Berkeley.
- [2] Baxter, P., and Jack, S., (2008), “Qualitative Case Study Methodology: Study design and implementation for Novic researchers”, *The Qualitative Report*, 13 (4), 544-559.
- [3] Canter, D., (1976), “The Psychology of Place”, Architectural Press, London.
- [4] Carmona, M., Tiesdell, S., Heath, T., and Oc, T., (2010), “public places public spaces: The dimensions of urban design”, Architectural press, UK.
- [5] Carr, S., Francis, M., Rivilin, L.G., Stone, A.M., (1992), “Public Space”, Cambridge university Press, Cambridge.
- [6] Cooper, M.C, Francis, C., (1998), “People Places: Design guidelines for urban open space”, John Wiley & Aons Inc. Toronto.
- [7] Cresswell, J., (2009), “Research design, qualitative, quantitative, and mixed methods approaches”, (3rd ed), Sage.
- [9] Gehl, J. (1987), “life between buildings: using public space, Van nostrand reinhold company, New York.
- [10] Golicnik, B., (2010), “Emerging relationships between design and use of urban park spaces”, *Journal of Landscape and Urban Planning*, 94 (1), 38-53.
- [11] Hillier, B., Penn, A., Hanson, J., T. Grojewski, J Xu, (1993), “Natural movement: or, configuration and attraction in urban pedestrian movement”, *Environment and planning B: Planning and Deisgn*, 20, 29-66.
- [12] Jacobs, J. (1961), “The Death and Life of Great American Cities: The Failure of Modern Town Planning”, Peregrine Books, London.
- [13] Lynch K., and Rodwin, L., (1958), “A Theory of Urban Form”, *Journal of the American Institute of Planners*, 24 (4), 201-214.
- [14] Lynch, K. (1981), “A theory of good city form”, MIT Press, Cambridge.

- [15] Lynch, K. (1960), "The Image of the City", MIT Press, Cambridge, Mass.
- [16] Madanipour, A. (2010), "Whose Public Space? International case studies in urban design and development", London; New York: Routledge.
- [17] Montgomery, J., (1998), "Making a city: Urbanity, Vitality and Urban Design", *Journal of Urban Design*, 3, 93-116.
- [18] Thompson, C., (2002), "Urban open space in the 21st century", *Journal of Landscape and Urban Planning*, 60 (2), 59-72.
- [19] Tibbalds, F., (2003), "Making people-friendly towns", Spon Press.
- [20] Urban Task Force (1999), "Towards an urban renaissance", Urban Task Force, London.
- [21] Van Melik, R., 2008. *Changing public space: The recent redevelopment of Dutch city squares*. Utrecht: Faculty of Geosciences, Utrecht University.
- [22] Varna, G., and Tiesdell, S., (2010), "Assessing the Publicness of Public Space: The Star Model of Publicness", *Journal of Urban Design*, 15: 4, 575 — 598.
- [23] Whyte, William.H. (1980), "The Social Life of Small Urban Spaces", The Conservation Foundation, Washington, D.C.

Modified Approach for Solving Maximum Clique Problem

Jaspreet Singh

M.Tech Scholar, LPU, Phagwara, Punjab, India.

ABSTRACT:

Maximum Clique problem is an NP Complete Problem which finds its applications in various fields ranging from networking to determination of structure of a protein molecule. The work suggests the solution of above problem with the help of Genetic Algorithms. Clique problem requires finding out all fully connected sub-graphs of a particular graph. This paper investigates the power of genetic algorithms at solving the maximum clique problem. Another feature of algorithm is based on population-driven search where the statistical properties of the initial population are controlled to produce efficient search. The technique can be extended to many unsolvable problems and can be used in many applications from loop determination to circuit solving.

KEYWORDS: MAXCLIQUE, Roulette Wheel Selection, Genetic Algorithm, Maximum Clique Problem (MCP).

I. INTRODUCTION:

1.1 Maximum Clique Problem

Assume that the finite undirected simple graph $G = (V, E)$ is given, where V is the set of nodes, $v \in V$, E is the set of edges. The arbitrary full graph is called a clique. The clique, which does not contain other cliques, is called a maximal Clique. The largest maximal clique is called a maximum clique. To extract all maximal cliques from the graph G . Many algorithms have been described to solve this problem. The best solution now a days is a procedure where the complexity is linear to the number of maximal cliques [1,2]. The theory and algorithms described in this paper can solve the problem. We assume that the graph G is presented in the form of an adjacency matrix X of order $N \times N$, the main diagonal of which has zeros. Given an undirected graph $G = (V, E)$, a clique S is a subset of V such that for any two elements $u, v \in S$, $(u, v) \in E$. Using the notation ES to represent the subset of edges which have both endpoints in clique S , the induced graph $GS = (S, ES)$ is complete. To Find Maximum clique in a graph is an NP-hard problem, called the maximum clique problem (MCP). Cliques are intimately related to vertex covers and independent sets. Given a graph G , and defining E^* to be the complement of E , S is a maximum independent set in the complementary graph $G^* = (V, E^*)$ if and only if S is a maximum clique in G . It follows that $V - S$ is a minimum vertex cover in G^* .

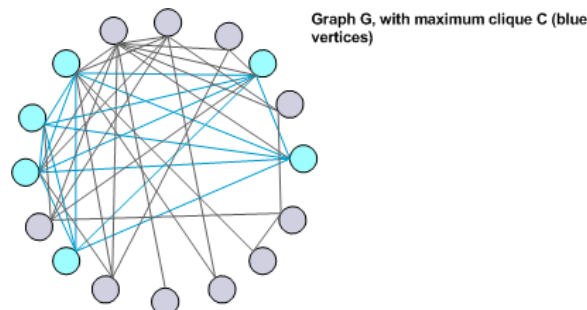


Fig. 1 An Example of Clique.

In other words a **clique** in an undirected graph $G = (V, E)$ is a subset of the vertex set $C \subseteq V$, such that for every two vertices in C , there is an edge connecting the two vertices. This is equivalent to saying that the sub graph induced by C is complete. A maximal clique is a clique that cannot be extended by including one more adjacent vertex to it, means and a clique which does not exist exclusively within the vertex set of a larger clique. A maximum clique is a clique of the largest possible size in a given graph. The clique number $\omega(G)$ of a graph G is defined the number of vertices in a maximum clique in G . The intersection number of G is also termed as the smallest number of cliques that together cover all edges of G .

The opposite of a clique is observed as an independent set, in the sense that every clique which corresponds to an independent set in the complement graph. The cliques cover problem concerns finding as few cliques as possible that include every vertex in the graph. A related concept is a bi-clique, a complete bipartite sub graph. The bipartite dimension of a graph is the minimum number of bi-cliques needed to cover all the edges of the graph.

1.2 GENETIC ALGORITHMS

Genetic algorithms are the closest computation model to natural evolution. Their success at searching complex non-linear spaces and general robustness has led to their use in a number of practical problems such as scheduling, financial modeling and optimization. The inventor of genetic algorithms, John Holland, took his inspiration for them from nature. Genetic algorithms contain a population of individuals, each of which has a known fitness. The population is evolved through successive generations; the individuals in each new generation are bred from the fitter individuals of the previous generation. Unlike Natural Evolution which is continuous indefinitely, we have to decide when to stop our GA. As with the breeding of domestic animals, we choose the individuals to breed from to drive the population's evolution in the direction we want it to go. As with domestic animals, it may take many generations to produce individuals with the required characteristics. Inside a computer an individual's fitness is usually calculated directly from its DNA and so only the DNA need be represented. Usually genetic algorithms represent DNA by a fixed length vector. Where a genetic algorithm is being used for optimization, each individual is a point in the search space and is evaluated by the fitness function to yield a number indicating how good that point is. If any point is good enough, the genetic algorithm stops and the solution is simply this point. If not then a new population, containing the next generation is bred. The breeding of a new generation is inspired by nature; new vectors are bred from the fitter vectors in the current generation, using either asexual or sexual reproduction. In asexual reproduction, the parent vector is simply copied. Chromosomes are selected from the population to be parents to crossover. The problem is how to select these chromosomes. According to Darwin's evolution theory the best ones should survive and create new offspring. There are many methods how to select the best chromosomes, for example roulette wheel selection, Boltzmann selection, tournament selection, rank selection, steady state selection and some others. Parents are selected according to their fitness. The better the chromosomes are, the more chances to be selected they have. Imagine a roulette wheel where are placed all chromosomes in the population, every chromosome has its place big accordingly to its fitness function.

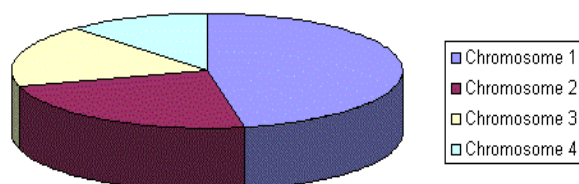


Fig.2 Roulette Wheel Selection

Then a marble is thrown there and selects the chromosome. Chromosome with bigger fitness will be selected more times. Figure 3 shows a child vector being created by mutating a single gene where each gene is represented by a single bit. With sexual reproduction, two of the fitter vectors are chosen and the new vector is created by sequentially copying sequences alternately from each parent. Typically only two or three sequences are used, and the point(s) where the copying crosses over to the other parent is chosen at random. This is known as crossover. Figure 4 shows a child being formed firstly by copying four genes from the left-hand parent then the three remaining genes are copied from the right-hand parent.

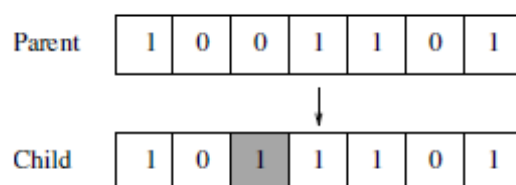


Fig. 3 Mutation

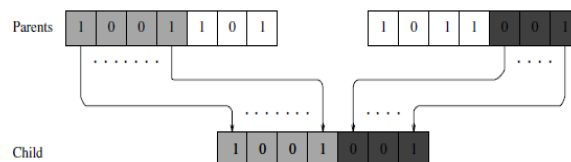


Fig. 4 Crossover

Holland in his paper "Genetic Algorithms and the Optimal Allocation of Trials" [Hol73] shows, via his schemata theorem, that in certain circumstances genetic algorithms make good use of information from the search so far to guide the choice of new points to search. Figure 5 shows the genetic algorithm cycle. The schemata theorem requires the vector representation and fitness function be designed so that the required solution can be composed of short fragments of vectors which, if present in a vector, give it a relatively high fitness regardless of the contents of the rest of the vector. These are known as building blocks. They can be thought of as collections of genes which work well together.

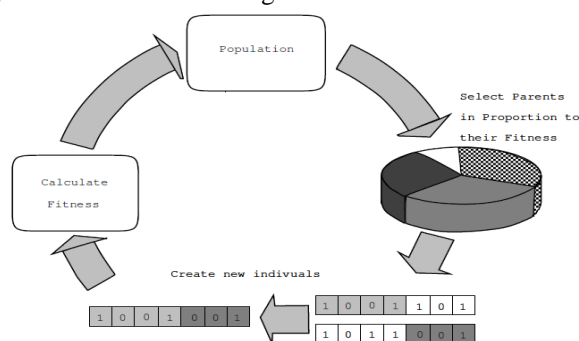


Fig. 5 The Genetic Algorithm Cycle.

1.3 OUTLINE OF THE BASIC GENETIC ALGORITHM

1. **[Start]** Generate random population of n chromosomes (suitable solutions for the problem)
2. **[Fitness]** Evaluate the fitness $f(x)$ of each chromosome x in the population
3. **[New population]** Create a new population by repeating following steps until the new population is complete
 - a. **[Selection]** Select two parent chromosomes from a population according to their fitness (the better fitness, the bigger chance to be selected)
 - b. **[Crossover]** With a crossover probability cross over the parents to form a new offspring (children). If no crossover was performed, offspring is an exact copy of parents.
 - c. **[Mutation]** With a mutation probability mutate new offspring at each locus (position in chromosome).
 - d. **[Accepting]** Place new offspring in a new population
4. **[Replace]** Use new generated population for a further run of algorithm
5. **[Test]** If the end condition is satisfied, **stop**, and return the best solution in current population
6. **[Loop]** Go to step 2

1.4 MAXIMUM CLIQUE PROBLEM IS NP HARD

Examples of difficult problems, which cannot be solved in "traditional" way, are NP problems. There are many tasks for which we know fast (polynomial) algorithms. There are also some problems that are not possible to be solved algorithmically. For some problems was proved that they are not solvable in polynomial time. But there are many important tasks, for which it is very difficult to find a solution, but once we have it, it is easy to check the solution. This fact led to **NP-complete** problems. NP stands for nondeterministic polynomial and it means that it is possible to "guess" the solution (by some nondeterministic algorithm) and then check it, both in polynomial time. If we had a machine that can guess, we would be able to find a solution in some reasonable time. Studying of NP-complete problems is for simplicity restricted to the problems, where the answer can be yes or no. Because there are tasks with complicated outputs, a class of problems called **NP-hard** problems has been introduced. This class is not as limited as class of NP-complete problems. For NP-problems is characteristic that some simple algorithm to find a solution is obvious at a first sight - just trying all

possible solutions. But this algorithm is very slow (usually $O(2^n)$) and even for a bit bigger instances of the problems it is not usable at all. Today nobody knows if some faster exact algorithm exists. Proving or disproving these remains as a big task for new researchers. Today many people think, that such an algorithm does not exist and so they are looking for some alternative methods – example of these methods are genetic algorithms. Examples of the NP problems are Maximum Clique Problem, Travelling Salesman Problem or Knapsack Problem.

1.5 APPLICATIONS OF MAXIMUM CLIQUE PROBLEM

The MAXCLIQUE Problem has many real world applications. It is encountered in many different fields in which either the underlying problem can be formulated as the MAXCLIQUE problem or finding the maximum clique is a precondition of solving the problem. Based on those applications, a collection of much diversified test graphs for the MAXCLIQUE problem has been created for evaluating the performance of algorithms for the MAXCLIQUE problem. They are available at <ftp://dimacs.rutgers.edu/pub/challenge/graph/> and consist of graphs derived from different problems such as coding theory, fault diagnosis and printed circuit board testing.

1.5.1 Coding theory

A common problem in coding theory is to find a binary code as large as possible that can correct a certain number of errors for a given binary word. A binary code is a set of binary vectors. The Hamming distance between two binary vectors is defined as the number of positions in which the two vectors have different values. A maximum clique of $H(n,d)$ represents the maximum number of binary vectors of size n with Hamming distance greater than or equal to d . Therefore, if we find the maximum clique C in $H(n,d)$, any binary code consisting of vectors represented by the vertices in C is able to correct $(d-1)/2$ errors.

1.5.2 Fault diagnosis

Fault diagnosis plays a very important role in studying the reliability of large multiprocessor systems. The goal is to identify all faulty processors (units) in the system. In the model designed by Berman and Pelc [1], the system is represented by an undirected graph $G = (V,E)$ whose vertices are processors and where edges are communication links.

1.5.3 Printed circuit board testing

A printed circuit board tester involves placing probes onto a board. A probe can determine if a portion of a board is working correctly. Since probes have a particular size, not every component can be checked in one pass. The problem of maximizing the number of components checked in one pass can be formulated as a clique problem: each node connects a component and an edge represents two nodes that are not too close to be checked simultaneously. A clique in this graph is then a set of components that can be checked in one pass.

1.6 OTHER TECHNIQUES OF FINDING MAXIMUM CLIQUE PROBLEMS

1.6.1 Simulated Annealing

Simulated annealing is a randomized neighborhood search algorithm inspired by the physical annealing process, where a solid is first heated up in a heat bath until it melts, and then cooled down until it solidifies into a low-energy state. It was first introduced by Kirkpatrick, Gelatt and Vecchi in 1983 [7]. This heuristic technique considers the solutions of a combinatorial optimization problem corresponding to the states of the physical system and the cost of a solution is equivalent to the energy of the state. A simulated annealing algorithm basically works as follows. First, a tentative solution in the state space is generated usually at random. Then the next state is produced from the current one. The new state is evaluated by a cost function f . If it improves, the new state is accepted. If not, the new state is accepted with probability $e^{-\Delta f/\tau}$, where Δf is the difference of the cost function between the new state and the current state, and τ is a parameter usually called the temperature in analogy with physical annealing, which is varied during the optimization process [8]. The simulated annealing heuristic has been ranked among one of the best heuristics for the MAXCLIQUE problem at the 1993 DIMACS challenges [6].

1.6.2 Neural Networks

An artificial neural network (ANN) is a parallel system inspired by the densely interconnected, parallel structure of the mammalian brain information- processing system [5]. Some mathematical models of the biology nervous systems show that the temporal evolution is controlled by a quadratic Lyapunov function (also called energy function), which is iteratively minimized as the process evolves. This feature can be applied to many combinatorial optimization problems. More than ten algorithms have been proposed for solving the MAX-CLIQUE problem using neural networks. They encode the problem in different models, but most of them are

based on the Hopfield model [5] and its variations. The problem is solved via several discrete (deterministic and stochastic) and continuous energy-descent dynamics. In general, algorithms based on neural networks can find significantly larger cliques than other simpler heuristics but the running time is slightly longer. On the other hand, comparing to those more sophisticated heuristics, they obtained significantly smaller cliques on average but were considerably faster [8].

1.6.3 Tabu Search

Tabu search is a modified local search algorithm, in which a prohibition-based strategy is employed to avoid cycles in the search trajectories and to explore new regions in the search space [8]. A tabu list is used to store historical information on the search path to prevent the algorithm from going back to recently visited solutions. Tabu solutions are accepted if they satisfy some aspiration level condition. Several tabu search algorithms for the MAXCLIQUE problem have been developed in the past ten years. They basically have the same structures but change the definition of the search space, the ways that tabu lists are used and the aspiration mechanism. In Battiti and Protasi's algorithm [3], a reactive local search method is used so that the size of the tabu list can be automatically determined. Also, an explicit restart procedure influenced by memory is activated to introduce diversification. The worst case complexity per iteration of this algorithm is $O(\max(|V|, |E|))$ where V is the vertex set and E is the edge set of the graph. The running time of the algorithm is better than those presented at the Second DIMACS Implementation Challenge [6]. There are also many simple heuristics that have been used to solve the MAX-CLIQUE problem such as the sequential greedy heuristics and local search heuristics. They usually have better running times than those advanced heuristics algorithms discussed above, but the quality of the results is worse on the average.

II. LITRATURE REVIEW

This observation was first mathematically formulated by John Holland in 1975 in his paper, "Adaptation in Natural and Artificial Systems" [5]. Usually the algorithm breeds a predetermined number of generations; each generation is populated with a predetermined number of fixed length binary strings. These binary strings are then translated (decoded) into a format that represents suitable parameters either for some controller, or as an output. The product resulting from evolution (whether natural or simulated) is not simply discovered by a random search through the problem state space, but by a directed search from random positions in that space. In fact, according to Goldberg, the simulated evolution of a solution through genetic algorithms is, in some cases, more efficient and robust than the random search, enumerative or calculus based techniques. The main reasons given by Goldberg are the probability of a multi-modal problem state space in non-linear problems, and that random or enumerative searches are exhaustive if the dimensions of the state space are too great [4]. David R. Wood, "An Algorithm for finding maximum clique in a graph", 1997 Elsevier Science, introduced a branch-and-bound algorithm for the maximum clique problem which applies existing clique finding and vertex coloring heuristics to determine lower and upper bounds for the size of a maximum clique [9]. Patric R. J. Ostergard, "A Fast Algorithm for the maximum clique problem", 2002 Elsevier Science, given a branch-and-bound algorithm for the maximum clique problem—which is computationally equivalent to the maximum independent (stable) set problem—is presented with the vertex order taken from a coloring of the vertices and with a new pruning strategy. The algorithm performs successfully for many instances when applied to random graphs and DIMACS benchmark graphs [10]. Xinchun Xu, Jun Ma, Jingsheng Lei, "Ant Colony Optimization for the Maximum Clique Problem" IEEE-ICNC 2007 introduced an evolutionary approach in which main task is to search for maximum cost path in a graph. Artificial Ants walk through graph and looking for high quality paths. Better results are found as emergent result of global cooperation among ants in colony. Li Lu, Yunhong Gu, Robert Grossman, "dMaximalCliques: A Distributed Algorithm for Enumerating All Maximal Cliques and Maximal Clique Distribution" IEEE- ICDMW-2010 presents a distributed algorithm which can obtain clique information from million-node graphs. It has used distribution of size of maximal cliques in a graph as a new measure for measuring structural properties of a graph. R.Rama, Suresh Badarla and Kamala krithivasan, "Clique-detection algorithm using clique-self-assembly", IEEE BIC-TA.2011, proposed a brute force algorithm where a large graph is being decomposed and these decomposed parts are cliques [11].

Hakan Yıldız, Christopher Kruegel, "Detecting Social Cliques for Automated Privacy Control in Online Social Networks", Fourth International Workshop on Security and Social Networking, Lugano (19 March 2012) proposed a privacy control approach that addresses this problem by automatically detecting social cliques among the friends of a user. To find cliques, given a small number of friends (seed), uses the structure of the social graph to generate an approximate clique that contains this seed. The cliques found by the algorithm can be transformed directly into friend lists, making sure that a piece of sensitive data is exposed only to the members of a particular clique. Harsh Bhasin, Rohan Mahajan, "Genetic Algorithms Based Solution To

Maximum Clique Problem”, ISSN: 0975-3397 Vol. 4 No. 08 Aug 2013, suggests the solution of above problem with the help of Genetic Algorithms (GAs). The work also takes into consideration, the various attempts that have been made to solve this problem and other such problems [12].

III. PRESENT WORK

3.1 Significance

Since the MAXCLIQUE problem has important applications, designing an algorithm with good performance becomes necessary and important. A lot of algorithms for solving the MAXCLIQUE problem have been proposed in the literature since the 1990's. The early work focused on the exact algorithms. Some of them achieved success on small graphs (less than 400 vertices). For example, Balas and Yu [2] improved the implicit enumeration algorithm by reducing the number of sub-problems generated from each node of the search tree, which in turn, reduced the size of the whole search tree. But still, the running time of exact algorithms increases exponentially with the size of graphs. So it is not practical to solve large problems by exact algorithms. The next step is to approximate the maximum clique size to be within a certain factor of the optimal solution. Therefore, it is necessary to solve the problem using heuristic algorithms. Heuristic algorithms cannot guarantee the quality of solutions but in practice they have been observed to produce very good solutions.

My area of research concentrates on solution of Maximum Clique Problem using a genetic algorithm which is a parallel search procedure inspired by the mechanisms of evolution in natural systems and the scenarios under which the solutions are applicable, the various qualitative parameters satisfied by the solutions and their associated costs in order to meet the current and future resource pool of a dynamic requirements in the most efficient way based on various qualitative and quantifiable parameters, so that virtualization or multi-tenancy can be easily deployed for providing various search services.

3.2 Objective

- [1] To identify various qualitative and quantifiable parameters for the fitness function to make intelligent decisions regarding fitness evaluation of chromosomes in a given population.
- [2] To design a solution for finding Maximum Clique Problem based upon extensive research of journals and articles in the field.
- [3] To identify various Clique finding algorithms and their solutions for helping Genetic Algorithm based solution to Maximum Clique Problem.
- [4] Implementation of the Maximum Clique Finding Algorithm in MATLAB.

3.3 Methodology

In order to build the Genetic Algorithm based solution to Maximum Clique Problem the following methodology is followed:-

[1] Identification

In this step the requirement analysis is done. This requires a task analysis to be done to determine the requirements, the inputs and outputs the prospective users.

[2] Conceptualization

In this the proposed program is designed to understand and define the specific relationships and interactions in the problem domain. The key concepts, the relationships, processes and control mechanisms are determined. This is the initial stage of knowledge acquisition.

[3] Formalization

This involves organizing the key concepts and information into formal representations i.e. rules for the Encoding and Crossover. It involves deciding the attributes to be determined to solve the problem and to build the initial mutated result.

[4] Implementation

This involves mapping of the formalized population into a framework of the development tool (MATLAB) to build a working Matrix. The contents of matrix structures, inference rules and control strategies established in the previous stages are organized into suitable format.

3.4 Sources of Data

The first population for the matrix computation will be developed through extensive study of journals, books, white papers etc. as well as experts in the field of Advanced Data Structures, Heuristic Searching Techniques and Evolutionary Search Strategies etc.

REFERENCES:-

- [1] P. Berman and A. Pelc, "Distributed Fault Diagnosis for Multiprocessor Systems" Proc. of the 20th Annual Int. Symp. On Fault-Tolerant Computing (Newcastle, UK), 1990, pp. 340-346.
- [2] E. Balas and C. S. Yu, "Finding a Maximum Clique in an Arbitrary Graph" SIAM J. Comput., 14, 1986, pp. 1054-1068.
- [3] R. Battiti and M. Protasi, "Reactive Local Search for the Maximum Clique Problem" Technical Report TR-95-052, International Computer Science Institute, Berkeley, CA, 1995.
- [4] D. E. Goldberg, "Genetic Algorithms in Search, Optimization and Machine Learning" Addison-Wesley, Boston, MA, 1989.
- [5] J.Hertz, A. Krogh and R. G. Palmer, "Introduction to the Theory of Neural Computation" Assison-Wesley, Redwood City, CA, 1991.
- [6] D. S. Johnson and M. A. Trick (eds.), "Cliques Coloring and Satisfiability, Second DIMACS Implementation Challenge" DIMACS 26, American Mathematical Society, 1996 (see also <http://dimacs.rutgers.edu/Volumes/Vol26.html>).
- [7] S. Kirkpatrick, C.D. Gelatt and M.P. Vecchi, "Optimization by Simulated Annealing" Science, 220, 1983, pp. 671 -680.
- [8] P. M. Pardalos and J. Xue. "The Maximum Clique Problem" Journal of Global Optimization, 4, 1994, pp. 301-328.
- [9] David R. Wood, "An algorithm for Finding a maximum clique in a graph" 1997 Elsevier Science B.V. PII S0167-6377(97)00054-0
- [10] Patric R. J. Ostergard, "A Fast Algorithm for the maximum clique problem", 2002 Elsevier Science B.V. PII: S0166-218X (01)00290-6
- [11] R.Rama, Suresh Badarla and Kamala krithivasan, "Clique-detection algorithm using clique-self-assembly", IEEE DOI 10.1109/BIC-TA.2011.32
- [12] Harsh Bhasin, Rohan Mahajan, "Genetic Algorithms Based Solution To Maximum Clique Problem", ISSN: 0975-3397 Vol. 4 No. 08 Aug 2013

Optimizing Design Cost of System by using Dynamic Programming

¹, K Indira Priyadarsini, ², Amanulla Mohammad

¹.M.TECH (SE) ². Assistant Professor (CSE)
G.I.E.T, RAJAHMUNDRY

ABSTRACT

Search based software engineering is an emerging discipline that optimizing the cost of system design by using algorithmic search techniques. For example in the design article intelligence system that help to crime investigation designs. Use the minimal amount of computing between to reduce weight and lost while supporting training and reorganization task running on board. Hard ware and software (system) design is a process which indentify software and hardware knapsack. Dynamic programming is a problem solving technique which solves the optimization design cost. This paper provide how cost. Constrained problem can be modeled as set of two dimensional knapsack problems and provides a frame work and algorithm to optimize design cost of system. An experimental result showing that results reaches the maximum of optimization solution value.

I. INTRODUCTION:

Software development organizations survive in a competitive market by profiting from the conversion of developers' effort to useful and successful software products. To build such products, the organization usually follows a process that divides the development effort into several activities. Each of these activities requires specific characteristics (e.g., such as skills, capabilities, and experience). Most of these characteristics are sought in human resources assigned to accomplish the activities. Search-based software engineering is an emerging discipline that aims to decrease the cost of optimizing system design by using algorithmic search techniques, such as genetic algorithms or simulated annealing, to automate the design search. In this paradigm, rather than performing the search manually, designers iteratively produce a design by using a search technique to find designs that optimize a specific system quality while adhering to design constraints. Each time a new design is produced, designers can use the knowledge they have gleaned from the new design solution to craft more precise constraints to guide the next design search. Search-based software engineering has been applied to the design of a number of software engineering aspects, ranging from generating test data to project management and staffing to software security. A common theme in domains where search-based software engineering is applied is that the design solution space is so large and tightly constrained that the time required to find an optimal solution grows at an exponential rate with the problem size. These vast and constrained solutions spaces make it hard for designers to derive good solutions manually. One domain with solution spaces that exhibit these challenging characteristics is hardware/software co-design. A key problem in these design scenarios is that they create a complex cost-constrained producer/consumer problem involving the software and hardware design. The hardware design determines the resources, such as processing power and memory, that are available to the software. Likewise, the hardware consumes a portion of the project budget and thus reduces resources remaining for the software (assuming a fixed budget). The software also consumes a portion of the budget and the resources produced by the hardware configuration. The perceived value of system comes from the attributes of the software design, e.g., image processing accuracy in the satellite example. The intricate dependencies between the hardware and software's production and consumption of resources, cost, and value make the design solution space so large and complex that finding an optimal and valid design configuration is hard.

II. MOTIVATING EXAMPLE:

This section presents a satellite design example to motivate the need to expand search-based software engineering techniques to encompass cost- constrained hardware/software producer consumer co-design problems. Designing satellites, such as the satellite for NASA's Magnetospheric Multiscale (MMS) mission [11], requires carefully balancing

hardware/software design subject to tight budgets Figure 1 shows a satellite with a number of possible variations in software and hardware design.

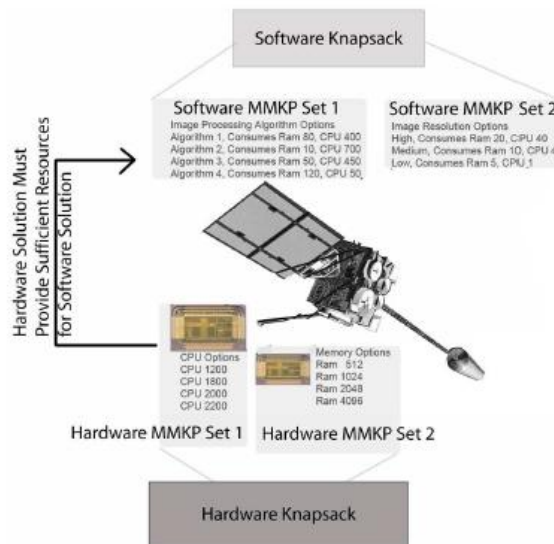


Fig. 1

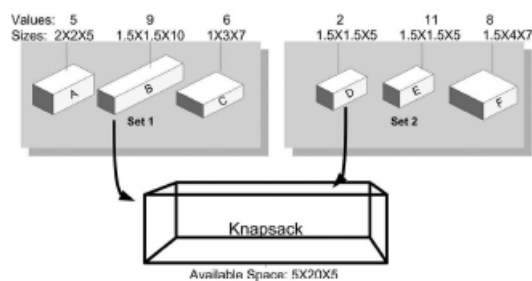


Fig.2

The software and hardware design problems are hard to solve individually. Each design problem consists of a number of design variability points that can be implemented by exactly one design option, such as a specific image processing algorithm. Each design option has an associated resource consumption, such as cost, and value associated with it. Moreover, the design options cannot be arbitrarily chosen because there is a limited amount of each resource available to consume.

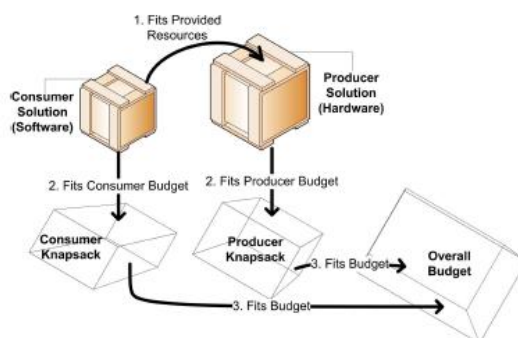


Fig.3

Figure 2 shows an example MMKP problem where two sets contain items of different sizes and values. At most one of the items A,B, and C can be put into the knapsack. Likewise, only one of the items D, E, and F can be put into the knapsack. The goal is to find the combination of two items, where one item is chosen from each set, that fits into the knapsack and maximizes the overall value.

III. PROBLEM DESCRIPTION:

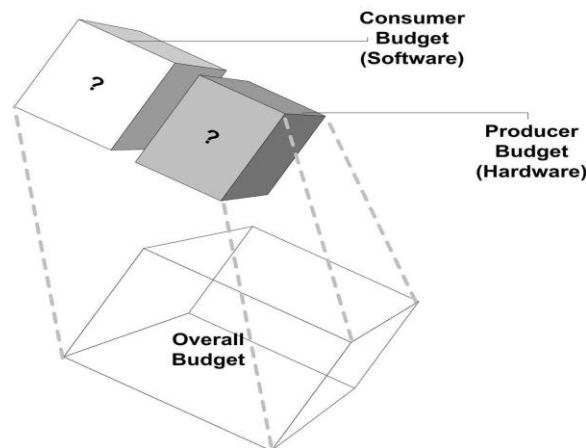
MMKP co-design problem, CoP, as an 8-tuple:
 CoP = < Pr, Co, S1, S2, S, R, Uc(x, k), Up(x, k) >
 where:

- Pr is the producer MMKP problem (e.g., the hardware choices).
- Co is the consumer MMKP problem (e.g., the software choices).
- S1 is the size of the producer, Pr, knapsack.
- S2 is the size of the consumer, Co, knapsack.
- R is the set of resource types (e.g., RAM, CPU, etc.) that can be produced and consumed by Pr and Co, respectively.
- S is the total allowed combined size of the two knapsacks for Pr and Co (e.g., total budget).
- Uc(x, k) is a function which calculates the amount of the resource $k \in R$ consumed by an item $x \in Co$ (e.g., RAM consumed).
- Up(x, k) is a function which calculates the amount of the resource $k \in R$ produced by an item $x \in Pr$ (e.g., RAM provided).

Let a solution to the MMKP co-design problem be defined as a 2-tuple, < p, c >, where $p \subset Pr$ is the set of items chosen from the producer MMKP problem and $c \subset Co$ is the set of items chosen from the consumer MMKP problem. A visualization of a solution tuple is shown in Figure 3. value of the solution as the sum of the values of the elements in the consumer solution:

$$V = \sum_0^j \text{valueof}(c_j)$$

where j is the total number of items in c, c_j is the jth item in c, and value of() is a uncton that returns the value of an item in the consumer solution.



IV. ALGORITHM OVERVIEW:

Inputs:

CoP = < Pr, Co, S1, S2, S, R, Uc(x, k), Up(x, k) >

D = stepsize

Algorithm:

1) For int i = 0 to $\lfloor S/D \rfloor$, set $S1 = i * D$ and $S2 = S - S1$

2) For each set of values for S1 and S2:

2.1) Solve for a solution, tc, to Co, given S2

2.2) Calculate a resource consumption heuristic

$V_r(k)$ for the resource in $r \in R$:

$V_r(r) = P|tc|$

$j=0 \sum Uc(tc_j, k)$

$P|R|$

$j=0 \sum P|tc|$

$k=0 \sum Uc(tc_j, k)$

2.3) Solve for a solution, p , to P_r that maximizes the sum of the values of the items selected for the knapsack, $P|p|$

$k=0$ Value(p_k), where the value of the k th item is calculated as:

Value(p_k) =

$|R|$

X

$j=0$

Value(r_j) * Up(p_k, r_j)

2.4) For each resource $r_j \in R$, calculate the amount of that resource, $P(r)$, produced by the items I_p :

$P(r) = Up(p_0, r_j) + Up(p_1, r_j) \dots Up(p|p|-1, r_j)$

2.5) Create a new multidimensional knapsack problem, C_{m0} , from C_0 , such that the maximum size

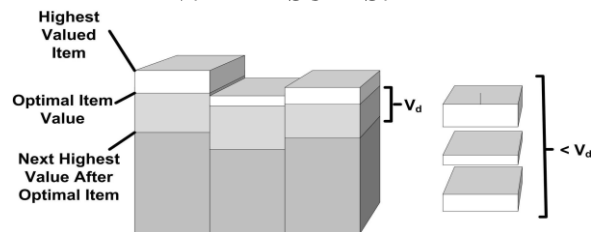
of each dimension of the new knapsack is defined by the vector:

$S_{m2} = (S_2, r_0, r_1, \dots, r_{|R|-1})$

2.6) Solve for a solution, c , to C_{m0} and add a solution tuple $\langle p, c \rangle$ to the list of candidate solutions, lc , for CoP

3) Sort the potential solutions, lc , of CoP and output both the highest valued solution and the list of other potential solutions.

V. RESULTS:



results are applicable to systems that have hard real time timing constraints and resource consumption characteristics. In particular, resources, such as CPU utilization, must have fixed limits. Moreover, the calculations are based on static worst-case bounds on resource consumption that must be known at design time. The results do not apply to systems where design decisions need to be based on dynamically changing resource consumption profiles. Each experiment used a total of 100 budget iterations ($T = 100$). We also used the MHEU MMKP approximation algorithm as our MMKP solver. All experiments were conducted on an Apple MacBook Pro with a 2.4 GHz Intel Core 2 Duo processor, 2 gigabytes of RAM, running OS X version 10.4.11, and a 1.5 Java Virtual Machine (JVM) run in client mode. The JVM was launched with a maximum heap size of 64mb ($-Xmx=64m$).

VI. EXPERIMENT RESULTS WITH RANDOM DATA:

When compared the algorithms on a series of problems that were completely randomly generated. For these problems, we did not know the true optimal value. We generated 100 problems with 50 sets per MMKP problem and 15 items per set. This yielded a solution space size of 15100. In order to ensure that we generated tractable problem instances, we set extremely loose resource constraints on the problems to create a high probability that a solution existed.

VII. CONCLUSION:

Designing hardware and software in tandem to maximize a system capability can be an NP-hard activity. Search-based software engineering is a promising approach that can be used to leverage algorithmic techniques during system co-design. This paper presented a polynomial-time search-based software engineering technique, called *Allocation-based Configuration Exploration Technique* (ASCENT), for finding near optimal hardware/software co-design solutions

This paper also provided how cost. Constrained problem could be modeled as set of two dimensional knapsack problems and provides a frame work and algorithm to optimize design cost of the system.

REFERENCES:

- [1] M. Abdelhalim and S.-D. Habib. Modeling Communication Cost and Hardware Alternatives in PSO Based HW/SW Partitioning. In *Proceedings of the International Conference on Microelectronics*, pages 111–114, Dec. 2007.
- [2] M. Akbar, E. Manning, G. Shoja, and S. Khan. Heuristic Solutions for the Multiple-Choice Multi-dimension Knapsack Problem. In *Proceedings of the International Conference on Computational Science-Part II*, pages 659–668. Springer-Verlag London, UK, 2001.
- [3] A. Barreto, M. Barros, and C. Werner. Staffing a Software Project: A Constraint Satisfaction and Optimization-based Approach. *Computers and Operations Research*, 35(10):3073–3089, 2008.
- [4] T. Wiantong, P. Cheung, and W. Luk. Comparing three heuristic search methods for functional partitioning inhardware–software codesign. *Design Automation for Embedded Systems*, 6(4):425–449, 2002.
- [5] K. Deb. An Efficient Constraint Handling Method for Genetic Algorithms. *Computer methods in applied mechanics and engineering*, 186(2-4):311–338, 2000.
- [6] T. Wiantong, P. Cheung, and W. Luk. Comparing three heuristic search methods for functional partitioning inhardware–software codesign. *Design Automation for Embedded Systems*, 6(4):425–449, 2002.
- [7] J. Clark and J. Jacob. Protocols are Programs Too: the Meta-heuristic Search for Security Protocols. *Information and Software Technology*, 43(14):891–904, 2001.
- [8] J. Gosling. *Introductory Statistics*. Pascal Press, Glebe, Australia, 1995. [9] M. Harman. The Current State and Future of Search Based Software Engineering. *International Conference on Software Engineering, Minneapolis, MN*, pages 342–357, May 2007.
- [9] P.-A. Hsiung, P.-H. Lu, and C.-W. Liu. Energy efficient co-scheduling in dynamically reconfigurable systems. In *Proceedings of the International Conference on Hardware/software Codesign and System Synthesis, Salzburg, Austria*, pages 87–92, October 2007.
- [10] G. Antoniol, M. Di Penta, and M. Harman. A RobustSearch-based Approach to Project Management in the Presence of Abandonment,Rework. *Proceedings of the International Symposium on Software Metrics*, pages 172–183, Sept. 2004.
- [11] L. Chung. *Non-Functional equirements in SoftwareEngineering*. Springer, 2000.
- [12] M. Harman and B. Jones. Search-based software engineering. *Information and Software Technology*, 43(14):833–839, 2001.
- [13] D. Vanderster, N. Dimopoulos, and R. Sobie. Metascheduling multiple resource types using the MMKP. In *Proceedings of the 7th IEEE/ACM International Conference on Grid Computing, Barcelona, Spain*, pages 231–237, Sept. 2006.
- [14] P. McMinn. Search-based software test data generation: a survey. *Software Testing, Verification & Reliability*, 14(2):105–156, 2004.
- [15] M. Harman. The Current State and Future of Search Based Software engineering. *International Conference on SoftwareEngineering, Minneapolis, MN*, pages 342–357, May 2007

Criteria for Choosing An Effective Cloud Storage Provider

Audu Jonathan Adoga¹, Garba M. Rabi², Anyesha Amos Audu³

^{1,2,3}Nasarawa State Polytechnic, Lafia, Nigeria

ABSTRACT:

Cloud storage, a revolutionary invention and a Cloud Computing model is changing the way computer users and organizations save their data. This review creates awareness on the benefits of cloud storage to the clients. The report also discusses Cloud's top ten risks, as presented by a professional body (OWASP). These risks serve as eye opener to those who want to employ cloud storage. Advantages of cloud storage have also been elaborated, but one may be left in confusion because the paper sheds light on both the advantages and the risks of Cloud Storage. It is in line with these that this review tries to create a crystal clear explanation by going further to expatiate on the functions that are required from a cloud storage provider. Clients can now make decisions that are devoid of mistakes during choices of cloud storage providers. The report also advises users and organizations to always check latest reviews about cloud storage providers based on the fact that, good or bad cloud storage providers of a particular year could change for better or worst.

KEYWORDS: Cloud Storage, advantages, computing model, risks, vulnerabilities, security holes, patched, Review, on-premises computing, Cloud Computing, identity federation, invisibility, resiliency.

OVERVIEW: This review is made up of seven sections. They are Introduction, Aims and Objectives of the Paper, Literature Review, Advantages of Cloud Storage, Bad Models Offered by Some Cloud Storage Providers, Conclusion, Bibliography and Appendix

I. INTRODUCTION

Conventional system of storing files is what almost everybody is aware of, but contemporary system of storage is cloud storage. What is this Cloud Storage and what does this system have that promises to be better than the conventional method? Who are the best storage providers and what are the criteria used in such rating? Imagine a situation where one has about eight devices that work on different or similar platforms such as iPod, Android Tablet, Android Phone, PC (Windows 7 – windows 8), Mac (OSX) and a Blackberry. If this owner needs a storage system that data from all the devices could be saved in and also accessed using any of the devices, without compatibility problem, then Cloud Storage is the solution. This is because; the owner of these devices may not travel with all the devices everywhere he/she goes but the need to get any of the saved data through any of the available device(s) may arise. You may also want to schedule backups of your specified files at the background, while working on your system locally or in the cloud. If you want synchronization of the files which helps a user to have both offline and online copies of files accessible through multiple devices, then you need the services of a good cloud storage provider. Based on the few points presented above and many more that will be discussed later, cloud storage could be defined as a model in Cloud Computing in which remote servers are used to store and accessed data online using virtualization techniques. "Cloud Storage is not just hardware, but network equipment, storage equipment, servers, applications, public access interface, the access network and the client program and other parts of the system" [1] Cloud Storage is a type of storage, accessible online, that stores data across multiple drives with different sizes, located in different areas [2]. Cloud Storage is a model that will transcend many centuries, considering the versatility of its functionalities. However, before a user or an organization chooses a cloud storage provider, it is wise to consider the services offered by such provider, whether they meet the needs of such user/organization. This is the reason why, Cloud Storage security risks from Open Web Application Security Project (OWASP) and the review presented by TopTenReviews are the subjects of discussions in this report.

II. AIMS AND OBJECTIVES OF THE REPORT

2.1 Source of information

Information will be sourced from secondary sources about cloud storage such as the professional websites on the internet, textbooks and reputable journals

2.2 History

This paper will give a brief history of the word cloud as used in computing. Though history is one aspect of life that is full of contradictions but this report will try as much as possible to do justice to that.

2.3 Advantages

Explicit discussion on the advantages that cloud storage has to offer to the modern computing world will be a matter of top priority in this paper.

2.4 Bad models

Despite the fact that there are many dividends of employing cloud storage, some of the most highly rated cloud storage providers still have some limitations and the limitations will be discussed in relation to those providers.

2.5 Awareness

This review will try to create awareness about cloud storage providers so that client can take informed decisions about them especially in the aspect of choosing cloud providers that could solve their data storage needs.

III. LITERATURE REVIEW

Cloud Computing has been defined by the National Institute of Standards and Technology (NIST) as a version of product, on-demand internet access to computer resources that can be deployed and also be released without much intervention by the provider of cloud storage[3].Cloud is a back to the future proposition which is as old as computing itself, but for the sake of history which is always subject to review, the term “cloud” was first coined by a communication industry in 1990s[4].Instead of the hardware from end to end type of network, companies started using virtual private networks for communications. It was not possible to predict accurately, what path data will follow between the user and the company hence, the phrase “the cloud” was used based on users’ point of view. Cloud Computing introduces to us a new world of computing where access to applications and storage of data that are executed locally are being transferred to the internet, but what are the implications in terms of transferring an organization’s data which may be very confidential to some servers on the internet instead of storing them locally? How do we trust the services of a cloud storage provider? Despite these hurdles that the client may pass through, there is good news. “ a company or individual is probably more likely to lose data in an on-premises solution than they are through many cloud-based services” [5].Moreover, On-premises Computing and Cloud Computing could be compared with car travel and air travel respectively. In car travel, both passengers and the car worker(s) contribute one way or the other to the success of the journey because, they may be familiar with so many things about car while in air travel, since most vital information about the plane is hidden such as no knowledge of airplane maintenance, but the convenience and more comfort travellers have when they change from travel by car to air travel can be compared with moving from conventional computing to cloud computing. Moving data from local systems to the internet may reduce one’s control over the data but does not necessarily means that the security of the data has been compromised. The cloud makes life easy for users because, software and data that reside on individual’s devices can now be accessed on any device, irrespective of the platform or the type of internet connectivity. Data can be accessed and applications could be loaded anytime and everywhere [6].

3.1 Top ten security risks that are associated with cloud storage

There are top ten security risks that are associated with Cloud Computing, especially Software as a Service (SaaS) model [7]. Despite the fact that, the top ten cloud providers have overcome many of their hurdles, So many others need improvement on their functionalities. The security risks, according to OWASP [7] are as follows:

3.1.0Data Ownership and Accountability. If an organization owns a traditional data centre, it is that organization’s responsibility to keep the data secure, physically and logically. But once a decision has been taken to host data using public cloud, the organization loses power in terms of the control it has over such data. There should be guarantee of data recovery and backups by all cloud storage providers.

3.1.1 User Identity Federation. The issue of federated authentication should be made compulsory. This is to avoid problems that are associated with migration of applications and services from one service provider to another. Identities needed for backend development could be serious problem during such migrations.

3.1.2 Business Continuity and Resiliency. Every IT compliant organization gives great priority to business continuity. But for an organization that employs the services of a storage provider, this responsibility is saddled on the cloud provider and it could be very risky because, there is no certainty on how the business can still be managed, if there is a disaster. **3.1.3 Regulatory Compliance.** Countries or continents may have legal differences when it comes to cloud storage and the regulatory body of an area must work in consonance with the laid down laws of the area it operates. This causes variance in security levels of cloud storage providers located in different parts of the world.

3.1.4 User Privacy and Secondary Usage of Data. For users of services such as Google Docs, YouTube and Yahoo Mail, their personal data are stored in the cloud and most of the providers are silent about what will happen to personal data of users in terms of usage. Moreover, the problem of default share to all used by some services such as Facebook, Twitter and LinkedIn, could allow personal details to be revealed to others. This issue triggers the need for creation of clear distinction data that can be used for security purposes and those that cannot. It is very common to see advertisements that are related to a user's recent communication. This is because; users' data are being used for secondary purposes.

3.1.5 Service and Data Integration. Cloud is susceptible to interception, based on this; clients cannot easily take this risk. Data ought to be transferred securely from a user to the cloud provider.

3.1.6 Multi Tenancy and Physical Security. Multi tenancy means the use of the same services and resources for so many clients such as the use of the same CPU, database and network. This is good but the challenge is this: the cloud provider must make sure that clients do not temper with the data security of one another. This can be achieved through tremendous increase in logical segregation by the cloud providers.

3.1.7 Incidence Analysis and Forensic Support. Sometimes, investigation during security incident could be very difficult in the cloud since logging may be a distributed type and data centres may be located in different parts of the world and this can bring difficulties when it comes to the legal handling of such cases because, laws have differences as one moves from one country or state to another. Moreover, through log files, different customers may be co-located on the same device, this brings about a concern to relevant agencies during forensic recovery.

3.1.8 Non Production Environment Exposure. If an IT company develops applications internally, then it uses non-production environments for its activities. But such environments are generally not as secure as production environments. If such organisation employs cloud as non-production environment, it could be riskier because of theft, illegal modification and fraudulent access.

3.1.9 Infrastructure Security. All infrastructures must work based on standard. All networks, systems and applications must be designed and developed with security zones. Access to administrative information should be based on role. The risk assessment of the storage facilities and their configurations should be done regularly by independent experts. A policy must come up that takes care of the problem of security holes and those vulnerabilities could be patched and updated. Customers should be informed appropriately.

3.2 Best Cloud Providers

A recent research [8] on the top ten 2013 cloud storage companies shows that the top ten cloud providers (Check Appendix) are just Cloud.com, Sugersync, Egnyte, HybrideCloud, YouSendIt, Dropbox, OpenDrive, Mozy, Online Storage, Carbonite and Box. These storage providers were rated based on what their storage services could do. It was discovered that some of the storage providers amongst the top ten were deficient in some functionalities such as Drag-and-drop-upload, Space provision for storage/price per month, versioning of file, sharing of file, link sharing using custom method, backup based on schedule, incremental backup, unlimited file size for every file, restoration of deleted files, event log, mobile app/website, all file format support, web access, mobile syncing, multiple computer syncing, SSL/TSL encryption, at-rest encryption, password protected sharing, permission settings for folders, email support, knowledgebase, tutorial using video, manual/guide for users, online chat, support for telephone, windows 8, 7, vista, xp, and mac os support.

IV. ADVANTAGES OF CLOUD STORAGE

It is crystal clear that what attracts people to a technology or an invention is the advantages it has over other related or former ones. Based on an online presentation by Nielsen [9] showed that, there are ten advantages of using online storage. Though, these advantages may not be possible with some cloud storage providers, but generally, clients of cloud storage providers are supposed to benefit from the following.

4.1 Cost

Backups of data are not always an easy thing to implement when it comes to practice. You have to consider the cost of the devices you want to use for the storage. Is it tapes or external drives? All these can cost an organisation a lot of money. Another thing one may also consider is the time it takes to perform the backups manually. Cloud storage providers now offer automatic backups of data. The storage space provided is of low monthly fee.

4.2 Invisibility

It is possible to pile up thousands of storage drives or tapes in an office. This is a space problem to such environment but with cloud storage, storage devices are invisible to any organisation that uses the services of a cloud storage provider. This has removed the problem of covering valuable space in the office with storage devices.

4.3 Security

The issue of confidentiality in any organisation is a serious matter that does not permit compromise. We have had situation where people embezzled money and burnt the office, just because they wanted the confidential document in the office to get burnt so that their secret will not be revealed. This cannot happen with cloud storage. Some storage providers make sure that, data is encrypted at the time of transmission as well as during storage. Illegal users are completely blocked from having access to the data.

4.4 Sharing

Cloud storage providers also make provision for information sharing. This is a good service since it takes care of users' needs of sharing some information. This does not mean that the security of users' information is compromised. A good storage model makes sure that, no body has access to what a user did not permit.

4.5 Automation

The idea about automation of cloud storage is this: tell the system what to do and also when to do it. The system does it automatically based on settings. Human attention could be taken away and a lot of damages could be done during such period but with automation, the system does not forget.

4.6 Accessibility

The idea of moving a file or files from one device you own to another could be cumbersome, especially when it comes to the updated version of the document. Why not store your file in one central zone that is easily accessible with any of the devices you own? This is one of the most powerful functions of cloud storage.

4.7 Syncing

This explanation is better done with example. Let us say you have three devices for developing your project. The moment a file is updated in any of the three devices, the technology and innovation of syncing helps you to get the updated version in all other devices automatically. This is great!

4.8 Collaboration

The possibility of stress less collaborative work, irrespective of one's geographical location is one of the greatest achievements of the internet. With the coming of cloud storage, it becomes much easier for people to execute collaborative work. In this case, you don't need to disturb yourself about tracking the latest version or the person that made the modification. It is as if all the members are in one place doing the work. This is worth embracing.

4.9 Protection

With some cloud storage providers, your files are well protected. There is additional layer of data protection given to precious files. This is achieved using series of security measures. Backups are kept by the cloud storage providers in a physical location that is different from where the originals are stored.

4.9.1 Recovery

With this method in place, if there is problem with the originals, it could be recovered from the backups and if there is problem with backups, they could easily be recovered from the originals. It is very rare for both to have problem at the same time. This is also a good aspect of cloud storage. The downtime for recovery is extremely short.

V. BAD MODELS OF CLOUD STORAGE OFFERED BY SOME ORGANISATIONS

There are so many definitions of a model in Oxford English Dictionary [10] but the one that is related to this report is “a particular version of a product”. From here, it is clear that bad cloud storage model simply means bad version of cloud storage. These bad versions of cloud storage have been implemented by some cloud storage providers and it is worth reporting.

In a recent review [8], TopTenReview was able to review and release a 2013 version of top ten cloud storage providers. just Cloud.com was the gold award winner, followed by SugarSync, Egnyte HybridCloud, YouSendIt, Dropbox, OpenDrive, Mozy, Online Storage, Carbonite and Box in that order. There were certain criteria they used to know what model of storage was good or better than others.

5.1 Storage space/price per month

In terms of storage, SugarSync, Egnyte HybridCloud, Dropbox, Mozy and Box though were among the top ten but offered bad models of storage because, they offered limited storage to their customers at flat rate per month.

5.2 Features

Box offered a bad model in terms of drag-and-drop functionality. Carbonite was not good at file sharing. Online Storage and Carbonite fell short of file versioning. Mozy and Carbonite were not good at file sharing and custom link sharing. YouSendIT and Box could not perform incremental backups and schedule backups. Mozy, Box and YouSendIt were not able to meet up with the demand for unlimited file size. It was not possible for YouSendIt and Online Storage to restore files that were deleted. Event log was not possible for SugarSync Egnyte HybridCloud, Mozy, Online Storage, Carbonite and Box. Finally, the functionality of file sharing was not possible for SugarSync, Egnyte HybridCloud, YouSendIt, Mozy, Carbonite and Box

5.3 Access

Cloud storage should allow one to store files of any format and have access to them as at when needed. Also, upload and access to files through different mobile devices and multiple systems should be possible. The cloud storage ought to be compatible with desktop applications and easy access to files from any browser. Some organisations have failed in this aspect. The review revealed that, Box could not implement desktop applications. Mobile and desktop application Syncing was not found in Carbonite.

5.4 Security

The issue of intrusion when it comes to internet is very high. As a result of this, a multi-layer security approach must be applied to data when it is stored and during transmission. Some of the security types are transport layer security (TLS), Secure Socket Layer (SSL), Advanced Encryption standard (AES), Folder permission and password protection. Carbonite failed in terms of folder permission but generally speaking, the top ten cloud storage providers were very good in the aspect of system security.

5.5 Help and support

Online Storage could not provide knowledgebase support. Support for customers on video tutorial was not provided by OpenDrive. YouSendIt failed in the aspect of user guide and manual. Egnyte HybridCloud, Dropbox, Online Storage and Box could not provide the functionality of charting with their customers. just Cloud.com, Mozy had no support for telephone though, SugarSync and OpenDrive provided telephone service to customers but not free.

5.6 Platforms

Almost all the top ten cloud storage providers had support for windows 8, 7, vista, xp and mac os except OpenDrive which had no support for windows 8.

VI. CONCLUSION

If the top ten cloud storage providers still had flaws in their functionalities. This report lacks what adjective that could be used to qualify the type of weaknesses in those that were not among the top ten. The regulatory bodies should take stringent actions against this and also alert the Government(s) on the inclusion of

such requirements in the constitution(s). Cloud storage is a back to future cloud computing model that cannot be ignored despite some of the current challenges. To the top ten cloud storage providers, keep it up, you are almost through but, this does not mean that you should relax. The attackers are there, mapping new strategies. So, you should consolidate on your areas of strength and improve on your weaknesses. We are almost there! Congratulations in advance. Individuals and organisations should not employ the services of a storage provider without checking latest reviews that exist on the internet. This indomitable computing model, signals success that could transcend centuries, but we must embrace it with precautions.

BIBLIOGRAPHY

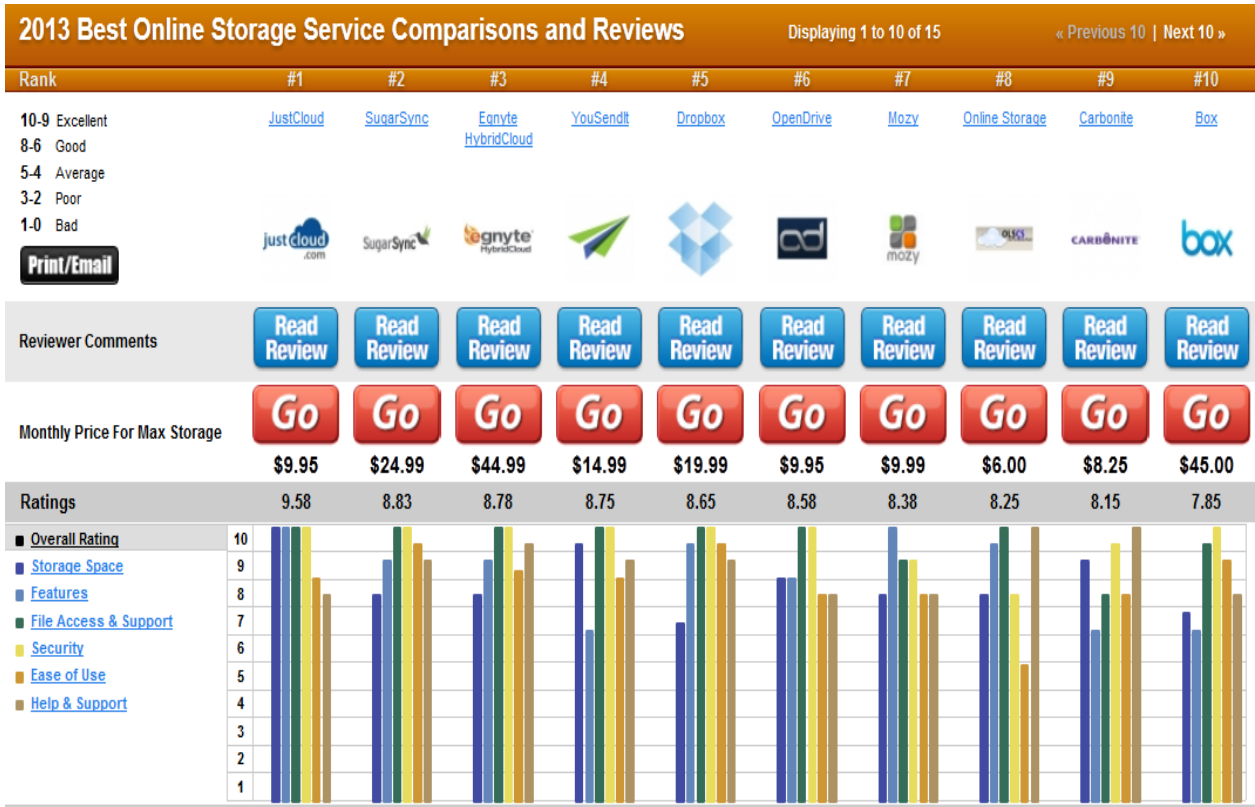
- [1] <http://www.sciencedirect.com/> Procedia Engineering, An Efficient Cloud Storage Model for Heterogeneous Cloud Infrastructures 2011 vol. 23 issue 2011
Dejun Wang
- [2] <http://www.cloudconsulting.com/storage/> CloudConsulting , Cloud Storage Overview 2014
- [3] International Conference on Application of Information and Communication Technologies (AICT), Towards a Wider Cloud Service Applicability by Security, Privacy and Trust Measurement 2010pp.1-6
Savola, R. M., Juhola, A. and Uusitalo, I.
- [4] <http://cit.srce.unizg.hr/index.php/CIT/article/view/1864>
CIT Journal of Computing and Information Technology, A Review on Cloud Computing: Design Challenges in Architecture and Security 2011 vol. 19, issue 1
Fei Hu, Meikang Qiu, Jiayin Li, Travis Grant, Drew Taylor, Seth McCaleb, Lee Butler, Richard Hammer
- [5] <http://Libweb.anglia.ac.uk> Computer Law & Security Review, Trust in the Cloud 2012 vol. 28, issue 5
Patrick Ryan, Sarah Falvey
- [6] <http://Libweb.anglia.ac.uk> Future Generation Computer Systems, Creating Optimal Cloud Storage Systems 2013 vol. 29, issue 4
Josef Spillner, Johannes Muller, Alexander Schill
- [7] https://www.owasp.org/index.php/Category:OWASP_Cloud_%E2%80%9010_Project
Open Web Application Security Project, Cloud Top Ten Security Risks 2014
- [8] <http://online-storage-service-review.toptenreviews.com/>
TopTenReviews, See Who is Number One in Online Storage Services 2013
- [9] <http://online-storage-service-review.toptenreviews.com/top-ten-advantages-of-using-online-storage-services.html>
TopTenReviews , Top Ten Advantages of Using Online Storage Services 2013
Katie Nielsen
- [10] Oxford(2012) Oxford English Dictionary. 7th ed. Oxford: Oxford University Press.

APPENDIX

See who is Number one in the Online Storage Services

The advertisement features a dark background with a navigation bar at the top containing categories like Software, Electronics, Mobile, Web Services, Appliances, Entertainment, Small Business, Auto Tech, and More. Below the navigation bar, there is a prominent yellow badge that reads '2013 Gold Award Winner' and 'Ranked #1 of 15 Companies'. The central focus is the 'justcloud.com' logo, accompanied by a quote: 'JustCloud is an excellent choice for an online data backup service. This web service offers a variety of backup features that are outstanding.' attributed to TopTenREVIEWS. To the right, another badge states 'Voted #1 Online Storage Provider' with a 'The Verdict' star rating and another '2013 Gold Award Winner' badge. A large orange button at the bottom right says 'Try Today For FREE'. A 'Read Review' button is also visible in the top right corner of the ad area.

Source: <http://online-storage-service-review.toptenreviews.com/>
TopTenReviews, (2013). See who is Number one in the Online Storage Services



Source: <http://online-storage-service-review.toptenreviews.com/>
 TopTenReviews, (2013) See who is Number one in the Online Storage Services



Source: <http://online-storage-service-review.toptenreviews.com/>
 TopTenReviews, (2013) See who is Number one in the Online Storage Services

Features										
Drag-and-Drop Upload	✓	✓	✓	✓	✓	✓	✓	✓	✓	✓
Folder Sharing	✓	✓	✓	✓	✓	✓	✓	✓	✓	✓
File Versioning	✓	✓	✓	✓	✓	✓	✓	✓	✓	✓
File Sharing	✓	✓	✓	✓	✓	✓	✓	✓	✓	✓
Custom Link Sharing	✓	✓	✓	✓	✓	✓	✓	✓	✓	✓
Scheduled Backup	✓	✓	✓	✓	✓	✓	✓	✓	✓	✓
Incremental Backups	✓	✓	✓	✓	✓	✓	✓	✓	✓	✓
Unlimited File Size Limit	✓	✓	✓	✓	✓	✓	✓	✓	✓	✓
Restore Deleted Files	✓	✓	✓	✓	✓	✓	✓	✓	✓	✓
Event Log	✓	✓	✓	✓	✓	✓	✓	✓	✓	✓
File Preview	✓	✓	✓	✓	✓	✓	✓	✓	✓	✓
Access										
Mobile App/Website	✓	✓	✓	✓	✓	✓	✓	✓	✓	✓
Supports all File Types	✓	✓	✓	✓	✓	✓	✓	✓	✓	✓
Web Access	✓	✓	✓	✓	✓	✓	✓	✓	✓	✓
Desktop App	✓	✓	✓	✓	✓	✓	✓	✓	✓	✓
Mobile Syncing	✓	✓	✓	✓	✓	✓	✓	✓	✓	✓
Multiple Computer Sync	✓	✓	✓	✓	✓	✓	✓	✓	✓	✓
Security										
SSL/TLS Encryption	✓	✓	✓	✓	✓	✓	✓	✓	✓	✓
At-Rest Encryption	✓	✓	✓	✓	✓	✓	✓	✓	✓	✓
Password Protected Sharing	✓	✓	✓	✓	✓	✓	✓	✓	✓	✓
Folder Permissions	✓	✓	✓	✓	✓	✓	✓	✓	✓	✓
Technical Help & Support										
Email Support	✓	✓	✓	✓	✓	✓	✓	✓	✓	✓
Knowledgebase	✓	✓	✓	✓	✓	✓	✓	✓	✓	✓
Video Tutorials	✓	✓	✓	✓	✓	✓	✓	✓	✓	✓
User Guide/Manual	✓	✓	✓	✓	✓	✓	✓	✓	✓	✓
Online Chat	✓	✓	✓	✓	✓	✓	✓	✓	✓	✓
Telephone Support	✓	5	✓	✓	✓	5	✓	✓	✓	✓
Supported Platforms										
Windows 8	✓	✓	✓	✓	✓	✓	✓	✓	✓	✓
Windows 7	✓	✓	✓	✓	✓	✓	✓	✓	✓	✓
Windows Vista	✓	✓	✓	✓	✓	✓	✓	✓	✓	✓
Windows XP	✓	✓	✓	✓	✓	✓	✓	✓	✓	✓

Source: <http://online-storage-service-review.toptenreviews.com/>

TopTenReviews, (2013) See who is Number one in the Online Storage Services

Design and Implementation of Area and Power Efficient Embedded Transition Inversion Coding For Serial Links

C.Jacob Ebbipeni¹ N.Bamakumari²

Department Of Electronics And Communication Engineering
Sri Venkateswara College Of Engineering And Technology, Thirupachur.

ABSTRACT

Advanced silicon technology offers possibility of integrating hundreds of millions of transistor into a single chip, which makes system on chip (SoC) design possible. With the continuous scaling of silicon technology, area and power dissipation of interconnects are one of the main bottlenecks for both on chip and off chip buses. Multiplexing parallel buses into a serial link enables an improvement in terms of reducing interconnect area, coupling capacitance and crosstalk, but it may increase the overall switching activity and energy dissipation. Therefore, an efficient coding method that reduce the switching activity is an important in serial interconnect design. Embedded Transition Inversion (ETI) is the coding method that reduces the switching activity and energy dissipation. Area is one of the important objective in integrated circuits. The main of this paper is reduce the area in ETI coding architecture. In this proposed method Alexander Phase Detector is replaced by Hogge Phase Detector. The proposed system done by using Xilinx 13.2 and ModelSim software to get efficient output. The proposed system result analysis shows better than the existing method.

INDEX TERMS :Serial Interconnection, Embedded Transition Inversion (ETI), Phase Encoder, Phase Decoder, Bit two inverter.

I. INTRODUCTION

Advanced silicon technology offers the possibility of integrating hundreds of millions of transistors into a single chip, which makes system-on-chip (SoC) design possible. With the continuous scaling of silicon technology, area and power dissipation of interconnects are one of the main bottlenecks for both on-chip and off-chip buses. Multiplexing parallel buses into a serial link enables an improvement in terms of reducing interconnect area, coupling capacitance, and crosstalk [1], but it may increase the overall switching activity factor (AF) and energy dissipation. Therefore, an efficient coding method that reduces the switching AF is an important issue in serial interconnect design. Many studies attempt to reduce the AF of parallel buses. For example, Stan and Burleson [2] introduced a bus-invert method that transmits the original or inverted pattern to minimize the switching activity. Researchers have proposed many techniques to improve the bus-invert coding method, such as the partial bus-invert coding [3] and weight-based businvert coding methods [4]. The schemes mentioned above use an extra channel to send the inversion indication signal. Kuo et al. [5] proposed the serial coding technique to solve the extra channel problem. They append extra information bits to the back of the original data word.

Although this approach resolves the area overhead problem, it increases data latency. Three level differential encoding is proposed for parallel bus [6] to enable multiple drivers at the transmitter and to recycle the same current and reduce power consumption [6]. Joint crosstalk avoidance code and error correction code are proposed to reduce the power in parallel bus [7]. Huang et al. [8] further proposed combining serializing bus with the joint crosstalk avoidance code and error correction code to reduce the power. Serialized low-energy transmission (SILENT) [1] is a coding method used in reducing the switching activity for serial links. This approach encodes every single bit in the parallel bus using the XOR gate, and multiplexes the encoded parallel buses into a serial link. The XOR operation sets an adjacent bit with the same value to zero. The greater the correlation is, the more zeros the encoder produces. This method is designed for data with strong correlation. Bharghava et al. [9] proposed the transition inversion coding (TIC) technique to reduce switching activity for random data and to detect errors. Their technique counts the transitions in the data word, and inverts the transition states if the number of transitions in a data word is more than half of the word length.

The scheme sets the current bit in the serial stream to be the same as the previous encoded bit when there is a transition. Otherwise, it is set to the inversion of the previous encoded bit. A transition indication bit is added in every data word. This extra bit not only increases the number of transmitted bits, but also increases the transitions and latency. Lee et al. [10]– [12] used serial links as communication channels on an on-chip network architecture for SoC. The serial links reduce the area of communication channels by 57% compared with a non-serialized approach [10]. This approach also reduces the switch activity because the coupling capacitance of the interconnect wires decreases [10]–[12]. Forward error correction (FEC) code is used to reduce the serial link power by trading off the FEC coding gain with specifications on transmit swing, analog-to-digital converter precision, jitter tolerance, receive amplification, and by enabling higher signal constellations [13]. By combining the single and differential signals and 8B/10B coding, a high speed phase tracking clock recovery is developed for serial link to reduce the power [14]. To utilize the relation between data in a link, the encoder reorders or shuffles the M bits in the parallel bus such that the encoded data are less correlated or silent [15]. Then the encoded data are serialized with one control bit. The silent coding with shuffling can reduce the power dissipation compared to the silent coding.

A serial link on-chip bus architecture is proposed to lower interconnect power [16]. Serialization reduces the number of wires and leads to a larger interconnect width and spacing. A large interconnect spacing reduces the coupling capacitance, while the wider interconnects reduce the resistivity. A significant improvement in the interconnect energy dissipation is achieved by applying different coding schemes and their proposed multiplexing techniques. However, the power reduction decreases when the degree of multiplexing increases. The embedded transition inversion (ETI) coding scheme to solve the issue of the extra indication bit [17]. This scheme eliminates the need of sending an extra bit by embedding the inversion information in the phase difference between the clock and the encoded data. When there is an inversion in the data word, a phase difference is generated between the clock and data. Otherwise, the data word remains unchanged and there is no phase difference between the clock and the data. This ETI coding scheme reduces transition by 31% compared with the SE scheme. The improvement of transition reduction is 19% compared with that of the TIC.

The receiver side adopts a phase detector (PD) to detect whether the received data word has been encoded or not. Statistical analysis and experimental results show that the proposed coding scheme has low transitions for different kinds of data patterns. Increasing the interconnect spacing reduces the coupling capacitance for on-chip buses. We also study about different phase detector to optimizes the performance of the ETI and also reduced the power and the area of the ETI system. The remainder of this paper is organized as follows. Section II presents ETI coding scheme. In Section III describe about ETI Architecture that includes the ETI encoder and decoder. Experimental result shown in Section IV and Conclude in Section V.

II. ETI CODING SCHEME

Although many coding algorithms can reduce the switching AF, most of them are designed for specific applications, such as video streaming or strongly correlated data. The TIC is one of the methods developed for random data [9]. This method adds a transition indication bit to every data word to indicate if there is an inversion or not. This inversion coding is performed on every bit of two consecutive bits in the serial stream. The extra indication bit increases the switching activity. This paper proposes the ETI coding scheme that operates on a two-bit basis and removes all the transition indication bits. Fig. 1. n/m ETI serial links with n input bitstreams under degree of multiplexing m . Fig. 1. ETI coding scheme for one serial link, word length = WL , $N_{th} = WL/2$, and number of transition = N_t . An n/m ETI serial links with n input bitstreams under degree of multiplexing m is shown in Fig. 1. Each serial link has m input bitstreams that are multiplexed by a serializer, followed by the ETI encoding. The encoded stream is transmitted through the serial link and followed by the ETI decoding and a deserializer. The ETI coding scheme includes the inversion coding and phase coding as shown in Fig. 2.

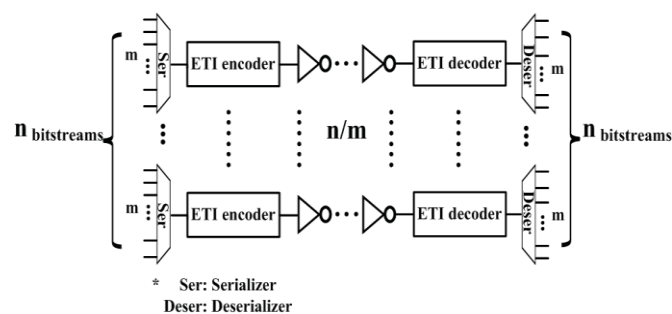


Fig 1. n/m ETI serial links with n input bitstreams under degree of multiplexing m .

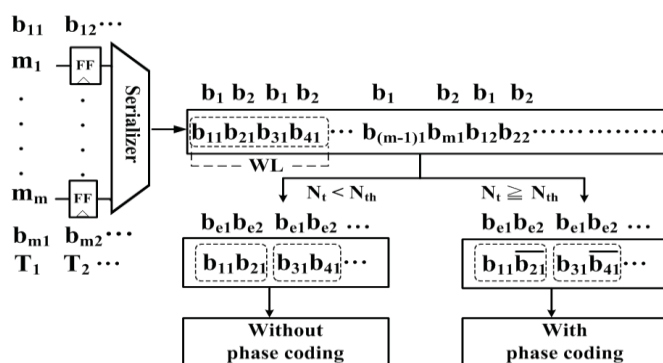


Fig 2. ETI coding scheme for one serial link, word length = WL, $N_{th} = WL/2$, and number of transition = N_t .

1) Inversion Coding: Define the word length (WL) as the number of bits in a data word and a threshold N_{th} as half of WL. A transition is defined as a bit changing from zero to one or from one to zero. For example, the bitstream “0100” has two transitions while “0101” has three transitions. When the number of transitions N_t in a data word exceeds the threshold N_{th} , the bits in the data word should be encoded. Otherwise, the data word remains the same.

When an encoding is needed in a data word, this method checks every two-bit in the data word, as Fig. 3 shows. Every two bit in the serial stream is combined as a base to be encoded. In this case, the $b_{11}b_{21}$ is a base and the $b_{31}b_{41}$ is another base. The 2-bit in a base is denoted as b_1b_2 and the encoded output is denoted as $b_{e1}b_{e2}$. When the N_t in a data word is less than N_{th} , b_1b_2 remains unchanged. Otherwise, we perform the inversion coding and the phase coding. For the inversion coding, the bitstreams “01” and “10” are mapped to “00” and “11,” respectively. The bitstreams “00” and “11” are mapped to “01” and “10,” respectively. For the phase coding, we embed the inversion information in the phase difference between the clock and the encoded data. The inversion encoding operation can be expressed as The inversion decoding operation for the decoded output $b_{d1} b_{d2}$ is Since this operation is on a two-bit basis and only the second bit is inverted, it is called bit-two inversion (B2INV).

2) Phase Coding: The ETI coding uses the phase difference between the data and the clock to encode the indication information. Table I shows the corresponding output data word after TIC, ETIpre, and ETI. The ETIpre has the same data word as the TIC, except that it removes the extra bit b_{ex} . Removing the b_{ex} leaves eight sets of data words that are exactly the same. For example, there are two “1000” data words after the ETIpre coding. Within every data word duration, the phase difference between the data and the clock distinguishes these two data words, as Fig. 4 illustrates. Same D_{out} “1000” in Fig. 3 and 4 is obtained from D_{in} “1000” and “1101” without and with inversion. A half clock cycle difference between D_{out} and CK is shown in Fig. 3, indicating that D_{in} has been encoded.

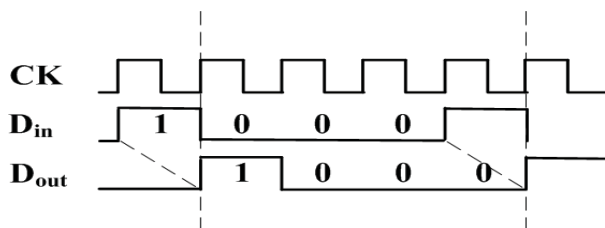


Fig 3. Din without encoding

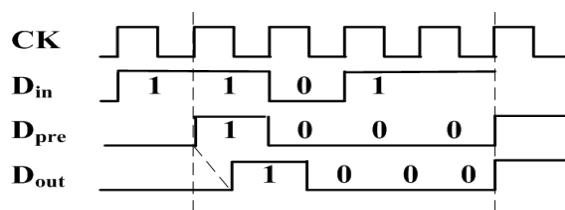


Fig 4. Data with encoding

This approach is able to identify whether Dout has been encoded or not as long as there is a half cycle delay between the Dout and CK. Although the phase difference can distinguish most of the data words of ETIpre, this method cannot be used for “0000” or “1111” because there is no transition inside the data word. The corresponding waveforms are shown in Fig. 5 for these two data words. The first bit of Dout in the “1000” and “0111” is aligned with CK and the duration of the bit is only half of the clock cycle.

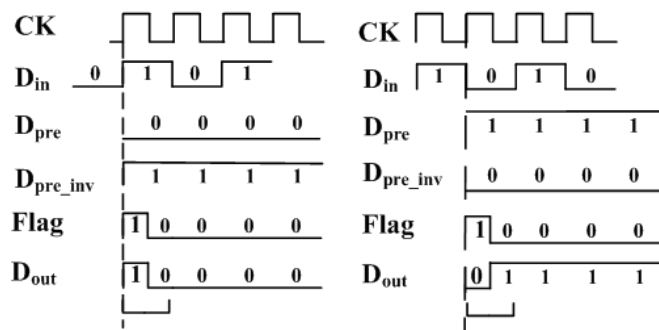


Fig 5. Waveform example for special data words

III. ETI ARCHITECTURE

A. ETI Encoder

The overall architecture of the ETI scheme is shown in Fig. 6. We add the ETIpre block and the TIC architecture for clarity. The ETIpre does not provide the decision bit information so it cannot be decoded in the receiver. The ETIpre encoder is shown by the dashed box in the ETI encoder in Fig. 6. The TIC counts the transitions in the data word then uses this information to perform encoding. The transition indication bit is added to every data word to indicate whether there is an inversion or not. The decoder adopts the transition indication bit to perform the decoding, as shown in Fig. 6. In the ETI encoder part, the input data Din are stored in the buffer to wait until the check transition operation is completed. The transition and threshold in a data word are used to set the decision bit. The decision bit is used to control the encoding process in the B2INV and the phase encoder block.

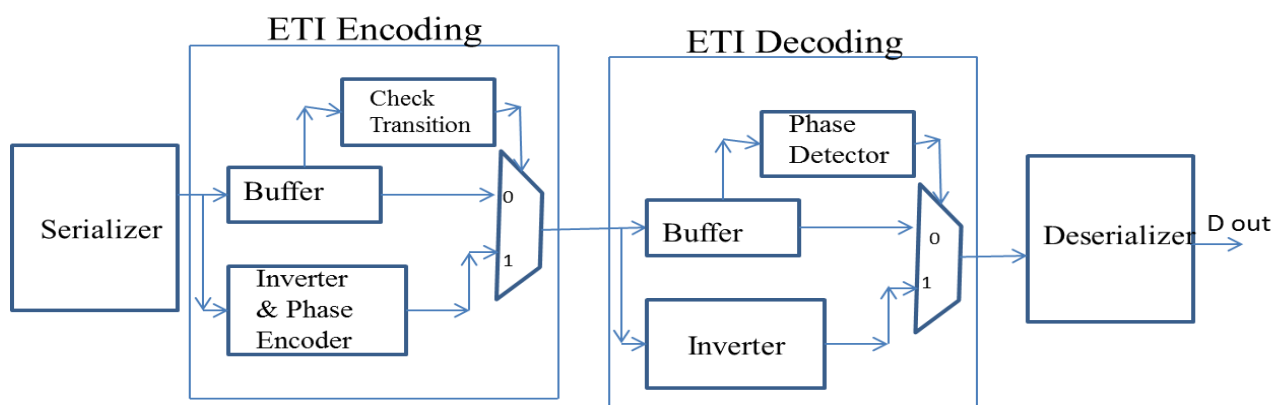


Fig 6. Architecture of the modified ETI scheme

The ETI encoder includes the check transitions block, buffer, B2INV, and phase encoder. The check transition block is shown in Fig. 7.

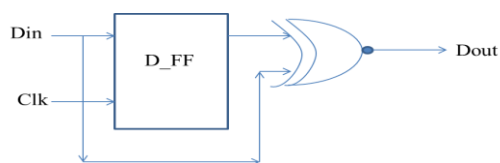


Fig 7. Check Transition Block

The check transition circuit is built by counting the transitions between consecutive bits in the bitstream. A transition between two bits is found in a simple manner by performing the equivalence operation of XOR (Exclusive OR) between them. The proposed circuit using a simple XOR gate between consecutive incoming bits of the bit stream. The WL indicator block counts the length of the data word and generates a high signal at the first bit of the data word. This signal is used to reset the adder and the D-flip-flop (D-FF). The D-FF stores the previous bit that is used to XOR with the current bit for transition checking. Before transmission, the number of transitions on a line is counted. This is just counting the transitions of the bitstream in that line. This can be done by a simple XOR gate between consecutive bits and counting the number of '1's. The adder block calculates the number of transition in a data word and sets the decision bit to high when the $N_t \geq N_{th}$. If the decision bit is set to 1 the input data becomes inverted.

Word length (WL) defines the number of bits in a data word and a threshold N_{th} defines half of WL. A transition is defined as a bit changing from zero to one or from one to zero. For example, the bit stream "0100" has two transitions while "0101" has three transitions. When the number of transitions N_t in a data word exceeds the threshold N_{th} , the bits in the data word should be encoded. Otherwise, the data word remains the same. When an encoding is needed in a data word, this method checks every two-bit in the data word. Every two bit in the serial stream is combined as a base to be encoded. In this case, the b_1b_2 is a base and the b_3b_4 is another base. The 2-bit in a base is denoted as b_1b_2 and the encoded output is denoted as be_1be_2 . When the N_t in a data word is less than N_{th} , b_1b_2 remains unchanged. Otherwise, we perform the inversion coding and the phase coding. For the inversion coding, the bit streams "01" and "10" are mapped to "00" and "11," respectively. The bit streams "00" and "11" are mapped to "01" and "10," respectively. For the phase coding, we embed the inversion information in the phase difference between the clock and the encoded data.

The inversion encoding operation can be expressed as

$$\begin{aligned}
 be_1 &= b_1 \\
 be_2 &= b_2, \quad \text{with } N_t < N_{th} \\
 &!\!b_2, \quad \text{with } N_t \geq N_{th} .
 \end{aligned}$$

The inversion decoding operation for the decoded output $bd_1 \ bd_2$ is

$$\begin{aligned}
 bd_1 &= be_1 \\
 bd_2 &= be_2, \quad \text{with } N_t < N_{th} \\
 &!\!be_2, \quad \text{with } N_t \geq N_{th} .
 \end{aligned}$$

The bit stream is encoded if a transition inversion is needed. This is done as the data is being put on the bus. This can be done in an on-the-fly manner since the encoder need to only process the current and next bit. The decision bit is used to control the encoding process in the B2INV and the phase encoder block. When the decision bit is set to zero, the B2INV passes the non inverted bit stream. Otherwise, the bit stream is encoded. This encoder needs to operate only for those cases where a transition inversion is needed. The D-FF on the incoming bit stream calculates the transition state just as the decision circuit did during the loading of the block. Once the transition state is known, it is inverted to generate an inverted state if the decision was to invert the transition. This inverted transition state is used to manipulate the next bit in such a way that the next bit will be in the inverted transition state in correspondence to the current bit. The inverter block is shown in the Fig. 8.

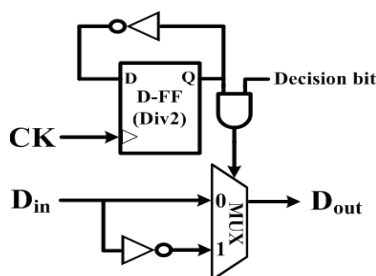


Fig 8. Bit Two Inverter

Within every data word duration, the phase difference between the data and the clock distinguishes these two data words. Same *Dout* “1000” in Fig. 9. is obtained from *Din* “1000” without inversion.

Dout “0100” in Fig. 9 is obtained from *Din* “1000” with inversion. A half clock cycle difference between *Dout* and *Clk*, indicating that *Din* has been encoded. The *Dout* and *Clk* are aligned in Fig. 9, indicating that *Din* has not changed. This approach is able to identify whether *Dout* has been encoded or not as long as there is a half cycle delay between the *Dout* and *Clk*. Although the phase difference can distinguish most of the data words of ETIpre.

This method cannot be used for “0000” or “1111” because there is no transition inside the data word. Under the inversion condition for these two data words, the “0000” and “1111” change to “1000” and “0111”. The first bit of *Dout* in the “1000” and “0111” is aligned with *Clk* and the duration of the bit is only half of the clock cycle.

The phase generator is used to generate phase difference between the encoded data (*Dpre*) and the clock (*Clk*) at each data word. Depending on the encoded data, there are three types of phase encoding: the one cycle delay, the half cycle delay and the special data word. The half cycle delay and the special data word are shown by the second and the third path Fig 9.

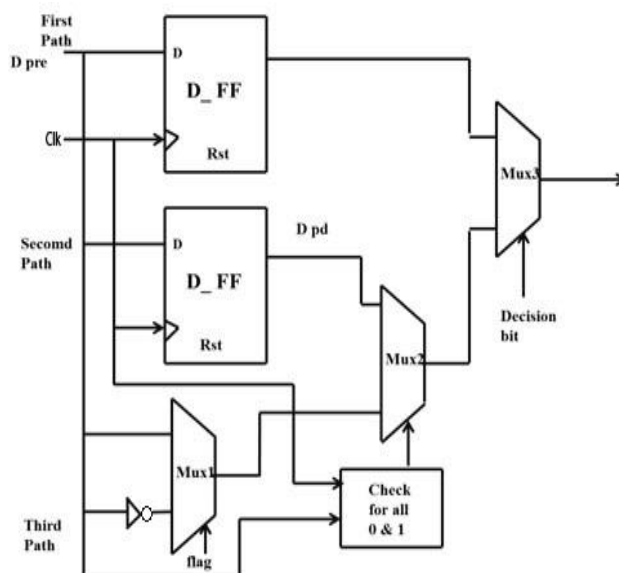


Fig 9. Phase Encoder

In the special data word, the predefined Flag signal is used to present the special data pattern. The “check all 0 and all 1” block is used to identify the special data word when the encoded data (*Dpre*) are “0000” or “1111.” If the encoded data are not the special data word, the second path is selected from the MUX1. Otherwise, the third path is selected. The decision bit then selects the data from the first path or the output of the MUX1.

B. ETI Decoder

The ETI encoder generates the phase difference between the clock and the data word. Normally, a PD identifies an early or delayed phase. A variety of PDs could detect the phase difference. This paper adopts the commonly used Hogge PD [18]. The Hogge PD architecture is shown in Fig. 10.

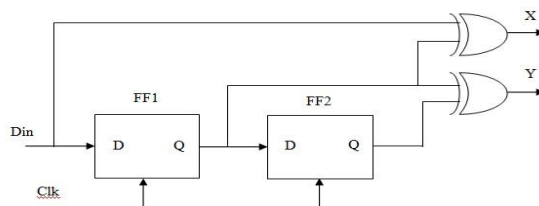


Fig 10. Hogge Phase Decoder

The PD is controlled by the clock CK and input data Din. When the clock CK and input data Din are valid, the PD is activated to identify the phase relation between the clock and the data. The PD can determine whether a data transition exists from the condition that the clock leads or lags the data.

The decision bit is used in the B2INV for the decoding. The decoding operator in the B2INV is the same as that in the encoder. Two D-FFs are added in the front of the B2INV block for buffering and alignment. A larger bandwidth is needed in the ETI coding scheme due to phase shift. The last bit has half the pulse width of the other bits so that the interconnect has twice the bandwidth. It means that the serial link needs to run at a much higher frequency. The higher clock frequency leads to problems, such as buffering, clock synchronization, and design complexity. The other way is to wait an extra bit to check the transition information but that would lower the overall bit rate. The disadvantage of this method is added in the revised paper. We send both data and clock from TX to RX in our proposed scheme. In our simulation, we assume the channel length of the clock and data links is equal and the phase skew between them is negligible.

IV. EXPERIMENTAL RESULT

The simulation result of the ETI scheme with Hogge phase detector is shown in the Fig 11. And the ETI scheme with Alexander PD and ETI scheme with Hogge PD comparison table is shown in Table 1.

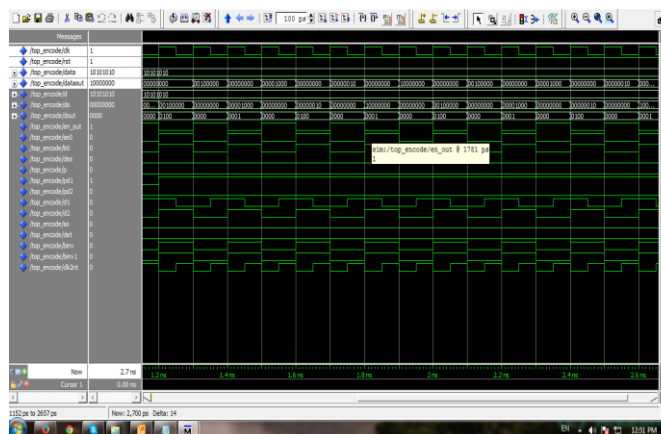


Fig 11. Simulation Result of the Proposed ETI Scheme

Spartan 3e Xc2s100e- 4tq144	AREA		DELAY(ns)	POWER(W)
	SLICE	LUT		
EXIT_ETI	37	59	9.061	0.654
PROPOSED_ETI	34	41	7.652	0.571

Table 1. Comparison of ETI Schemes

V. CONCLUSION

The ETI scheme is reduces the extra bit used in the TIC scheme and reduces the crosstalk, energy dissipation. ETI scheme uses the phase difference between the data and clock to indicate the bit inversion. In this paper the proposed ETI scheme is reduces the area and power compare with the existing ETI scheme.

REFERENCES

- [1] K. Lee, S. J. Lee, and H. J. Yoo, "SILENT: Serialized low energy transmission coding for on-chip interconnection networks," in *Proc. IEEE Int. Conf. Comput.-Aided Design Conf.*, Nov. 2004, pp. 448–451.
- [2] M. R. Stan and W. P. Burleson, "Bus-invert coding for low-power I/O," *IEEE Trans. Very Large Scale Integr. (VLSI) Syst.*, vol. 3, no. 1, pp. 49–58, Mar. 1995.
- [3] Y. Shin, S. I. Chae, and K. Choi, "Partial bus-invert coding for power optimization of application-specific systems," *IEEE Trans. Very Large Scale Integr. (VLSI) Syst.*, vol. 9, no. 2, pp. 377–383, Apr. 2001.
- [4] R. B. Lin and C. M. Tsai, "Weight-based bus-invert coding for lowpower applications," in *Proc. Int. Conf. VLSI Design*, Jan. 2002, pp. 121–125.

- [5] C. H. Kuo, W. B. Wu, Y. J. Wu, and J. H. Lin, "Serial low power bus coding for VLSI," in *Proc. IEEE Int. Conf. Commun., Circuits Syst.*, Jun. 2006, pp. 2449–2453.
- [6] S. Zogopoulos and W. Namgoong, "High-speed single-ended parallel link based on three-level differential encoding," *IEEE J. Solid-State Circuits*, vol. 44, no. 2, pp. 549–558, Feb. 2009.
- [7] S. R. Sridhara and N. R. Shanbhag, "Coding for reliable on-chip buses: A class of fundamental bounds and practical codes," *IEEE Trans. Comput.-Aided Design Integr. Circuits Syst.*, vol. 26, no. 5, pp. 977–983, May 2007.
- [8] P. T. Huang, W.-L. Fang, Y.-L. Wang, and W. Hwang, "Low power and reliable interconnection with self-corrected green coding scheme for network-on-chip," in *Proc. 2nd ACM/IEEE Int. Symp. Netw. Chip*, Apr. 2008, pp. 77–84.
- [9] R. Abinesh, R. Bharghava, and M. B. Srinivas, "Transition inversion based low power data coding scheme for synchronous serial communication," in *Proc. IEEE Comput. Soc. Annu. Symp. VLSI Conf.*, May 2009, pp. 103–108.
- [10] S. J. Lee, S. J. Song, K. Lee, J. H. Woo, S. E. Kim, B. G. Nam, and H. J. Yoo, "An 800 MHz star-connected on-chip network for application to systems on a chip," in *IEEE Int. Solid-State Circuits Conf. Technol. Dig.*, Feb. 2003, pp. 468–469.
- [11] K. Lee, S. J. Lee, and S. E. Kim, "A 51 mW 1.6 GHz on-chip network for low-power heterogeneous SoC platform," in *Proc. IEEE Int. Solid-State Circuits Conf.*, Feb. 2004, pp. 152–158.
- [12] K. Lee, S. J. Lee, and H. J. Yoo, "Low-power network-on-chip for highperformance SoC design," *IEEE Trans. Very Large Scale Integr. (VLSI) Syst.*, vol. 14, no. 2, pp. 148–160, Feb. 2006.
- [13] C.T. Chiu, W.C. Huang, C.H. Lin, W.C. Lai, and Y.F. Tsao, "Embedded Transition Inversion Coding With Low Switching Activity for Serial Links", *IEEE Trans. Very Large Scale Integration (Vlsi) Systems*, vol. 21, no. 10, Oct. 2013.
- [14]. R. Abinesh, R. Bharghava, and M. B. Srinivas, "Transition inversion based low power data coding scheme for synchronous serial communication," in *Proc. IEEE Comput. Soc. Annu. Symp. VLSI Journal.*, May 2009, pp. 103–108.
- [15]. Brajesh Kumar Kaushik n, Deepika Agarwal, Nagendra G. Babu "Bus encoder design for reduced crosstalk, power and area in coupled VLSI interconnects" *Microelectronics Journal*. Elsevire April 2013
- [16]. J. Bhasker "VHDL Primer", third edition.
- [17]. M. Ghoneima, Y. Ismail, M. Khellah, J. Tschanz, and V. De, "Serial-link bus: A low-power on-chip bus architecture," *IEEE Trans. Circuits Syst. I, Reg. Papers*, vol. 56, no. 9, pp. 2020–2032, Sep. 2009.

An Improved Software Reliability Growth Model

B. Anniprincy¹ & Dr. S. Sridhar²

¹Research Scholar, Sathyabama University, Chennai,

²Dean-Cognitive & Central Computing Facility, RV College of Engineering, Bangalore-560059

ABSTRACT

Software reliability is the possibility of the failure free operation of software in a given period of time under some certain conditions. Software testing can be defined as the process to detect the faults in whole and worth of developed computer software. Optimum amount of code also needs to be covered to make sure that the software is of good quality. Testing time alone may not give the correct picture of the number of faults removed in the software. Therefore to capture the combined effect of testing time and testing coverage we propose two dimensional software reliability growth models by using Cobb-Douglas production function by incorporating the effect of testing time and testing coverage on the number of faults removed in the software system. The proposed model is validated on real data sets.

KEYWORDS: Software Reliability, Two dimensional, Testing Coverage (TC), Cobb-Douglas Model, Imperfect Debugging, S-Shaped Model.

I. INTRODUCTION

The role of software is expanding rapidly in modern society. Hence, quality, reliability, and customer satisfaction become the main goals for software engineers and very important considerations for software development organizations. Testing is the major quality control used during software development [7]. The quality of the software system has many attributes such as maintainability, portability, usability, security, reliability, availability, etc. Software reliability is the most dynamic attribute which can measure and predict the operational quality of the product [3]. Software Reliability is defined as the probability of failure-free software operation for a specified period of time in a specified environment. The aim of software reliability engineers is to increase the probability that a designed program will work as intended in the hands of the customers [1]. Modeling of software reliability accurately and predicting its possible trends are essential for determining overall reliability of the software. It is easy to determine some important metrics like time period, number of remaining faults, mean time between failures (MTBF), and mean time to failure (MTTF) through SRGMs [6]. A software reliability growth model is known as one of the useful mathematical tool for quantitative assessment of software reliability. This mathematical model enables us to describe a software reliability growth process observed in the actual testing-phase by treating the software failure-occurrence or the software fault-detection phenomenon as random variables [5]. In the context of software testing, the key elements are the testing effort, and effectiveness of the test-cases. Many published models either assumes that the consumption rate of testing resources is constant, or do not explicitly consider neither the testing effort nor its effectiveness [1]. During software testing phase, much testing-effort is consumed itself. The consumed testing-effort indicates how the errors are detected effectively in the software and can be modified by different distributions [6]. Limitations of software reliability growth models that are applied to a safety-critical software system also need to be considered. One of the most serious limitations is the expected total number of inherent software faults calculated by the software reliability growth models that are highly sensitive to time-to-failure data [8]. However, there are several limitations when applying the software reliability growth models to safety-critical software. One of the most serious limitations is that the expected total number of inherent software faults calculated by the software reliability growth models is highly sensitive to the time-to-failure data [14].

II. REVIEWS OF SOFTWARE RELIABILITY GROWTH MODELS

A handful of researches have been presented in the literature for developing software reliability growth models in the presence of imperfect debugging and error generation. The objective of such studies is to improve software performance. These studies can be placed in one of the two categories. The first category emphasizes empirical analysis of data collected from software projects.

The second category deals with the developments of models for quantitative assessment of software performance. A brief review of some recent researches is presented here. Carina Andersson [7] presented a replication of a method for selecting software reliability growth models to decide whether to stop testing and release software. They have applied the selection method in an empirical study, conducted in a different development environment than the original study. Over the last several decades, more number of Software Reliability Growth Models (SRGM) have been developed to greatly facilitate engineers and managers in tracking and measuring the growth of reliability as software is being improved. However, some research work indicates that the delayed S-shaped model may not fit the software failure data well when the testing-effort spent on fault detection is not a constant. Chin-Yu Huang *et al.* [1] have first reviewed the logistic testing-effort function that can be used to describe the amount of testing-effort spent on software testing. They described how to incorporate the logistic testing-effort function into both exponential type, and S-shaped software reliability models. The proposed models are also discussed under both ideal, and imperfect debugging conditions. Results from applying the proposed models to two real data sets are discussed, and compared with other traditional SRGM to show that the proposed models can give better predictions, and that the logistic testing-effort function is suitable for incorporating directly into both exponential-type, and S-shaped software reliability models. V. B. Singh *et al.* [9] reviewed that how different software reliability growth models have been developed, where fault detection process was dependent not only on the number of residual fault content but also on the testing time, and saw how these models can be reinterpreted as the delayed fault detection model by using a delay effect factor. Based on the power function of the testing time concept, they proposed four new SRGMs that assumed the presence of two types of faults in the software: leading and dependent faults. Leading faults are those that can be removed upon a failure being observed. However, dependent faults were masked by leading faults and can only be removed after the corresponding leading fault had been removed with a debugging time lag. These models have been tested on real software error data to show its goodness of fit, predictive validity and applicability.

Han Seong Son *et al.* [8] proposed an application procedure of software RGM, which is used practically to quantify software reliability to NPP PSAs. Reliability goal setting and application ranging are essential steps of the procedure. Through the steps, a selected software reliability growth model can be efficiently validated in view of adequacy for the project before real application. Lev V. Utkin *et al.* [10] proposed a new framework which was explored for combining imprecise Bayesian methods with likelihood inference, and it is presented in the context of reliability growth models. The main idea of the framework is to divide a set of the model parameters of interest into two sub-sets related to fundamentally different aspects of the overall model, and to combine Walley's idea of imprecise Bayesian models related to one of the sub-sets of the model parameters with maximum likelihood estimation for the other subset. N. Ahmad *et al.* [4] proposed a material which compares the predictive capability of two popular software reliability growth models (SRGM), say exponential growth and inflection S-shaped growth models. They first reviewed the exponentiated Weibull (EW) testing-effort functions and discussed the exponential type and inflection S-shaped type SRGM with EW testing-effort. Then they analyzed the actual data applications and compared the predictive capability of those two SRGM graphically.

The findings reveal that inflection S-shaped type SRGM had better prediction capability as compared to exponential type SRGM. P. K. Kapur *et al.* [2] proposed two general frameworks for deriving several software reliability growth models based on a non homogeneous Poisson process (NHPP) in the presence of imperfect debugging and error generation. The proposed models are initially formulated for the case when there is no differentiation between failure observation and fault removal testing processes, and then extended for the case when there is a clear differentiation between failure observation and fault removal testing processes. S. M. K. Quadri *et al.* [6] proposed a method for constructing software reliability growth model based on Non-Homogeneous Poisson Process. In that method, they have considered the case where the time dependent behaviors of testing-effort expenditures are described by Generalized Exponential Distribution (GED). Software Reliability Growth Models (SRGM) based on the NHPP are developed which incorporates the (GED) testing-effort expenditure during the software-testing phase. It was assumed that the error detection rate to the amount of testing-effort spent during the testing phase is proportional to the current error content. Models parameters are estimated by the Least Square and the Maximum Likelihood estimation methods, and software measures are investigated through numerical experiments on real data from various software projects. R. Satya Prasad *et al.* [11] proposed that, software reliability may be used as a measure of the Software system's success in providing its function properly. Software process improvement helps in finishing with reliable software product. Software process improvement includes monitoring software development practices and actively seeking ways to increase value, reduce errors, increase productivity, and enhance the developer's environment.

III. INCORPORATING S-SHAPED FLEXIBLE MODEL AND COBB DOUGLAS PRODUCTION FUNCTION INTO SOFTWARE RELIABILITY GROWTH MODELS

In this paper we will develop a two-dimensional model which shows the united effect of testing time and testing coverage to remove the faults mendacious dormant in the software. We will assume that the number of faults detached in the software by a fixed time is dependent on the total testing resources accessible to the testing team. This testing resource will be a fusion of both testing time and testing coverage. We have used cobb-douglas production function to develop the two dimensional model incorporating the effect of testing time and testing coverage on the number of faults removed in the software system. The faults in the software may not be removed perfectly. When the faults are not removed perfectly and lead to further generation of faults. In this paper, we develop an s shaped model with imperfect debugging and fault generation. The proposed method is implemented using JAVA and it is validated on real data sets.

Time Dependent Model

The time dependent behavior of fault removal process is explained by a Software Reliability Growth Model (SRGM). Most of the software reliability models can be categorized under Non Homogeneous Poisson Process (NHPP) models. The assumption that governs these models is software failure occurs at random times during testing caused by faults lying dormant in software. And, for modeling the software fault detection phenomenon, counting process $\{N(t); t \geq 0\}$ is defined which represents the cumulative number of software faults detected by testing time t . The SRGM based on NHPP is formulated as:

$$\Pr\{N(t) = n\} = \frac{m(t)^n \cdot \exp(-m(t))}{n!} \quad (1)$$

Where

$$n = 0, 1, 2, 3, \dots$$

$m(t)$ is the mean value function of the counting process $N(t)$

Testing Coverage Based Modeling

The testing coverage based software reliability growth model can be formulated as follows:

$$\frac{dm(t)}{dt} = \frac{c'(t)}{1-c(t)} (N - m(t)) \quad (2)$$

Where,

$m(t)$ is the expected number of faults identified in the time interval $(0, t]$

$c(t)$ is the testing coverage as a function of time t .

N is the constant, representing the number of faults lying dormant in the software at the beginning of testing.

Here $c(t)$ defines the percentage of the coded statements that has been observed till time t . So, $1 - c(t)$ defines the percentage of the coded statements which has not yet been covered till time t . Then, the first order derivative of $c(t)$, denoted by $c'(t)$, represents the testing coverage rate.

Therefore, function $\frac{c'(t)}{1-c(t)}$ can be taken as a measure of the fault detection rate. In one dimensional SRGM with

testing coverage we need to define coverage function $c(t)$ although in a two dimensional modeling approach we need not define a coverage function and it can be estimated directly from the data.

S-Shaped Flexible Model

In 1992 Kapur and Garg developed an S-shaped model with assuming that when we remove the different faults in the software some additional faults in the software are removed without actually affecting the system. The revised Kapur garg model is derived by using a logistic rate as the detection rate to capture the effect of imperfect debugging and fault generation. This model was based on the assumption of Non-Homogeneous Poisson Process. The basic assumptions of the model are as follows:

- [1] Failure /fault removal phenomenon is modeled by NHPP.
- [2] Software is subject to failures during execution caused by faults remaining in the software.
- [3] Failure rate is equally affected by all the faults remaining in the software.
- [4] Fault detection / removal rate may change at any time moment.

The differential equation of the representing the rate of change of cumulative number of faults detected in time t is given as Eq. (3)

$$m'(t) = \frac{b}{1 - \beta \exp(-bt)} (N - m(t)) \tag{3}$$

The below Eq. (4) gives the mean value function of the number of faults detected in time t

$$m(\tau) = \frac{N(1 - \exp(-b\tau))}{1 + \beta \exp(-b\tau)} \tag{4}$$

Where,

- b is the rate at which a fault is detected/removed in the software.
- m is the mean number of faults detected/ Corrected corresponding to testing time t .
- β is the constant.
- x is the rate of error generation.
- p is the probability of imperfect debugging.

Cobb Douglas Production Function

The Cobb–Douglas functional form of production functions is broadly used to represent the relationship of an output to inputs. It was proposed by Knut Wicksell (1851–1926), and tested against statistical evidence by Charles Cobb and Paul Douglas in 1900–1928. The Cobb-Douglas function considered a simplified view of the economy in which production output is determined by the amount of labor involved and the amount of capital invested. Even if there are many factors affecting economic performance, still their model proved to be remarkably accurate.

The mathematical form of the production function is given as follows

$$Y = AL^\nu K^{1-\nu} \tag{5}$$

Where,

- Y is the total production per year.
- L is the labor input.
- K is the capital input.
- A is the total factor productivity.
- ν is the elasticity of labor which is constant and determined by available technology.

Cobb and Douglas made some assumptions which are stated as follows:

- [1] If either labor or capital vanishes, then so will production.
- [2] The marginal productivity of labor is proportional to the amount of production per unit of labor.
- [3] The marginal productivity of capital is proportional to the amount of production per unit of capital.

Cobb Douglas Model

Software Testing involves operation of a system or application under controlled conditions and evaluating the results. The controlled conditions should include both normal and abnormal conditions. Testing should intentionally attempt to make things go wrong to determine if things happen when they shouldn't or things don't happen when they should. It is oriented to detection. The testing team has many resources of testing to make sure that software hence formed is of quality. These include software testing man hours, CPU time, testing effort testing coverage etc.

$$\tau \cong s^\alpha u^{1-\alpha} \quad 0 \leq \alpha \leq 1 \tag{6}$$

Where,

τ is the testing resources

s is the testing time

u is the testing coverage

α is the Effect of testing time

Let $\{N(s, u), s \geq 0, u \geq 0\}$ be a two-dimensional stochastic process representing the cumulative number of software failures by time s and testing coverage u . A two-dimensional NHPP with a mean value function $m(s, u)$ is formulated as

$$\Pr(N(s, u) = n) = \frac{(m(s, u))^n}{n!} \exp(-m(s, u)), n = 0, 1, 2, \dots \tag{7}$$

$$m(s, u) = \int_0^s \int_0^u \lambda(\zeta, \xi) d\zeta d\xi \tag{8}$$

Two-Dimensional S-Shaped Model

In this proposed method, we develop a two dimension S-shaped model determining the combined effect of testing time and testing coverage. The differential equation of the representing the rate of change of cumulative number of faults detected with respect to the total testing resources is given as

$$m'(\tau) = \frac{b}{1 + \beta \exp(-b\tau)} (N - m(\tau)) \tag{9}$$

The mean value function of the number of faults detected with testing resources x using the initial condition $x(0) = 0$ is given as

$$m(\tau) = \frac{N(1 - \exp(-b\tau))}{1 + \beta \exp(-b\tau)} \tag{10}$$

Now we extend the testing resource of one dimensional S-shaped model to a two dimensional problem. Using the cobb-douglas production the corresponding mean value function is given as

$$m(\tau) = \frac{N(1 - \exp(-bs^\alpha u^{1-\alpha}))}{1 + \beta \exp(-bs^\alpha u^{1-\alpha})} \tag{11}$$

In the above two-dimensional mean value function, if $\alpha = 1$, then the above mean value function can be regarded as a traditional one dimensional time dependent SRGM and if $\alpha = 0$ it becomes a testing coverage dependent SRGM.

Two-Dimensional S-Shaped Model with Imperfect Debugging

Mostly, the debugging process in real life won't be much perfect. While during the fault removal process two possibilities can occur. It may happen that the fault, which was considered to be perfectly fixed, had been improperly repaired and resulted in same type of failure again. There is also a fine chance that some new faults might get introduced during the course of correcting. This situation is much dangerous than the former one, because in the first case the total fault content is not altered, whereas in latter, error generation resulted in

increased fault content. The effects of both type of imperfect debugging during testing phase are incorporated in our proposed model. The rate equation of flexible model with imperfect debugging and error generation can be written as follows

$$\frac{d}{dt}m(\tau) = \frac{bp}{1 + \beta \exp^{-b\tau}} [N + xm(\tau) - m(\tau)] \quad (12)$$

We use logistic function to incorporate the effect of imperfect debugging and error generation. By solving the above equation using initial condition $N(0) = 0$, we get

$$N(t) = \frac{N}{1-x} \left\{ 1 - \left(\frac{(1+\beta)}{1+\beta \exp^{-bp\tau}} \right)^{p(1-x)} \exp^{-bp(1-x)} \right\} \quad (13)$$

Reliability Evaluation

Software evaluation is a very significant phenomenon in quantitative software reliability assessment. The software reliability function signifies the probability that a software failure does not occur in time-interval $(t, t+x)$ ($t \geq 0, x \geq 0$) given that the testing team or the user operation has been going up to time t . In two dimensional SRGM, we can assess software reliability in an operation phase where we assume that the testing coverage is not expanded. We can derive the probability that the software failure does not occur in time-interval $[s_\pi, s_\pi + \omega]$ ($s_\pi > 0, \omega > 0$) that testing has been going up to s_π and the value of testing coverage has been attained up to u_π by testing termination time s_π as:

$$R(\omega / s_\pi, u_\pi) = \exp \left\{ - \left[m((s_\pi + \omega), u_\pi / k) - m(s_\pi, u_\pi / k) \right] \right\} \quad (14)$$

Where k indicates the set of parameter estimates of a two dimension SRGM

IV. CRITERIA FOR SRGM'S COMPARISON

Using the proposed imperfect-debugging model, we now show a real numerical illustration for software reliability measurement. Here, in order to validate the imperfect-debugging model, the AE and MSF are selected as the evaluation criteria.

The Accuracy of Estimate (AE) is defined as

$$AE = \left| \frac{M_a - a}{M_a} \right| \quad (15)$$

Where M_a is the actual cumulative number of is detected errors after the test, and a is the estimated number of initial errors. For practical purposes, M_a is obtained from software error tracking after software testing.

The mean of Squared Errors (Long-term predictions) is defined as

$$MSE = \frac{1}{k} \sum_{i=1}^k [m(t_i) - m_i]^2 \quad (16)$$

Where $m(t_i)$ is the expected number of errors at time t_i estimated by a model, and m_i is the observed number of errors at time t_i . MSE gives the qualitative comparison for long-term predictions. A smaller MSE indicates a minimum fitting error and better performance.

The proposed method is compared with Yamanda Rayleigh Model and Huang Logistic Model. The comparison values of the proposed method, and Yamanda Rayleigh model and Huang Logistic Model are given in the below table.

Table I. Comparative results of different SRGM

Model	a	r	AE(%)	MSE
Proposed Model	628.87	0.0824	69.97	83.29
Yamanda Rayleigh Model	565.35	0.0196	57.91	122.09
Huang Logistic Model	394.08	0.0427	10.06	118.59

V. CONCLUSION

In this paper we have developed a common approach in deriving more general models based on simple assumptions, constant with the basic software reliability growth modeling. The proposed models embed a broader hypothetical structure which accounts for interaction between different dimensions of software reliability metrics. Incorporating the dynamics of testing time of the software and the testing coverage has allowed us the model to be a two dimensional framework. The proposed models use the Cobb Douglas production function to capture the combined effect of testing time and testing coverage. The proposed models are validated on real data sets and analyses are done using goodness of fit criterion. We also conclude that the proposed SRGM has better performance as compare to the other SRGM and gives a reasonable predictive capability for the actual software failure data. Therefore, this model can be applied to a wide range of software.

REFERENCES

- [1] Chin-Yu Huang, Sy-Yen Kuo and Michael R. Lyu, "An Assessment of Testing-Effort Dependent Software Reliability Growth Models," IEEE Transactions on Reliability, Vol. 56, No. 2, pp. 198-211, Jun 2007.
- [2] P. K. Kapur, H. Pham, Sameer Anand and Kalpana Yadav, "A Unified Approach for Developing Software Reliability Growth Models in the Presence of Imperfect Debugging and Error Generation," IEEE Transactions on Reliability, Vol. 60, No. 1, pp. 331-340, Mar 2011.
- [3] Khurshid Ahmad Mir, "A Software Reliability Growth Model," Journal of Modern Mathematics and Statistics, Vol. 5, No. 1, pp. 13-16, 2011.
- [4] N. Ahmad, S. M. K Quadri and Razeef Mohd, "Comparison of Predictive Capability of Software Reliability Growth Models with Exponentiated Weibull Distribution," International Journal of Computer Applications, Vol. 15, No. 6, pp. 40-43, Feb 2011.
- [5] Shinji Inoue and Shigeru Yamada, "A Bivariate Software Reliability Model with Change-Point and Its Applications," American Journal of Operations Research, Vol. 1, No. 1, pp. 1-7, Mar 2011.
- [6] S. M. K. Quadri, N. Ahmad and Sheikh Umar Farooq, "Software Reliability Growth modeling with Generalized Exponential testing -effort and optimal Software Release policy," Global Journal of Computer Science and Technology, Vol. 11, No. 2, pp. 27-42, Feb 2011.
- [7] Carina Andersson, "A replicated empirical study of a selection method for software reliability growth models," Journal of Empirical Software Engineering, Vol. 12, No. 2, pp. 161-182, Apr 2007.
- [8] Han Seong Son, Hyun Gook Kang and Seung Cheol Chang, "Procedure for Application of Software Reliability Growth Models to NPP PSA," Journal of Nuclear Engineering and Technology, Vol. 41 No. 8, pp. 1065-1072, Oct 2009.
- [9] V. B. Singh1; Kalpana Yadav, Reecha Kapur and V. S. S. Yadavalli, "Considering the Fault Dependency Concept with Debugging Time Lag in Software Reliability Growth Modeling Using a Power Function of Testing Time," International Journal of Automation and Computing, Vol. 4, No. 4, pp. 359-368, Oct 2007.
- [10] Lev V. Utkin, Svetlana I. Zatenko and Frank P.A. Coolen, "Combining imprecise Bayesian and maximum likelihood estimation for reliability growth models," In Proc. of the Sixth International Symposium on Imprecise Probability: Theories and Applications, Durham, UK, 2009.
- [11] Dr. R. Satya Prasad, K. Ramchand H Rao and Dr. R.R.L. Kantha, "Software Reliability Measuring using Modified Maximum Likelihood Estimation and SPC," International Journal of Computer Applications, Vol. 21, No.7, pp. 1-5, May 2011.
- [12] Andy Ozment, "Software Security Growth Modeling: Examining Vulnerabilities with Reliability Growth Models," Journal of Advances in Information Security, Vol. 23, No. 2, pp. 25-36, 2006.
- [13] Martin Baumer, Patrick Seidler, Richard Torkar and Robert Feldt, "Predicting Fault Inflow in Highly Iterative Software Development Processes: An Industrial Evaluation," In Proc. of the 19th IEEE International Symposium on Software Reliability Engineering, Seattle, USA, 2008.
- [14] Man Cheol Kim, Seung Cheol Jang and Jae Joo Ha, "Possibilities And Limitations of Applying Software Reliability Growth Models To Safetycritical Software," Journal of Nuclear Engineering and Technology, Vol. 39, No. 2, pp. 145-148, Apr 2007.
- [15] Chin-Yu Huang, Jung-Hua Lo, Sy-Yen Kuo and Michael R. Lyu, "Software Reliability Modeling and Cost Estimation Incorporating Testing-Effort and Efficiency," In Proc. of the 10th International Symposium on Software Reliability Engineering, Boca Raton, FL, pp. 62-72, Nov 1999.
- [16] Swapna S. Gokhale, Michael R. Lyu, and Kishor S. Trivedi, "Incorporating Fault Debugging Activities Into Software Reliability Models: A Simulation Approach," IEEE Transactions on Reliability, Vol. 55, No. 2, pp. 281-292, Jun 2006.
- [17] Katerina Goseva-Popstojanova, and Kishor S. Trivedi, "Failure Correlation in Software Reliability Models," IEEE Transactions on Reliability, Vol. 49, No. 1, pp. 37-48, Mar 2000.
- [18] Swapna S. Gokhale, Michael R. Lyu and Kishor S. Trivedi, "Software Reliability Analysis Incorporating Fault Detection and Debugging Activities," In Proc. of the Ninth International Symposium on Software Reliability Engineering, Paderborn, Germany, pp. 202-211, Nov 1998.

Electronic Waste Status in Jharkhand Cities

¹Umesh Kumar, ²Dr D N Singh,

¹Electronics & Communication Engg, Dept of Science & Technology,
G W P Ranchi Tharpakhna, Ranchi 834001

²Jt Secretary, Dept of Science & Technology, SBTE, Patna

ABSTRACT:

The use of Electrical Electronic Equipments (EEE) in day to day life is increasing and changing with rapid and frequent changes in technology. Like any product these EEE have also their life and at end of life when they lose their credibility and usability turn to waste and are popularly known as Electronic Waste (e waste). These e wastes contain many toxic and hazardous constituents in it which are dangerous and harmful to health and environment. The e wastes are day by day increasing and are posing threats to the mankind by increasing the pollution. India being developing country with extreme poverty and has vast unskilled manpower ready for doing any work without knowing the hazards is more liable to risks of the e wastes. In India also we notice the various states representing the various levels of economic strata and affordability. The developed states are moving towards managing e wastes through regulations but the less developed states lacks on this front also. The study of the Jharkhand developed cities and relatively less developed cities has been carried out. The study reveals that the maximum volumes and weights of the e wastes are from the larger and bigger EEE products i.e. AC, Refrigerator, Washing Machine etc. The major eight products present in everyone's life have been considered in this study. The reuse and recycle takes place in formal and informal sectors. 95 % of recycling is done in informal sector which is performed and actuated in most toxic and hazardous environment. The extended producers responsibility (ERP) which requires the producer or propagators to take back e wastes for recycling or disposal as buy back with fees or without financial initiatives is day to day becoming fact and figure for strict requirement for proper tackling of e wastes. The lack of knowledge of the user that wastes of EEE also have reusable components can entitle them good return often lead to ignorance of consumers to hand back to the manufacturer and lack of market of reusable components among the manufacturers also leads to e waste in bulk though meaningful components can be extracted and reduction of waste volumes can be noticed. The main concerns are the following of western thinking of "one size fit all", eco label initiative or oligopoly approach of Indian Government and pollution control boards. The large scale imports with inappropriate technology and imports of junks in name of up gradation from developed countries lead to increased e waste. The employment generation, lack of job potential and poverty compels the user and workforce to drive themselves into these. The status of Jharkhand is also same as there is no specific state government initiative for tackling the e wastes. The production of e waste is in line of any other state in India. The scenario of this state is in confirmation to the states of affairs in the developing states category, if India has developed, developing and underdeveloped states. The worst sufferers are the common man and the poor users who inherit the junk in name of technological upgradation and making the life easier by automating the lifestyle.

KEYWORD: EEE, e waste, Environment, Technology, End-of-life, Disposal, Household, Discard, Pollution.

I. INTRODUCTION

The rapid growth & industrialization and desire of common man to lead a easy life leads to the boom in the rapidly growing electronics in particular and electrical and electronic equipments (EEE) and information technology industry is the fastest growing sector in particular. The information technology industry in India is equally prominent sector as witnessed in the global scenario. The influx of leading multinational brands and companies in the manufacturing sector of these EEE has reported as a result of changing policies and exchange of R&D facilities. The advancement in technology results in increase in updated EEE products and this leads to a situation of obsolesce of old products as they lose their usefulness and this leads to end of life rise and hence generation of Waste of Electrical & Electronic Equipments (WEEE) i.e. electronics waste (e waste).The popular EEE products include computers, laptops ,Printers, mobiles , electronic gadgets, televisions, VCRs, DVD, stereos, copiers, fax machines, lamps, audio equipment , electronic toys , electrical home appliances, electric equipments and batteries etc. The recent past has witnessed accelerated manifold growth of e waste. Various factors for rise of e waste includes the imports of used and obsolete EEE products in name of technology up gradation aimed to the third world countries who have vast potential of consumerisation or market from the developed countries. The e waste amounts to 2.7. to 3 % of the total waste whose handling itself is a complex phenomenon. The issue of e waste handling are concentrated at manufacturer, distributor or consumer levels. The initiative of the regulatory mechanism for such issues is being talked about and are at initial stage only. The consumer handling of e waste is itself a complex issue as the e wastes constitute hazardous elements also. The making use of products at various levels and through various techniques includes its recycling; reuse and sometimes mixing of components for making it usable are prevalent in India, though are rarely evident in the developed countries. The developed nations mostly follow use and throw policy. The dependence on the EEE is still a status symbol and its affordability is to the elite and economically affordable section of the society only. The economical betterment and affordability of citizens is creating larger markets for EEE. The gray market mostly for the computers where assembled computers market is evident, resale and reuse is prominently evident. The survey and research for estimation of e waste is only taken up by limited organizations and are in stray condition. This is the sole reason that we lack reliable data of e waste and e waste generation.

The Information Technology (IT) sector is the most promising sector which is generating employment. The outsourcing of software development and solutions are day by day outreaching the far flung areas. The needs and changes are faster and this results in increased demand of optimized and recent hardware and software. Hence this sector is another area which is responsible for the e waste generation. The availability of finance and increase in affordability as the EEE prices are lowering down the tendency of procurement of new TV sets, mobiles, house hold appliances, electronic toys and other EEE are increasing many fold. With increase in consumption pattern e waste generation is also resulting. Jharkhand state has many cities like Jamshedpur, Ranchi, Bokaro, Dhanbad which are at high peaks of economic activity at one end and other cities like Dumka, Daltongang, Hazribagh, Ramghar are at lesser peaks. The cities in the vicinity of developed cities and well connected metros are developing as potential centres of software and hardware development in the IT sector and have traditional consumers of EEE. The industrial giants, hubs in the cities and rising network of BPO throughout state are creating high end society are also responsible for growth of EEE consumers and networks. As rough estimate the state has more than 800 numbers of software industries/ developers and numerous hardware industries/organisations established and several (BPO's) companies with more than fifty thousand employees. State cities like Jamshedpur, Ranchi, Dhanbad and Bokaro have emerged as important destination and or hub for reuse recycling of EEE and as a result e-waste generator. The reuse and recycling centers available in the areas are in informal and unorganized sectors only. Instances of shifting the ewastes to nearby metro are also in sight. The informal and unorganized sectors involvement in the recycling sector is leading to pollution and hazardous environment and is causing health concerns to the workers and persons involved in it. The higher consumption and disposal rates of the consumers are responsible for increased growth of e waste. Immediate concerns for the health and pollution and strict measures for the pollution control and proper recycling and reuse technology and training to personals is the emergent need of the day. The work being reported here is based on the exploratory sample estimation of e waste generation in the state.

II. PRESENT E WASTE SCENARIO AND CONCERNS / TRENDS

As an estimate the e waste amount piled up in India is 800000 tones in India in 2012 as per Manufacturers Association of Information Technology Companies (MAIT) and GTZ study. The e-waste strategic Management Systems in the key developing and underdeveloped countries can be seen as a comparative way among sets of countries can be as depicted in the table 1. The table shows a comparative view of Prevailing overall Technology, E waste Management , Actors , Formal e waste collection, Disposal / dumping sites, techniques , uniqueness financial aspects and legal framework and its adherence in the India , China very fast developing country, south Africa example of third world nations and Switzerland sample of developed nation has been briefly outlined.

Table 1 Approach Details of India, Developing country China, Third World Country S Africa Developed Country Switzerland

Important aspect	India	China	South Africa	Switzerland
Technology	Mostly borrowed , few indigenous	Indigenous and borrowed	Borrowed	Developed , trans boarder migrated
Prevailing overall waste management system	Semi Organised in metropolitans but unorganized in other areas	Only organized in urban areas	Mostly unorganized	Organized , Swiss Association for the Information, Communication and Organizational Technologies (SWICO) system
E waste management	Partly specific through unorganized and informal	Non specific but Semi organized	Not specific	Not specific
Actors	Manufacturers, distributors, traders, importers, consumers, formal and informal recyclers and scrap dealers.	Manufacturers, distributors, traders, importers, consumers, recyclers, scrap dealers and disposers.	Distributors, traders, importers, consumers, recyclers, collectors, sorters and disposers.	Manufacturers, distributors, traders, importers, consumers, recyclers, licensed collectors and licensed dismelters and refiners.
Formal e waste collection centres	Mostly under Pollution control boards	EMPA, GTZ and EECZ	DESCO Electronic recyclers ND Universal recycling co.	SWICO and SENS (Swiss Foundation for Waste Management)
Disposal / dumping sites	Mostly in landfills	Municipal sites and mostly illegal sites	In Landfills	In Landfills
Disposal site technologies	No proper collection system	No legal methods	Permitted sites with technology	Systematic and meticulous process
Uniqueness	Reusable and secondary raw material segregation	Multiple conditioning and refining process	Unique processing and screening	Landfill capacity adherence
Financial Uniqueness	Lacking of defined system	Individuals are paid for the collected e waste	Payments are made by metal scrap dealers for the metals in the waste	Provision of Advanced Recycling Fees (ARF)
Legal framework and adherence alertness	100% prohibited in principle but no definite adherence	Legally imports prohibited	Stringent laws but loose in adherence	Strict tougher laws and adherence to norms

The e waste scenario as per various studies available till 2012 for all the states in India in terms of percentage of the total production of e waste (in India) can be viewed as mentioned in Table 2.

Table 2 Showing Details of State wise E Waste Contribution in India

Sl	States	WEEE in % in India	Sl	States	WEEE in % in India
1	Maharashtra	13.88121	19	Uttarakhand	1.123886
2	Tamil Nadu	9.235316	20	Himachal	1.092317
3	Andhra Pradesh	8.751912	21	Jammu & Kashmir	1.041916
4	Uttar Pradesh	7.108937	22	Goa	0.292682
5	West Bengal	6.888625	23	Tripura	0.259058
6	Delhi	6.662478	24	Chandigarh	0.246321
7	Karnataka	6.244472	25	Pondicherry	0.194619
8	Gujarat	6.159256	26	Meghalaya	0.144903
9	Madhya Pradesh	5.341829	27	Nagaland	0.099364
10	Punjab	4.765149	28	Arunachal Pradesh	0.090188
11	Rajasthan	4.332633	29	Andaman Nicobar	0.063138
12	Kerala	4.226421	30	Mizoram	0.054647
13	Haryana	3.086305	31	Manipur	0.05451
14	Bihar	2.092461	32	Sikkim	0.053483
15	Orissa	2.011792	33	Diu & Daman	0.02794
16	Assam	1.490594	34	Dadar & Nagar Haweli	0.019928
17	Chhattisgarh	1.472242	35	Lakshadweep	0.005067
18	Jharkhand	1.384383			

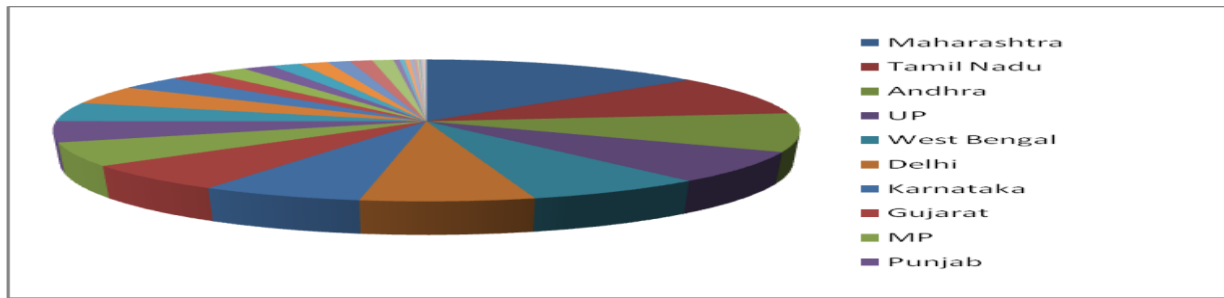


Figure Showing percentage representation of E waste generation in India state wise

III. JHARKHAND STATE CITIES STUDIES AND DATA OUTLINES

The following strategies were employed for data collection and studies:-

1. Questioner were developed and data's based on the questioner were received basically from the diversified socio economic groups across the sections for proper ascertaining practical sample data of the state so far practicable particularly from the following groups
 - a) Households,
 - b) Business organizations & institutions including offices
 - c) Manufacturers, Importers / exporters, EEE collectors, EEE second-hand shops, EEE repair shops, Recyclers / dismantlers, Processors of recyclable materials, Re-users, R&D units and similar institutions.
 2. Selective interview with the selected group were conducted to ascertain the facts and figures and principle of thoughts
 3. The purchasing pattern, recycling, reuse and disposal practices were collected i.e. ascertained
- Broadly main seven types of consumer commodity of EEE were considered for determination of pattern of e waste disposal. The seven EEE are Computers inclusive of monitors (LCD / CRT both types),Laptops, Mobiles , Refrigerators , Air conditioners (AC) , Batteries including the mobile batteries.

In all 300 sets of questioners in equal numbers i.e. 100 each to the mentioned three groups were sent through email, post and distributed manually.

Responses from the three categories of target groups are as follows mentioned in the table

In household category for the eight cities total of 800 questionnaires supplied 734 were received back. The responses mentioned in table 4 are mainly the response that reflects the mood of the consumers on individual basis. Business organizations & institutions including offices: Out of total 800 targets the 600 receipts reveals the mood of the bulk user and policymakers. The details of responses are in table 5. The Manufacturers, Importers / exporters responses are in conformity of the e waste generation as it was most likely that the e waste would be nil only as the EEE products are not put to use themselves and are extended to others only for conversion to e waste after extensive use and handling, recycling and reuse. The details are in table 6.

Table 3 Showing the Responses in the three Segments Identified and Planned

Household			Business organizations & institutions including offices			Manufacturers, Importers/exporters etc.		
City	Questionnaire sent	Questionnaire received	City	Questionnaire sent	Questionnaire received	City	Questionnaire sent	Questionnaire received
Jamshedpur	100	95	Jamshedpur	100	90	Jamshedpur	100	89
Ranchi	100	99	Ranchi	100	87	Ranchi	100	92
Dhanbad	100	94	Dhanbad	100	88	Dhanbad	100	94
Bokaro	100	96	Bokaro	100	78	Bokaro	100	89
Hazaribagh	100	95	Hazaribagh	100	67	Hazaribagh	100	81
Ramghar	100	93	Ramghar	100	56	Ramghar	100	78
Daltonganj	100	94	Daltonganj	100	73	Daltonganj	100	74
Dumka	100	86	Dumka	100	61	Dumka	100	86

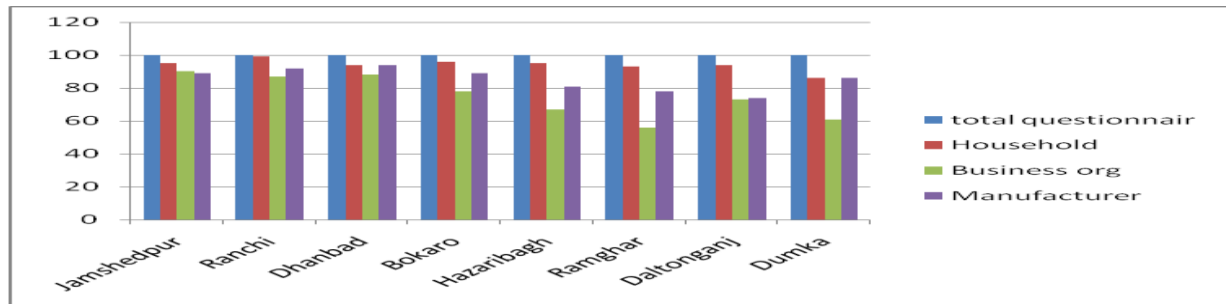


Figure depicting distributed and received questionnaire for individual three groups

IV. DETAILS OF SAMPLE SURVEYS

In Sample survey for household e wastes all together 800 questionnaires were sent and in all 752 were received i.e. 48 did not reply.

In case of business organizations and institutions the received number was 600 i.e. 200 chose not to reply.

In the manufacturers, importers / exporters etc category it was 683 indicates that 117 were non responsive.

Reusers / Recyclers/ Second hand market holders Questionnaires

In this category mainly four groups existed and they were

- Scrap metal collectors
- Second hand repair shops
- Formal pollution board listed/licensed vendors and
- Informal vendors active in this field.

Mostly the details were collected by the interview of such groups. The questionnaires were not responded and to collect data interview was only option left. The volumes and weight of the e wastes calculated in this study are as per the report of UNEP volume I published.

Details of collected data for the eight listed segments of the e waste are as mentioned in the tables listed here under.

Table4 Showing E waste generation from household

Components	Household sector e waste survey (Total received records 752 from all the 8 districts)								
	Large scale			Medium scale			Small scale		
	Used	Repaired/discarded	E waste	Used	Repaired/discarded	E waste	Used	Repaired / discarded	E waste
Computers with monitors	409	121	3533.2	131	26	75.92	12	3	8.72
Laptops	242	67	234.5	98	23	80.5	32	4	14
Printers	54	11	55	23	12	60	9	2	10
Mobile phones	1052	246	922.17	678	154	12.63	890	341	27.96
TV	1436	203	4060	1231	401	802.0	776	456	91.2
Refrigerator	259	37	1110	328	41	123	35	6	18
AC	498	53	1065	541	48	94.6	4	2	1.2
Washing machines	256	23	460	349	71	92	80	36	6.4
Total e waste	11439.87 kg/yr			1340.67 kg/yr			177.48 kg/yr		

The major e waste generated in this segment is in the TV field followed by computers although the mobile users was the second largest i.e. after TV. The e wastes figures from the Jamshedpur and Ranchi cities were largest compared to the cities of Ramghar showing the least one. His understandably so as the availability of the products and paying capacity of the members in the cities of Jamshedpur and Ranchi are higher compared to the other cities.

Table 5 showing E waste generation from Business organizations & institutions including offices

Components	Software sector e waste survey (Total received records 75 from all the 8 districts)								
	Large scale			Medium scale			Small scale		
	Used	Repaired / discarded	E waste	Used	Repaired / discarded	E waste	Used	Repaired / discarded	E waste
Computers with monitors	21265	2098	61802	987	112	3360	298	46	1343
Laptops	9826	965	3377.5	421	46	161	68	23	80.5
Printers	872	176	880	321	38	190	121	28	140
Mobile phones	748	89	7.3	173	56	4.59	114	41	3.36
TV	357	91	3276	162	16	756	75	4	144
Refrigerator	67	23	1108	46	18	540	41	23	690
AC	189	41	1640	56	32	1280	12	4	160
Washing machines	23	9	180	11	2	40	3	1	20
Total e waste	72271.8 kg/yr			6151.59 kg/yr			2580.86 kg/yr		

As the major business, official and educational organizations are situated in the Jamshedpur, Ranchi and Dhanbad cities the bulk users are in the computer and laptop segments. These sections show the major e waste generations also. The small cities like Ramghar and Dumka generated lower e waste in this segment.

Table 6 Showing E waste generation from Manufacturers, Importers/exporters etc.

Components	Software sector e waste survey (Total received records 75 from all the 8 districts)								
	Large scale			Medium scale			Small scale		
	Used	Repaired / discarded	E waste	Used	Repaired / discarded	E waste	Used	Repaired / discarded	E waste
Computers with monitors	8046	03	Returned	1208	6	Returned	1561	4	0
Laptops	3471	2	Returned	189	0	0	0	0	0
Printers	4847	7	Returned	231	0	0	0	0	0
Mobile phones	16123	8	Returned	431	2	Returned	0	0	0
TV	11347	7	Returned	2028	39	Returned	1091	81	0
Refrigerator	6711	4	Returned	0	0	0	0	0	0
AC	958	2	Returned	871	9	Returned	0	0	0
Washing machines	3218	3	Returned	592	7	Returned	682	43	0

The major manufacturer/importer/exporter units are located in Jamshedpur followed by Ranchi and Dhanbad. The connectivity of Jamshedpur and Dhanbad to Kolkata is easier and hence these cities were better having facilities of returning the damaged products. The company owned maintenance and service centres are mostly in Ranchi followed in Jamshedpur. The Dhanbad is well connected to Kolkata so the service providers are mostly attending from there only.

V. SEGMENT WISE RESULTS AND DISCUSSIONS

Household: Survey of total of 752 out of 800 houses to get a trend of generation of e waste was done. Here the number of family members count divided the large, medium and small section. The overall trend for these shows that the EEE are in properly maintained conditions. They often get repaired when they get defects. The authorized centres personals come for the repairing. The care and frequency are the sole causes of low generation of e waste. The outdated Computers , Laptops Printers , TV AC etc get exchanged in the market and often get their reflection as e waste in the next group where we dealt with the reusers and recyclers etc. The table shows the details of use and e waste generation. The e waste generation is from the products which came from the gray market. The items and products of the standard companies did not contribute much to the e waste. The Maximum of e waste generated in computer is because of the low life span and fast technology upgradation and tendency that the latest version of software are not supported by the

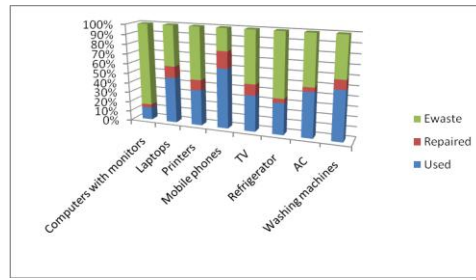


Figure showing Household E waste details

Old computers which offer low generation and lesser speed peripherals. The choice of lesser repairs is also reason for e-waste generation. In case of TV the changing pattern of consumers for changing technology is the basic cause of shifting of product to lower groups and ultimately resulting in the obsolescence i.e. e waste. The refrigerator is the other EEE product which often gets converted to e waste as the repairing cost is high and recovery of the items is easy and volumes of metallic part results in the major e waste by weight and volume. The second hand market is not that high.

Methods of disposal of EEE in the sample survey of 752 studies noticed is as mentioned herein :

Activity	Frequency	Percentage
Disposable EEE keep in house	111	14.76
Send to manufacturer	36	4.79
To Repair/ Recycle centre	99	13.16
Transfer to relative	54	7.18
Charity transfer	72	9.57
Waste bins	293	38.96
Others	87	11.57

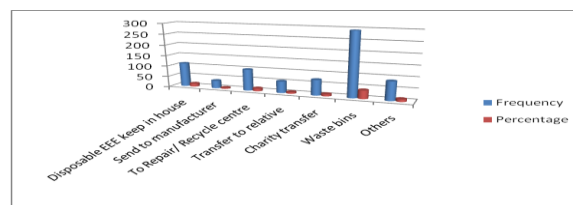


Figure showing Disposal Activity Freq. & Percentage

Business organizations & institutions including offices: The survey for the 800 sent information questionnaire out of which 600 were received details / information were gathered. The trends of e waste generation percentage and volume can be explained in different ways. The volume wise e waste generation is maximum in computers and printers followed by TV, AC, fridge, printer, washing machine and mobile. The e waste generation percentage wise is maximum in Refrigerator section followed by AC, TV, Washing machine, Computers, Printers, laptops and Mobile. The amount of e waste generated is understandably largest in the large scale sector and minimum in small sector.

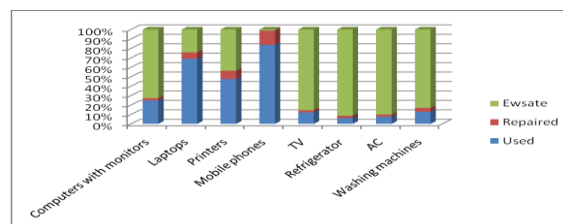


Figure showing e waste in Business etc organisations

E waste generation from Manufacturers, Importers/exporters etc: In this category we observe that since the products are not in use and only few in transportation get damaged and hence require repairs. The e waste produced is nonexistent in this case. The damaged items are returned back to the importers / exporters / manufacturers or assemblers. These parties make use of the new parts to other unit and hence the e waste is negligible. The branded parties and reputed assemblers of the area and region were only contacted hence the real story of the very small or cottage type industries scenario could not be studied.

VI. CHALLENGES, CONCERNS AND ECONOMICS OF E WASTES

The mammoth growth and arising concerns for the Electronics Waste in a sustainable and sound environmental technological development with updating processing advancements and growth of use and throw mindset is increasingly making e waste management task bit challenging one. The outburst of hazardous toxic constituents of the e wastes in the environment has proved that we have failed to strike balance between safety, cost and advancement of technology with proper environment protection for green world. We need to address the facts of reduction of e waste through recovery, reuse and recycle to minimize toxic substances in order to arrive at technology for such labour intensive and safe product development with enhanced participation of stakeholders in fixing responsibility of managing e waste in more sensible manner. The e waste gets recycled in formal and informal sectors. As per initial estimate 90-95 % of e-waste gets recycled in India in the informal sector which is performed and actuated in highly hazardous conditions. The e waste is one which simultaneously poses threat and opportunity at same time. It contains different hazardous and toxic elements responsible for even health problem, if not properly treated and managed. The positive aspect of e waste is that E-waste also offers employment and handsome returns and offers great opportunity to small manufacturers in formal and informal sectors by providing means of supply of many inputs, recovered through recycling and dismantling process, at a vary cheaper rates.

Remains and scraps of the end of life products are the main source of e waste, in other words one can say that products which suffers from the technological obsolescence and permanent damage conditions results in e waste. Separate designated location for storage of e waste becomes inevitable. The extended producers responsibility which entitles the manufacturers or its importers / agents to take back e wastes for disposal as buy back or otherwise arrangement is day by day becoming fact and figure for strict requirement. The lack of awareness of the contents and toxicity and hazardousness among the users sometimes becomes consumer's ignorance for the handing over of the product even in case of buy back offers. The lack of knowledge of the user that wastes of EEE also have reusable components can feed them good return often lead to ignorance of consumers to hand back to the manufacturer and lack of market of reusable components among the manufacturers also leads to e waste in bulk though meaningful components can be extracted and reduction of waste volumes can be noticed. The response of the lack of awareness among the users and manufactures were noticed in the responses received. The proper awareness about belongingness of e wastes among the handler group was divided i.e. they are not fully aware that to whom this belongs and so was the case among the consumers / user. The situation of regulations and strictness of adherence was also divided lot. The overall reaction is that the "it carries" is the situation among the different groups. The Indian business leaders are reluctant towards e waste handling and its proper management. The duty of user is to handle the e waste is feeling in majority of the business leaders. The main concerns are the following of western thinking of "one size fit all", eco label initiative or oligopoly approach of Indian Govt. and pollution control boards. The large scale imports with inappropriate technology and imports of junks in name of upgradation from developed countries lead to increased e waste. The monopoly and oligopoly lukewarm approach of dominant players in cases environmental regulations and weak loopholes in the regulatory mechanism and governmental initiative for creating proper awareness among users are the main concerns.

The employment generation, lack of job potential and poverty compels the user and workforce to drive themselves into these. The underdeveloped or least developed countries are since not having more sophisticated gadgets and EEE so the level of pollution is low and can afford cuts in the pollution levels for the developed nations. The environmental protection from pollution among the developed and under developed nation has given rise to economics in needed items and trade. The health and aesthetic reasons for environmental protection has become luxury of the developed nations. The reduction of pollution is increasingly becoming need of these nations as they are becoming experimental grounds of the developed nations.

VII. CONCLUSIONS

In the study regarding the e waste in the Jharkhand it came out that the situation is no different from the other states in India. There is lack of proper awareness among the users about the hazardousness and toxicity of the EEE products resulting in e wastes. There is lack of proper regulatory and awareness (propaganda) mechanism in the areas and requires that the manufacturers / agencies the governmental agencies who owe the responsibility to protect the consumers / users setup cells throughout in general and in each district in particular. The principle of polluter's pays and extended producer responsibility should be strictly implemented. The green technology and appropriate technology for information technology industries and similar organizations be implemented so that minimum e waste is generated. The reuse and recycle capacity and tendency must be applauded and increasingly adopted. The educational establishments, hospitals government establishments and common users must be encouraged to store and collect the e wastes separately and safely handled. The extended producer responsibility, take back or exchange or buy back initiatives must be encouraged in order to hand over the nearing end of life product to safe hand for proper e waste handling. The bulky items are more responsible for volume and weight wise e waste generation. The mobiles and small EEE products are more in numbers but volume-wise and weight-wise e waste produce are less. The bulkier AC, Washing Machines, Computers etc contribute volume-wise and weight-wise more in the e waste generation. The common man / consumer / user houses the e waste due to lack of awareness in their possession. Lack of awareness of toxicity and hazardousness of the constitutes of the e wastes puts the user in vernable condition and they suffer most. The awareness, binding regulations and strict confirmation to them by the three potential groups i.e. Household users, Business organizations and entities and the Manufacturers / importers / exporters / agencies responsible for EEE production / distribution and buy back and liable for extended producer responsibility is must for dealing the e wastes in effective manner. The adherence to regulations laws and awareness in handling e wastes will relive from further getting environment deterioration.

The study of the present case summarily reveals that following:-
Household e waste generation due to large scale is 11439.87 kg/year, for medium scale it is 1340.67 kg/year and for small scale it is 177.48 kg / year. Business organizations including offices generate e waste to the tune of 72271.8 kg/year, 6151.59 kg/year and 2580.86 kg/year for large scale, medium scale and small scale respectively. In case of Manufacturers , Importers / Exporters etc the e waste understandably is minimal i.e. almost non existable as the e waste chances are due to breakage during transportation etc only and there also chances of maximum utilization of components and constituents reuse is maximum.

The assemblers of the computers don't produce e wastes. They are mostly associated as dealer of the reputed companies for computers, laptops and printers.

REFERENCES

- [1.] E-waste Manual: Volume 1, compiled by UNEP (United Nations Environmental Programme) Study on E-waste recycling in Delhi Region, conducted in 2003-04 by IRGSSA in collaboration with Toxics Link and EMPA Swiss Federal Labs
- [2.] Johri Rajesh, "E-Waste: Implications, Regulations and Management in India and Current Global Best Practices", TERI Press, 2008
- [3.] The e-Waste Guide, a knowledge base for the sustainable recycling of e-waste at <http://www.ewaste.ch>
- [4.] US Environmental Protection Agency at <http://www.epa.gov>
- [5.] The Basel Action Network (BAN) at <http://www.ban.org>
- [6.] Recycling technologies, ewasteguide_info.mht, 2011.
- [7.] E. Roche, India's poor risk 'slow death' recycling 'e-waste' by (AFP) – Jul 5, 2010.
- [8.] Alan Finlay (2005), E-Waste Challenges In Developing Countries: South Africa Case Study, APC "Issue Papers" Series 2005: APC-200511-CIPP-IEN- PDF-0007, <http://www.apc.org>
- [9.] Donation of used Computers and Reduce E-Waste, e-nam (EWA Newsletter for Awareness & Management), Volume 1: Issue 3, January 2008, <http://www.ewa.co.in>
- [10.] e – Waste Management, website: <http://www.cqmsju.org>
- [11.] Central Pollution Control Board: Draft Guidelines for Environmentally Sound Management of Electronic Waste, Ministry of Environment & Forests, Government of India.
- [12.] WEEE Stakeholders, 2008, MoEF.
- [13.] Rolf Widmer, Heidi Oswald-Krapf, Deepali Sinha-Khetriwal, Max Schnellmann, Heinz Boni (2005), Global Perspectives on e-waste, Environmental Impact Assessment Review 25 (2005) 436-458, ELSEVIER.
- [14.] Guidelines for Environmentally Sound Management of E-waste by Central Pollution Control Board-2008.
- [15.] Implementation of E-waste Rules 2011" by Central Pollution Control Board.
- [16.] E-waste (Management and Handling) Rules, 2011-GOI, Ministry of Environment and forest.
- [17.] Umesh Kr, D N Singh papers in 2013 from various international journals on e waste.
- [18.] Various internet web based papers on e waste.
- [19.] Various e waste reviews and statistics on web sites on internets.
- [20.] Topics on e wastes in newspapers and scientific magazines.

Introducing Parallelism in Privacy Preserving Data Mining Algorithms

¹ Mrs.P.Cynthia Selvi, ² Dr.A.R.Mohamed Shanavas

¹Associate Professor, Dept. of Comp. Sci.

K.N.Govt.Arts College for Women, Thanjavur, Tamilnadu, India

²Associate Professor, Dept. of Comp. Sci.

Jamal Mohamed College Trichirapalli, Tamilnadu, India

ABSTRACT

The development of parallel and distributed data mining algorithms in various functionalities have been motivated by the huge size and wide distribution of the databases and also by the computational complexity of the data mining methods. Such algorithms make partitions of the huge database that is being used into segments that are processed in parallel. The results obtained from the processed segments of database are then merged; This reduces the computational complexity and improves the speed. This article aims at introducing parallelism in data sanitization technique in order to improve the performance and throughput.

KEYWORDS: Cover, Parallelism, Privacy Preserving Data Mining, Restrictive Patterns, Sanitization, Sensitive Transactions, Transaction-based Maxcover Algorithm.

I. INTRODUCTION

Data mining is an emerging technology that enable the discovery of interesting patterns from large collections of data. As the amount of data being collected continues to increase very rapidly, scalable algorithms for data mining becomes essential; Moreover, it is a challenging task for data mining approaches to handle large amount of data effectively and efficiently. Scaling up the data mining algorithms to be run in high-performance parallel and distributed computing environments offers an alternative solution for effective data mining. Parallelization is a process that consist of breaking up a large single process into multiple smaller tasks which can run in parallel and the results of those tasks are combined to obtain an overall improvement in performance. With a lot of information accessible in electronic forms and available on the web, and with increasingly powerful data mining tools being developed and put into use, there are increasing concerns that data mining pose a threat to privacy and data security. This motivated the area of Privacy Preserving Data Mining(PPDM) and its main objective is to develop algorithms to transform the original data to protect the private data and knowledge without much utility loss. There are many approaches for preserving privacy in data mining; to name a few are perturbation, encryption, swapping, distortion, blocking, sanitization. The task of transforming the source database into a new database that hides some sensitive knowledge is called sanitization process[1].This article introduce the concept of parallelism in PPDM algorithms. Section-2 narrates the previous work on PPDM. Section-3 introduces the basic terminologies and the proposed algorithm is presented in section-4. Section-5 gives implementation details and the observed results.

II. LITERATURE SURVEY

The idea behind data sanitization was introduced in [2], which considered the problem of modifying a given database so that the support of a given set of sensitive rules decreases below the minimum support value. The authors focused on the theoretical approach and showed that the optimal sanitization is an NP-hard problem. In [3], the authors investigated confidentiality issues of a broad category of association rules and proposed some algorithms to preserve privacy of such rules above a given privacy threshold.In the same direction, Saygin[4] introduced some algorithms to obscure a given set of sensitive rules by replacing known values with unknowns, while minimizing the side-effects on non-sensitive rules. Like the algorithms proposed in [3], these algorithms are CPU-sensitive and require various scans depending on the no. of association rules to be hidden. In [5,6], heuristic-based sanitization algorithms have been proposed. All these algorithms concentrated on data hiding principle to be implemented on the source database as a whole and parallelism is not dealt with. Hence this work makes an attempt to introduce parallelism in Transaction-based Maxcover Algorithm(TMA) proposed in [6] and improved performance is obtained from the observed results.

III. BASIC CONCEPTS OF PPDM ALGORITHM

Transactional Database : A transactional database consists of a file where each record represents a transaction that typically includes a unique identity number (*trans_id*) and a list of items that make up the transaction. Let D be a source database which is a transactional database containing a set of transactions T , where each transaction t contain an itemset $X \in D$. Also, every $X \subseteq I$ has an associated set of transactions $T \subseteq D$, where $X \subseteq t$ and $t \in T$.

Association Rule : It is an expression of the form $X \Rightarrow Y$, where X and Y contain one or more itemsets (categorical values) without common elements ($X \cap Y = \phi$).

Frequent Pattern : An itemset or pattern that forms an association rule is said to be frequent if it satisfies a prespecified minimum support threshold (*min_sup*).

Restrictive Patterns : Let P be a set of significant patterns that can be mined from transactional source database D , and R_H be a set of rules to be hidden according to some privacy policies. A set of all patterns rp_i denoted by R_P is said to be *restrictive*, if $R_P \subset P$ and if and only if R_P would derive the set R_H . $\sim R_P$ is the set of *non-restrictive patterns* such that $\sim R_P \cup R_P = P$ [4].

Sensitive Transactions : A set of transactions is said to be *sensitive*, denoted by S_T , if every $t \in S_T$ contain atleast one restrictive pattern rp_i . ie $S_T = \{ t \in T / \exists rp_i \in R_P, rp_i \subseteq t \}$.

Cover : The *Cover*[5] of an item A_k can be defined as,

$$C_{A_k} = \{ rp_i / A_k \in rp_i \subset R_P, 1 \leq i \leq |R_P| \}$$

i.e., set of all restrictive patterns which contain A_k . The item that is included in a maximum number of rp_i 's is the one with *maximal cover* or *maxCover*;

i.e., $maxCover = \max(|C_{A_1}|, |C_{A_2}|, \dots, |C_{A_n}|)$ such that $A_k \in rp_i \subset R_P$.

Principle of Transaction-based Maxcover Algorithm(TMA) [6]: Initially, identify the transaction-list of each $rp_i \subset R_P$. Starting with rp_i having larger *supCount*, for every transaction t in *t-list*(rp_i), find the *cover*(A_k) within t such that $A_k \in rp_i \subset t$. Delete item A_k with *maxCover* in t , and decrease the *supCount* of all rp_i 's which are included in t . Also mark this t as *victim transaction* in the *t-list* of the corresponding rp_i 's. Repeat this process until the *supCount* of all rp_i 's are reduced to 0.

IV. ALGORITHM

The sanitization task is distributed among the Server (a server is an entity that has some resource that can be shared) and the Clients (a client is simply any other entity which wants to gain access to a particular server) and the task is implemented as two modules namely Server Module and Client Module.

Procedure(Server module):

Input : Source transactional database(D)

Output : Sanitized database(D')

Start;

Get Source Database(D);

Get N; //N- no. of data segments;

Horizontally partition the D into N segments;

Initialize Lookup Tables;

Allocate the segment to client; // one each

Merge the sanitized segments received from N clients;

Display Sanitized Database(D');

End

Procedure(Client module):

Start;

Get data segment from Server;

Access the Lookup Tables;

Run TMA algorithm to sanitize the data segment;

Return Sanitized segment to Server;

Stop.

V. IMPLEMENTATION

The proposed algorithm was tested on real databases *RETAIL* & *T1014D100K*[7] with samples of transactions between 1000 and 10000. The restrictive patterns were chosen in a random manner with their support ranging between 0.6 and 5, confidence between 32.5 and 85.7 and length between 2 and 6. The test run was made on AMD Turion II N550 Dual core processor with 2.6 GHz speed and 2GB RAM operating on 32 bit OS; The implementation of the proposed algorithm was done with windows 7 - Netbeans 6.9.1 - SQL 2005. The coding part is done with JDK 1.7; because Java’s clean and type-safe object-oriented programming model together with its support for parallel and distributed computing make it an attractive environment for writing reliable and parallel programs. The characteristics of Source and Sanitized databases are given in table-I & II respectively; the improved performance in terms of execution time is shown in Table-III & IV and the graphs.

Table-I. Characteristics of source databases

Database Name	No. of Transactions	No. of Distinct Items	Min. Length	Max. Length	Min. no. of Sensitive Transactions	Max. no. of Sensitive Transactions	Database Size (MB)
Retail	1K – 10K	3176 – 8126	1	58	22	2706	90.2KB–928 KB
<i>T1014D100K</i>	1K – 10K	795 - 862	1	26	7	78	94.8KB–786 KB

Table-II. Characteristics of sanitized databases

Database Name	No. of Transactions	No. of Distinct Items	Min. Length	Max. Length	Database Size(MB)
Retail	1K – 10K	3176 – 8126	1	58	90.0KB – 916KB
<i>T1014D100K</i>	1K – 10K	795 - 862	1	26	94.0KB – 778KB

5.1. Results

Table-III. Results on the database *Retail*

Size (No. of Transactions)	Execution Time (in seconds)			Merge Time (in seconds)	Turnaround Time(TT) in seconds TT=Max(Execution Time of Clients) + Merge Time
	Without Parallelism	With Parallelism			
	Server	Client-1	Client-2		
1000	50.90	0.297	0.218	0.009	0.306
5000	151.39	11.138	10.701	0.016	11.154
10000	110.03	23.08	20.65	0.02	23.10

Table-IV. Results on the database *T1014D100K*

Size (No. of Transactions)	Execution Time(seconds)			Merge Time (seconds)	Turnaround Time(TT) in seconds TT=Max(Execution Time of Clients) + Merge Time
	Without Parallelism	With Parallelism			
	Server	Client-1	Client-2		
1000	8.80	0.015	0.018	0.015	0.033
5000	19.42	2.50	0.031	0.016	2.516
10000	29.00	1.747	0.973	0.031	1.778

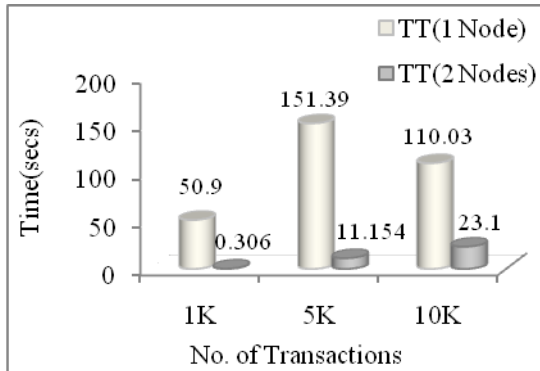


Fig.1. Execution time(Retail Database)

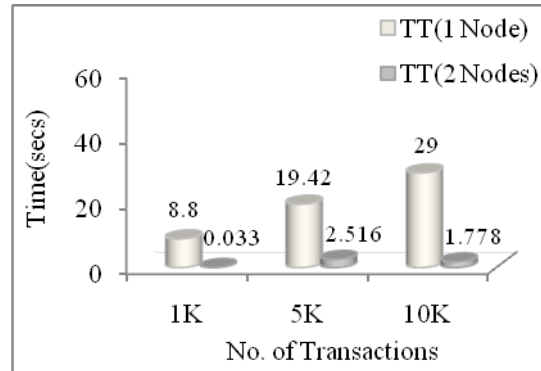


Fig.2. Execution time(T10I4D100K)

VI. CONCLUSION

The main objective of this study is to improve the performance of the Privacy Preserving Data Mining Algorithm, TMA which was proposed and proved its performance in the earlier work[6]. In this article we implemented a parallel processing on TMA and we have observed very good improvement in the processing speed. Hence this empirical study showed that improved performance can be achieved but performance would degrade as the number of processors increased.

REFERENCES

- [1] A.Evfimievski, R.Srikant, R.Agarwal, Gehrke. Privacy Preserving mining of association rules. Proceedings of 8th ACM SIGKDD international conference on Knowledge discovery and data mining, Alberta, Canada. p.217-28. 2002.
- [2] M.Atallah, E.Bertino, A.Elamagarmid, M.Ibrahim and V.Verykios. Disclosure Limitation of Sensitive Rules. In Proc. of IEEE knowledge and Data Engg.workshop. p.45-52. Chicogo, Illinois. Nov.1999.
- [3] E.Dessani, V.S.Verykios, A.K.Elamagarmid and E.Bertino. Hiding association rules by using confidence and support. In 4th information hiding workshop. p.369-383. Pitsburg, PA. Apr 2001.
- [4] Y.Saygin, V.S.Verikios and C.Clifton. Using unknowns to Prevent Discovery of Association Rules. SIGMOD Record. 30(4):45-54. Dec.2001.
- [5] P.Cynthia Selvi, A.R.Mohamed Shanavas. An Improved Item-based Maxcover Algorithm to Protect Sensitive Patterns in Large Databases. IOSR-Journal on Computer Engineering. Volume 14, Issue 4 (Sep-Oct, 2013). PP 01-05. DOI. 10.9790/0661-1440105.
- [6] P.Cynthia Selvi, A.R.Mohamed Shanavas. Towards Information Privacy using Transaction-based Maxcover Algorithm. Presented on International Conference on Data Mining and SoftComputing Techniques. SASTRA University, India. 25th & 26th Oct'2013.
- [7] The Dataset used in this work for experimental analysis was generated using the generator from IBM Almaden Quest research group and is publicly available from <http://fimi.ua.ac.be/data/>

Comparative Aspects of Single & Multiple PV Arrays Connected With UPQC

Payal Deshpande, Amit Shrivastava,

Department Of Electrical & Electronics Engineering, PG Scholar, Oriental College Of Technology, Bhopal,
Department of Electrical & Electronics Engineering, Professor, Oriental College of Technology, Bhopal
Corresponding Author; Payal Deshpande, Oriental College Of Technology, Bhopal, INDIA

ABSTRACT

This paper deals with the comparative aspect if single and multiple PV Arrays connected with UPQC. Dynamic model of the UPQC is developed in the MATLAB/SIMULINK environment and the simulation results demonstrating the power quality improvement in the system are presented.

INDEX TERMS: Photovoltaic Arrays (PV Arrays), UPQC, Energy Storage Devices.

I. INTRODUCTION

One of the comparative structures of the electric power is back to back converter. In respect to controlling structure, these converters may have various operations in compensation. For example, they can operate as series or shunt active filters for compensating the load current harmonics and voltage oscillation [1]. This is called Unified Power Quality Conditioner (UPQC) [2]. UPQC is greatly studied by researchers [3-5] as a basic device to control the power quality. The duty of UPQC is to reduce perturbations which affect the operation of sensitive loads. UPQC is able to compensate voltage using shunt and series inverters. In spite of this issue, UPQC is not able to compensate voltage interruption and active power injection to grid, because in its DC link, there is no energy source. The attention to Distributed Generating (DG) sources is increasing day by day. The reason is their important roll they likely play in the future of power system [6-8]. Recently, several studies are accomplished in the field of connecting DGs to grid using power electronic converters. Here, grid's interface shunt inverters are considered more where the reason is low sensitive of DGs to grids parameters and DG power transferring facility using this approach. Although DG needs more controls to reduce the problems like grid power quality and reliability, Photovoltaic array (PV) energy is one of the distributed generation sources which provides a part of human required energy nowadays and will provide in the future. The greatest shares of applying this kind of energy in the future will be its usage in interconnect systems.

Nowadays, European countries have shown inter – connected systems development in their countries by choosing supporting policies. In this study, UPQC and PV combined system has been presented. UPQC introduced by Chen et al., [9], it has the ability to compensate voltage sag voltage swell, harmonics and reactive power. A structure has been proposed in [10, 12-15], as shown in Figure 1, where DG sources are connected to a DC link in the UPQC as an energy source.

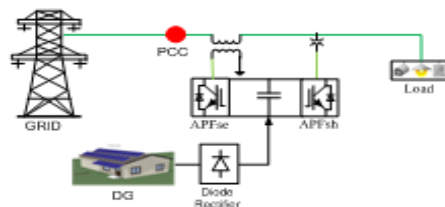


Fig.1.UPQC with DG connected to the DC link

This configuration works both in interconnected and islanded mode (shown in Figure 3.1; 3.2). In Interconnected mode, DG provides power to the source and loads whereas in islanded mode DG (within its power rating) supplies the power to the load only. In Addition, UPQC has the ability to inject power using DG to sensitive loads during source voltage interruption. The advantage of this system is voltage interruption compensation and active power injection to the grid in addition to the other normal UPQC abilities. The system's functionality may be compromised if the DG resources are not sufficient during the voltage

interruption conditions. Economical operation of the system can also be achieved by proper controlling of the active power transfer between the supply and DG source through a series APF [16-19].

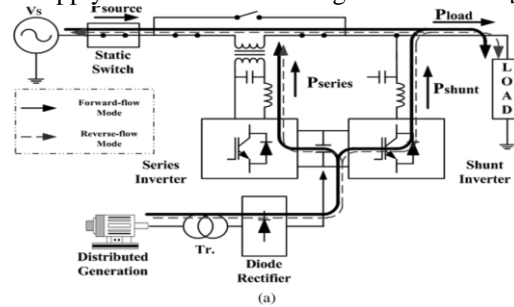


Fig.3 (DG-UPQC) DC- linked System operation concept. (a) Interconnected mode.

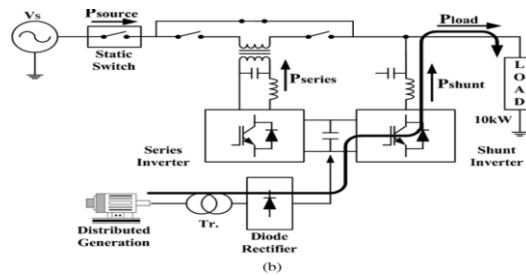


Fig.4. (DG-UPQC) DC- linked System operation concept. (b) Islanding mode

Major advantages of the photovoltaic power are as follows:

- Short lead time to design, install, and start up a new plant.
- Highly modular, hence, the plant economy is not a strong function of size.
- Power output matches very well with peak load demands.
- Static structure, no moving parts, hence, no noise.
- High power capability per unit of weight.
- Longer life with little maintenance because of no moving parts.
- Highly mobile and portable because of light weight.

II. INTRODUCTION TO UPQC WITH PV ARRAYS

Although DG needs more controls to reduce the problems like grid power quality and reliability, PV energy is one of the distributed generation sources which provides a part of human required energy nowadays and will provide in the future. The greatest share of applying this kind of energy in the future will be its usage in interconnected systems. Nowadays, European countries, has caused interconnected systems development in their countries by choosing supporting policies. Hence, UPQC and PV combined system has been presented. UPQC introduced in has the ability to compensate voltage interruption along with voltage sag and swell, harmonics and reactive power [20 -22]. Here, PV energy conversion system has high efficiency, low cost and high functionality. In the following figure, converter 1 (PV converter) is responsible to convert the PV energy to the grid as well as to compensate current harmonics and reactive power. The converter 2 (DVR Converter) is responsible to compensate voltage harmonics or voltage sags. Thus, the utilization of two controlled converters makes the system to have the most structure applied as energy conditioner[23].

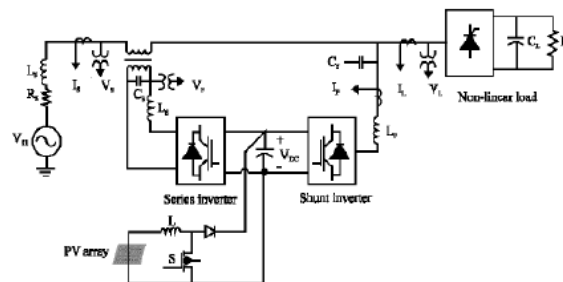


Fig.4. UPQC connected with PV arrays.

III. A.UPQC WITH SINGLE PV ARRAY

In this paper the role of Unified power quality conditioner is the power quality improvement of Distributed networks (PV Arrays). Here, UPQC is integrated with single PV Array and then with multiple PV Arrays. The comparative aspect of UPQC with single and multiple PV Array is studied with the help of MATLAB SIMULINK models. Figures shown in Fig.5 and Fig.6 represent the circuit models of both UPQC with single and multiple PV Arrays respectively and battery is taken as the energy storage device. In the figure shown single PV array is connected with UPQC. The DC output required by the UPQC is obtained from the PV Array. Since this DC voltage generated by a photovoltaic array varies and is low in magnitude, a step-up DC-DC converter is essential to generate a regulated higher DC voltage. The DC-DC converter is responsible for absorbing power from the photovoltaic array, and therefore should be designed to match photovoltaic array ripple current specifications and should not conduct any negative current into the photovoltaic array. Following figure shows the internal model of the PV Array.

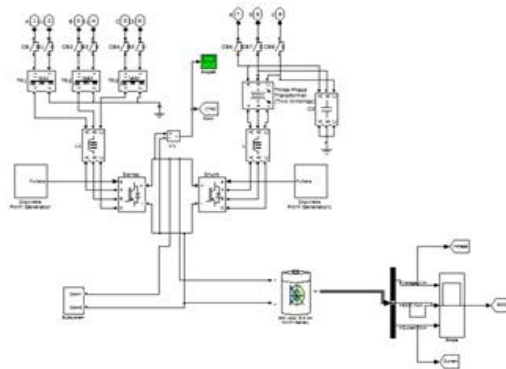


Fig.5. UPQC with single PV Array

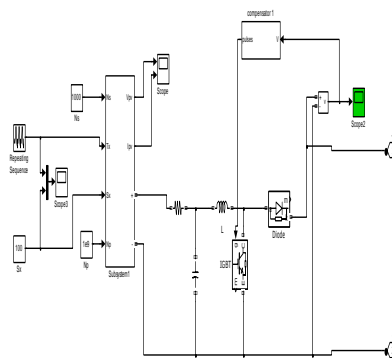


Fig.6. Internal of PV Array

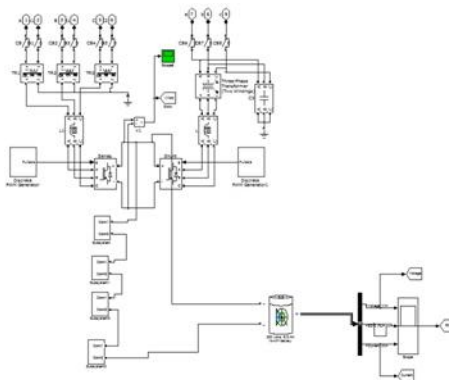


Fig.7. UPQC with multiple PV Arrays

IV. B.UPQC WITH MULTIPLE PV ARRAYS

The multiple input single output (MISO) DC-DC converters is useful for combining several distributed generation sources whose power capacity and/or voltage levels are different to obtain well-regulated higher output voltage [24]. The converter topology used for the combination of DC output of photovoltaic array units is shown in Fig. 8. In the control system of MISO DC-DC converter, the output voltage of converter has been compared with a reference value and the error signal is applied to PI-controller. The output signal of this controller is the one input of PWM switching for adjusting the duty cycle. Here, as an example a Triple-Input Single-Output (TISO) DC-DC converter has been designed and studied.

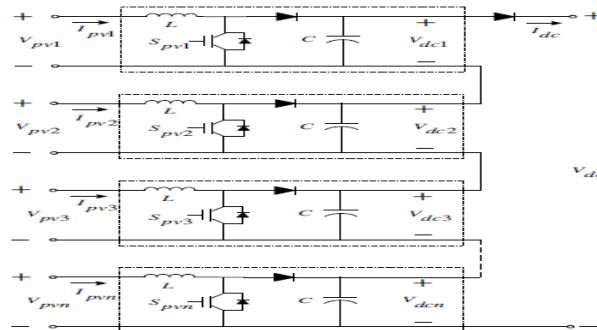


Fig.8. TISO DC - DC Converter

5.2 Control Scheme of the Proposed System

Instantaneous power theory is used to control of the proposed system. This scheme includes Photovoltaic (PV) energy resource to deliver PV power to loads and maintaining DC link voltage as well as other condition tasks. The theory is based on converting three axis parameters into two axes by defining well-known transfer matrix. The active and reactive instantaneous power can be decomposed by DC component and AC harmonic components, which consist of negative sequence component and harmonic component. Following sections provide the shunt and series inverter control strategies.

If shunt inverter is used simultaneously for reactive, negative and harmonic component compensation, the α - β axis current reference is given by the following equation

$$\begin{bmatrix} i_{c\alpha}^* \\ i_{c\beta}^* \end{bmatrix} = \frac{1}{v_{\alpha}^2 + v_{\beta}^2} \begin{bmatrix} v_{\alpha} & -v_{\beta} \\ v_{\beta} & v_{\alpha} \end{bmatrix} \begin{bmatrix} -p_{control} \\ -q_{control} \end{bmatrix} \quad (1)$$

When the series converter of the proposed configuration is used simultaneously for reactive, negative and harmonic compensation, the α - β axis voltage reference is given by equation (4).

$$\begin{bmatrix} v_{c\alpha}^* \\ v_{c\beta}^* \end{bmatrix} = \frac{1}{i_{\alpha}^2 + i_{\beta}^2} \begin{bmatrix} i_{\alpha} & -i_{\beta} \\ i_{\beta} & i_{\alpha} \end{bmatrix} \begin{bmatrix} -p_{control} \\ -q_{control} \end{bmatrix} \quad (2)$$

When the shunt converter of the proposed configuration is used for the charge control of battery, the active reactive power control is becoming the main issue, and the proposed system still satisfy the compensation demand of load such as negative and harmonic compensation. Then the α - β axis current reference is given by equation (3).

$$\begin{bmatrix} i_{c\alpha}^* \\ i_{c\beta}^* \end{bmatrix} = \frac{1}{v_{\alpha}^2 + v_{\beta}^2} \begin{bmatrix} v_{\alpha} & -v_{\beta} \\ v_{\beta} & v_{\alpha} \end{bmatrix} \begin{bmatrix} p_{control} + p_{pv} \\ q_{control} \end{bmatrix} \quad (3)$$

Where, p_{pv} is the PV power delivered to local loads by shunt converter. It should be noted that, it is so difficult to compensate reactive power and harmonic current using series converter only and because the signals from converter output terminals must be passed through the filters, the filter design strongly depends on the system parameters like load size and transformer turns ratio.

V. SINGLE LINE DIAGRAM OF TEST SYSTEM

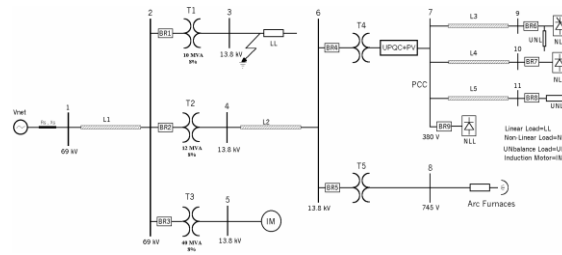


Fig.9. Single line diagram of test system used under consideration

As mentioned earlier this paper focuses on the comparison of UPQC with single PV Array and Multiple PV Arrays with compensation being performed at the distribution voltage level (13.8 kV in this case)[24]. Above designed new UPQC with PV Array models are installed in the secondary side of transformer between bus bars 6 and 7 near the point of common coupling (PCC). Following figures show the single line diagram and MATLAB model of the test system under consideration. Initially working of system is observed for UPQC with single PV Array and then with multiple PV arrays. The effectiveness of the both of UPQC models can be observed from the outputs of the system with UPQC.

VI. SIMULATIONS AND RESULTS

The values for inductance and capacitance are 0.112mH and 138.455 μF respectively for multiple PV arrays. The output voltage of MISO DC-DC converter V_{dc} can be expressed by the following (4):

$$V_{dc} = V_{dc1} + V_{dc2} + V_{dc3} + \dots + V_{dcn}$$

$$= \frac{V_{pv1}}{1-D_{pv1}} + \frac{V_{pv2}}{1-D_{pv2}} + \frac{V_{pv3}}{1-D_{pv3}} + \dots + \frac{V_{pvn}}{1-D_{pvn}} \tag{4}$$

Where D_{pv1} , D_{pv2} , D_{pv3} and D_{pvn} are the duty cycles of boost converters and V_{dc1} , V_{dc2} , V_{dc3} and V_{dcn} are the output voltages of boost converters.

Following are the outputs obtained for the UPQC with single and multiple PV arrays. And FFT analysis is done to analyze the THD % differences for voltage and current of the system.

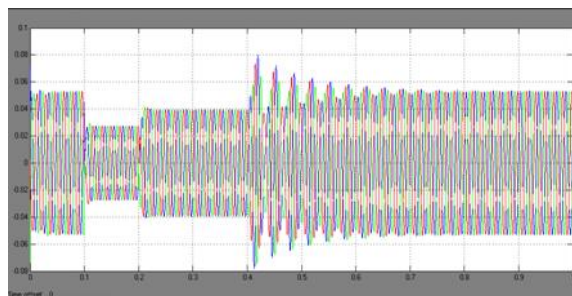


Fig.10. Voltage of the system integrated with UPQC and single PV Array

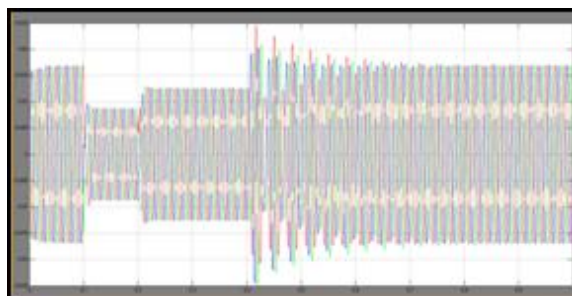


Fig.11. Current of the system integrated with UPQC and single PV Array

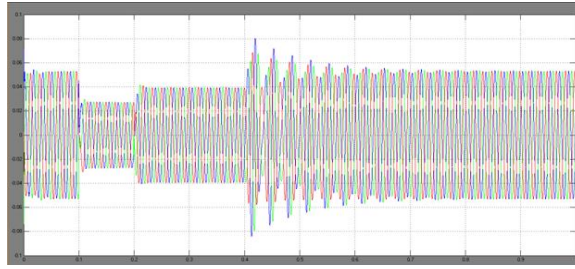


Fig.12. Voltage of the system integrated with UPQC and multiple PV Arrays

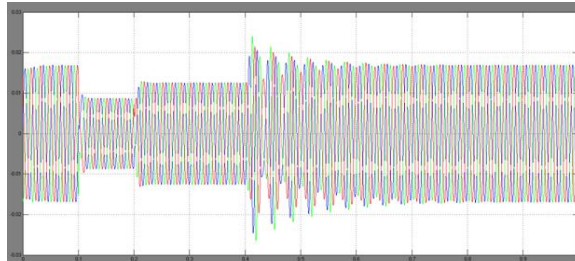


Fig.13. Current of the system integrated with UPQC and multiple PV Arrays

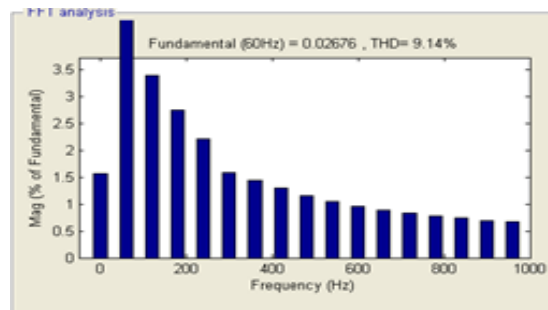


Fig.14. FFT Analysis for voltage of the system integrated with UPQC and single PV Array.

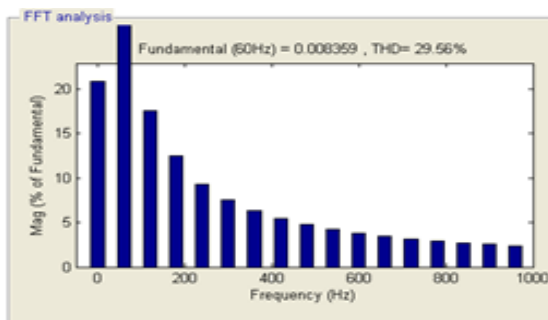


Fig.15. FFT Analysis for current of the system integrated with UPQC and single PV Array.

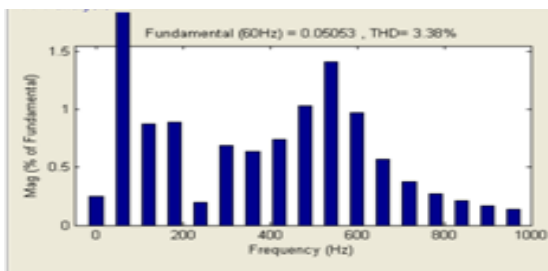


Fig.16. FFT Analysis for voltage of the system integrated with UPQC and multiple PV Arrays.

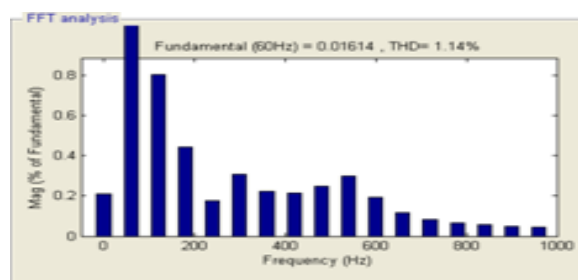


Fig.17. FFT Analysis for current of the system integrated with UPQC and multiple PV Arrays.

Figures 10 & 11 shows greater distortions in voltage and current output of the system integrated with UPQC and single PV arrays as compared to that in figures 13 & 14 outputs of system with multiple PV arrays. It can also be cleared from FFT analysis for the THD% shown in the table below:

TABLE I. FFT ANALYSIS

PV Arrays	Voltage THD%	Current THD%
Single	9.14	29.56
Multiple	3.38	1.14

VII. CONCLUSIONS & FUTURE ASPECTS

This paper proposes the comparative aspect of UPQC model s with single and multiple PV Arrays and the concept of Multi Input Single Output is studied. Results obtained show the effectiveness of the UPQC with multiple PV Arrays over the UPQC with single PV Arrays. The THD% level of the system is reduced in the case of multiple PV arrays. Hence it can be a better option where more accuracy in the system is required and multiple PV arrays can be easily installed. The performance of the proposed system was analyzed using simulations with MATLAB SIMULINK and validates the improvement of the power reliability of the system.

TABLE II. LIST of PARAMETERS USED

Sr. No.	System Quantities	Standards
1	Source	3 phase, 69 kV, 60Hz
2	Inverter parameters	IGBT based, 3-arm, 6-Pulse, Carrier Frequency=2000 Hz, Sample Time=5 μ s
3	PI Controller	Kp=0.5, Ki=1000 for series control Kp=0.5, Ki=1000 for shunt control, Sample time=50 μ s
4	RL load	Active Power = 5kW; Inductive Reactive Power = 2kVAR
5	Transformer 1	Δ \Yg, 69/138kV
6	Transformer 2	Δ \Delta; 69/138kV
7	Transformer 3	Δ \Yg, 69/138kV
8	Transformer 4	Δ \Yg,138\745kV
9	Motor Load (NLL)	Voltage V_{rms} = 138kV, Frequency = 60Hz

REFERENCES

- [1] Akagi H. and H.Fujita, "A new power line conditional for harmonic compensation" in power systems IEEE Trans power delivery, 10, 1570-1575, 1995.
- [2] Akagi, H.Y., Kanazawa and A.Nabae, "Instantaneous reactive power compensator comprising switching devices without energy storage components." IEEE Trans. India Appl.20:625-630, 2007
- [3] Aredes, M. and E.H.Watanabe, "New control algorithms for series and shunt three-phase four wire active power filters." IEEE Trans. Power delivery 10: 1649-1656. 1995.
- [4] Barker P.P. and R.W.De Mello, "Determining the impact of distributed generation on power systems.Part Radial distribution systems." Proc. IEEE power Eng.Sec.Summer Meeting, 3: 1645-1656, 2000.
- [5] Basu, M.S.P. Das and G.K.Dubey, "Comparative evaluation of two models of UPQC for suitable interface to enhance power quality." Elec. power system Res.77: 821-830, 2007.
- [6] Blaabjerg, F.Z Chen and S.B.Kjaer, "Power electronics as efficient interface in dispersed power generation systems." IEEE Trans. Power Elect, 19: 1184-1194, 2004.
- [7] Chen, Y.X.Zha and J.Wang, "Unified power quality conditioner (UPQC). The theory, modeling and application." Proc. Power syst. Technol. Conf.,3: 1329-1333, 2000.
- [8] Fujita, H.andH.Akagi,"The unified power quality conditioner.The integration of series and shunt active filters.IEEE Trans. Power Elect, 13: 315-322, 1998.
- [9] Ghosh, A. and G.Ledwich, "A unified power quality conditioner (UPQC) for simultaneous voltage and current compensation."Electric Power. Syst.Res.59: 55-63, 2001.
- [10] E.W.Gunther and H.Mehta, "A survey of distribution system power quality",IEEE Trans. on Power Delivery, vol.10, No.1, pp.322-329, Jan.1995.
- [11] B. Singh, AL.K.Haddad & A. Chandra, "A review of active filters for power quality improvement," IEEE Trans. on Ind. Electron, vol.46, pp. 960-971, 1999.
- [12] H Akagi, "New trends in active Filters for power conditioning", IEEE Trans.on Ind. Appl., 1996, 32, pp. 1312-1322
- [13] B.Singh,V. Verma,A. Chandra and K. Al-Haddad, " Hybrid filters for power quality improvement,"Proc. IEE on Generation, Transmission and Distribution, vol.152,pp.365-378,May2005.
- [14] Arindam Ghosh, Gerard Ledwich, "*Power Quality Enhancement Using Custom Power Devices*",Kulwer International Series in Engineering and Computer Science, 2002.
- [15] N. G. Hingorani, "Introducing custom power," Proc. IEEE Spectrum, vol.32, pp.41-48, June1995.
- [16] P. Jayaprakash, B. Singh and D.P. Kothari, "Star/Hexagon transformer Based Three-Phase Four-Wire DSTATCOM for Power Quality Improvement," International Journal of Emerging Electric Power Syatem,vol.9,no.8,Article1,Dec.2008.
- [17] B. Singh, P. Jayaprakash and D. P. Kothari, "A T-Connected Transformer and Three-leg VSC Based DSTATCOM for Power Quality Improvement," *IEEE Transactions on Power Electronics*, Vol. 23 , pp.2710-2718,2008.
- [18] A.Ghosh and G.Ledwich, "Compensation of distribution system voltage using DVR," IEEE Trans. on Power Delivery, vol.17, pp.1030-1036, Oct.2002.
- [19] J.Praveen, B.P. Muni, S. Venkateshwarlu and H.V. Makthal, " Review of dynamic voltage restorer for power quality Improvement," Proc.IEEE on IECON2004, Nov.2004, vol.1, pp.749-754.
- [20] M. Aredes, K. Heumann, and E. H. Walandble, "An universal active power line conditioner," *IEEE Trans. Power Del.*, vol. 13, no. 2, pp. 545- 551, Apr. 1998.
- [21] H. Fujita and H. Akagi, "The unified power quality conditioner: the integration of series- and shunt-active filters," *IEEE Trans. Power Electron.*, vol. 13, no. 2, pp. 315-322, Mar. 1998.
- [22] B. Han, B. Bae, H. Kim, and S. Baek, "Combined operation of unified power-quality conditioner with distributed generation," *IEEE Trans. Power Del.*, vol. 21, no. 1, pp. 330-338, Jan. 2006.
- [23] Hideaki Fujita and Hirofumi Akagi,"The Unified Power Quality Conditioner: The Integration of Series- and Shunt-Active Filters" IEEE transaction on power electronics, vol. 13, no. 2, March 1998
- [24]. M. Davari, S.M. Ale-Emran, H. Yazdanpanahi and G. B. Gharehpetian, "Modeling the Combination of UPQC and Photovoltaic Arrays with Multi-Input Single-Output DC-DC Converter", IEEE, 2009

Analytical Solution Of Unsteady Flow Past An Accelerated Vertical Plate With Constant Temperature and Variable Mass Transfer

¹I. J. Uwanta and ²I. D. Yale

¹Department of Mathematics, Usmanu Danfodiyo University, Sokoto, Nigeria

²Department of Mathematics, Kebbi State University of Science and Technology, Aliero, Nigeria

ABSTRACT

Analytical solution of unsteady flow past an accelerated vertical plate has been carried out in the presence of variable temperature and mass transfer. The dimensionless governing equations are solved using Laplace transform technique. The results are obtained for velocity, temperature, and concentration were obtained for different physical parameters like thermal Grashof number, mass Grashof number, Schmidt number and time. It is observed that the velocity increases with increase in Sc , t , Gr , and Gc .

KEY WORDS: Mass transfer, unsteady, accelerated vertical plate, variable temperature.

I. INTRODUCTION

Heat and mass transfer plays an important role in manufacturing industries for the design of fins, steel rolling, nuclear power plants, gas turbines and various propulsion devices for aircraft, missiles, space craft design, solar energy collectors, design of chemical processing equipment, satellites and space vehicles are example of such engineering applications. Mass transfer certainly occurs within the mantle and cores of planets of the size of or larger than the earth. It is therefore interesting to investigate this phenomenon and to study in particular, the case of mass transfer in the free convection flow. Several researches have been carried out to investigate unsteady flow past an accelerated vertical plate with mass transfer effect. Singh (1983) have investigated the mass transfer effects on flow past an accelerated vertical plate with uniform heat flux. Jha (1990) studied mass transfer effects and the flow past accelerated infinite vertical plate with heat sources. Mohammed and Karim (2000) have investigated the combined effects of transpiration and free convective current on the unsteady flow of viscous incompressible fluid past an exponential accelerated vertical permeable plate which is at a uniform temperature.

In their course of studies, expressions for the velocity -field, temperature- field, and Skin- friction were obtained in closed form by Laplace transform. Gupta *et al.* (2003) have analysed the flow in the Ekman layer on an oscillating plate. Mass transfer effects on unsteady flow plate an accelerated vertical plate with suction have been investigated by Das *et al.* (2006). A mass transfer effect on vertical oscillating plate with heat flux was studied by Muthucumaraswamy and Manivannan (2007). In their work, it shows that the temperature from the plate to the fluid at a uniform rate and the mass is diffused uniformly. They observed that the velocity increases with decreasing phase angle ωt . Muthucumaraswamy *et al.* (2009) have studied the unsteady flow past an accelerated infinite vertical plate with variable temperature and uniform mass diffusion. They analysed the velocity profiles and concentration for different physical parameters like the thermal Grashof number, mass Grashof number, Schmidt number and time. They also observed that the velocity increases with decreasing values of the Schmidt number. Okedoye and Lamidi, (2009) have investigated analytical solution of mass transfer effects on unsteady flow past an accelerated vertical porous plate with suction.

This present study investigates mass transfer effects on unsteady flow past an accelerated vertical plate with wall temperature. The dimensionless governing equations are solved using Laplace – transform technique. The solutions are obtained in terms of exponential and error functions

II. FORMULATION OF THE PROBLEM

Analytical solution of Mass transfer effects on unsteady flow past an accelerated vertical plate with variable temperature has been considered. The x' -axis is taken along the plate in the vertically upward direction and also the y' -axis is taken normal to the plate. At $t' > 0$, velocity of the plate raise with respect to time in its own plane, the temperature from the plate raise to T_w , and the concentration is raised linearly with respect to time.

2.1 THE GOVERNING EQUATION

Then under the usual Boussinesq's approximation the unsteady flow equations are momentum equation, energy equation, and mass equation respectively.

$$\frac{\partial u}{\partial t'} = g\beta(T - T_\infty) + g\beta^*(C' - C'_\infty) + \nu \frac{\partial^2 u}{\partial y^2} \quad (1)$$

$$\rho C_p \frac{\partial T}{\partial t'} = \kappa \frac{\partial^2 T}{\partial y^2} \quad (2)$$

$$\frac{\partial C'}{\partial t'} = D \frac{\partial^2 C'}{\partial y^2} \quad (3)$$

where u is the velocity of the fluid, T is the fluid temperature, C' is the concentration, g is the

gravitational constant, β and β^* are the thermal expansions of fluid and concentration respectively, t' is the time,

ρ is the fluid density, C_p is the specific heat capacity, ν is the viscosity of the fluid, κ is the thermal conductivity.

The initial and boundary conditions are:

$$\left. \begin{aligned} u = 0 & & T = T_\infty & & C' = C'_\infty & \text{for all } y, t' \leq 0 \\ t' > 0: u = u_0 t & & T = T_\omega & & C' = C'_\infty + (C'_\omega - C'_\infty) A t' & \text{at } y = 0 \\ u \rightarrow 0 & & T \rightarrow T_\infty & & C' \rightarrow C'_\infty & \text{at } y \rightarrow \infty \end{aligned} \right\} \quad (4)$$

where $A = \left(\frac{u_0^2}{\nu} \right)^{\frac{1}{3}}$

The non-dimensional quantities are:

$$\left. \begin{aligned} U = \frac{u}{(v u_0)^{\frac{1}{3}}}, t = t' \left(\frac{u_0^2}{\nu} \right)^{\frac{1}{3}}, Y = y \left(\frac{u_0}{\nu} \right)^{\frac{1}{3}} \\ \theta = \frac{T - T_\infty}{T_\omega - T_\infty}, Gr = \frac{g\beta(T_\omega - T_\infty)}{u_0}, C = \frac{C' - C'_\infty}{C'_\omega - C'_\infty} \\ Gc = \frac{g\beta^*(C'_\omega - C'_\infty)}{u_0}, Pr = \frac{\mu c_p}{\kappa}, Sc = \frac{\nu}{D} \end{aligned} \right\} \quad (5)$$

The non-dimensional quantities of equation (5) which analysed (1) to (4), and they lead to the dimensionless equations as follows;

$$\frac{\partial U}{\partial t} = Gr\theta + GcC + \frac{\partial^2 U}{\partial Y^2} \quad (6)$$

$$\frac{\partial \theta}{\partial t} = \frac{1}{Pr} \frac{\partial^2 \theta}{\partial Y^2} \quad (7)$$

$$\frac{\partial C}{\partial t} = \frac{1}{Sc} \frac{\partial^2 C}{\partial Y^2} \quad (8)$$

Where Sc is the Schmidt number, Pr is prandtl number, and Gr and Gc are the Grashof numbers

The initial and boundary conditions are reduces to:

$$\left. \begin{aligned} U = 0, \theta = 0, C = 0, & \text{for all } Y, t \leq 0 \\ t > 0: U = t, \theta = 1, C = t & \text{at } Y = 0 \\ U \rightarrow 0, \theta \rightarrow 0, C \rightarrow 0 & \text{as } Y \rightarrow \infty \end{aligned} \right\} \quad (9)$$

III. SOLUTION TO THE PROBLEM

Equations (6) – (8), are solved subjected to the boundary conditions of (9), and the solutions are obtained for concentration, temperature and velocity flow in terms of exponential and complementary error function using the Laplace- transform technique as follows;

$$C = t \left[(1 + 2\eta^2 Sc) \operatorname{erfc}(\eta\sqrt{Sc}) - \frac{2\eta\sqrt{Sc}}{\sqrt{\pi}} \exp(-\eta^2 Sc) \right] \quad (10)$$

$$\theta = \operatorname{erfc}(\eta\sqrt{\operatorname{Pr}}),$$

(11)

$$U = \left[(1 + 2\eta^2) \operatorname{erfc}(\eta) - \frac{2\eta}{\sqrt{\pi}} e^{-\eta^2} \right] + \frac{Gr t}{\operatorname{Pr} - 1} \left[(1 + 2\eta^2) \operatorname{erfc}(\eta) - \frac{2\eta}{\sqrt{\pi}} e^{-\eta^2} (1 + 2\eta^2 \operatorname{Pr}) \operatorname{erfc}(\eta\sqrt{\operatorname{Pr}}) \right. \\ \left. + \frac{2\eta\sqrt{\operatorname{Pr}}}{\sqrt{\pi}} e^{-\eta^2 \operatorname{Pr}} \right] + \frac{Gc \cdot t^2}{6(Sc - 1)} \left[(3 + 12\eta^2 + 4\eta^4) \operatorname{erfc}(\eta) - \frac{\eta}{\sqrt{\pi}} (10 + 4\eta^2) e^{-\eta^2} - (3 + 12\eta^2 Sc + 4\eta^4 (Sc)^2) \right. \\ \left. \operatorname{erfc}(\eta\sqrt{Sc}) + \frac{\eta\sqrt{\operatorname{Pr}}}{\sqrt{\pi}} (10 + 4\eta^2 Sc) e^{-\eta^2 Sc} \right] \quad (12)$$

where $\eta = \frac{y}{\sqrt{2t}}$

IV. RESULTS AND DISCUSSION

The problem of unsteady flow past an accelerated vertical plate with variable temperature and mass transfer has here been formulated, analyzed and solved analytically. In other to point out the effects of different physical parameters like Gr, Gc, Sc, Pr, and t on the flow, the computations of this parameter are carried out, and the following discussions are made. The value of the Prandtl number (Pr=0.71) is chosen to represent air. The value of the Schmidt number (Sc=0.6) is chosen to represent the presence of species by water vapour. Figures 4.1 to 4.7 represent the solutions of the problem, and is investigated for the physical parameters namely thermal Grashof number Gr, mass Grashof number Gc, Schmidt number Sc, Prandtl number Pr, and time t. The effect of velocity for different values of time (Sc =0.16, 0.3, 0.6, 2.01) is presented in Figure 4.1. It shows that velocity increases with increasing values of Sc.

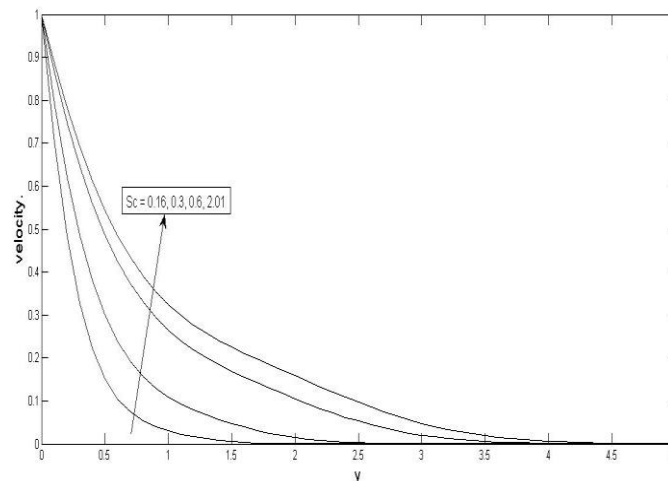


Figure 4.1 Velocity profiles for different values of Sc

The effect of velocity for different values of time (t=0.1, 0.4, 0.8, 1.2) is presented in Figure 4.2. It shows that velocity increases with increasing values of t.

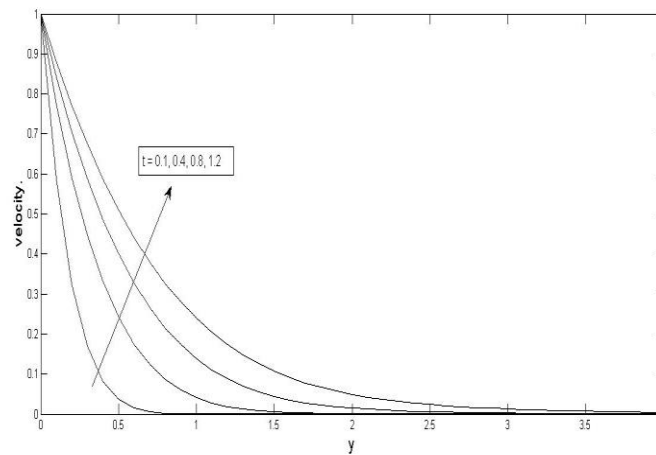


Figure 4.2 Velocity profiles for different values of t

The velocity profiles for different values of mass Grashof number ($G_c = 0.2, 0.4, 0.6, 0.8$) is presented in Figure

4.3 It is observed that velocity increases with increasing G_c .

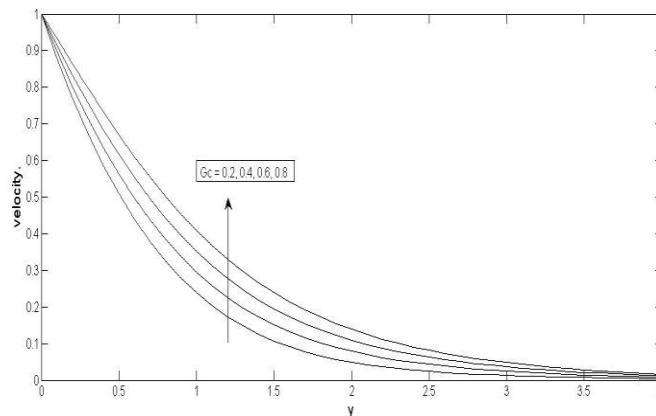


Figure 4.3 Velocity profiles for different values of G_c

The velocity profiles for different values of thermal Grashof number ($Gr = 0, 0.2, 0.4, 0.6$) is seen in Figure 4.4.

It is observed that velocity increases with increasing Gr .

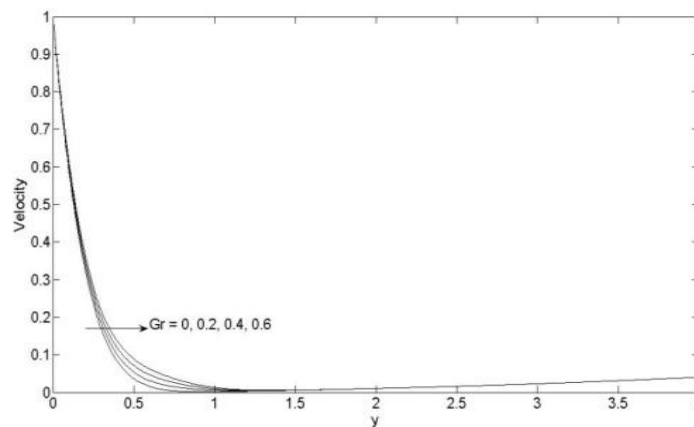


Figure 4.4 Velocity profiles for different values of Gr

The effect of temperature for different values of time ($t=0.1, 0.4, 0.8, 1.2$) is presented in Figure 4.5. It shows that temperature rises with increasing t

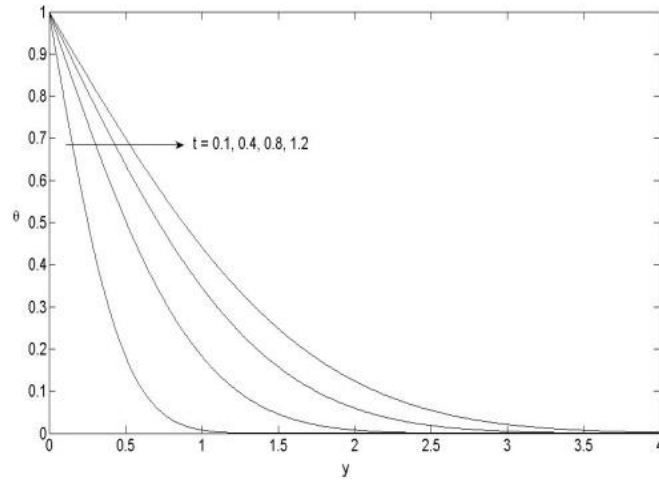


Figure 4.5 Temperature profiles for different values of t

The temperature profiles for different values Prandtl number ($Pr= 1.71, 1, 0.85, 0.71$) is presented in figure 4.6. It is observed that increases in Prandtl number Pr with decreases the temperature.

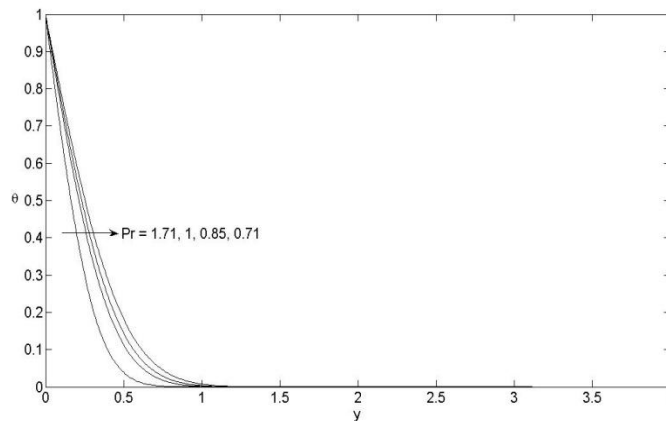


Figure 4.6 Temperature profiles for different values of Pr

The effect of concentration for different values of time ($t = 0.1, 0.2, 0.3, 0.4$) is presented in Figure 4.7. It is observed that time increases with increase in concentration.

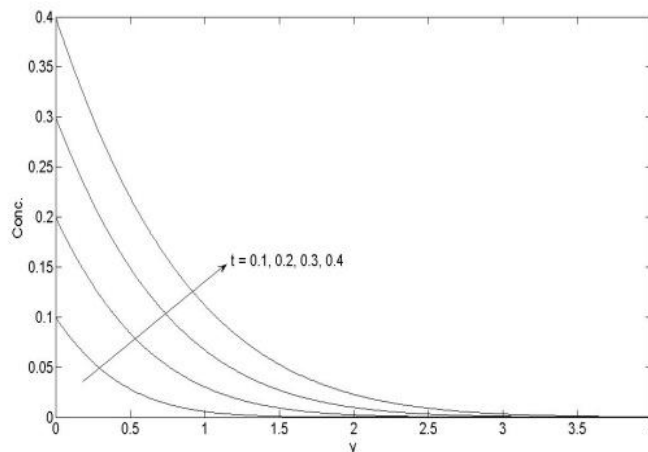


Figure 4.7 Concentration profiles for different values of t

The concentration profiles for different values of Schmidt number ($Sc = 0.16, 0.3, 0.6, 2.01$) is presented Figure 4.8. It is observed that the concentration increase with decreasing Sc .

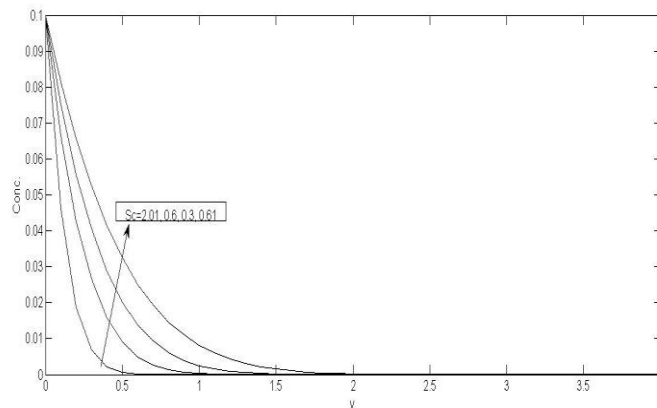


Figure 4.8 Concentration profiles for values of Sc

V. SUMMARY AND CONCLUSION

Analytical solutions of unsteady flow past an accelerated vertical plate with variable temperature and mass transfer have been studied. The dimensional governing equations are solved by Laplace transform technique and computed for different parameters using MATLAB. The effect of different parameters like Schmidt number, prandtl number, mass Grashof number, thermal Grashof number, and time are presented graphically. It is observed that velocity profile increases with increasing parameter like Sc , t , G_c , and Gr . It also observed that temperature increases with increasing t , but increases with decreasing Pr . The concentration profiles is observed also that rise in t increases the concentration profile.

REFERENCES

- [1] Singh A. K and Singh.J. (1983). Mass Transfer Effects on the Flow Past an Accelerated Vertical Plate with Constant Heat Flux. *Astrophysics and Space Science*.**97**, 57-61.
- [2] Jha. B. K and Prasad.R. (1990). "Free convection and Mass Transfer Effects on the flow past an Accelerated Vertical Plate with Heat Sources". *Mechanics Research Communication*.**17**, 143- 148.
- [3] Mohammed, I., and Karim, R. (2000). "Free Convection Flow Past a Vertical Plate". *Journal of the Tennessee Academy of Science*.
- [4] Gupta, A. S., Mishra, J.C., Raze, M., and Soundalgekar, V. M. (2003). "Flow in the Ekman Layer in an Oscillating Porous Plate". *ACTA Mechanica*. (165). 1-16.
- [5] Das, S. S., Shao, S. K., Dash, G. C. (2006). "Numerical Solution of Mass Transfer Effects on Unsteady Flow Past an Accelerated Vertical Porous Plate with Solution". *Bulletin Malaysian Mathematics Science Society*.**29** (1). 33- 42
- [6] Muthucumaraswamy, R., and Manivarannan, K. (2007). "Mass Transfer on Vertical Oscillating Plate with Heat Flux". *Theoretical Applied Mechanic*, (34). 309-322.
- [7] Muthucumaraswamy, R., Sundaraj, M., and Subramanian, V. S. A. (2009). "Unsteady Flow Past an Accelerated Vertical Plate with Variable Temperature and Mass Diffusion". *International Journal of Applied Mathematics and Mechanics*. **5**(6). 51-56
- [8] Okedoye .A.M., and Lamidi .O.T., (2009). "Analytical Solution of Mass Transfer Effects Unsteady flow Past an Accelerated Vertical Porous Plate with Suction". *Journal of Nigeria Association Mathematical Physics (JNAMP)* .**15**, 501-512.

Identification of Fault Location in Multiple Transmission Lines by Wavelet Transform

Subba Reddy.B¹, D.Sreenuvasulu Reddy², Dr.G.V.Marutheswar³

¹Assitant Professor, Department Of E.E.E., Sree Vidyanikethan Engineering College,

²Assitant Professor, Department Of E.E.E., Sree Vidyanikethan Engineering College,

³Professor, Department Of E.E.E., S.V.University College Of Engineering

ABSTRACT

Distance protection is one of the most common methods used to protect transmission lines. Many techniques have been proposed to achieve accurate results. The main target of these techniques is to calculate impedance at the fundamental frequency between the relay and the fault point. This impedance is calculated from the measured voltage and current signals at the relay location. In addition to the fundamental frequency, the signals usually contain some harmonics and dc component, which affect the accuracy of the phasor estimation. Distance relays have experienced much improvement due to the adoption of digital relaying. Signal processing is one of the most important parts of the operation of the digital distance protection. Wavelets are recently developed mathematical tool for signal processing and the basic concept in wavelet transform (WT) is to select an appropriate wavelet function "mother wavelet" and then perform analysis using shifted and dilated versions of this wavelet. The WT uses short windows at high frequencies and long windows at low frequencies. Wavelet transform (WT) has the ability to decompose signals into different frequency bands using multi resolution analysis (MRA). It can be utilized in detecting faults and to estimate voltage and current of the fault signals without any DC offset in these signals, which are essential for transmission line distance protection. This paper presents a distance protection scheme for transmission lines based on analyzing the measured voltage and current signals using WT with MRA.

KEYWORDS: Distance-protection relaying, multi-resolution analysis, power systems, wavelet transform (WT).

I. INTRODUCTION.

This paper focuses the use of wavelet transform, a unified framework for analyzing power system fault identification in a multi-transmission line. Wavelet transform possesses excellent features such as a little wave, little in the sense of being of short duration with finite energy which integrates to zero [1]. Wavelet is well suited to wide band signals that are not periodic and may contain both sinusoidal and impulse components as it is typical for power system transients. In this paper, a new scheme is proposed for fast and reliable fault classification. The proposed method uses a wavelet-based scheme. Various transient system faults are modeled and a Wavelet based algorithm is used for classification of faults. Performance of the proposed scheme is evaluated using various fault types and encouraging results are obtained. It is shown that the algorithm is able to perform fast and correctly for different combinations of fault conditions, e.g. fault type, fault location, pre-fault power flow direction and system short circuit level [2]. In power system, wavelet transforms (WTs) are better suited for the analysis of certain types of transient waveforms than the Fourier Transforms (FT) and Short-Time Fourier Transforms (STFT) approaches. A wavelet is described as a little wave, little in the sense of being of short duration with finite energy which integrates to zero, and hence if its suitability for transients. Power system transients, which often have an adverse effect on the normal operation of the system, are quite common like, lighting transients, transformer inrush currents, motor starting currents, capacitor and line-switching transients are just a few of the typical electromagnetic power system transients that occur in practice. Some of the methods employed for analysis of the transient phenomena at present are, transforming the data into the frequency domain via Fourier and STFT. These methods also have served the power engineering community. Fourier has a few drawbacks, they require periodicity in all the time functions involved and also location of transient in time axis is lost. STFT have the following drawbacks, they have the limitations of fixed window width and it will consume more time in transient location. If WTs are opted, they overcome the above discussed

disadvantages, as wavelet transforms employ analysis functions that are both in time and frequency domain. It focuses on short-time intervals for high frequency components and long-time intervals for low frequency components. Wavelets have a window that automatically adapts to give appropriate resolution. In unsymmetrical faults only one or two phases are involved. In such fault the voltages and currents become unbalanced (unsymmetrical) and each phase is to be treated individually for calculation purposes. Most of the faults that occur are unsymmetrical faults. Since any unsymmetrical fault causes unbalanced currents to flow in the system, the unsymmetrical faults are analyzed using symmetrical components.

2.1 INTRODUCTION TO WAVELET TRANSFORMS

Wavelet transform is a powerful signal analysis tool that has been used successfully in many areas for than a decade. The Multi-Resolution Analysis (MRA) is one of the most active branches of the Wavelet Transforms. The main algorithm dates back to the work of Stephane Mallet in 1989 [3]. MRA provides an effective way to examine the features of a signal at different frequency bands. Hence, it is suited for the fault classification and location problems in the power system [4], [1]. The fundamental idea behind wavelets is to analyze according to scale. Wavelets are functions that satisfy certain mathematical requirements and are used in representing data or other functions. However, in wavelet analysis, the scale that we use to look at data plays a special role. Wavelet algorithms process data at different scales or resolutions. If we look at a signal with a large “window”, we would notice gross features. Similarly, if we look at a signal with a small “window”, we would notice small features. For many decades, scientists have wanted more appropriate functions than the sine’s and cosines which comprise the basis of Fourier analysis, to approximate choppy signals. By their definition, these functions are non-local (and stretch out to infinity). They therefore do a very poor job in approximating sharp spikes. But with wavelet analysis, we can use approximating functions that are contained neatly infinite domains. Wavelets are well-suited for approximating data with sharp discontinuities. The wavelet analysis procedure is to adopt a wavelet prototype function, called an analyzing wavelet or mother wavelet. Temporal analysis is performed with a contracted, high-frequency version of the prototype wavelet, while frequency analysis is performed with a dilated, low-frequency version of the same wavelet. Because the original signal or function can be represented in terms of a wavelet expansion (using coefficients in a linear combination of the wavelet functions), data operations can be performed using just the corresponding wavelet coefficients, and if you further choose the best wavelets adapted to your data, or truncate the coefficients below a threshold, your data is sparsely represented. This sparse coding makes wavelets an excellent tool in the field of data compression.

2.2 Motivation to Use WT

The increasing complexity of the power systems, concomitant with a demand to drive the network harder without compromising on the quality of power supply, has meant that power engineers it continuously strive for a improved alternative methods of transient analysis, for the purposes of designing new equipment to efficiently and expeditiously deal with abnormal transient phenomena. In this respect, the present methods of transients analysis have limitations. For instance, a Fourier series requires periodicity of all the time functions involved, this effectively means that the basic functions (i.e. sine and cosine waves) used in Fourier analysis. Traditional Fourier analysis does not consider frequencies that evolve with time, i.e. non-stationary signal. Finally, certain adverse effect such as the Gibbs phenomenon and aliasing associated with the discrete FT (DFT) exists when analyzing certain waveforms. However, the drawback is the windowed FT (Also known as the short-time FT or STFT) has the limitations of the fixed window width which needs to be fixed a prior, this effectively means that it does not provide the requisite good resolution in both time and frequency, which is an important character for analyzing transient signals comprising both high and low-frequency components [5]. Wavelet analysis overcomes the limitations of the Fourier methods by employing analysis functions that are local both in time and frequency. The WT is well suited to wideband signals that are not periodic and may contain both sinusoidal and impulse components as is typical of fast power system transients. In particular, the ability of wavelets to focus on short-time intervals for high frequency components improves the analysis of signals with localized impulses and oscillation, practically in the presence of fundamental and low-order harmonics. In a sense, wavelets have a window that automatically adapts to give the appropriate resolution.

2.3 Basic Concepts of Wavelet Transforms

A wavelet is a waveform of effectively limited duration that has an average value of zero. Compare wavelets with sine waves, which are the basis of Fourier analysis. Sinusoids do not have limited duration they extend from minus to plus infinity, and where sinusoids are smooth and predictable, wavelets tend to be irregular and asymmetric. Fourier analysis consists of breaking up a signal into sine waves of various frequencies. Similarly, wavelet analysis is the breaking up of a signal into shifted and scaled versions of the original (or mother) wavelet. It also makes sense that local features can be described better with wavelets that

have local extent [5]. The wavelet transform allows resolving the resolution problem encountered in STFT. The basic functions allow to trade off the time and frequency resolution in different ways. If a large region of low frequency signal is to be analyzed, a wide basis function will be used. Similarly, if a small region of high frequency signal is to be analyzed, a small basis function will be used. The basic functions of the wavelet transform are known as wavelets. There are a variety of different wavelet functions to suit the needs of different applications. In general, a wavelet is a small wave that has finite energy concentrated in time as shown in Figure 1. This is the characteristic about a wavelet that gives it the ability to analyze any time-varying signals.

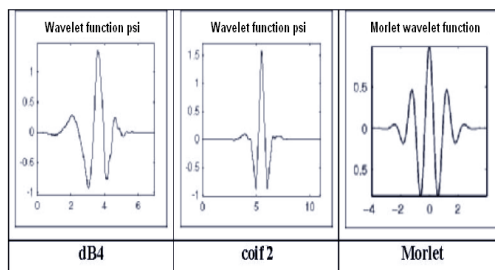


Fig. 1 Types of Wavelet

II. WAVELET FAMILIES

There are a number of basic functions that can be used as the mother wavelet for Wavelet Transformation. Since the mother wavelet produces all wavelet functions used in the transformation through translation and scaling, it determines the characteristics of the resulting Wavelet Transform. Therefore, the details of the particular application should be taken into account and the appropriate mother wavelet should be chosen in order to use the Wavelet Transform effectively. Figure 2 illustrates some of the commonly used wavelet functions. Haar wavelet is one of the oldest and simplest wavelet. Daubechies wavelets are the most popular wavelets. They represent the foundations of wavelet signal processing and are used in numerous applications.

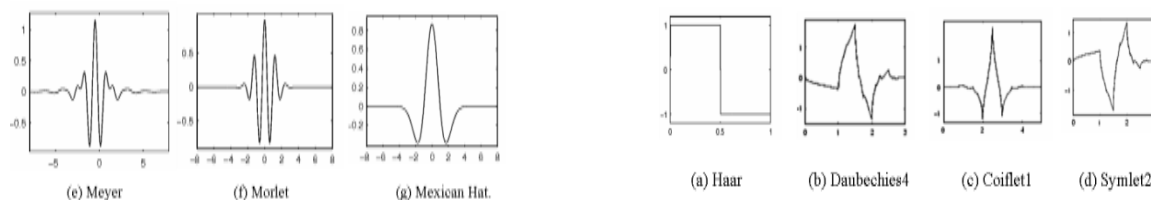


Fig. 2 Wavelet families

These are also called Maxflat wavelets as their frequency responses have maximum flatness at frequencies 0 and π . This is a very desirable property in some applications. The Haar, Daubechies, Symlets and Coiflets are compactly supported orthogonal wavelets. These wavelets along with Meyer wavelets are capable of perfect reconstruction. The Meyer, Morlet and Mexican Hat wavelets are symmetric in shape. The wavelets are chosen based on their shape and their ability to analyze the signal in a particular application.

3.1 Daubechies Family

The names of the Daubechies family wavelets are written dbN, where N is the order, and db is the “surname” of the wavelet. The db1 wavelet, as mentioned above, is the same as Haar wavelet. Here are the wavelet functions of the next nine members of the family. Figure 3 shows the members of the Daubechies family.

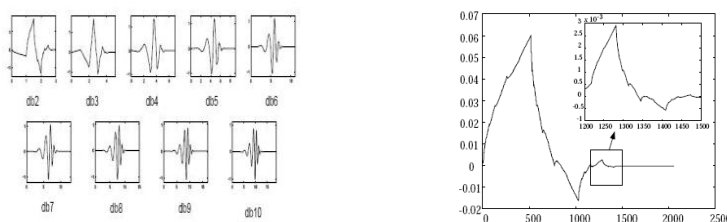


Fig. 3 Daubechies family wavelets

3.2 Continuous Wavelet Transform

The continuous wavelet transform was developed as an alternative approach to the short time Fourier transforms to overcome the resolution problem. The wavelet analysis is done in a similar way to the STFT analysis, in the sense that the signal is multiplied with a function, similar to the window function in the STFT, and the transform is computed separately for different segments of the time-domain signal. However, there are two main differences between the STFT and the CWT:

- [1] The Fourier transforms of the windowed signals are not taken, and therefore single peak will be seen corresponding to a sinusoid, i.e., negative frequencies are not computed.
 - [2] The width of the window is changed as the transform is computed for every single spectral component, which is probably the most significant characteristic of the wavelet transform.
- a. Mathematically, the continuous wavelet transform (CWT) of a given signal $x(t)$ with respect to a mother wavelet $g(t)$ is generically defined as shown in Equation 1.

$$CWT(a,b) = \frac{1}{a} \int_{-\infty}^{\infty} x(t)g\left(\frac{t-b}{a}\right)dt \tag{1}$$

Where ‘a’ is the dilation of scale factor and ‘b’ is the translation factor, and both variables are continuous. It is apparent from Equation (1) that the original one-domain signal $x(t)$ is mapped to a new time-dimensional function space across scale ‘a’ and translation ‘b’ by the wavelet transforms (WT). A WT coefficients CWT (a,b) at particular scale and translation represents how well the original signal $x(t)$ and scaled and translated mother wavelet match. Thus, the set of all wavelet coefficients CWT (a,b) associated with a particular signal are the wavelet representation of the original signal $x(t)$ with respect to the mother wavelet $g(t)$.

The parameter scale used in wavelet transformation is similar to the scale used in the maps. At high scale, the wavelet seeks for global information or low frequency information about the signal. At low scale, the wavelet seeks for detailed information or high frequencies information about the signal.

3.3 Discrete Wavelet Transform

The foundations of the DWT go back to 1976 when Croiser, Esteban, and Galand devised a technique to decompose discrete time signals [2]. Analogous to the relationship between continuous Fourier transform and discrete Fourier transform, the continuous wavelet transform has digitally implementable counterpart called the discrete wavelet transform and is defined as

$$DWT(a,b) = \frac{1}{a^m} \sum_n x(n)g\left(\frac{k-nb_0 a_0^m}{a_0^m}\right) \tag{2}$$

Where ‘a’ and ‘b’ are the scaling and translation parameters. Where $a=a_0^m$ and $b=nb_0 a_0^m$ giving rise to a family of dilated mother wavelet, i.e. daughter wavelet. Scaling gives the DWT logarithmic frequency coverage in contrast to the uniform frequency coverage of, say, the windowed-DFT (i.e. WDFT). The DWT output can be represented in a two-dimensional grid in a manner similar to the WDFT but with very different divisions in time and frequency.

III. MULTI-RESOLUTION AND WAVELET DECOMPOSITION

The Wavelet represents a powerful signal processing with a wide variety of applications:

Acoustics, communications, transient analysis, medicine etc. the main reason for this growing activity is the ability of the wavelet transform not to be decompose a signal into its frequency components, but also unlike the Fourier transforms to provide a non-uniform division of frequency domain [5]. Whereby it focuses on short time Fourier intervals for the high frequency components and long intervals for low frequencies. This attribute to tailor the frequency resolution can be greatly facilitate signal analysis and the detection of the signal features, which can be very useful in characterizing the sources of the transients and or the state of the post disturbance system. The wavelet transforms normally uses both the analysis and synthesis wavelet pair. Synthesis is used for wavelet reconstruction. The original signal is decomposed into its constituent wavelet sub bands or levels. Each of these levels represents that part of original signal occurring at the particular time and in that particular frequency band. These individual frequency bands are logarithmically spaced rather than uniform spaced as in the Fourier transforms. The decomposed signal posses a powerful property which is one of the major benefits provided by the WT. The resulting decomposed signal can be analyzed in both time and frequency domains. Multi-resolution analysis is a procedure to obtain low-pass approximates band-pass details from original signals [2]. An approximates is a low resolution representation of a original signal, while a detail is the difference between two successive low-resolution representations of the original signal.

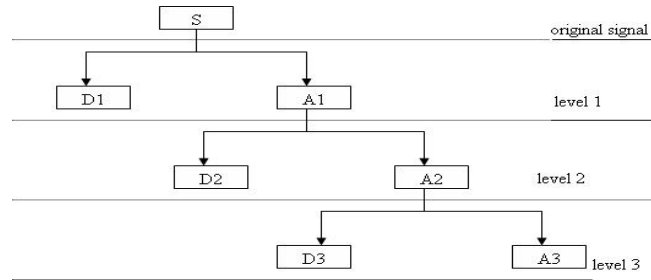


Fig. 4 Multi-Resolution and Wavelet Decomposition

An approximation contains the general trend of the original signal while a detail embodies the high-frequency content of the original signal. Approximation and detail are obtained through a succession of convolution processes. The original signal is divided into different scales of resolution, rather than different frequencies, as in the case of Fourier analysis. The algorithm of multi-resolution decomposition is illustrated in Figure 4, where three levels of decomposition are taken as an example of illustration. The details and approximations of the original signal S are obtained by passing through a filter bank, which consists of low-pass and high-pass filter. A low-pass filter picks out high frequency contents in the signal being analyzed. With reference to Figure 3, the multi-resolution decomposition procedures are defined as:

$$D_j(n) = \sum h(k)A_{j-1}(n-k) \quad (3)$$

$$A_j(n) = \sum L(k)A_{j-1}(n-k) \quad (4)$$

Where l and h are low-pass and high-pass filter vectors, respectively D_j , A_j are detail and approximation at resolution j , $j=1,2,\dots,j$ respectively, A_{j-1} is the approximation of the level immediately above level j , $k=1,2,\dots,k$ where k is length of the filter vector.

To have a non-redundant representation and unique representation and unique reconstruction of the original signal, orthogonal filter banks are required. WT and multi-resolution decomposition are closely related. Also, as shown in Figure 3, wavelet decomposition is accomplished by including down-sampling operations into the multi-resolution analysis. The maximum number of wavelet decomposition levels for WT is determined by the length of original signal, the particular wavelet being selected, and the level of detail required. The low-pass and high-pass filter is determined by the scaling function and wavelet function respectively. Signal processing uses exclusively orthogonal wavelets [1]. The non-redundant representation and perfect reconstruction of the original signal can only realize through compactly supported orthogonal wavelets. The ones that are frequently used for signal processing are daubechies, morlets, and coiflets and symlets. The wavelets exhibit different attributes and performance criterion when applied to specific applications, such as detection of transients, signal compression and denoising.

4.1 IMPLEMENTATION OF DWT

The interchange of the variables n , k and rearrangement of the Equation (2) gives.

$$DWT(m,n) = \frac{1}{a^m} \sum_n x(n)g(a_o^{-m}n - b_o k) \quad (5)$$

On closer observation of this equation, we notice that there is a remarkable similarity to the convolution equation for the finite impulse response (FIR) digital filters, namely

$$y(n) = \frac{1}{c} \sum x(k)h(n-k) \quad (6)$$

where $h(n-k)$ is the impulse responses of the FIR filter.

By comparing Equation (5) and Equation (6), it is evident that the impulse response of the filter in the DWT equation is

$$g(a_o^{-m}n - b_o k) \quad (7)$$

Therefore mentioned characteristic feature of the DWT is very different from the WDFT. The DWT is thus very effective in isolating the highest frequency band at precisely the quarter cycle of its occurrence while the 50Hz power frequency is fully preserved as a continuous magnitude. This simple example clearly explains the multi-resolution attributes of the wavelet transforms in analyzing a non-stationary transient signal comprising both high and low-frequency components.

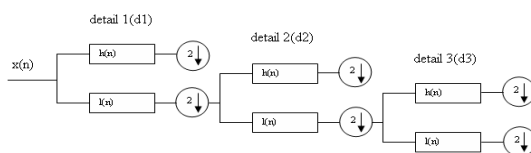


Fig. 5 Implementation of the Discrete Wavelet Transform

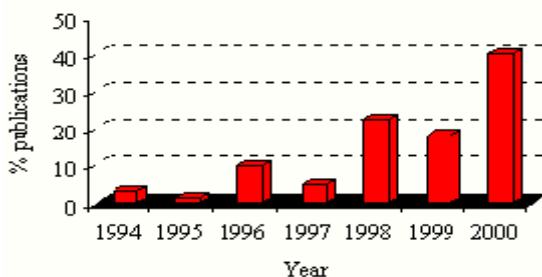
By selecting a_2 and $b_0=1$, the CWT can be implemented by using a multi-stage filter with the mother wavelet as the low-pass filter $l(n)$ and its dual as the high-pass filter $h(n)$, as shown in Figure 5. As evident from the example considered, down sampling the output of the low-pass filter $l(n)$ by factor 2(2) effectively scales the wavelet by a factor of 2 for the next stage, thereby simplifying the process of dilation.

$$h[l-1-n] = (-1)^n l(n) \tag{8}$$

Where l is the filter length. Note that the filter length are ‘odd index’ alternated reversed versions of each other, and the low-pass to high-pass conversion is provided by the $(-1)^n$ term, filters satisfying this condition are commonly used in signal processing, and they are known as the ‘quadrature mirror filters’. The implementation of the DWT with a filter bank is computationally efficient. The output of the high-pass filter in Figure 5 gives the detailed version of the high-frequency component of the signal. As can be seen, the low-frequency component is further split further to get the other detail of the input signal.

4.2 APPLICATIONS OF WAVELET TRANSFORMS IN POWER SYSTEM

Wavelet transform has received great attention in power community in the last years, because are better suited for the analysis of certain types of transient waveforms than the other transforms approach. The aim of this paper is to provide a descriptive overview of the wavelet transform applications in power systems to those who are novel in the study of this subject. A specific application of wavelet MRA in transmission line fault detection, classification, and location is discussed briefly in the following sections. The wavelets were first applied to power system in 1994 by Robertson [6] and Ribeiro. From this year the number of publications



in this area has increased as Figure 6 shows.

Fig. 6 Evolution of Wavelet Publications in Power Systems

The main focus in the literature has been on identification and classification methods from the analysis of measured signals, however, few works use wavelet transform as an analysis technique [7] for the solution of voltages and currents which propagate throughout the system due, for example, a transient disturbance popular wavelet transform applications in power systems are the following:

- Power system protection
- Power quality
- Power system transients
- Load forecasting
- Power system measurement

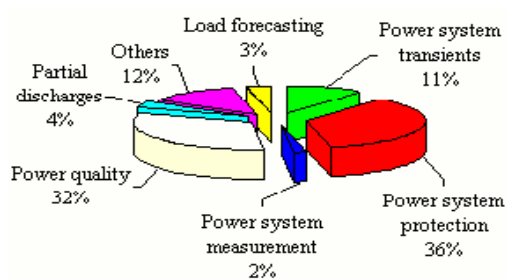


Fig. 7 Percentage of Wavelet Publications in Different Power System Areas

Figure 7 shows the percentage of publications in each area; the areas in which more works have been developed are the protection and power quality field [8]. The goal in each of the above is to “reduce the large volume of transient signal data to a much smaller and higher quality information packet to archive or actively distribute to the power system” [9]. The result is to enhance the value of transient data from digital recording equipment through increased use of day-to-day transient event monitoring.

IV. MATLAB SIMULATION

A simulation model is developed for the system shown in figure 8 using simulink.

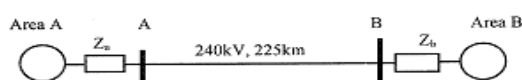


Fig. 8 schematic diagram of power system

- [1] Generator ratings: 240 KV, 60Hz.
- [2] Transmission line parameters:

R	0.01844 (Ω /km)
L	3.73e-3 (H/km)
C	5.08e-9 (F/km)
Z1 & Z2	(8.05+j110.66) Ω
Z0	(79.19+j302.77) Ω
Z _L	(4.15+j84.6) Ω

5.1 The phase currents and voltages for the simulation model without fault

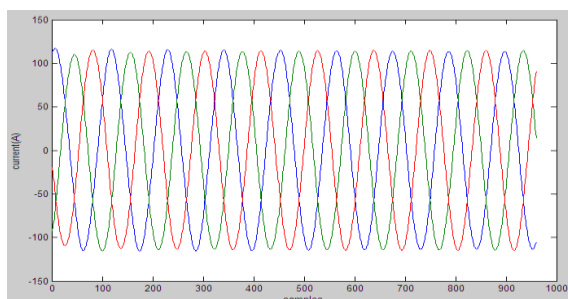


Fig. 9 Healthy phase current signal

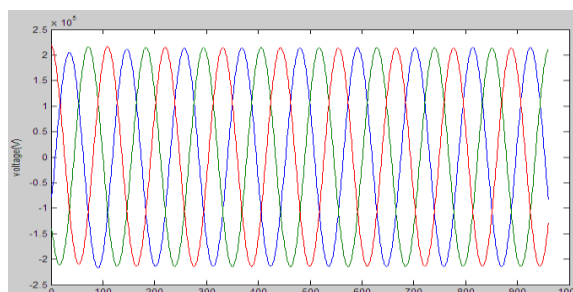


Fig. 10 Healthy phase voltage signals

5.3 Phase currents and voltages of the simulation model with L-G fault are shown below

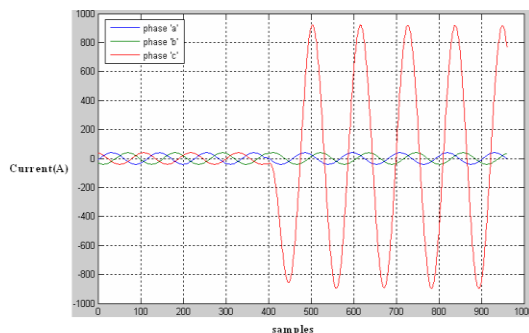


Fig. 11 current waveforms for an L-G fault

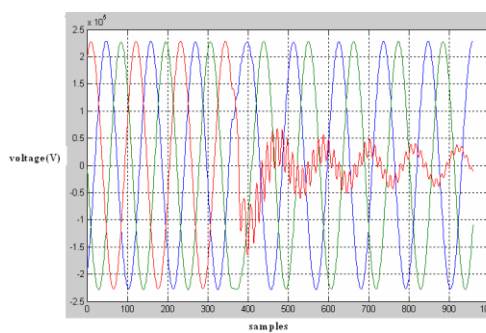


Fig. 12 Voltage waveforms for L-G fault

VI. RESULTS AND DISCUSSIONS

6.1 Wavelet distance protection algorithm.

In order to investigate the applicability of the proposed wavelet transform distance protection algorithm, a simulation of transmission line model is developed. Fault simulations were carried out using MATLAB. The three phase current and voltage signals are sampled at 960Hz (16 samples/fundamental power cycle). These signals are then filtered using the pre-band-pass filters to attenuate the dc component. The output filtered signals are the input to the proposed wavelet distance protection algorithm.

6.2. Analysis of L-G fault.

The simulated fault signals are being analyzed through the Wavelet transform using MATLAB wavelet toolbox as follows. Three phase current and voltage signals[10] Figure 8 are loaded to the multisignal analysis1-D in the wavelet toolbox main menu.

The proposed technique is divided into two sections

6.2.1 Fault detection.

The first section is detection of the fault by observing the output of the high pass filter details of the first decomposition level. This decomposition level has the ability to detect any disturbances in the original current waveform. The loaded current signals (Figure 8) are decomposed at one level with the db1 wavelet.

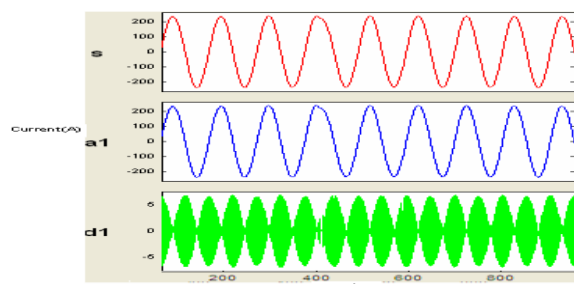


Fig. 13 First level decomposition of phase 'a'

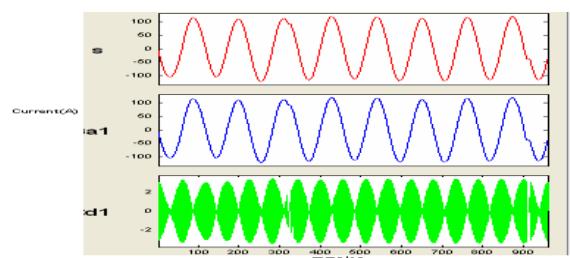


Fig. 14 First level decomposition of phase 'b'

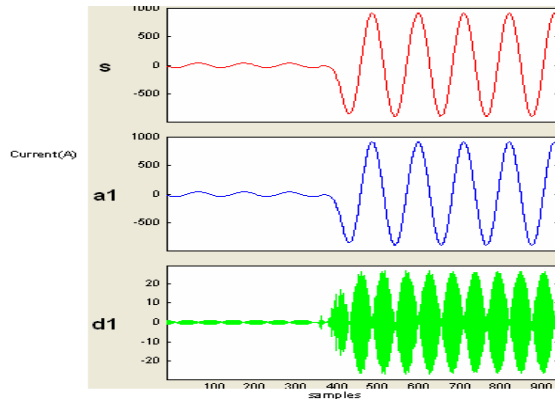


Fig. 15 First level decomposition of phase 'c'

6.2.2 Estimation of current and voltages.

The second section of the algorithm is the estimation of the fundamental frequency voltage and currents. It can be done by observing the output of the low-pass filter at the fourth decomposition level (A4). The fourth level of decomposition gives good approximation of the phasors. At this level the High frequencies in the signal are eliminated by the high-pass filters of the first, second and third decomposition levels and DC component has already been eliminated by pre-band-pass filtering the signal. The estimation of phasors is based on capturing the peak value of each signal (magnitude). The three phase current and voltage signals are decomposed by the db4 wavelet.

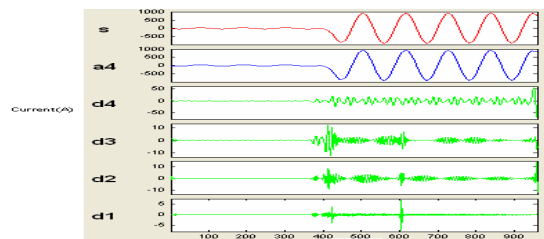
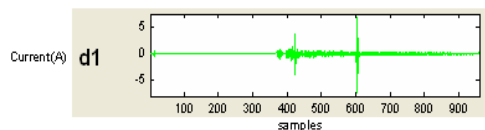


Fig. 16 4-levels of decomposition of phase 'c'

6.2.3 Fault distance measurement



No of samples : 182
 Simulation time : 0.22 sec
 Time interval between two peaks : 0.22/182
 : 1.208 m sec
 Traveling wave velocity : 1.82×10^5 miles/sec
 Fault distance $D = (v \cdot T_d) / 2$
 = 109.89 miles
 = 175.83Km.

VII. CONCLUSIONS

The present work proposed an efficient wavelet based transmission line distance protection. It has the ability of detecting faults and to estimate the voltages and currents of signals without any DC offset in the signals, which are fundamental for distance protection. This wavelet based technique allows decompose the signal into frequency bands (multi-resolution) in both time and frequency allows accurate fault detection as well as estimation of fault signal currents and voltages at the fundamental frequency. Various faults on the transmission line can be identified and cleared within one cycle according to the fault location.

REFERENCES

- [1]. S. G. Mallat, "A theory for multi resolution signal decomposition: The Wavelet representation," IEEE Trans. Pattern Anal. Machine Intell, vol.11, pp. 674–693, July 1989.
- [2]. D. C. Robertson, O. I. Camps, J. S.Mayer, and W. B. Gish, "Wavelet and electromagnetic power system transients," IEEE Trans. Power Delivery, A. H. Osman (S'01) received the B.Sc. and M.Sc. degrees in electrical engi-vol. 11, pp. 1050–1056, Apr. 1996.
- [3]. A.H.Osman and O. P. Malik, "Wavelet transform approach to distance protection of transmission lines," in Proc. PES 2001 Summer Meeting, Vancouver, BC, Canada.
- [4]. A.H.Osman, Student member, IEEE, and O.P. Malik, Life fellow, IEEE"Transmission line distance protection based on wavelet transform"2004 IEEE.
- [5]. C.L. Wadhwa, "Electrical Power Systems", New Age International (P) Ltd., New Delhi, July 1998.
- [6]. C.-K. Wong et al., "A novel algorithm for phasor calculation based on wavelet analysis," in Proc. PES 2001 Summer Meeting, Vancouver, BC, Canada.
- [7]. S.El Safty,A.El-Zonkoly Applying Wavelet entropy principle in fault classification" PWACET VOLUME 30 JULY 2008.
- [8]. Chaari, M. Meunier, and F. Brouaye, "Wavelets: A new tool for the resonant grounded power distribution systems relaying", Teee Trans. on Power Delivery, Vol. 1, No. 3, July 1996, pp. 1301-1308,7..T.
- [9]. M. Lai, L. A. Snider, E. Lo, D. Sutanto "High- Impedance Fault Detection Using Discrete Wavelet Transform and Frequency Range and RMS Conversion," IEEE Trans. on Power Delivery, , January 2005, vol.20, no. 1, pp. 397-407.
- [10]. Wai, and X. Yibin, "A novel technique for high impedance fault identification", IEEE Trans. on Power Delivery, Vol. 13, No. 3, July 1998, pp. 738-744.



B.SUBBAREDDY received B.Tech degree in Electrical and Electronics Engineering from JNT University Hyderabad and M.Tech degree in Power System Operation and Control from S.V.University, Tirupati. Presently working as Assistant Professor in Sree Vidyanikethan Engineering College, Tirupathi. His research areas are power system operation and control and Special Machines.



D.SREENIVASULU REDDY received B.Tech degree in Electrical and Electronics Engineering from JNT University Hyderabad and M.Tech degree in Electrical Power System from from JNT University, Anapapur. Presently working as Assistant Professor in Sree Vidyanikethan Engineering College, Tirupathi. His research areas are power system operation and control and Special Machines.



Dr G.V. MARUTHESWAR received B.Tech degree in Electrical and Electronics Engineering and M.Tech degree in Instrumentation and Control Systems from S.V.University, Tirupati and received Ph.D from S.V.University, Tirupati. Presently working as Professor in Department of Electrical and Electronics Engineering in SVU College of Engineering Tirupati. His research areas are Control Systems and Special Machines.

Data Storage in Secured Multi-Cloud Storage in Cloud Computing

Archana Waghmare¹, Rahul Patil², Pramod Mane³, Shruti Bhosale⁴.

^{1, 2, 3, 4} S.V.P.M's COE Malegaon(Bk). Department Of Computer Engg.

ABSTRACT

Now a day even though Cloud services offer flexibility, scalability, there have been proportionate concerns about security. As more data moves from centrally located server storage to the cloud storage. Security is the most important factor related to the cloud computing. As the users can stores his private data on cloud with the help of cloud service providers. Data stored on single cloud is risk of service availability failure due to attacker enters in single cloud. Our approach is to movement towards multi-clouds that is data stored on multi-cloud service providers. In this system we propose a secured cost-effective multi-cloud storage (SCMCS) model in cloud computing in which holds an economical distribution of data among the available cloud service provider (SP) in the market, instead of single cloud to provide the customers with advanced data availability as well as security. This work aims to encourage the use of multi-clouds due to its ability to reduce security risks that affect the cloud computing user. Our proposed model provides a better security for customer's data according to their available budgets from that they can choose cloud service provider.

KEYWORDS: Cloud Networks , Service provider ,Multi- Cloud Storage ,Security, Cloud Services, Cloud Computing.

I. INTRODUCTION

Cloud computing is nothing but rate server and internet based model .A huge amount of data being retrieved from geographically distributed data sources and non localized data handling requirements. The industrial information technology towards a subscription based or pay-per-use service business model known as cloud computing. One of the advantage of cloud computing is cloud data storage, in which users do not have to store his own data on their own servers [1], where instead their data will be stored on the cloud service provider's servers. For that reason users have to pay the service charge to service provider for this storage service. This service does not provide only flexibility and scalability for the data storage it also provides customers with the benefit of paying a charge only amount of data they need to store for particular time.To access this cloud services security and reliability we are using different modules like: 1) Using single cloud service provider. 2) Using multiple cloud service providers. The drawback of single cloud service provider is that it can be easily hacked by any attacker. In multiple cloud service provider model gives better security and availability of user private data.

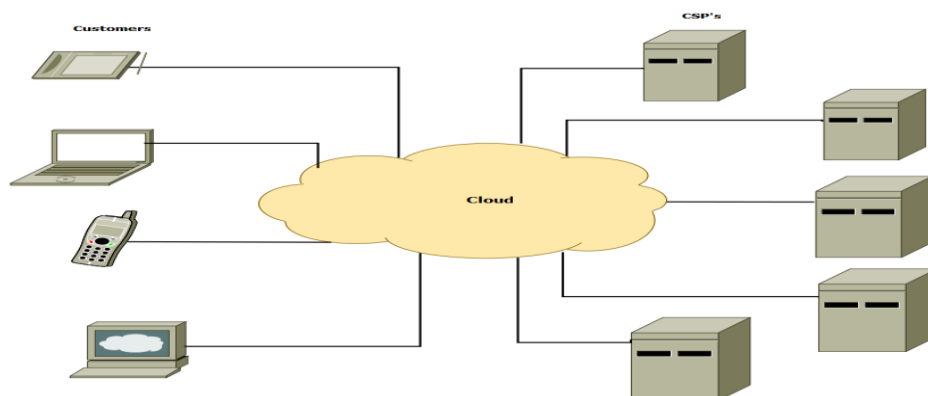


Fig 1: Cloud Computing Architecture

Data integrity and privacy of the data are the most critical issues in cloud storage. For that reason cloud service provider have standard techniques and hybrid model [4][3][5]. In this work we provide better privacy and availability of user's data can be achieved by dividing into block of data pieces and distributing them among the cloud service provider's in such way that for retrieving original data specific number of cloud service providers are required. Our proposed approach will provide the cloud computing users a decision model, That will provide a better security by distributing data over multiple cloud service providers in such a manner, none of the SP can successfully retrieve meaningful information from the data pieces allocated at their servers. Also in addition, we may provide user with better assurance of availability of their data.

II. BACKGROUND

We found these some existing system is related to our proposed system having their advantages and limitations. From these we can say that our proposed system is better than existing one.

	Existing System	Advantages	Limitations
1	Single Cloud Computing	i. Availability of data is maintained.	i. Require high cost. ii. Does not provide flexibility and scalability.
2	Data Storage only with Cryptography.	i. Due to encryption and decryption of data, confidentiality is achieved.	i. Only cryptography does not provide full security. ii. Cryptography does not provide integrity and availability.
3	Data Storage Over Untrusted Networks.	i. If Attacker hacks any one network still he does not retrieve any meaningful data.	i. Secret key get be shared with every user. ii. Losses of data.

In one of the above system we consider threat model which will losses data availability because of failure or crash of server of cloud service provider which makes difficult for customer to retrieve his stored data on the server [2]. Customer cannot depend on single cloud service provider to ensure the storage of confidential data. For understanding this threat model we take example in Fig 1. Let us consider three customers (customer1, customer2 and customer3) and stored their data on three different cloud service providers (CSP1, CSP2 and CSP3) respectively. Each customer can retrieve his own data from the cloud service provider who it has dealing with. If a failure occurs at CSP1, due to internal problem with the server all customer1 data which was stored on CSP1's servers will be lost and cannot be retrieved.

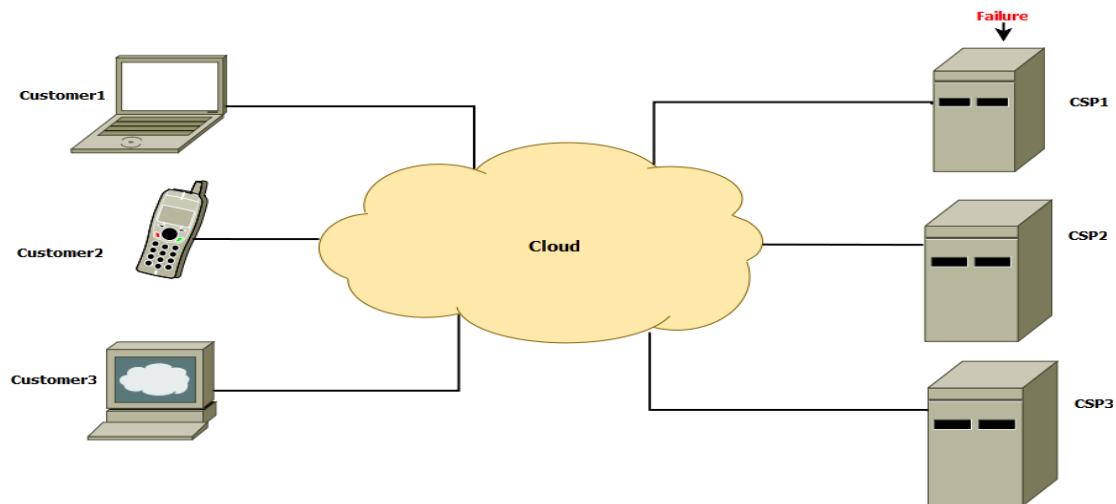


Fig. 3: CSP Failure

III. SYSTEM OVERVIEW

In our system, we are considering 1] Customer (C1): The person who has some files to store on the cloud (i.e. Cloud Server). 2] Cloud service provider (CSP): To manage Cloud Server, having considerable storage space and to provide effective services for data storage and maintenance. The cloud service provider priced to customers which is based on two factors, how much data is going to be stored on the cloud servers and for how long time the data is to be stored. In our system, we consider that specific number cloud service providers for data storage and retrieve. Hence, customer can store his private data on multiple clouds according his budgets.

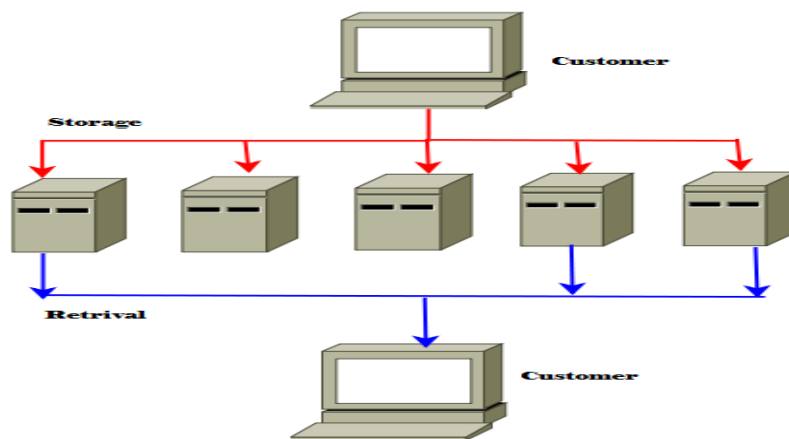


Fig 2: Data Storage And Retrieval

IV. PROPOSED MODEL

In this system, we proposed distribution of user's data among the available service providers in the market, to provide all the cloud users with data availability as well as better security of data storage. In our model, the customer divides his data among several CSP's available in the market, based on user available budget. Also we provide a choice for the customer, to choose different CSP. User may choose CSP to store or to access the data.

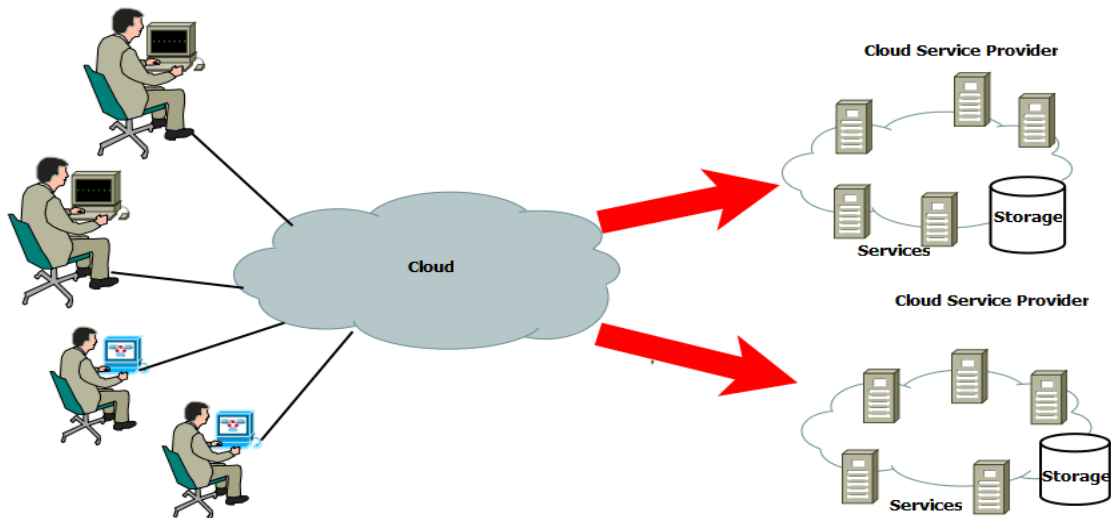


Fig. 4: Multi-Cloud Storage in Cloud Computing

Our proposed approach provides a better security by distributing the data over multiple cloud service providers in such a way that, none of the service provider can successfully retrieve meaningful data from the data stored at their own servers and provides better availability of data. If any hacker hacks any of the network still user can access his data by retrieving it from other cloud service providers.

3.1. Advantages

- 1) The system provides data Integrity, Availability, Confidentiality in short Security.
- 2) By using cryptography data is secured.
- 3) Less cost and cost based on client requirements.
- 4) Cloud data storage also redefines security issues targeted on customers outsourced data.
- 5) Easy to maintain large databases with security.
- 6) Avoid database losses.

3.2. Algorithms

The Algorithms to be used in our system:

- 1) Shamir Secret Sharing Algorithm

In cryptography, secret sharing refers to a method for distributing a "secret" amongst a group of shares, each of them gets allocated a share of the secret. The secret can be only reconstructed when the shares are combined together; individual shares are of no use on their own. 2) Message Digest (MD5) This algorithm used for checking integrity of retrieved data. It takes as input a message of arbitrary length and produces as output a 128 bit fingerprint or message digest of the input. It is conjectured, so it is computationally infeasible to produce two messages having the same message digest intended, where such a large file should be compressed in a secure manner before being encrypted with a private key under a public-key crypto-system.

V. CONCLUSION

It is clear that although the use of cloud computing has rapidly increased, its security is still considered the major issue in the cloud computing environment. The customers do not want to lose their private information as a result of malicious insiders in the cloud. In addition, loss of service availability has caused many problems for a large number of customers. Furthermore, data intrusion leads to many problems for the users of cloud computing. The purpose of this work is to check the recent research on single clouds and multi-clouds to address the security risks and solutions.

REFERENCES

- [1] P. Mell, T. Grance, "Draft NIST working definition of cloud computing", Referenced on June. 3rd, 2009, Online at <http://csrc.nist.gov/groups/SNS/cloud-computing/index.html>, 2009.
- [2] N. Gruschka, M. Jensen, "Attack surfaces: A taxonomy for attacks on cloud services", Cloud Computing (CLOUD), 2010 IEEE 3rd International Conference on, 5-10 July 2010.
- [3] J. Kincaid, "MediaMax/TheLinkup Closes Its Doors", Online at <http://www.techcrunch.com/2008/-7/10/mediamaxthelinkupcloses-itsdoors/>, July 2008.
- [4] B. Krebs, "Payment Processor Breach May Be Largest Ever", Online at [payment processor breach may b.html](http://paymentprocessorbreachmayb.html), Jan, 2009 <http://voices.washingtonpost.com/securityfix/2009/01/>.
- [5] Amazon.com, "Amazon s3 availability event: July 20, 2008", Online at <http://status.aws.amazon.com/s3-20080720.html>, 2008.
- [6] P. S. Browne, "Data privacy and integrity: an overview", In Proceeding of SIGFIDET 71 Proceedings of the ACM SIGFIDET (now SIGMOD), 1971.
- [7] W. Itani, A. Kayssi, A. Chehab, "Privacy as a Service: Privacy-Aware Data Storage and Processing in Cloud Computing Architectures," Eighth IEEE International Conference on Dependable, Autonomic and Secure Computing, Dec 2009.
- [8] M. Dijk, A. Juels, "On the Impossibility of Cryptography Alone for Privacy-Preserving Cloud Computing", HotSec 2010.
- [9] P. F. Oliveira, L. Lima, T. T. V. Vinhoza, J. Barros, M. Medard "Trusted storage over untrusted networks", IEEE GLOBECOM 2010, Miami, FL, USA.